Kingdom of Saudi Arabia

Ministry of Education

Northern Border University

Faculty of Science

Department of Chemistry

Methods of Instrumental Analysis

(Theory)

(1102-312)

(طرق التحليل الآلي)

(نظري)

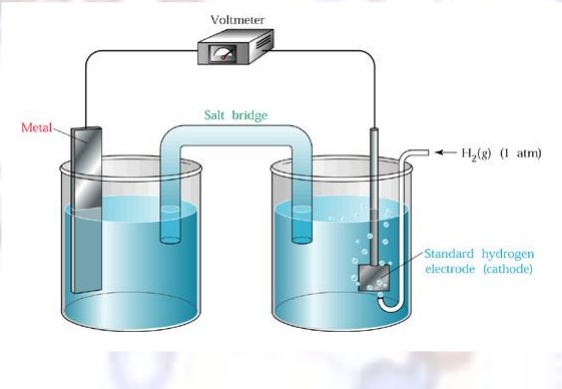

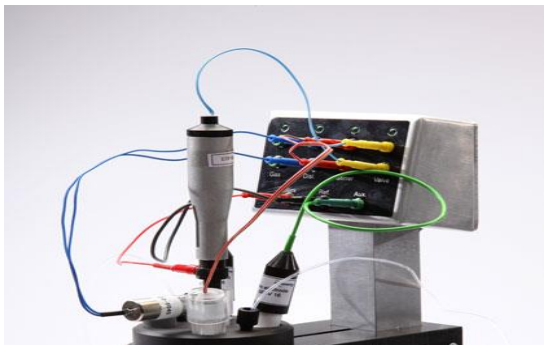

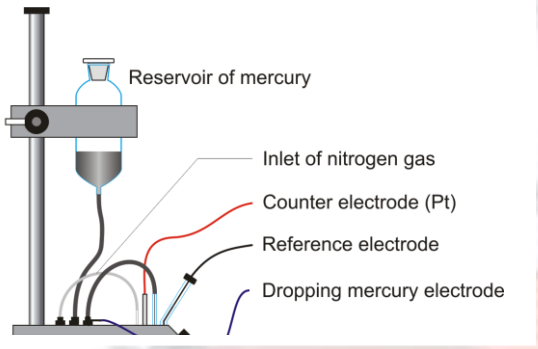

1445H

Spectrochemical Analysis

PART V

CHAPTER 24

Introduction to Spectrochemical Methods

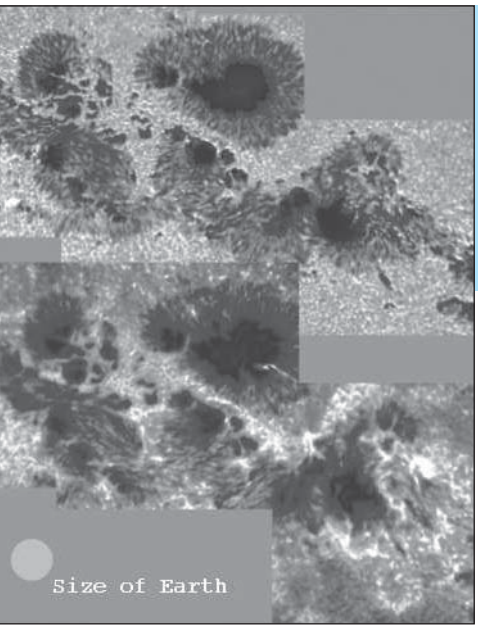

M. Sigwarth, J. Elrod, K.S. Balasubramaniam, S. Fletcher/NSO/AURA/NSF

This composite image is a sunspot group collected with the Dunn Solar Telescope at the Sacramento Peak Observatory in New Mexico on March 29, 2001. The lower portion consisting of four frames was collected at a wavelength of 393.4 nm, and the upper portion was collected at 430.4 nm. The lower image represents calcium ion concentration, with the intensity of the radiation proportional to the amount of the ion in the sunspot. The upper image shows the presence of the CH molecule. Using data like these, it is possible to determine the location and abundance of virtually any chemical species in the universe. Note that the Earth could fit in the large black core sunspot at the upper left of each of the composite images.

Methods that use or produce UV, visible, or IR radiation are often called optical spectroscopic methods. Other useful methods include those that use the γ-ray, X-ray, microwave, and RF spectral regions.

Measurements based on light and other forms of electromagnetic radiation are widely used throughout analytical chemistry. The interactions of radiation and matter are the subject of the science called **spectroscopy**. Spectroscopic analytical methods are based on measuring the amount of radiation produced or absorbed by molecular or atomic species of interest.[1] We can classify spectroscopic methods according to the region of the electromagnetic spectrum used or produced in the measurement. The γ-ray, X-ray, ultraviolet (UV), visible, infrared (IR), microwave, and radio-frequency (RF) regions have been used. Indeed, current usage extends the meaning of spectroscopy yet further to include techniques such as acoustic, mass, and electron spectroscopy in which electromagnetic radiation is not a part of the measurement.

Spectroscopy has played a vital role in the development of modern atomic theory. In addition, **spectrochemical methods** have provided perhaps the most widely used tools for the elucidation of molecular structure as well as the quantitative and qualitative determination of both inorganic and organic compounds.

In this chapter, we discuss the basic principles that are necessary to understand measurements made with electromagnetic radiation, particularly those dealing with the absorption of UV, visible, and IR radiation. The nature of electromagnetic radiation and its interactions with matter are stressed. The next five chapters are devoted to spectroscopic instruments (Chapter 25), molecular absorption spectroscopy (Chapter 26), molecular fluorescence spectroscopy (Chapter 27), atomic spectroscopy (Chapter 28), and mass spectrometry (Chapter 29).

[1]For further study, see D. A. Skoog, F. J. Holler, and S. R. Crouch, *Principles of Instrumental Analysis,* 6th ed., Sections 2–3, Belmont, CA: Brooks/Cole, 2007; F. Settle, ed., *Handbook of Instrumental Techniques for Analytical Chemistry,* Sections III–IV, Upper Saddle River, NJ: Prentice-Hall, 1997; J. D. Ingle, Jr., and S. R. Crouch, *Spectrochemical Analysis*, Upper Saddle River, NJ: Prentice-Hall, 1988; E. J. Meehan, in *Treatise on Analytical Chemistry*, 2nd ed., P. J. Elving, E. J. Meehan, and I. M. Kolthoff, eds., Part I, Vol. 7, Chs. 1–3, New York: Wiley, 1981.

24A PROPERTIES OF ELECTROMAGNETIC RADIATION

Electromagnetic radiation is a form of energy that is transmitted through space at enormous velocities. We will call electromagnetic radiation in the UV/visible and sometimes in the IR region, **light**, although strictly speaking the term refers only to visible radiation. Electromagnetic radiation can be described as a wave with properties of wavelength, frequency, velocity, and amplitude. In contrast to sound waves, light requires no transmitting medium; thus, it can travel readily through a vacuum. Light also travels nearly a million times faster than sound.

The wave model fails to account for phenomena associated with the absorption and emission of radiant energy. For these processes, electromagnetic radiation can be treated as discrete packets of energy or particles called **photons** or **quanta**. These dual views of radiation as particles and waves are not mutually exclusive but complementary. In fact, the energy of a photon is directly proportional to its frequency as we shall see. Similarly, this duality applies to streams of electrons, protons, and other elementary particles, which can produce interference and diffraction effects that are typically associated with wave behavior.

Courtesy of the Archives, California Institute of Technology

Richard P. Feynman (1918–1988) was one of the most renowned scientists of the twentieth century. He was awarded the Nobel Prize in Physics in 1965 for his role in the development of quantum electrodynamics. In addition to his many and varied scientific contributions, he was a skilled teacher, and his lectures and books had a major influence on physics education and science education in general.

24A-1 Wave Properties

In dealing with phenomena such as reflection, refraction, interference, and diffraction, electromagnetic radiation is conveniently modeled as waves consisting of perpendicularly oscillating electric and magnetic fields, as shown in **Figure 24-1a**. The electric field for a single frequency wave oscillates sinusoidally in space and time, as shown in **Figure 24-1b**. The electric field is represented as a vector whose length is proportional to the field strength. The *x* axis in this plot is either time as the radiation passes a fixed point in space or distance at a fixed time. Note that the direction in which the field oscillates is perpendicular to the direction in which the radiation propagates.

> *Now we know how the electrons and photons behave. But what can I call it? If I say they behave like particles I give the wrong impression; also if I say they behave like waves. They behave in their own inimitable way, which technically could be called a quantum mechanical way. They behave in a way that is like nothing that you have ever seen before.* — R. P. Feynman[2]

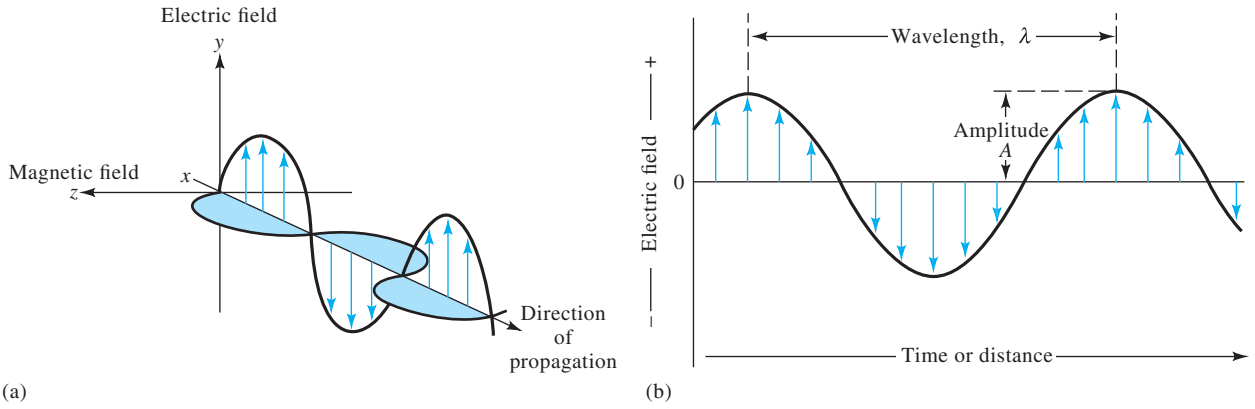

Figure 24-1 Wave nature of a beam of single frequency electromagnetic radiation. In (a), a plane-polarized wave is shown propagating along the *x* axis. The electric field oscillates in a plane perpendicular to the magnetic field. If the radiation were unpolarized, a component of the electric field would be seen in all planes. In (b), only the electric field oscillations are shown. The amplitude of the wave is the length of the electric field vector at the wave maximum, while the wavelength is the distance between successive maxima.

[2]R. P. Feynman, *The Character of Physical Law,* New York: Random House, 1994, p. 122.

The **amplitude** of an electromagnetic wave is a vector quantity that provides a measure of the electric or magnetic field strength at a maximum in the wave.

The **period** of an electromagnetic wave is the time in seconds for successive maxima or minima to pass a point in space.

The **frequency** of an electromagnetic wave is the number of oscillations that occur in one second.

The unit of frequency is the **hertz** (Hz), which corresponds to one cycle per second, that is, 1 Hz = 1 s^{-1}. The frequency of a beam of electromagnetic radiation does not change as it passes through different media.

Radiation velocity and wavelength both decrease as the radiation passes from a vacuum or from air to a denser medium. Frequency remains constant.

Note in Equation 24-1, v (distance/time) = ν ~~waves~~/time) × λ(distance/~~wave~~)

To three significant figures, Equation 24-2 is equally applicable in air or vacuum.

The **refractive index**, η, of a medium measures the extent of interaction between electromagnetic radiation and the medium through which it passes. It is defined by $\eta = c/v$. For example, the refractive index of water at room temperature is 1.33, which means that radiation passes through water at a rate of $c/1.33$ or 2.26×10^{10} cm s^{-1}. In other words, light travels 1.33 times slower in water than it does in vacuum. The velocity and wavelength of radiation become proportionally smaller as the radiation passes from a vacuum or from air to a denser medium while the frequency remains constant.

TABLE 24-1

Wavelength Units for Various Spectral Regions

Region	Unit	Definition
X-ray	Angstrom unit, Å	10^{-10} m
Ultraviolet/visible	Nanometer, nm	10^{-9} m
Infrared	Micrometer, μm	10^{-6} m

Wave Characteristics

In Figure 24-1b, the **amplitude** of the sine wave is shown, and the wavelength is defined. The time in seconds required for the passage of successive maxima or minima through a fixed point in space is called the **period**, p, of the radiation. The **frequency**, ν, is the number of oscillations of the electric field vector per unit time and is equal to $1/p$.

The frequency of a light wave or any wave of electromagnetic radiation is determined by the source that emits it and remains constant regardless of the medium traversed. In contrast, the **velocity**, v, of the wave front through a medium depends on both the medium and the frequency. The **wavelength**, λ, is the linear distance between successive maxima or minima of a wave, as shown in Figure 24-1b. The product of the frequency in waves per unit time and the wavelength in distance per wave is the velocity v of the wave in distance per unit time (cm s^{-1} or m s^{-1}), as shown in Equation 24-1. Note that both the velocity and the wavelength depend on the medium.

$$v = \nu\lambda \tag{24-1}$$

Table 24-1 gives the units used to express wavelengths in various regions of the spectrum.

The Speed of Light

In a vacuum, light travels at its maximum velocity. This velocity, which is given the special symbol c, is 2.99792×10^8 m s^{-1}. The velocity of light in air is only about 0.03 % less than its velocity in vacuum. Thus, for a vacuum, or for air, Equation 24-1 can be written to three significant figures as

$$c = \nu\lambda = 3.00 \times 10^8 \text{ m s}^{-1} = 3.00 \times 10^{10} \text{ cm s}^{-1} \tag{24-2}$$

In a medium containing matter, light travels with a velocity less than c because of interaction between the electromagnetic field and electrons in the atoms or molecules of the medium. Since the frequency of the radiation is constant, the wavelength must decrease as the light passes from a vacuum to a medium containing matter (see Equation 24-1). This effect is illustrated in **Figure 24-2** for a beam of visible radiation. Note that the effect can be quite large.

The **wavenumber**, $\bar{\nu}$, is another way to describe electromagnetic radiation. It is defined as the number of waves per centimeter and is equal to $1/\lambda$. By definition, $\bar{\nu}$ has the units of cm^{-1}.

EXAMPLE 24-1

Calculate the wavenumber of a beam of infrared radiation with a wavelength of 5.00 μm.

Solution

$$\bar{\nu} = \frac{1}{\lambda} = \frac{1}{5.00\ \cancel{\mu\text{m}} \times 10^{-4}\ \text{cm}/\cancel{\mu\text{m}}} = 2000\ \text{cm}^{-1}$$

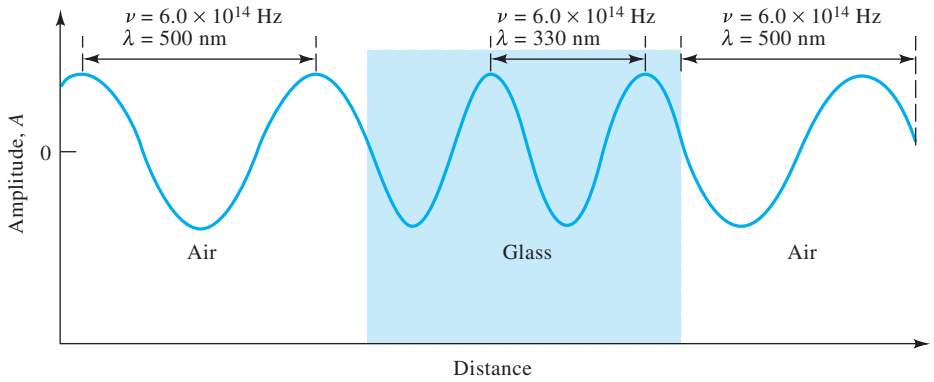

Figure 24-2 Change in wavelength as radiation passes from air into a dense glass and back to air. Note that the wavelength shortens by nearly 200 nm, or more than 30%, as it passes into glass; a reverse change occurs as the radiation again enters air.

Radiant Power and Intensity

The **radiant power**, P, in watts (W) is the energy of a beam that reaches a given area per unit time. The **intensity** is the radiant power-per-unit solid angle.[3] Both quantities are proportional to the square of the amplitude of the electric field (see Figure 24-1b). Although not strictly correct, radiant power and intensity are frequently used interchangeably.

The **wavenumber** $\bar{\nu}$ in cm^{-1} (Kayser) is most often used to describe radiation in the infrared region. The most useful part of the infrared spectrum for the detection and determination of organic species is from 2.5 to 15 μm, which corresponds to a wavenumber range of 4000 to 667 cm^{-1}. As shown below, the wavenumber of a beam of electromagnetic radiation is directly proportional to its energy and thus its frequency.

24A-2 The Particle Nature of Light: Photons

In many radiation/matter interactions, it is useful to emphasize the particle nature of light as a stream of photons or quanta. We relate the energy of a single photon to its wavelength, frequency, and wavenumber by

$$E = h\nu = \frac{hc}{\lambda} = hc\bar{\nu} \tag{24-3}$$

A **photon** is a particle of electromagnetic radiation having zero mass and an energy of $h\nu$.

where h is Planck's constant (6.63×10^{-34} J·s). Note that the wavenumber and frequency in contrast to the wavelength are directly proportional to the photon energy. Wavelength is inversely proportional to energy. The radiant power of a beam of radiation is directly proportional to the number of photons per second.

Equation 24-3 gives the energy of radiation in SI units of **joules**, where one joule (J) is the work done by a force of one newton (N) acting over a distance of one meter.

Both frequency and wavenumber are proportional to the energy of a photon.

EXAMPLE 24-2

Calculate the energy in joules of one photon of radiation with the wavelength given in Example 24-1.

Solution

Applying Equation 24-3, we can write

$$E = hc\bar{\nu} = 6.63 \times 10^{-34}\ \text{J}\cdot\text{s} \times 3.00 \times 10^{10}\ \frac{\text{cm}}{\text{s}} \times 2000\ \text{cm}^{-1}$$
$$= 3.98 \times 10^{-20}\ \text{J}$$

We sometimes speak of "a mole of photons", meaning 6.022×10^{23} packets of radiation of a given wavelength. The energy of one mole of photons with a wavelength of 5.00 μm is 6.022×10^{23} photons/mol × 1 mol × 3.98×10^{-20} J/photon = 2.40×10^{4} J = 24.0 kJ.

[3]Solid angle is the three dimensional spread at the vertex of a cone measured as the area intercepted by the cone on a unit sphere whose center is at the vertex. The angle is measured in stereradians (sr).

24B INTERACTION OF RADIATION AND MATTER

The most interesting and useful interactions in spectroscopy are those in which transitions occur between different energy levels of chemical species. Other interactions, such as reflection, refraction, elastic scattering, interference, and diffraction, are often related to the bulk properties of materials rather than to the unique energy levels of specific molecules or atoms. Although these bulk interactions are also of interest in spectroscopy, we will limit our discussion here to those interactions in which energy level transitions occur. The specific types of interactions observed depend strongly on the energy of the radiation used and the mode of detection.

TABLE 24-2

Regions of the UV, Visible, and IR Spectrum

Region	Wavelength Range
UV	180–380 nm
Visible	380–780 nm
Near-IR	0.78–2.5 μm
Mid-IR	2.5–50 μm

One easy way to recall the order of the colors in the spectrum is by the mnemonic **ROY G BIV**, which is short for **R**ed, **O**range, **Y**ellow, **G**reen, **B**lue, **I**ndigo, and **V**iolet.

The **visible region** of the spectrum extends from about 400 nm to almost 800 nm (see Table 24-2).

24B-1 The Electromagnetic Spectrum

The electromagnetic spectrum covers an enormous range of energies (frequencies) and thus wavelengths (see **Table 24-2**). Useful frequencies vary from $>10^{19}$ Hz (γ-ray) to 10^3 Hz (radio waves). An X-ray photon ($\nu \approx 3 \times 10^{18}$ Hz, $\lambda \approx 10^{-10}$ m), for example, is 10,000 times as energetic as a photon emitted by an ordinary light bulb ($\nu \approx 3 \times 10^{14}$ Hz, $\lambda \approx 10^{-6}$ m) and 10^{15} times as energetic as a radio-frequency photon ($\nu \approx 3 \times 10^3$ Hz $\lambda \approx 10^5$ m).

The major divisions of the spectrum are shown in color in Color Plate 21. Note that the visible region, to which our eyes respond, is only a tiny fraction of the entire spectrum. Different types of radiation such as gamma (γ) rays or radio waves differ from visible light only in the energy (frequency) of their photons.

Figure 24-3 shows the regions of electromagnetic spectrum that are used for spectroscopic analyses. Also shown are the types of atomic and molecular transitions that result from interactions of the radiation with a sample. Note that the

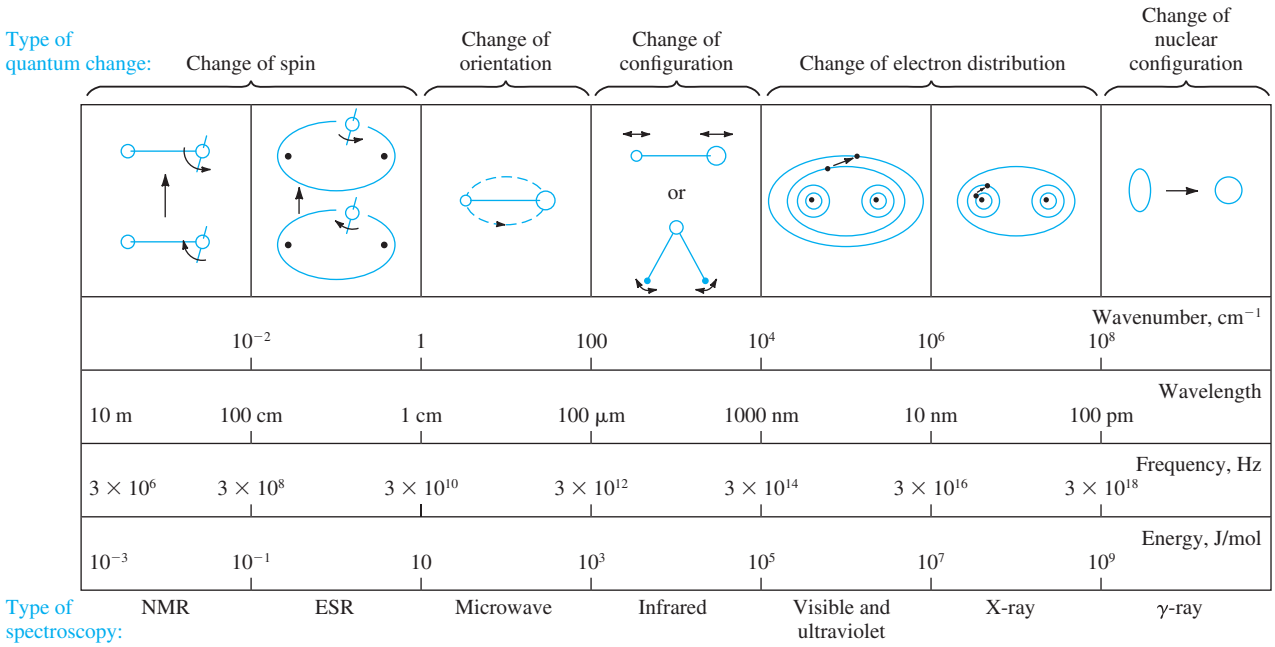

Figure 24-3 The regions of the electromagnetic spectrum. Interaction of an analyte with electromagnetic radiation can result in the types of changes shown. Note that changes in electron distributions occur in the UV/visible region. The wavenumber, wavelength, frequency, and energy are characteristics that describe electromagnetic radiation. (From C. N. Banwell, *Fundamentals of Molecular Spectroscopy,* 3rd ed., New York; McGraw-Hill, 1983, p. 7.)

low-energy radiation used in nuclear magnetic resonance (NMR) and electron spin resonance (ESR) spectroscopy causes subtle changes, such as changes in spin; the high-energy radiation used in γ-ray spectroscopy can cause much more dramatic changes, such as nuclear configuration changes.

Spectrochemical methods that use not only visible but also ultraviolet and infrared radiation are often called **optical methods** in spite of the fact that the human eye is not sensitive to UV or IR radiation. This terminology arises from the many common features of instruments for the three spectral regions and the similarities in the way we view the interactions of the three types of radiation with matter.

Optical methods are spectroscopic methods based on ultraviolet, visible, and infrared radiation.

24B-2 Spectroscopic Measurements

Spectroscopists use the interactions of radiation with matter to obtain information about a sample. Several of the chemical elements were discovered by spectroscopy (see Feature 24-1). The sample is usually stimulated in some way by applying energy in the form of heat, electrical energy, light, particles, or a chemical reaction. Prior to applying the stimulus, the analyte is predominately in its lowest-energy or **ground state**. The stimulus then causes some of the analyte species to undergo a transition to a higher-energy or **excited state**. We acquire information about the analyte by measuring the electromagnetic radiation emitted as it returns to the ground state or by measuring the amount of electromagnetic radiation absorbed as a result of excitation.

Figure 24-4 illustrates the processes that occur in emission and chemiluminescence spectroscopy. The analyte is stimulated by applying heat or electrical energy or by a chemical reaction. The term **emission spectroscopy** usually refers to methods in which the stimulus is heat or electrical energy, while **chemiluminescence spectroscopy** refers to excitation of the analyte by a chemical reaction. In both cases, measurement of the radiant power emitted as the analyte returns to the ground state can give information about its identity and concentration. The results of such a measurement are often expressed graphically by a **spectrum**, which is a plot of the emitted radiation as a function of frequency or wavelength.

A familiar example of **chemiluminescence** is found in the light emitted by a firefly. In the firefly reaction, an enzyme luciferase catalyzes the oxidative phosphorylation reaction of luciferin with adenosine triphosphate (ATP) to produce oxyluciferin, carbon dioxide, adenosine monophosphate (AMP), and light. Chemiluminescence involving a biological or enzyme reaction is often termed **bioluminescence**. The popular light stick is another familiar example of chemiluminescence.

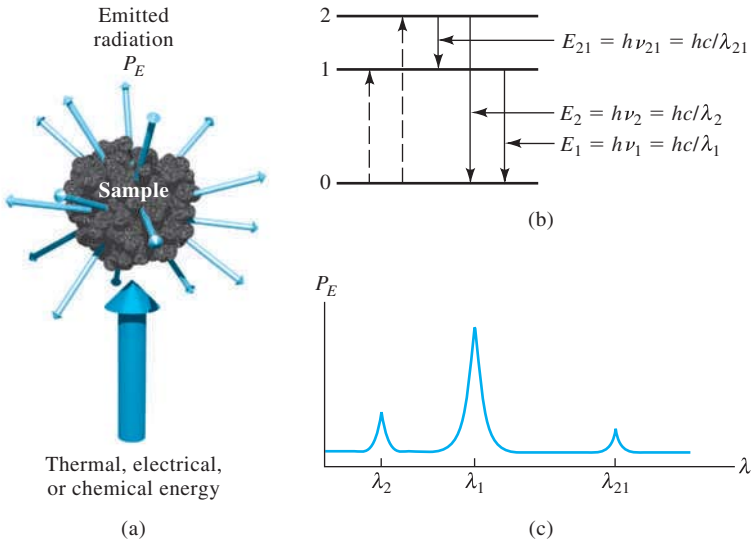

Figure 24-4 Emission or chemiluminescence processes. In (a), the sample is excited by applying thermal, electrical, or chemical energy. No radiant energy is used to produce excited states, and so, these are called non-radiative processes. In the energy level diagram (b), the dashed lines with upward pointing arrows symbolize these nonradiative excitation processes, while the solid lines with downward pointing arrows indicate that the analyte loses its energy by emission of a photon. In (c), the resulting spectrum is shown as a measurement of the radiant power emitted, P_E, as a function of wavelength, λ.

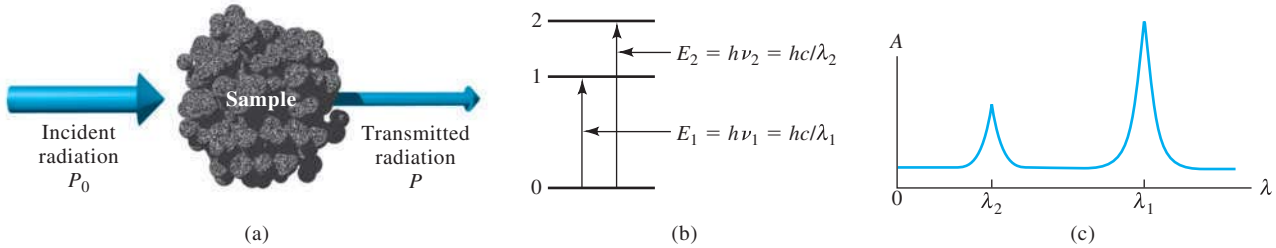

Figure 24-5 Absorption methods. In (a), radiation of incident radiant power P_0 can be absorbed by the analyte, resulting in a transmitted beam of lower radiant power P. For absorption to occur the energy of the incident beam must correspond to one of the energy differences shown in (b). The resulting absorption spectrum is shown in (c).

When the sample is stimulated by applying an external electromagnetic radiation source, several processes are possible. For example, the radiation can be scattered or reflected. What is important to us is that some of the incident radiation can be absorbed and promote some of the analyte species to an excited state, as shown in Figure 24-5. In **absorption spectroscopy**, we measure the amount of light absorbed as a function of wavelength. Absorption measurements can give both qualitative and quantitative information about the sample. In **photoluminescence spectroscopy** (see Figure 24-6), the emission of photons is measured following absorption. The most important forms of photoluminescence for analytical purposes are **fluorescence** and **phosphorescence spectroscopy**.

We focus here on absorption spectroscopy in the UV/visible region of the spectrum because it is so widely used in chemistry, biology, forensic science, engineering, agriculture, clinical chemistry, and many other fields. Note that the processes shown in Figures 24-4 through 24-6 can occur in any region of the electromagnetic spectrum; the different energy levels can be nuclear levels, electronic levels, vibrational levels, or spin levels.

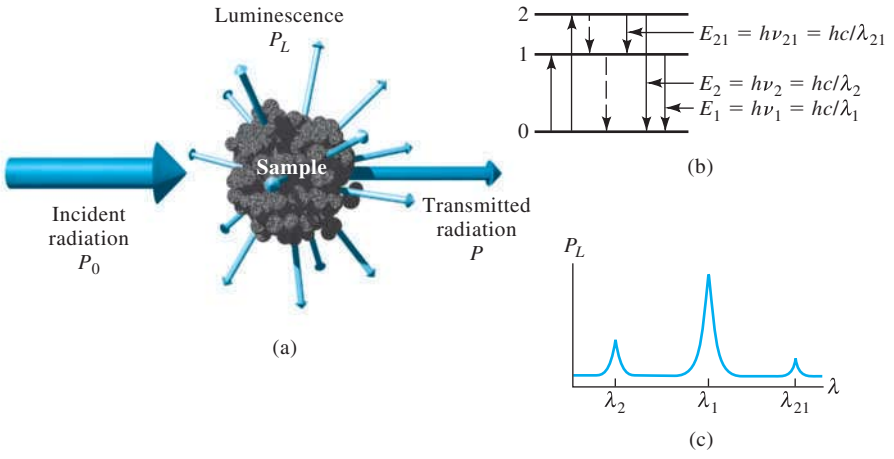

Figure 24-6 Photoluminescence methods (fluorescence and phosphorescence). Fluorescence and phosphorescence result from absorption of electromagnetic radiation and then dissipation of the energy by emission of radiation, as shown in (a). In (b), the absorption can cause excitation of the analyte to state 1 or state 2. Once excited, the excess energy can be lost by emission of a photon (luminescence shown as solid lines) or by nonradiative processes (dashed lines). The emission occurs over all angles, and the wavelengths emitted (c) correspond to energy differences between levels. The major distinction between fluorescence and phosphorescence is the time scale of emission with fluorescence being prompt and phosphorescence being delayed.

FEATURE 24-1

Spectroscopy and the Discovery of Elements

The modern era of spectroscopy began with the observation of the spectrum of the sun by Sir Isaac Newton in 1672. In his experiment, Newton passed rays from the sun through a small opening into a dark room where they struck a prism and dispersed into the colors of the spectrum. The first description of spectral features beyond the simple observation of colors was in 1802 by Wollaston, who noticed dark lines on a photographic image of the solar spectrum. These lines along with more than 500 others, which are shown in the solar spectrum of **Figure 24F-1**, were later described in detail by Fraunhofer. Based on his observations, which began in 1817, Fraunhofer gave the prominent lines letters starting with "A" at the red end of the spectrum. The solar spectrum is shown in color plate 17.

It remained, however, for Gustav Kirchhoff and Robert Wilhelm Bunsen in 1859 and 1860 to explain the origin of the Fraunhofer lines. Bunsen had invented his famous burner (see **Figure 24F-2**) a few years earlier, which made possible spectral observations of emission and absorption phenomena in a nearly transparent flame. Kirchhoff concluded that the Fraunhofer "D" lines were due to sodium in the sun's atmosphere and the "A" and "B" lines were due to potassium. To this day, we call the emission lines of sodium the sodium "D" lines. These lines are responsible for the familiar yellow color seen in flames containing sodium or in sodium vapor lamps. The absence of lithium in the sun's spectrum led Kirchhoff to conclude that there was little lithium present in the sun. During these studies, Kirchhoff also developed his famous laws relating the absorption and emission of light from bodies and at interfaces. Together with Bunsen, Kirchhoff observed that different elements could impart different colors to flames and produce spectra exhibiting differently colored bands or lines. Kirchhoff and Bunsen are thus credited with discovering the use of spectroscopy for chemical analysis. Emission spectra of several elements are shown in color plate 16. The method was soon put to many practical uses, including the discovery of new elements. In 1860, the elements cesium and rubidium were discovered with spectroscopy, followed in 1861 by thallium and in 1864 by indium. The age of spectroscopic analysis had begun.

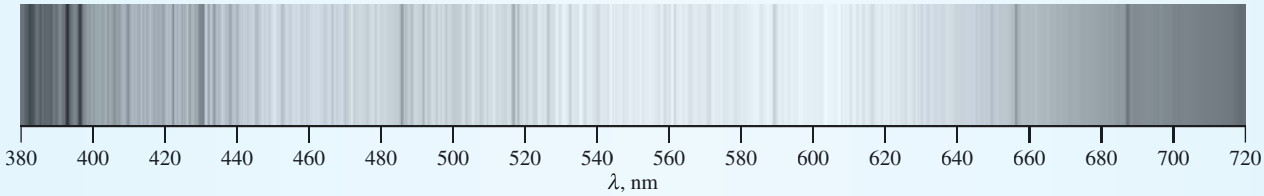

Figure 24F-1 The solar spectrum. The dark vertical lines are the Fraunhofer lines. See color plate 17 for a full-color version of the spectrum. Data for the image were collated by Dr. Donald Mickey, University of Hawaii Institute for Astronomy, from National Solar Observatory spectral data. NSO/Kitt Peak FTS data used here were produced by NSF/NOAO.

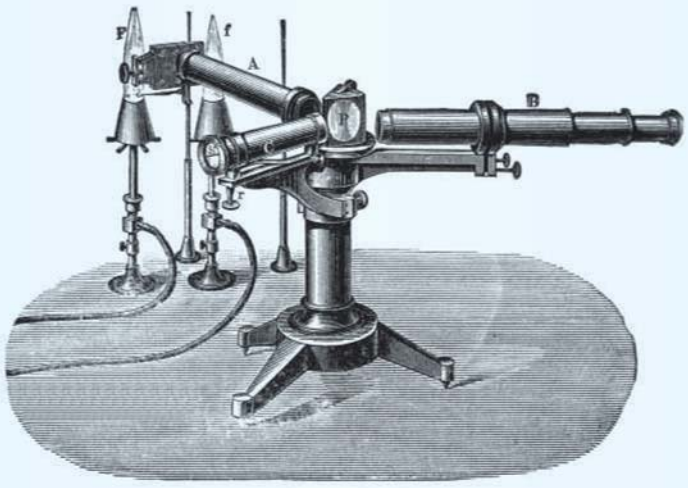

Figure 24F-2 Bunsen burner of the type used in early spectroscopic studies with a prism spectroscope of type used by Kirchhoff. (From H. Kayser, *Handbuch der Spectroscopie,* Stuttgart, Germany: S. Hirzel Verlag GmbH, 1900.)

24C ABSORPTION OF RADIATION

Every molecular species is capable of absorbing its own characteristic frequencies of electromagnetic radiation, as described in Figure 24-5. This process transfers energy to the molecule and results in a decrease in the intensity of the incident electromagnetic radiation. Absorption of the radiation thus **attenuates** the beam in accordance with the absorption law as described in Section 24C-1.

In spectroscopy, **attenuate** means to decrease the energy per unit area of a beam of radiation. In terms of the photon model, attenuate means to decrease the number of photons per second in the beam.

24C-1 The Absorption Process

The absorption law, also known as the **Beer-Lambert law** or just **Beer's law**, tells us quantitatively how the amount of attenuation depends on the concentration of the absorbing molecules and the path length over which absorption occurs. As light traverses a medium containing an absorbing analyte, the intensity decreases as the analyte becomes excited. For an analyte solution of a given concentration, the longer the length of the medium through which the light passes (path length of light), the more absorbers are in the path, and the greater the attenuation. Similarly, for a given path length of light, the higher the concentration of absorbers, the stronger the attenuation.

The term **monochromatic radiation** refers to radiation of a single color; that is, a single wavelength or frequency. In practice, it is virtually impossible to produce a single color of light. We discuss the practical problems associated with producing monochromatic radiation in Chapter 25.

Figure 24-7 depicts the attenuation of a parallel beam of **monochromatic radiation** as it passes through an absorbing solution of thickness b cm and concentration c moles per liter. Because of interactions between the photons and absorbing particles (recall Figure 24-5), the radiant power of the beam decreases from P_0 to P. The **transmittance** T of the solution is the fraction of incident radiation transmitted by the solution, as shown in Equation 24-4. Transmittance is often expressed as a percentage and called the **percent transmittance**.

$$T = P/P_0 \tag{24-4}$$

Percent transmittance $= \%T = \dfrac{P}{P_0} \times 100\%$.

Absorbance

The **absorbance**, A, of a solution is related to the transmittance in a logarithmic manner as shown in Equation 24-5. Notice that as the absorbance of a solution increases, the transmittance decreases. The relationship between transmittance and absorbance is illustrated by the conversion spreadsheet shown in **Figure 24-8**. The scales on earlier instruments were linear in transmittance or sometimes in absorbance. In modern instruments, a computer calculates absorbance from measured quantities.

$$A = -\log T = -\log \frac{P}{P_0} = \log \frac{P_0}{P} \tag{24-5}$$

Absorbance can be calculated from percent transmittance as follows:

$$T = \frac{\%T}{100\%}$$

$$A = -\log T$$
$$= -\log \%T + \log 100$$
$$= 2 - \log \%T$$

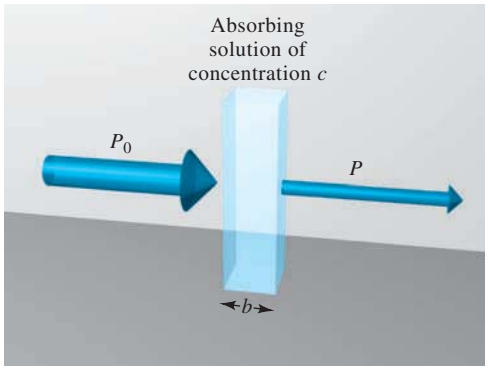

Figure 24-7 Attenuation of a beam of radiation by an absorbing solution. The larger arrow on the incident beam signifies a higher radiant power P_0 than that transmitted by the solution P. The path length of the absorbing solution is b and the concentration is c.

	A	B	C	D
1	Calculation of Absorbance from Transmittance			
2	*T*	%*T*	*A* = -log *T*	*A* = 2-log %*T*
3	0.001	0.1	3.000	3.000
4	0.010	1.0	2.000	2.000
5	0.050	5.0	1.301	1.301
6	0.075	7.5	1.125	1.125
7	0.100	10.0	1.000	1.000
8	0.200	20.0	0.699	0.699
9	0.300	30.0	0.523	0.523
10	0.400	40.0	0.398	0.398
11	0.500	50.0	0.301	0.301
12	0.600	60.0	0.222	0.222
13	0.700	70.0	0.155	0.155
14	0.800	80.0	0.097	0.097
15	0.900	90.0	0.046	0.046
16	1.000	100.0	0.000	0.000
17				
18	Spreadsheet Documentation			
19	Cell B3=A3*100			
20	Cell C3=-LOG10(A3)			
21	Cell D3=2-LOG10(B3)			

Figure 24-8 Conversion spreadsheet relating transmittance T, percent transmittance $\%T$, and absorbance A. The transmittance data to be converted are entered in cells A3 through A16. The percent transmittance is calculated in cells B3 by the formula shown in the documentation section, cell A19. This formula is copied into cells B4 through B16. The absorbance is calculated from $-\log T$ in cells C3 through C16 and from $2 - \log \%T$ in cells D3 through D16. The formulas for the first cell in the C and D columns are shown in cells A20 and A21.

Measuring Transmittance and Absorbance

Transmittance and absorbance, as defined by Equations 24-4 and 24-5 and depicted in Figure 24-7, usually cannot be measured as shown because the solution to be studied must be held in a container (cell or cuvette). Reflection and scattering losses can occur at the cell walls, as shown in **Figure 24-9**. These losses can be substantial. For example, about 8.5% of a beam of yellow light is lost by reflection when it passes through a glass cell. Light can also be scattered in all directions from the surface of large molecules or particles, such as dust, in the solvent, and this scattering can cause further attenuation of the beam as it passes through the solution.

To compensate for these effects, the power of the beam transmitted through a cell containing the analyte solution is compared with one that traverses an identical cell containing only the solvent, or a reagent blank. An experimental absorbance that closely approximates the true absorbance for the solution is thus obtained, that is,

$$A = \log \frac{P_0}{P} \approx \log \frac{P_{\text{solvent}}}{P_{\text{solution}}} \tag{24-6}$$

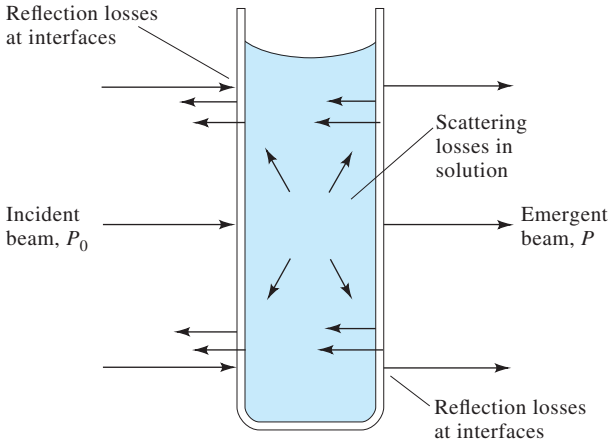

Figure 24-9 Reflection and scattering losses with a solution contained in a typical glass cell. Losses by reflection can occur at all the boundaries that separate the different materials. In this example, the light passes through the following boundaries, called interfaces: air-glass, glass-solution, solution-glass, and glass-air.

Because of this close approximation, the terms P_0 and P will henceforth refer to the power of a beam that has passed through cells containing the solvent (or blank) and the analyte solution, respectively.

Beer's Law

According to Beer's law, absorbance is directly proportional to the concentration of the absorbing species, c, and to the path length, b, of the absorbing medium as expressed by Equation 24-7.

$$A = \log(P_0/P) = abc \tag{24-7}$$

The molar absorptivity of a species at an absorption maximum is characteristic of that species. Peak molar absorptivities for many organic compounds range from 10 or less to 10,000 or more. Some transition metal complexes have molar absorptivities of 10,000 to 50,000. High molar absorptivities are desirable for quantitative analysis because they lead to high analytical sensitivity.

In Equation 24-7, a is a proportionality constant called the **absorptivity**. Because absorbance is a unitless quantity, the absorptivity must have units that cancel the units of b and c. If, for example, c has the units of g L^{-1} and b has the units of cm, absorptivity has the units of L g^{-1} cm^{-1}.

When we express the concentration in Equation 24-7 in moles per liter and b in cm, the proportionality constant is called the **molar absorptivity** and is given the symbol ε. Thus,

$$A = \varepsilon bc \tag{24-8}$$

where ε has the units of L mol^{-1} cm^{-1}.

FEATURE 24-2

Deriving Beer's Law

To derive Beer's law, we consider the block of absorbing matter (solid, liquid, or gas) shown in **Figure 24F-3**. A beam of parallel monochromatic radiation with power P_0 strikes the block perpendicular to a surface; after passing through a length b of the material, which contains n absorbing particles (atoms, ions, or molecules), its power is decreased to P as a result of absorption. Consider now a cross section of the block having an area S and an infinitesimal thickness dx. Within this section, there are dn absorbing particles. Associated with each particle, we can imagine a surface at which photon capture will occur, that is, if a photon reaches one of these

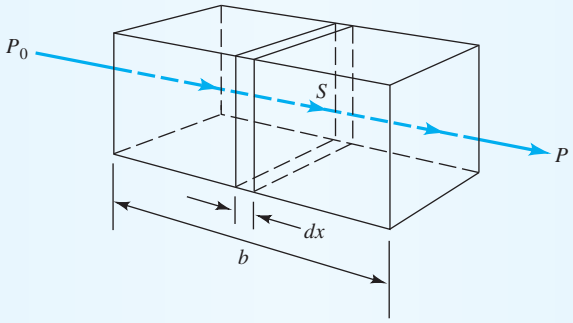

Figure 24F-3 Attenuation of a beam of electromagnetic radiation with initial power P_0 by a solution containing c mol/L of absorbing solute and a path length of b cm. The transmitted beam has a radiant power P ($P < P_0$).

areas by chance, absorption will follow immediately. The total projected area of these capture surfaces within the section is designated as dS; the ratio of the capture area to the total area then is dS/S. On a statistical average, this ratio represents the probability for the capture of photons within the section. The power of the beam entering the section, P_x, is proportional to the number of photons per square centimeter per second, and dP_x represents the quantity removed per second within the section. The fraction absorbed is then $-dP_x/P_x$, and this ratio also equals the average probability for capture. The term is given a minus sign to indicate that *the* radiant power undergoes a decrease. Thus,

$$-\frac{dP_x}{P_x} = \frac{dS}{S} \tag{24-9}$$

Recall now that dS is the sum of the capture areas for particles within the section. It must, therefore, be proportional to the number of particles, or

$$dS = a \times dn \tag{24-10}$$

where dn is the number of particles and a is a proportionality constant, which is called the *capture cross section*. By combining Equations 24-9 and 24-10 and integrating over the interval between 0 and n, we obtain

$$-\int_{P_x}^{P} \frac{dP_x}{P_x} = \int_0^n \frac{a \times dn}{S}$$

which, when integrated, gives

$$-\ln \frac{P}{P_0} = \frac{an}{S}$$

We then convert to base 10 logarithms, invert the fraction to change the sign, and obtain

$$\log \frac{P_0}{P} = \frac{an}{2.303\ S} \tag{24-11}$$

where n is the total number of particles within the block shown in Figure 24F-3. The cross-sectional area S can be expressed in terms of the volume of the block V in cm^3 and its length b in cm. Thus,

$$S = \frac{V}{b}\ cm^2$$

By substituting this quantity into Equation 24-11, we find

$$\log \frac{P_0}{P} = \frac{anb}{2.303\ V} \tag{24-12}$$

Notice that n/V has the units of concentration (that is, number of particles per cubic centimeter). To convert n/V to moles per liter, we find the number of moles by

$$\text{number mol} = \frac{n\ \text{particles}}{6.022 \times 10^{23}\ \text{particles/mol}}$$

(continued)

The concentration c in mol/L is then

$$c = \frac{n}{6.022 \times 10^{23}} \text{ mol} \times \frac{1000 \text{ cm}^3/\text{L}}{V \text{ cm}^3}$$

$$= \frac{1000\,n}{6.022 \times 10^{23}} \text{ mol/L}$$

By combining this relationship with Equation 24-12, we have

$$\log \frac{P_0}{P} = \frac{6.022 \times 10^3\, abc}{2.303 \times 1000}$$

Finally, the constants in this equation can be collected into a single term ε to give

$$A = \log \frac{P_0}{P} = \varepsilon bc \qquad (24\text{-}13)$$

which is Beer's law.

Terms Used in Absorption Spectrometry

In addition to the terms we have introduced to describe absorption of radiant energy, you may encounter other terms in the literature or with older instruments. The terms, symbols, and definitions given in **Table 24-3** are recommended by the Society for Applied Spectroscopy and the American Chemical Society. The third column contains the older names and symbols. Because a standard nomenclature is highly desirable to avoid ambiguities, we urge you to learn and use the recommended terms and symbols and to avoid the older terms.

TABLE 24-3

Important Terms and Symbols Employed in Absorption Measurements

Term and Symbol*	Definition	Alternative Name and Symbol
Incident radiant power, P_0	Radiant power in watts incident on sample	Incident intensity, I_0
Transmitted radiant power, P	Radiant power transmitted by sample	Transmitted intensity, I
Absorbance, A	$\log(P_0/P)$	Optical density, D; extinction, E
Transmittance, T	P/P_0	Transmission, T
Path length of sample, b	Length over which attenuation occurs	l, d
Absorptivity†, a	$A/(bc)$	α, k
Molar absorptivity‡, ε	$A/(bc)$	Molar absorption coefficient

*Compilation of terminology recommended by the American Chemical Society and the Society for Applied Spectroscopy (*Appl. Spectrosc.*, **2012**, *66*, 132).

† c may be expressed in g L^{-1} or in other specified concentration units; b may be expressed in cm or other units of length.

‡ c is expressed in mol L^{-1}; b is expressed in cm.

Using Beer's Law

Beer's law, as expressed in Equations 24-6 and 24-8, can be used in several different ways. We can calculate molar absorptivities of species if the concentration is known, as shown in Example 24-3. We can use the measured value of absorbance to obtain concentration if absorptivity and path length are known. Absorptivities, however, are functions of such variables as solvent, solution composition, and temperature. Because of variations in absorptivity with conditions, it is never a good idea to depend on literature values for quantitative work. Hence, a standard solution of the analyte in the same solvent and at a similar temperature is used to obtain the absorptivity at the time of the analysis. Most often, we use a series of standard solutions of the analyte to construct a calibration curve, or working curve, of A versus c or to obtain a linear regression equation (for the method of external standards and linear regression, see Section 8D-2). It may also be necessary to duplicate closely the overall composition of the analyte solution in order to compensate for matrix effects. Alternatively, the method of standard additions (see Section 8D-3 and Section 26A-3) is used for the same purpose.

EXAMPLE 24-3

A 7.25×10^{-5} M solution of potassium permanganate has a transmittance of 44.1% when measured in a 2.10-cm cell at a wavelength of 525 nm. Calculate (a) the absorbance of this solution and (b) the molar absorptivity of $KMnO_4$.

Solution

(a) $A = -\log T = -\log 0.441 = -(-0.356) = 0.356$

(b) From Equation 24-8,

$$\varepsilon = A/bc = 0.356/(2.10 \text{ cm} \times 7.25 \times 10^{-5} \text{mol L}^{-1})$$
$$= 2.34 \times 10^{3} \text{ L mol}^{-1} \text{ cm}^{-1}$$

Spreadsheet Summary In the first exercise in Chapter 12 of *Applications of Microsoft® Excel in Analytical Chemistry,* 2nd ed., a spreadsheet is developed to calculate the molar absorptivity of permanganate ion. A plot of absorbance versus permanganate concentration is constructed, and least-squares analysis of the linear plot is carried out. The data are analyzed statistically to determine the uncertainty of the molar absorptivity. In addition, other spreadsheets are presented for calibration in quantitative spectrophotometric experiments and for calculating concentrations of unknown solutions.

Applying Beer's Law to Mixtures

Beer's law also applies to solutions containing more than one kind of absorbing substance. Provided that there is no interaction among the various species, the total

absorbance for a multicomponent system at a single wavelength is the sum of the individual absorbances. In other words,

Absorbances are additive if the absorbing species do not interact.

$$A_{\text{total}} = A_1 + A_2 + \cdots + A_n = \varepsilon_1 b c_1 + \varepsilon_2 b c_2 + \cdots + \varepsilon_n b c_n \qquad (24\text{-}14)$$

where the subscripts refer to absorbing components 1, 2, . . . , n.

24C-2 Absorption Spectra

A bit of Latin. One plot of absorbance versus wavelength is called a spectr**um**; two or more plots are called spectr**a**.

An **absorption spectrum** is a plot of absorbance versus wavelength, as illustrated in **Figure 24-10**. Absorbance could also be plotted against wavenumber or frequency. Modern scanning spectrophotometers produce such an absorption spectrum directly. Older instruments sometimes displayed transmittance and produced plots of T or $\%T$ versus wavelength. Occasionally plots with log A as the ordinate are used. The logarithmic axis leads to a loss of spectral detail, but it is convenient for comparing solutions of widely different concentrations. A plot of molar absorptivity ε as a function of wavelength is independent of concentration. This type of spectral plot is characteristic for a given molecule and is sometimes used to aid in identifying or confirming the identity of a particular species. The color of a solution is related to its absorption spectrum (see Feature 24-3).

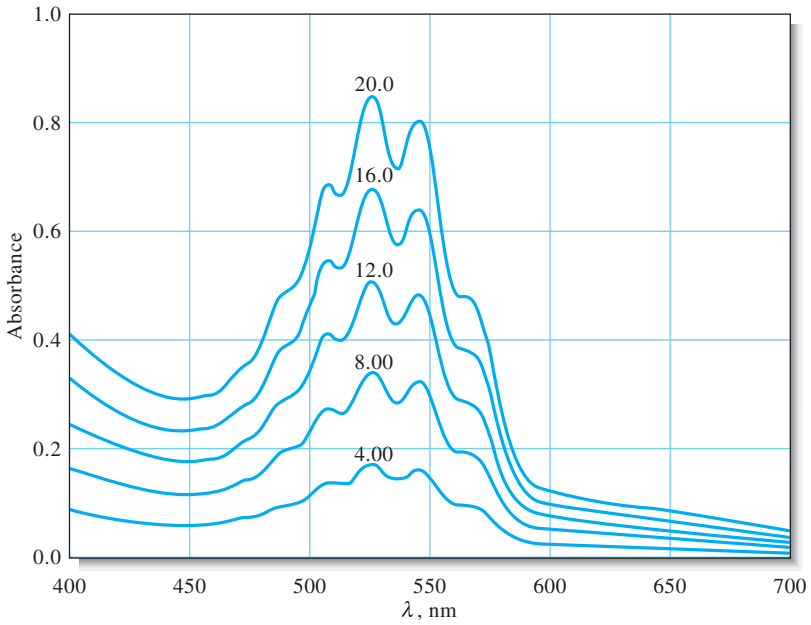

Figure 24-10 Typical absorption spectra of potassium permanganate at five different concentrations. The numbers adjacent to the curves indicate concentration of manganese in ppm, and the absorbing species is permanganate ion, MnO_4^-. The cell path length b is 1.00 cm. A plot of absorbance at the peak wavelength at 525 nm versus concentration of permanganate is linear and thus the absorber obeys Beer's law.

FEATURE 24-3

Why Is a Red Solution Red?

An aqueous solution of the complex $Fe(SCN)^{2+}$ is not red because the complex adds red radiation to the solvent. Instead, it absorbs green from the incoming white radiation and transmits the red component (see **Figure 24F-4**). Thus, in a colorimetric determination of iron based on its thiocyanate complex, the maximum change in absorbance with concentration occurs with green radiation; the absorbance change with red radiation is negligible. In general, then, the radiation used for a colorimetric analysis should be the complementary color of the analyte solution. The following table shows this relationship for various parts of the visible spectrum.

The Visible Spectrum

Wavelength Region Absorbed, nm	Color of Light Absorbed	Complementary Color Transmitted
400–435	Violet	Yellow-green
435–480	Blue	Yellow
480–490	Blue-green	Orange
490–500	Green-blue	Red
500–560	Green	Purple
560–580	Yellow-green	Violet
580–595	Yellow	Blue
595–650	Orange	Blue-green
650–750	Red	Green-blue

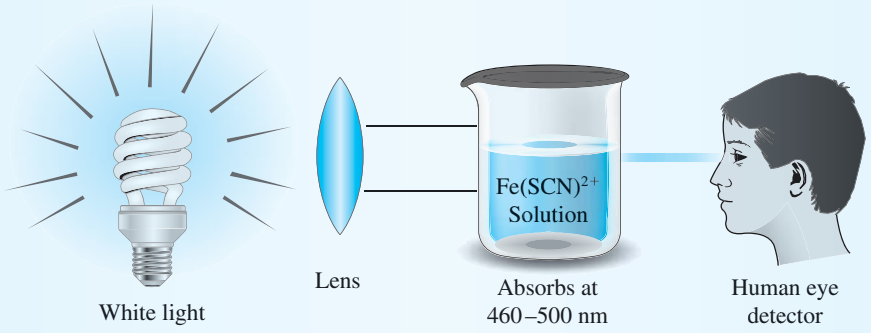

Figure 24F-4 Color of a solution. White light from a lamp or the sun strikes an aqueous solution of $Fe(SCN)^{2+}$. The fairly broad absorption spectrum shows a maximum absorbance in the 460 to 500 nm range (see Figure 26-4a). The complementary red color is transmitted.

Atomic Absorption

When a beam of polychromatic ultraviolet or visible radiation passes through a medium containing gaseous atoms, only a few frequencies are attenuated by absorption, and when recorded on a very high resolution spectrometer, the spectrum consists of a number of very narrow absorption lines.

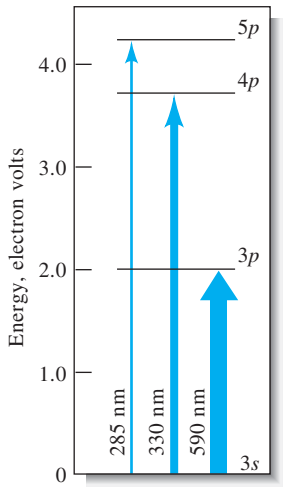

Figure 24-11 Partial energy level diagram for sodium, showing the transitions resulting from absorption at 590, 330, and 285 nm.

The **electron volt** (eV) is a unit of energy. When an electron with charge $q = 1.60 \times 10^{-19}$ coulombs is moved through a potential difference of 1 volt = 1 joule/coulomb, the energy expended (or released) is then equal to $E = qV = (1.60 \times 10^{-19}$ coulombs$)(1$ joule/coulomb$) = 1.60 \times 10^{-19}$ joule = 1 eV.

$$1 \text{ eV} = 1.60 \times 10^{-19} \text{ J} = 3.83 \times 10^{-20} \text{ calories} = 1.58 \times 10^{-21} \text{ L atm}$$

In an **electronic transition,** an electron moves from one orbital to another. Transitions occur between atomic orbitals in atoms and between molecular orbitals in molecules.

Vibrational and rotational transitions occur with polyatomic species because only this type of species has vibrational and rotational states with different energies.

The **ground state** of an atom or a molecular species is the minimum energy state of the species. At room temperature, most atoms and molecules are in their ground state.

Figure 24-11 is a partial energy level diagram for sodium that shows the major atomic absorption transitions. The transitions, shown as colored arrows between levels, occur when the single outer electron of sodium is excited from its room temperature or ground state 3*s* orbital to the 3*p*, 4*p*, and 5*p* orbitals. These excitations are brought on by absorption of photons of radiation whose energies exactly match the differences in energies between the excited states and the 3*s* ground state. Transitions between two different orbitals are termed **electronic transitions**. Atomic absorption spectra are not usually recorded because of instrumental difficulties. Instead, atomic absorption is measured at a single wavelength using a very narrow, nearly monochromatic source (see Section 28D).

EXAMPLE 24-4

The energy difference between the 3*p* and the 3*s* orbitals in Figure 24-11b is 2.107 eV. Calculate the wavelength of radiation that would be absorbed in exciting the 3*s* electron to the 3*p* state (1 eV = 1.60×10^{-19} J).

Solution

Rearranging Equation 24-3 gives

$$\lambda = \frac{hc}{E} = \frac{6.63 \times 10^{-34} \cancel{\text{J}}\cancel{\text{s}} \times 3.00 \times 10^{10} \cancel{\text{cm}}/\cancel{\text{s}} \times 10^{7} \text{ nm}/\cancel{\text{cm}}}{2.107 \cancel{\text{eV}} \times 1.60 \times 10^{-19} \text{ J}/\cancel{\text{eV}}} = 590 \text{ nm}$$

Molecular Absorption

Molecules undergo three types of quantized transitions when excited by ultraviolet, visible, and infrared radiation. For ultraviolet and visible radiation, excitation occurs when an electron residing in a low-energy molecular or atomic orbital is promoted to a higher-energy orbital. We mentioned previously that the energy $h\nu$ of the photon must be exactly the same as the energy difference between the two orbital energies.

In addition to electronic transitions, molecules exhibit two other types of radiation-induced transitions: **vibrational transitions** and **rotational transitions**. Vibrational transitions occur because a molecule has a multitude of quantized energy levels, or vibrational states, associated with the bonds that hold the molecule together.

Figure 24-12 is a partial energy level diagram that depicts some of the processes that occur when a polyatomic species absorbs infrared, visible, and ultraviolet radiation. The energies E_1 and E_2, two of the several electronically excited states of a molecule, are shown relative to the energy of the ground state E_0. In addition, the relative energies of a few of the many vibrational states associated with each electronic state are indicated by the lighter horizontal lines.

You can get an idea of the nature of vibrational states by picturing a bond in a molecule as a vibrating spring with atoms attached to both ends. In **Figure 24-13a**, two types of stretching vibration are shown. With each vibration, atoms first approach and then move away from one another. The potential energy of such a system at any instant depends on the extent to which the spring is stretched or compressed. For a real-world macroscopic spring, the energy of the system varies continuously and

reaches a maximum when the spring is fully stretched or fully compressed. In contrast, the energy of a spring system of atomic dimensions (a chemical bond) can have only certain discrete energies called vibrational energy levels.

Figure 24-13b shows four other types of molecular vibrations. The energies associated with these vibrational states usually differ from one another and from the energies associated with stretching vibrations. Some of the vibrational energy levels associated with each of the electronic states of a molecule are depicted by the lines labeled 1, 2, 3, and 4 in Figure 24-12 (the lowest vibrational levels are labeled 0). Note that the differences in energy among the vibrational states are significantly smaller than among energy levels of the electronic states (typically an order of magnitude smaller). Although they are not shown, a molecule has many quantized rotational states that are associated with the rotational motion of a molecule around its center of gravity. These rotational energy states are superimposed on each of the vibrational states shown in the energy diagram. The energy differences among these states are smaller than those among vibrational states by an order of magnitude and so are not shown in the diagram. The total energy E associated with a molecule is then given by

$$E = E_{\text{electronic}} + E_{\text{vibrational}} + E_{\text{rotational}} \qquad (24\text{-}15)$$

where $E_{\text{electronic}}$ is the energy associated with the electrons in the various outer orbitals of the molecule, $E_{\text{vibrational}}$ is the energy of the molecule as a whole due to interatomic vibrations, and $E_{\text{rotational}}$ accounts for the energy associated with rotation of the molecule about its center of gravity.

Infrared Absorption. Infrared radiation generally is not energetic enough to cause electronic transitions, but it can induce transitions in the vibrational and rotational states associated with the ground electronic state of the molecule. Four of these

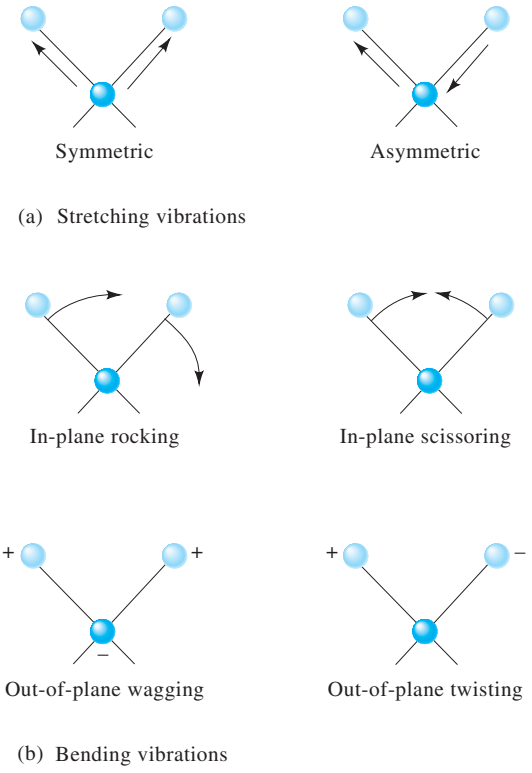

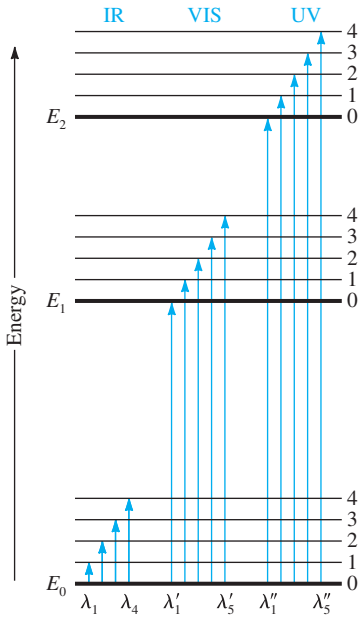

Figure 24-12 Energy level diagram showing some of the energy changes that occur during absorption of infrared (IR), visible (VIS), and ultraviolet (UV) radiation by a molecular species. Note that with some molecules a transition from E_0 to E_1 may require UV radiation instead of visible radiation. With other molecules, the transition from E_0 to E_2 may occur with visible radiation instead of UV radiation. Only a few vibrational levels (0–4) are shown. The rotational levels associated with each vibrational level are not shown because they are too closely spaced.

Figure 24-13 Types of molecular vibrations. The plus sign indicates motion out of the page; the minus sign indicates motion into the page.

transitions are depicted in the lower left part of Figure 24-12 (λ_1 to λ_4). For absorption to occur, the radiation source has to emit frequencies corresponding exactly to the energies indicated by the lengths of the four arrows.

Absorption of Ultraviolet and Visible Radiation. The center arrows in Figure 24-12 suggest that the molecules under consideration absorb visible radiation of five wavelengths (λ_1' to λ_5'), thereby promoting electrons to the five vibrational levels of the excited electronic level E_1. Ultraviolet photons that are more energetic are required to produce the absorption indicated by the five arrows to the right.

Figure 24-12 suggests that molecular absorption in the ultraviolet and visible regions produces **absorption bands** made up of closely spaced lines. A real molecule has many more energy levels than can be shown in the diagram. Thus, a typical absorption band consists of a large number of lines. In a solution, the absorbing species are surrounded by solvent molecules, and the band nature of molecular absorption often becomes blurred because collisions tend to spread the energies of the quantum states, giving smooth and continuous absorption peaks.

Figure 21-14 shows visible spectra for 1,2,4,5-tetrazine that were obtained under three different conditions: gas phase, nonpolar solvent, and polar solvent (aqueous solution). Notice that in the gas phase (see Figure 24-14a), the individual tetrazine molecules are sufficiently separated from one another to vibrate and rotate freely so that many individual absorption peaks resulting from transitions among the various vibrational and rotational states appear in the spectrum. In the liquid state and in nonpolar solvents (see Figure 24-14b), however, tetrazine molecules are unable to rotate freely so that we see no fine structure in the spectrum. Furthermore, in a polar solvent such as water (see Figure 24-14c), frequent collisions and interactions between tetrazine and water molecules cause the vibrational levels to be modified

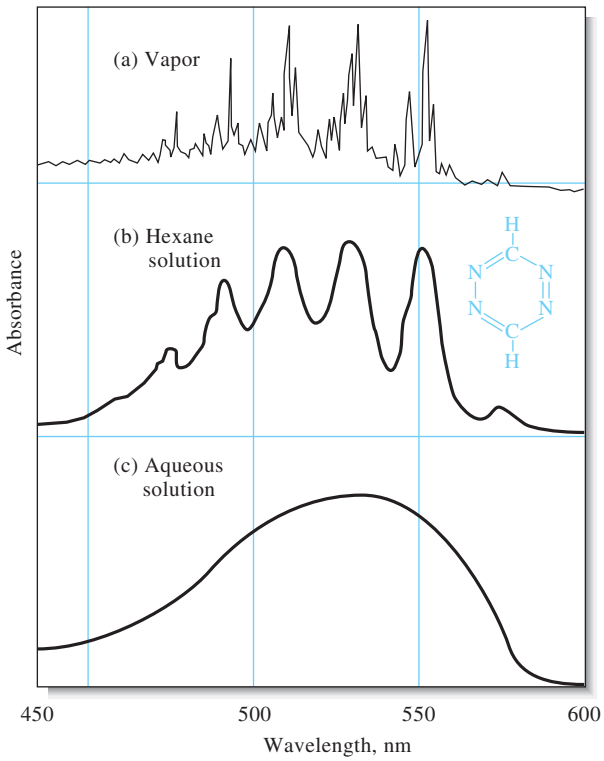

Figure 24-14 Typical visible absorption spectra. The compound is 1,2,4,5-tetrazine. In (a), the spectrum is shown in the gas phase where many lines due to electronic, vibrational, and rotational transitions are seen. In a nonpolar solvent (b), the electronic transitions can be observed, but the vibrational and rotational structure has been lost. In a polar solvent (c), the strong intermolecular forces have caused the electronic peaks to blend together to give only a single smooth absorption peak. (Reproduced from S. F. Mason, *J. Chem. Soc.*, **1959**, 1263, **DOI**: 10.1039/JR9590001263, with permission of The Royal Society of Chemistry.)

energetically in an irregular way. Hence, the spectrum appears as a single broad peak. The trends shown in the spectra of tetrazine in this figure are typical of UV-visible spectra of other molecules recorded under similar conditions.

24C-3 Limits to Beer's Law

There are few exceptions to the linear relationship between absorbance and path length at a fixed concentration. We frequently observe deviations from the direct proportionality between absorbance and concentration, however, when the path length b is a constant. Some of these deviations, called **real deviations**, are fundamental and represent real limitations to the law. Others are a result of the method that we use to measure absorbance (**instrumental deviations**) or from chemical changes that occur when the concentration changes (**chemical deviations**).

Real Limitations to Beer's Law

Beer's law describes the absorption behavior only of dilute solutions and in this sense is a **limiting law**. At concentrations exceeding about 0.01 M, the average distances between ions or molecules of the absorbing species are diminished to the point where each particle affects the charge distribution and thus the extent of absorption of its neighbors. Because the extent of interaction depends on concentration, the occurrence of this phenomenon causes deviations from the linear relationship between absorbance and concentration. A similar effect sometimes occurs in dilute solutions of absorbers that contain high concentrations of other species, particularly electrolytes. When ions are very close to one another, the molar absorptivity of the analyte can be altered because of electrostatic interactions which can lead to departures from Beer's law.

Limiting laws in science are those that hold under limiting conditions such as dilute solutions. In addition to Beer's law, the Debye-Hückel law (see Chapter 10) and the law of independent migration that describes the conductance of electricity by ions are limiting laws.

Chemical Deviations

As shown in Example 24-5, deviations from Beer's law appear when the absorbing species undergoes association, dissociation, or reaction with the solvent to give products that absorb differently from the analyte. The extent of such departures can be predicted from the molar absorptivities of the absorbing species and the equilibrium constants for these equilibria. Unfortunately, since we are usually unaware that such processes are affecting the analyte, there is often no opportunity to correct the measurement. Typical equilibria that give rise to this effect include monomer-dimer equilibria, metal complexation equilibria where more than one complex is present, acid/base equilibria, and solvent-analyte association equilibria.

EXAMPLE 24-5

Solutions containing various concentrations of the acidic indicator HIn with $K_a = 1.42 \times 10^{-5}$ were prepared in 0.1 M HCl and 0.1 M NaOH. In both media, plots of absorbance at either 430 nm or 570 nm versus the total indicator concentration are nonlinear. However, in both media, the individual species HIn or In^- obey Beer's law at 430 nm and 570 nm. Hence, if we knew the equilibrium concentrations of HIn and In^-, we could compensate for the fact that dissociation of HIn occurs. Usually, though, the individual concentrations are unknown, and only the total concentration $c_{total} = [HIn] + [In^-]$ is known. Let us now calculate the absorbance for a solution with $c_{total} = 2.00 \times 10^{-5}$ M. The magnitude of the

(*continued*)

acid dissociation constant suggests that, for all practical purposes, the indicator is entirely in the undissociated form (HIn) in the HCl solution and completely dissociated as In^- in NaOH. The molar absorptivities at the two wavelengths were found to be

	ε_{430}	ε_{570}
HIn (HCl solution)	6.30×10^2	7.12×10^3
In^- (NaOH solution)	2.06×10^4	9.60×10^2

We would now like to find the absorbances (1.00-cm cell) of unbuffered solutions of the indicator ranging in concentration from 2.00×10^{-5} M to 16.00×10^{-5} M. Let us first find the concentration of HIn and In^- in the unbuffered 2×10^{-5} M solution. From the equation for the dissociation reaction, we know that $[H^+] = [In^-]$. Furthermore, the mass-balance expression for the indicator tells us that $[In^-] + [HIn] = 2.00 \times 10^{-5}$ M. By substituting these relationships into the K_a expression, we find that

$$\frac{[In^-]^2}{2.00 \times 10^{-5} - [In^-]} = 1.42 \times 10^{-5}$$

This equation can be solved to give $[In^-] = 1.12 \times 10^{-5}$ M and $[HIn] = 0.88 \times 10^{-5}$ M. The absorbances at the two wavelengths are found by substituting the values for ε, b, and c into Equation 24-13 (Beer's Law). The result is that $A_{430} = 0.236$ and $A_{570} = 0.073$. We could similarly calculate A for several other values of c_{total}. Additional data, obtained in the same way, are shown in **Table 24-4**. **Figure 24-15** shows plots at the two wavelengths that were constructed from data obtained in a similar manner.

CHALLENGE: Perform calculations to confirm that $A_{430} = 0.596$ and $A_{570} = 0.401$ for a solution in which the analytical concentration of HIn is 8.00×10^{-5} M.

The plots of Figure 24-15 illustrate the kinds of departures from Beer's law that occur when the absorbing system undergoes dissociation or association. Notice that the direction of curvature is opposite at the two wavelengths.

TABLE 24-4

Absorbance Data for Several Concentrations of the Indicator in Example 24-5

c_{Hin}, M	[HIn]	$[In^-]$	A_{430}	A_{570}
2.00×10^{-5}	0.88×10^{-5}	1.12×10^{-5}	0.236	0.073
4.00×10^{-5}	2.22×10^{-5}	1.78×10^{-5}	0.381	0.175
8.00×10^{-5}	5.27×10^{-5}	2.73×10^{-5}	0.596	0.401
12.0×10^{-5}	8.52×10^{-5}	3.48×10^{-5}	0.771	0.640
16.0×10^{-5}	11.9×10^{-5}	4.11×10^{-5}	0.922	0.887

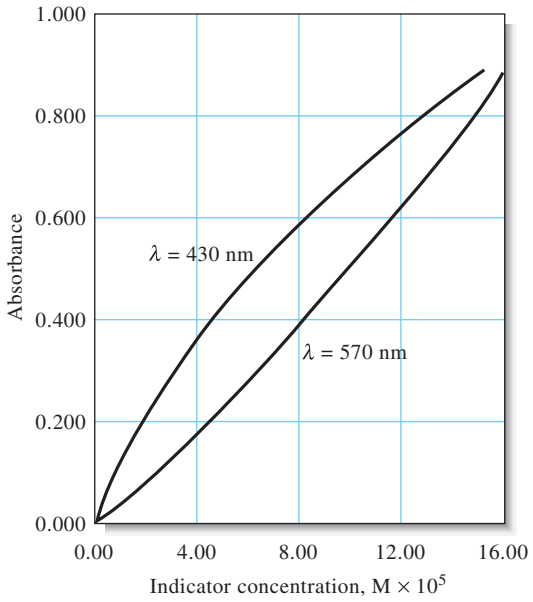

Figure 24-15 Chemical deviations from Beer's law for unbuffered solutions of the indicator HIn. The absorbance values were calculated at various indicator concentrations, as shown in Example 24-5. Note that there are positive deviations at 430 nm and negative deviations at 570 nm. At 430 nm, the absorbance is primarily due to the ionized In^- form of the indicator and is in fact proportional to the fraction ionized. The fraction ionized varies nonlinearly with total concentration. At lower total concentrations ([HIn] + [In^-]), the fraction ionized is larger than at high total concentrations. Hence, a positive error occurs. At 570 nm, the absorbance is due principally to the undissociated acid HIn. The fraction in this form begins as a low amount and increases nonlinearly with the total concentration, giving rise to the negative deviation shown.

Instrumental Deviations: Polychromatic Radiation

Deviations from Beer's law often occur when polychromatic radiation is used to measure absorbance.

Beer's law strictly applies only when measurements are made with monochromatic source radiation. In practice, polychromatic sources that have a continuous distribution of wavelengths are used in conjunction with a grating or a filter to isolate a nearly symmetric band of wavelengths surrounding the wavelength to be employed (see Chapter 25, Section 25A-3).

The following derivation shows the effect of polychromatic radiation on Beer's law. Consider a beam of radiation consisting of just two wavelengths λ' and λ''. Assuming that Beer's law applies strictly for each wavelength, we may write for λ'

$$A' = \log \frac{P_0'}{P'} = \varepsilon' bc$$

or

$$\frac{P_0'}{P'} = 10^{\varepsilon' bc}$$

where P_0' is the incident power and P' is the resultant power at λ'. The symbols b and c are the path length and concentration of the absorber, and ε' is the molar absorptivity at λ'. Then,

$$P' = P_0' 10^{-\varepsilon' bc}$$

Similarly, for λ'',

$$P'' = P_0'' 10^{-\varepsilon'' bc}$$

When an absorbance measurement is made with radiation composed of both wavelengths, the power of the beam emerging from the solution is the sum of the powers

emerging at the two wavelengths $P' + P''$. Likewise, the total incident power is the sum $P_0' + P_0''$. Therefore, the measured absorbance A_m is

$$A_m = \log\left(\frac{P_0' + P_0''}{P' + P''}\right)$$

We then substitute for P' and P'' and find that

$$A_m = \log\left(\frac{P_0' + P_0''}{P_0' 10^{-\varepsilon' bc} + P_0'' 10^{-\varepsilon'' bc}}\right)$$

or

$$A_m = \log(P_0' + P_0'') - \log(P_0' 10^{-\varepsilon' bc} + P_0'' 10^{-\varepsilon'' bc})$$

We see that, when $\varepsilon' = \varepsilon''$, this equation simplifies to

$$\begin{aligned} A_m &= \log(P_0' + P_0'') - \log[(P_0' + P_0'')(10^{-\varepsilon' bc})] \\ &= \log(P_0' + P_0'') - \log(P_0' + P_0'') - \log(10^{-\varepsilon' bc}) \\ &= \varepsilon' bc = \varepsilon'' bc \end{aligned}$$

High-quality spectrophotometers produce narrow bands of radiation and are less likely to suffer deviations from Beer's law due to polychromatic radiation than low-quality instruments.

Polychromatic light, literally multicolored light, is light of many wavelengths, such as that from a tungsten light bulb. Light that is essentially monochromatic can be produced by filtering, diffracting, or refracting polychromatic light, as discussed in Chapter 25, Section 25A-3.

and Beer's law is followed. As shown in **Figure 24-16**, however, the relationship between A_m and concentration is no longer linear when the molar absorptivities differ. In addition, as the difference between ε' and ε'' increases, the deviation from linearity increases. When this derivation is expanded to include additional wavelengths, the effect remains the same.

If the band of wavelengths selected for spectrophotometric measurements corresponds to a region of the absorption spectrum in which the molar absorptivity of the analyte is essentially constant, departures from Beer's law will be minimal. Many molecular bands in the UV/visible region of the spectrum fit this description. For these bands, Beer's law is obeyed, as demonstrated by Band *A* in **Figure 24-17**. On the other hand, some absorption bands in the UV-visible region and many in the IR region are very narrow, and departures from Beer's law are common, as illustrated for Band *B* in Figure 24-17. To avoid such deviations, it is best to select a wavelength

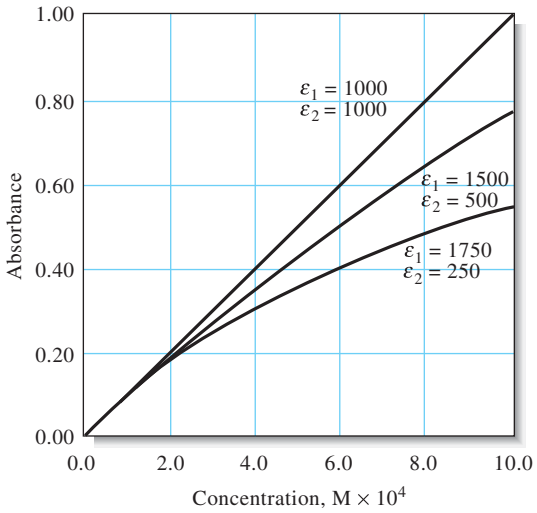

Figure 24-16 Deviations from Beer's law with polychromatic radiation. The absorber has the indicated molar absorptivities at the two wavelengths λ' and λ''.

band near the wavelength of maximum absorption where the analyte absorptivity changes little with wavelength. Atomic absorption lines are so narrow that they require special sources to obtain adherence to Beer's law as discussed in Chapter 25, Section 25A-2.

Instrumental Deviations: Stray Light

Stray radiation, commonly called **stray light**, is defined as radiation from the instrument that is outside the nominal wavelength band chosen for the determination. This stray radiation often is the result of scattering and reflection off the surfaces of gratings, lenses or mirrors, filters, and windows. When measurements are made in the presence of stray light, the observed absorbance A' is given by

$$A' = \log\left(\frac{P_0 + P_s}{P + P_s}\right)$$

where P_s is the radiant power of the stray light. **Figure 24-18** shows a plot of the apparent absorbance A' versus concentration for various levels of P_s, relative to P_0. Stray light always causes the apparent absorbance to be lower than the true absorbance. The deviations due to stray light are most significant at high absorbance values. Because stray radiation levels can be as high as 0.5% in modern instruments, absorbance levels above 2.0 are rarely measured unless special precautions are taken or special instruments with extremely low stray light levels are used. Some inexpensive filter instruments show deviations from Beer's law at absorbances as low as 1.0 because of high stray light levels and/or the presence of polychromatic light.

Mismatched Cells

Another almost trivial, but important, deviation from adherence to Beer's law is caused by mismatched cells. If the cells holding the analyte and blank solutions are not of equal path length and equivalent in optical characteristics, an intercept will occur in the calibration curve, and $A = \varepsilon bc + k$ will be the equation for the

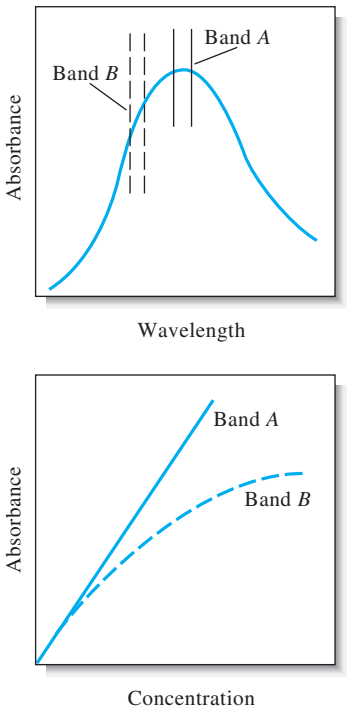

Figure 24-17 The effect of polychromatic radiation on Beer's law. In the absorption spectrum at the top, the absorptivity of the analyte is seen to be nearly constant over Band *A* from the source. Note in the Beer's law plot at the bottom that using Band *A* gives a linear relationship. In the spectrum, band *B* coincides with a region of the spectrum over which the absorptivity of the analyte changes. Note the dramatic deviation from Beer's law that results in the lower plot.

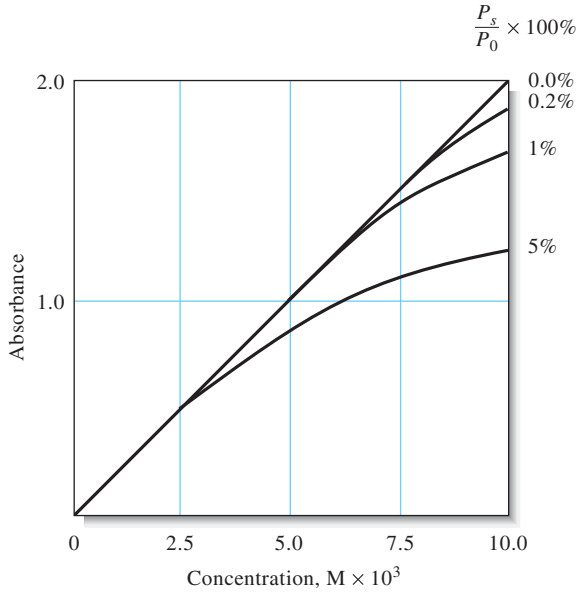

Figure 24-18 Deviation from Beer's law caused by various levels of stray light. Note that absorbance begins to level off with concentration at high stray light levels. Stray light always limits the maximum absorbance that can be obtained because, when the absorbance is high, the radiant power transmitted through the sample can become comparable to or lower than the stray light level.

curve instead of Equation 24-8. This error can be avoided either by using carefully matched cells or by using a linear regression procedure to calculate both the slope and intercept of the calibration curve. In most cases, linear regression is the best strategy because an intercept can also occur if the blank solution does not totally compensate for interferences. Another way to avoid the mismatched-cell problem with single beam instruments is to use only one cell and keep it in the same position for both blank and analyte measurements. After obtaining the blank reading, the cell is emptied by aspiration, washed, and filled with analyte solution.

Spreadsheet Summary In Chapter 12 of *Applications of Microsoft® Excel in Analytical Chemistry,* 2nd ed., spreadsheets are presented for modeling the effects of chemical equilibria and stray light on absorption measurements. Chemical and physical variables may be changed to observe their effects on instrument readouts.

24D EMISSION OF ELECTROMAGNETIC RADIATION

Chemical species can be caused to emit light by (1) bombardment with electrons; (2) heating in a plasma, flame, or an electric arc; or (3) irradiation with a beam of light.

Atoms, ions, and molecules can be excited to one or more higher energy levels by any of several processes, including bombardment with electrons or other elementary particles; exposure to a high-temperature plasma, flame, or electric arc; or exposure to a source of electromagnetic radiation. The lifetime of an excited species is generally transitory (10^{-9} to 10^{-6} s), and relaxation to a lower energy level or the ground state takes place with a release of the excess energy in the form of electromagnetic radiation, heat, or perhaps both.

24D-1 Emission Spectra

Radiation from a source is conveniently characterized by means of an emission spectrum, which usually takes the form of a plot of the relative power of the emitted radiation as a function of wavelength or frequency. **Figure 24-19** illustrates a typical emission spectrum, which was obtained by aspirating a brine solution into an oxyhydrogen flame. Three types of spectra are superimposed in the figure: a **line spectrum**, a **band spectrum**, and a **continuum spectrum**. The line spectrum, marked lines in Figure 24-19, consists of a series of sharp, well-defined spectral lines caused by excitation of individual atoms. The band spectrum, marked bands, is comprised of several groups of lines so closely spaced that they are not completely resolved. The source of the bands is small molecules or radicals in the source flame. Finally, the continuum spectrum, shown as a green dashed line in the figure, is responsible for the increase in the background that appears above about 350 nm. The line and band spectra are superimposed on this continuum. The source of the continuum is described on page 677.

The line widths of atoms in a medium such as a flame or plasma are about 0.1–0.01 Å. The wavelengths of atomic lines are unique for each element and are often used for qualitative analysis.

Line Spectra

Line spectra occur when the radiating species are individual atoms or ions that are well separated, as in a gas. The individual particles in a gaseous medium behave independently of one another, and the spectrum in most media consists of a series of sharp lines with widths of 10^{-1}–10^{-2} Å (10^{-2}–10^{-3} nm). In Figure 24-19, lines for sodium, potassium, strontium, calcium, and magnesium are identified.

The energy level diagram in **Figure 24-20** shows the source of three of the lines that appear in the emission spectrum of Figure 24-19. The horizontal line labeled 3*s* in Figure 24-20 corresponds to the lowest, or ground state, energy of the atom E_0. The horizontal lines labeled 3*p,* 4*p,* and 4*d* are three higher-energy electronic levels

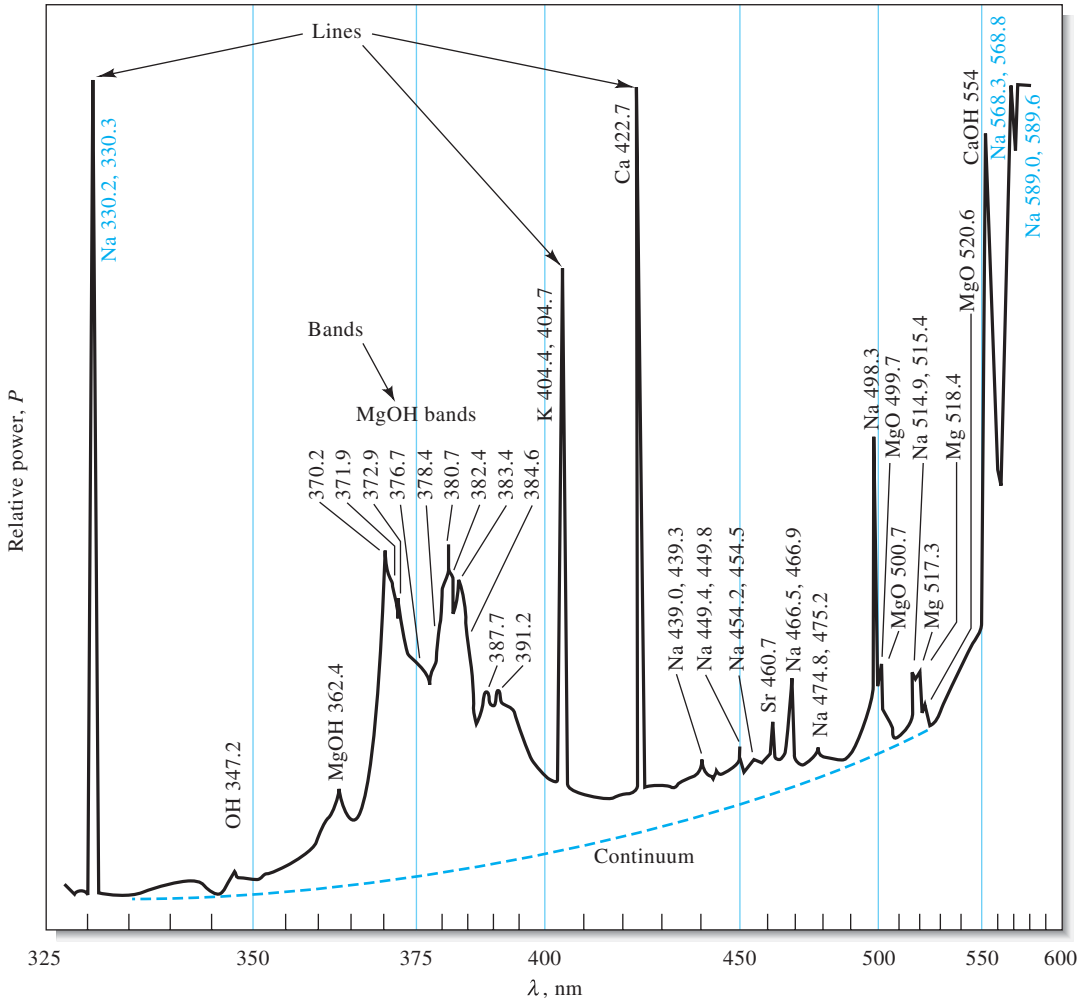

Figure 24-19 Emission spectrum of a brine sample obtained with an oxyhydrogen flame. The spectrum consists of the superimposed line, band, and continuum spectra of the constituents of the sample and flame. The characteristic wavelengths of the species contributing to the spectrum are listed beside each feature. (R. Hermann and C. T. J. Alkemade, *Chemical Analysis by Flame Photometry,* 2nd ed., New York: Interscience, 1979, p. 484.)

of sodium. Note that each of the *p* and *d* states are split into two closely spaced energy levels as a result of electron spin. The single outer shell electron in the ground state 3*s* orbital of a sodium atom can be excited into either of these levels by absorption of thermal, electrical, or radiant energy. Energy levels E_{3p} and E'_{3p} then represent the energies of the atom when this electron has been promoted to the two 3*p* states by absorption. The promotion to these states is depicted by the green line between the 3*s* and the two 3*p* levels in Figure 24-20. A few nanoseconds after excitation, the electron returns from the 3*p* state to the ground state, emitting a photon whose wavelength is given by Equation 24-3.

$$\lambda_1 = \frac{hc}{(E_{3p} - E_0)} = 589.6 \text{ nm}$$

In a similar way, relaxation from the 3*p*′ state to the ground state yields a photon with $\lambda_2 = 589.0$ nm. This emission process is once again shown by the green line between the 3*s* and 3*p* levels in Figure 24-20. The result is that the emission process from the two closely spaced 3*p* levels produces two corresponding closely spaced lines

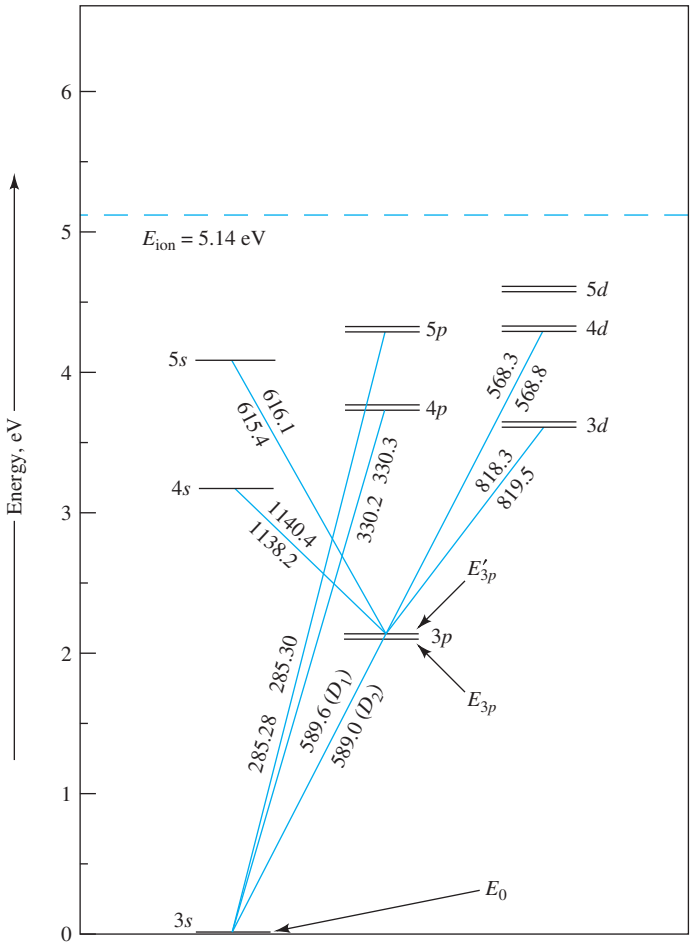

Figure 24-20 Energy level diagram for sodium in which the horizontal lines represent the atomic orbitals, which are identified with their respective labels. The vertical scale is orbital energy in electron volts (eV), and the energies of excited states relative to the ground state 3*s* orbital can be read from the vertical axis. The lines in color show the allowed transitions resulting in emission of various wavelengths (in nm), indicated adjacent to the lines. The horizontal dashed line represents the ionization energy of sodium. (INGLE, JAMES D., CROUCH, STANLEY R., *SPECTROCHEMICAL ANALYSIS*, 1st Edition, © 1988, p.206. Reprinted by permission of Pearson Education, Inc., Upper Saddle River, NJ.)

in the emission spectrum called a **doublet**. These lines, indicated by the transitions labeled D_1 and D_2 in Figure 24-20, are the famous Fraunhofer "D" lines discussed in Feature 24-1. They are so intense that they are completely off scale in the upper right corner of the emission spectrum of Figure 24-19.

The transition from the more energetic 4*p* state to the ground state (see Figure 24-20) produces a second doublet at a shorter wavelength. The line appearing at about 330 nm in Figure 24-19 results from these transitions. The 4*d*-to-3*p* transition provides a third doublet at about 568 nm. Notice that all three of these doublets appear in the emission spectrum of Figure 24-19 as just single lines. This is a result of the limited resolution of the spectrometer used to produce the spectrum, as discussed in Sections 25A-3 and 28A-4. It is important to note that the emitted wavelengths are identical to the wavelengths of the absorption peaks for sodium (see Figure 24-11) because the transitions are between the same pairs of states.

At first glance, it may appear that radiation could be absorbed and emitted by atoms between any pair of the states shown in Figure 24-20, but in fact, only certain transitions are allowed, while others are forbidden. The transitions that are allowed and forbidden to produce lines in the atomic spectra of the elements are determined by the laws of quantum mechanics in what are called **selection rules**. These rules are beyond the scope of our discussion.[4]

[4]See J. D. Ingle, Jr., and S. R. Crouch, *Spectrochemical Analysis,* Upper Saddle River, NJ: Prentice-Hall, 1988, p. 205.

Band Spectra

An emission band spectrum is made up of many closely spaced lines that are difficult to resolve.

Band spectra are often produced in spectral sources because of the presence of gaseous radicals or small molecules. For example, in Figure 24-19, bands for OH, MgOH, and MgO are labeled and consist of a series of closely spaced lines that are not fully resolved by the instrument used to obtain the spectrum. Bands arise from the numerous quantized vibrational levels that are superimposed on the ground state electronic energy level of a molecule. For further discussion of band spectra, see Section 28B-3.

Continuum Spectrum

A spectral continuum has no line character and is generally produced by heating solids to a high temperature.

As shown in **Figure 24-21**, a spectral continuum of radiation is produced when solids such as carbon and tungsten are heated to incandescence. Thermal radiation of this kind, which is called **blackbody radiation**, is more characteristic of the temperature of the emitting surface than of its surface material. Blackbody radiation is produced by the innumerable atomic and molecular oscillations excited in the condensed solid by the thermal energy. Note that the energy peaks in Figure 24-21 shift to shorter wavelengths with increasing temperature. As the figure shows, very high temperatures are required to cause a thermally excited source to emit a substantial fraction of its energy as ultraviolet radiation.

Part of the continuum background radiation in the flame spectrum shown in Figure 24-19 is probably thermal emission from incandescent particles in the flame. Note that this background decreases rapidly as the wavelength approaches the ultraviolet region of the spectrum.

Heated solids are important sources of infrared, visible, and longer-wavelength ultraviolet radiation for analytical instruments, as we will see in Chapter 25.

Effect of Concentration on Line and Band Spectra

The radiant power P of a line or a band depends directly on the number of excited atoms or molecules, which in turn is proportional to the total concentration c of the species present in the source. Thus, we can write

$$P = kc \tag{24-16}$$

where k is a proportionality constant. This relationship is the basis of quantitative emission spectroscopy, which is described in some detail in Section 28C.

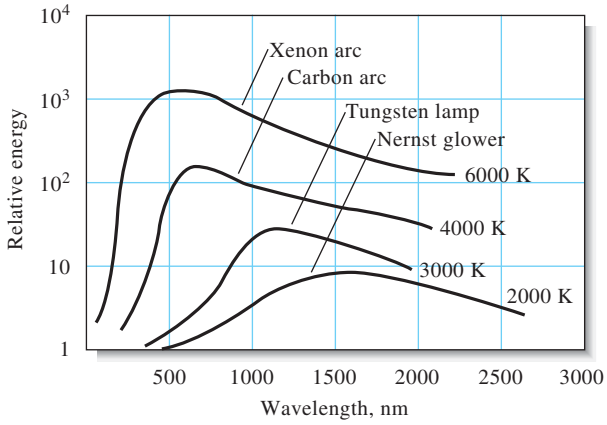

Figure 24-21 Blackbody radiation curves for various light sources. Note the shift in the wavelengths of maximum emission as the temperature of the sources changes.

In 1900, Max Planck (1858–1947) discovered a formula (now often called the Planck radiation law) that modeled curves like those shown in Figure 24-21 nearly perfectly. He followed this discovery by developing a theory that made two bold assumptions regarding the oscillating atoms or molecules in blackbody radiators. He assumed (1) that these species could have only discrete energies and (2) that they could absorb or emit energy in discrete units, or quanta. These assumptions, which are implicit in Equation 24-3, laid the foundation for the development of quantum theory.

Resonance fluorescence is radiation that is identical in wavelength to the radiation that excited the fluorescence.

24D-2 Emission by Fluorescence and Phosphorescence

Fluorescence and phosphorescence are analytically important emission processes in which atoms or molecules are excited by the absorption of a beam of electromagnetic radiation. The excited species then relax to the ground state, giving up their excess energy as photons. Fluorescence takes place much more rapidly than phosphorescence and is generally complete in 10^{-5} s or less from the time of excitation. Phosphorescence emission may extend for minutes or even hours after irradiation has ceased. Fluorescence is considerably more important than phosphorescence in analytical chemistry, so our discussions focus primarily on fluorescence.

Atomic Fluorescence

Gaseous atoms fluoresce when they are exposed to radiation that has a wavelength that exactly matches that of one of the absorption (or emission) lines of the element in question. For example, gaseous sodium atoms are promoted to the excited energy state, E_{3p}, shown in Figure 24-20 through absorption of 589-nm radiation. Relaxation may then take place by reemission of radiation of the identical wavelength. When excitation and emission wavelengths are the same, the resulting emission is called **resonance fluorescence**. Sodium atoms could also exhibit resonance fluorescence when exposed to 330-nm or 285-nm radiation. In addition, however, the element could also produce nonresonance fluorescence by first relaxing from E_{5p} or E_{4p} to energy level E_{3p} through a series of nonradiative collisions with other species in the medium. Further relaxation to the ground state can then take place either by the emission of a 589-nm photon or by further collisional deactivation.

Molecular Fluorescence

Fluorescence is a photoluminescence process in which atoms or molecules are excited by absorption of electromagnetic radiation, as shown in **Figure 24-22a**. The excited species then relax back to the ground state, giving up their excess energy as photons. As we have noted, the lifetime of an excited species is brief because there are several mechanisms for an excited atom or molecule to give up its excess energy and relax to its ground state. Two of the most important of these mechanisms, **nonradiative relaxation** and **fluorescence emission**, are illustrated in **Figures 24-22b** and **c**.

Nonradiative Relaxation. Two types of nonradiative relaxation are shown in Figure 24-22b. **Vibrational deactivation**, or **relaxation**, depicted by the short wavy arrows between vibrational energy levels, takes place during collisions between excited molecules and molecules of the solvent. During the collisions, the excess vibrational energy is transferred to solvent molecules in a series of steps as indicated in the figure. The gain in vibrational energy of the solvent is reflected in a tiny increase in the temperature of the medium. Vibrational relaxation is such an efficient process that the average lifetime of an excited vibrational state is only about 10^{-15} s. Nonradiative relaxation between the lowest vibrational level of an excited electronic state and the upper vibrational level of another electronic state can also occur. This type of relaxation, which is called **internal conversion**, depicted by the two longer wavy arrows in Figure 24-22b, is much less efficient than vibrational relaxation so that the average lifetime of an electronic excited state is between 10^{-9} and 10^{-6} s. The mechanisms by which this type of relaxation occurs are not fully understood, but the net effect is again a very small rise in the temperature of the medium.

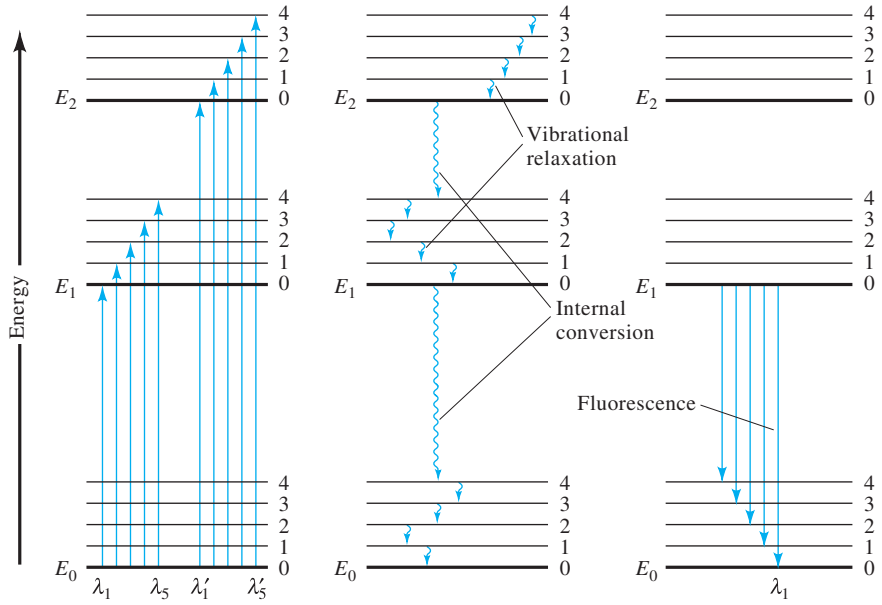

Figure 24-22 Energy level diagram showing some of the energy changes that occur during absorption, nonradiative relaxation, and fluorescence by a molecular species.

Fluorescence. The relative number of molecules that fluoresce is small because fluorescence requires structural features that slow the rate of the nonradiative relaxation processes illustrated in Figure 24-22b and enhance the rate of fluorescence emission shown in Figure 24-22c. Most molecules lack these features and undergo nonradiative relaxation at a rate that is significantly greater than the radiative relaxation rate, and so fluorescence does not occur. As shown in Figure 24-22c, bands of radiation are produced when molecules relax from the lowest-lying vibrational state of an excited state, E_1, to the many vibrational levels of the ground state, E_0. Like molecular absorption bands, molecular fluorescence bands are made up of a large number of closely spaced lines that are usually difficult to resolve. Notice that the transition from E_1 to the lowest-lying vibrational state of the ground state (λ_1) has the highest energy of all of the transitions in the band. As a result, all of the other lines that terminate in higher vibrational levels of the ground state are lower in energy and produce fluorescence emission at longer wavelengths than λ_1. In other words, molecular fluorescence bands consist largely of lines that are longer in wavelength than the band of absorbed radiation responsible for their excitation. This shift in wavelength is called the **Stokes shift**. A more detailed discussion of molecular fluorescence is given in Chapter 27.

The **Stokes shift** refers to fluorescence radiation that occurs at wavelengths that are longer than the wavelength of radiation used to excite the fluorescence.

WEB WORKS

To learn more about Beer's law, use a search engine to find the IUPAC "Glossary of Terms Used in Photochemistry." Find how the molar absorptivity (the IUPAC "Glossary" uses **molar absorption coefficient**) of a compound (ε) relates to the absorption cross section (σ). Multiply the absorption cross section by Avogadro's number and note the result. How would the result change if absorbance were expressed as $A = -\ln(P/P_0)$ rather than the usual definition in terms of base 10 logarithms? What are the units of σ? Which of the quantities ε or σ is a macroscopic quantity? Which of the terms, molar absorptivity or molar absorption coefficient, is most descriptive? Explain and justify your answer.

QUESTIONS AND PROBLEMS

*24-1. In a solution of pH 5.3, the indicator bromocresol purple exhibits a yellow color, but when the pH is 6.0, the indicator solution changes to purple. Discuss why these colors are observed in terms of the wavelength regions and colors absorbed and transmitted.

24-2. What is the relationship between
*(a) absorbance and transmittance?
(b) absorptivity a and molar absorptivity ε?

*24-3. Identify factors that cause the Beer's law relationship to be nonlinear.

24-4. Describe the differences between "real" deviations from Beer's law and those due to instrumental or chemical factors.

24-5. How does an electronic transition resemble a vibrational transition? How do they differ?

24-6. Calculate the frequency in hertz of
*(a) an X-ray beam with a wavelength of 2.65 Å.
(b) an emission line for copper at 211.0 nm.
*(c) the line at 694.3 nm produced by a ruby laser.
(d) the output of a CO_2 laser at 10.6 μm.
*(e) an infrared absorption peak at 19.6 μm.
(f) a microwave beam at 1.86 cm.

24-7. Calculate the wavelength in centimeters of
*(a) an airport tower transmitting at 118.6 MHz.
(b) a VOR (radio navigation aid) transmitting at 114.10 kHz.
*(c) an NMR signal at 105 MHz.
(d) an infrared absorption peak with a wavenumber of 1210 cm^{-1}.

24-8. A sophisticated ultraviolet/visible/near-IR instrument has a wavelength range of 185 to 3000 nm. What are its wavenumber and frequency ranges?

*24-9. A typical simple infrared spectrophotometer covers a wavelength range from 3 to 15 μm. Express its range (a) in wavenumbers and (b) in hertz.

24-10. Calculate the frequency in hertz and the energy in joules of an X-ray photon with a wavelength of 2.70 Å.

*24-11. Calculate the wavelength and the energy in joules associated with a signal at 220 MHz.

24-12. Calculate the wavelength of
*(a) the sodium line at 589 nm in an aqueous solution with a refractive index of 1.35.
(b) the output of a ruby laser at 694.3 nm when it is passing through a piece of quartz that has a refractive index of 1.55.

24-13. What are the units for absorptivity when the path length is given in centimeters and the concentration is expressed in
*(a) parts per million?
(b) micrograms per liter?
*(c) mass-volume percent?
(d) grams per liter?

24-14. Express the following absorbances in terms of percent transmittance
*(a) 0.0356
(b) 0.895
*(c) 0.379
(d) 0.167
*(e) 0.485
(f) 0.753

24-15. Convert the accompanying transmittance data to absorbances.
*(a) 27.2%
(b) 0.579
*(c) 30.6%
(d) 3.98%
*(e) 0.093
(f) 63.7%

24-16. Calculate the percent transmittance of solutions that have twice the absorbance of the solutions in Problem 24-14.

24-17. Calculate the absorbances of solutions with half the transmittance of those in Problem 24-15.

24-18. Evaluate the missing quantities in the accompanying table. Where needed, use 200 for the molar mass of the analyte.

			ε	a	b	c	
	A	$\%T$	L mol^{-1} cm^{-1}	cm^{-1} ppm^{-1}	cm	M	ppm
*(a)	0.172		4.23×10^3		1.00		
(b)		44.9		0.0258		1.35×10^{-4}	
*(c)	0.520		7.95×10^3		1.00		
(d)		39.6		0.0912			1.76
*(e)			3.73×10^3		0.100	1.71×10^{-3}	
(f)		83.6			1.00	8.07×10^{-6}	
*(g)	0.798				1.50		33.6
(h)		11.1	1.35×10^4			7.07×10^{-5}	
*(i)		5.23	9.78×10^3				5.24
(j)	0.179				1.00	7.19×10^{-5}	

24-19. A solution containing 4.48 ppm $KMnO_4$ exhibits 85.9 %T in a 1.00-cm cell at 520 nm. Calculate the molar absorptivity of $KMnO_4$ at this wavelength.

24-20. Beryllium(II) forms a complex with acetylacetone (166.2 g/mol). Calculate the molar absorptivity of the complex, given that a 2.25 ppm solution has a transmittance of 37.5% when measured in a 1.00-cm cell at 295 nm, the wavelength of maximum absorption.

***24-21.** At 580 nm, the wavelength of its maximum absorption, the complex $Fe(SCN)^{2+}$ has a molar absorptivity of 7.00×10^3 L cm^{-1} mol^{-1}. Calculate

(a) the absorbance of a 3.40×10^{-5} M solution of the complex at 580 nm in a 1.00-cm cell.
(b) the absorbance of a solution in which the concentration of the complex is twice that in (a).
(c) the transmittance of the solutions described in (a) and (b).
(d) the absorbance of a solution that has half the transmittance of that described in (a).

24-22. A 2.50-mL aliquot of a solution that contains 4.33 ppm iron(III) is treated with an appropriate excess of KSCN and diluted to 50.0 mL. What is the absorbance of the resulting solution at 580 nm in a 2.50-cm cell? See Problem 24-21 for absorptivity data.

***24-23.** A solution containing the complex formed between Bi(III) and thiourea has a molar absorptivity of 9.32×10^3 L cm^{-1} mol^{-1} at 470 nm.

(a) What is the absorbance of a 5.67×10^{-5} M solution of the complex at 470 nm in a 1.00-cm cell?
(b) What is the percent transmittance of the solution described in (a)?
(c) What is the molar concentration of the complex in a solution that has the absorbance described in (a) when measured at 470 nm in a 2.50-cm cell?

24-24. The complex formed between Cu(I) and 1,10-phenanthroline has a molar absorptivity of 7000 L cm^{-1} mol^{-1} at 435 nm, the wavelength of maximum absorption. Calculate

(a) the absorbance of a 6.17×10^{-5} M solution of the complex when measured in a 1.00-cm cell at 435 nm.
(b) the percent transmittance of the solution in (a).
(c) the concentration of a solution that in a 5.00-cm cell has the same absorbance as the solution in (a).
(d) the path length through a 3.13×10^{-5} M solution of the complex that is needed for an absorbance that is the same as the solution in (a).

***24-25.** A solution with a "true" absorbance [$A = -\log(P_0/P)$] of 2.10 was placed in a spectrophotometer with a stray light percentage (P_s/P_0) of 0.75. What absorbance A' would be measured? What percentage error would result?

24-26. A compound X is to be determined by UV/visible spectrophotometry. A calibration curve is constructed from standard solutions of X with the following results: 0.50 ppm, $A = 0.24$; 1.5 ppm, $A = 0.36$; 2.5 ppm, $A = 0.44$; 3.5 ppm, $A = 0.59$; and 4.5 ppm, $A = 0.70$. Find the slope and intercept of the calibration curve, the standard error in Y, the concentration of the solution of unknown X concentration, and the standard deviation in the concentration of X. Construct a plot of the calibration curve and determine the unknown concentration by hand from the plot.

24-27. One common way to determine phosphorus in urine is to treat the sample after removing the protein with molybdenum (VI) and then reducing the resulting 12-molybdophosphate complex with ascorbic acid to give an intense blue-colored species called molybdenum blue. The absorbance of molybdenum blue can be measured at 650 nm. A 24-hour urine sample was collected, and the patient produced 1122 mL in 24 hours. A 1.00 mL aliquot of the sample was treated with Mo(VI) and ascorbic acid and diluted to a volume of 50.00 mL. A calibration curve was prepared by treating 1.00 mL aliquots of phosphate standard solutions in the same manner as the urine sample. The absorbances of the standards and the urine sample were obtained at 650 nm and the following results obtained:

Solution	Absorbance at 650 nm
1.00 ppm P	0.230
2.00 ppm P	0.436
3.00 ppm P	0.638
4.00 ppm P	0.848
Urine sample	0.518

(a) Find the slope, intercept, and standard error in y of the calibration curve. Construct a calibration curve. Determine the concentration number of phosphorus in ppm in the urine sample and its standard deviation from the least-squares equation of the line. Compare the unknown concentration to that obtained manually from a calibration curve.
(b) What mass in grams of phosphorus was eliminated per day by the patient?
(c) What is the phosphate concentration in urine in mM?

24-28. Nitrite is commonly determined by a colorimetric procedure using a reaction called the Griess reaction. In this reaction, the sample containing nitrite is reacted with sulfanilimide and N-(1-Napthyl) ethylenediamine to form a colored species that absorbs at 550 nm. Using an automated flow analysis

instrument, the following results were obtained for standard solutions of nitrite and for a sample containing an unknown amount:

Solution	Absorbance at 550 nm
2.00 μM	0.065
6.00 μM	0.205
10.00 μM	0.338
14.00 μM	0.474
18.00 μM	0.598
Unknown	0.402

(a) Find the slope, intercept, and standard deviation of the calibration curve.
(b) Construct the calibration curve.
(c) Determine the concentration of nitrite in the sample and its standard deviation.

24-29. The equilibrium constant for the reaction

$$2CrO_4^{2-} + 2H^+ \rightleftharpoons Cr_2O_7^{2-} + H_2O$$

is 4.2×10^{14}. The molar absorptivities for the two principal species in a solution of K_2CrO_7 are

λ, nm	ε_1 (CrO_4^{2-})	ε_2 ($Cr_2O_7^{2-}$)
345	1.84×10^3	10.7×10^2
370	4.81×10^3	7.28×10^2
400	1.88×10^3	1.89×10^2

Four solutions were prepared by dissolving 4.00×10^{-4}, 3.00×10^{-4}, 2.00×10^{-4}, and 1.00×10^{-4} moles of $K_2Cr_2O_7$ in water and diluting to 1.00 L with a pH 5.60 buffer. Calculate theoretical absorbance values (1.00-cm cells) for each solution and plot the data for (a) 345 nm; (b) 370 nm; and (c) 400 nm.

24-30. **Challenge Problem**: NIST maintains a database of the spectra of the elements at *http://www.nist.gov/pml/data/asd_contents.cfm*. The following energy levels for neutral lithium were obtained from this database:

Electronic Configuration	Level, eV
$1s^2 2s^1$	0.00000
$1s^2 2p^1$	1.847818
	1.847860
$1s^2 3s^1$	3.373129
$1s^2 3p^1$	3.834258
	3.834258
$1s^2 3d^1$	3.878607
	3.878612
$1s^2 4s^1$	4.340942
$1s^2 4p^1$	4.521648
	4.521648
$1s^2 4d^1$	4.540720
	4.540723

(a) Construct a partial energy level diagram similar to the one in Figure 24-20. Label each energy level with its corresponding orbital.
(b) Browse to the NIST website and click on the Physical Reference Data link. Locate and click on the link for the Atomic Spectral Database and click on the Lines icon. Use the form to retrieve the spectral lines for Li I between 300 nm and 700 nm, including energy level information. Note that the retrieved table contains wavelength, relative intensity, and changes in electron configuration for the transitions that give rise to each line. Add connecting lines to the partial energy level diagram from (a) to illustrate the transitions and label each line with the wavelength of the emission. Which of the transitions in your diagram are doublets?
(c) Use the intensity versus wavelength data that you retrieved in (b) to sketch an emission spectrum for lithium. If you placed a sample of $LiCO_3$ in a flame, what color would the flame be?
(d) Describe how the flame spectrum of an ionic lithium compound, such as $LiCO_3$, displays the spectrum of neutral lithium atoms.
(e) There appear to be no emission lines for lithium between 544 nm and 610 nm. Why is this?
(f) Describe how the information obtained in this problem could be used to detect the presence of lithium in urine. How would you determine the amount of lithium quantitatively?

CHAPTER 26

Molecular Absorption Spectrometry

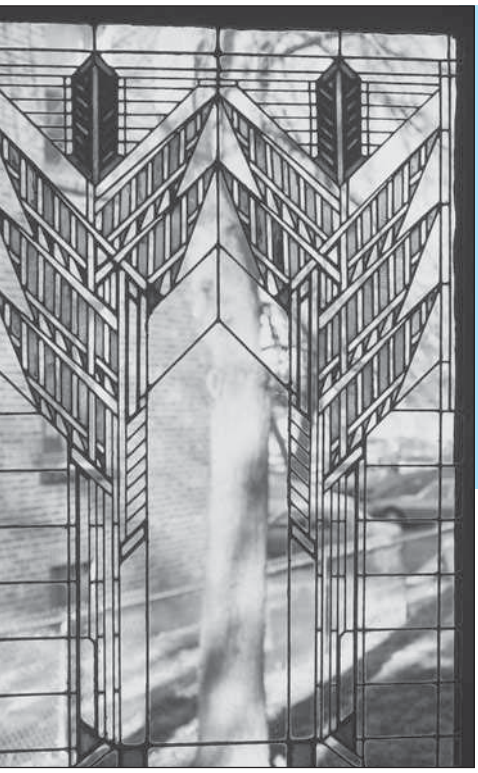

© Thomas A. Heinz

Glassmaking is among the oldest technologies, dating from the Neolithic period nearly 10,000 years ago. Ordinary glass is transparent because valence electrons in the silicate structure do not receive sufficient energy from visible light to be excited from their ground states in the valence band of the silicate structure to the conduction band. Beginning with the Egyptians in the second millennium B.C.E., glassmakers learned to add various compounds to glasses to produce colored glass. These additives often contain transition metals to provide accessible energy levels so that absorption of light occurs, and the resulting glass is colored. Colored glass is used widely in art and architecture as, for example, in the stained glass window shown here. Optical spectroscopy is used to characterize colored glasses by recording their absorption spectra. This information is used in several different fields. For example, in art history absorption spectra are used to characterize, identify, and trace the origin and development of works of art, in archeology spectra are used to explore the origins of humankind, and in forensics they are used to correlate evidence in crime investigations.

The absorption of ultraviolet, visible, and infrared radiation is widely used to identify and determine many inorganic, organic, and biochemical species.[1] Ultraviolet and visible molecular absorption spectroscopy is used primarily for quantitative analysis and is probably applied more extensively in chemical and clinical laboratories than any other single technique. Infrared absorption spectroscopy is a very powerful tool for determining the identity and structure of both inorganic and organic compounds. In addition, it now plays an important role in quantitative analysis, particularly in the area of environmental pollution.

26A ULTRAVIOLET AND VISIBLE MOLECULAR ABSORPTION SPECTROSCOPY

Several types of molecular species absorb ultraviolet and visible radiation. Molecular absorption by these species can be used for qualitative and quantitative analyses. UV-visible absorption is also used to monitor titrations and to study the composition of

[1]For more detailed treatment of absorption spectroscopy, see E. J. Meehan, in *Treatise on Analytical Chemistry,* 2nd ed., P. J. Elving, E. J. Meehan, and I. M. Kolthoff, eds., Part I, Vol. 7, Ch. 2, New York: Wiley, 1981; C. Burgess and A. Knowles, eds., *Techniques in Visible and Ultraviolet Spectrometry,* Vol. 1, New York: Chapman and Hall, 1981; J. D. Ingle, Jr., and S. R. Crouch, *Spectrochemical Analysis,* Chs. 12–14, Englewood Cliffs, NJ: Prentice-Hall, 1988; D. A. Skoog, F. J. Holler, and S. R. Crouch, *Principles of Instrumental Analysis,* 6th ed., Chs. 13, 14, 16, 17, Belmont, CA: Brooks/Cole, 2007.

complex ions. The use of absorption spectrometry to follow the kinetics of chemical reactions for quantitative purposes is described in Chapter 30.

26A-1 Absorbing Species

As noted in Section 24C-2, absorption of ultraviolet and visible radiation by molecules generally occurs in one or more electronic absorption bands, each of which is made up of many closely packed but discrete lines. Each line arises from the transition of an electron from the ground state to one of the many vibrational and rotational energy states associated with each excited electronic energy state. Because there are so many of these vibrational and rotational states and because their energies differ only slightly, the number of lines contained in the typical band is quite large and their separation from one another is very small.

A band consists of a large number of closely spaced vibrational and rotational lines. The energies associated with these lines differ little from one another.

As we saw previously in Figure 24-14a, the visible absorption spectrum for 1,2,3,4-tetrazine vapor shows the fine structure that is due to the numerous rotational and vibrational levels associated with the excited electronic states of this aromatic molecule. In the gaseous state, the individual tetrazine molecules are sufficiently separated from one another to vibrate and rotate freely, and many individual absorption lines appear as a result of the large number of vibrational and rotational energy states. As a pure liquid or in solution, however, the tetrazine molecules have little freedom to rotate, so lines due to differences in rotational energy levels disappear. Furthermore, when solvent molecules surround the tetrazine molecules, energies of the various vibrational levels are modified in a nonuniform way, and the energy of a given state in a sample of solute molecules appears as a single broad peak. This effect is more pronounced in polar solvents, such as water, than in nonpolar hydrocarbon media. This solvent effect is illustrated in Figures 24-14b and 24-14c.

Absorption by Organic Compounds

Absorption of radiation by organic molecules in the wavelength region between 180 and 780 nm results from interactions between photons and electrons that either participate directly in bond formation (and are thus associated with more than one atom) or that are localized about such atoms as oxygen, sulfur, nitrogen, and the halogens.

The wavelength of absorption of an organic molecule depends on how tightly its electrons are bound. The shared electrons in carbon-carbon or carbon-hydrogen single bonds are so firmly held that their excitation requires energies corresponding to wavelengths in the vacuum ultraviolet region below 180 nm. Single-bond spectra have not been widely exploited for analytical purposes because of the experimental difficulties of working in this region. These difficulties occur because both quartz and atmospheric components absorb in this region, which requires that evacuated spectrophotometers with lithium fluoride optics be used.

Electrons in double and triple bonds of organic molecules are not as strongly held and are therefore more easily excited by electromagnetic radiation. Thus, species with unsaturated bonds generally exhibit useful absorption bands. Unsaturated organic functional groups that absorb in the ultraviolet or visible regions are known as **chromophores**. **Table 26-1** lists common chromophores and the approximate wavelengths at which they absorb. The wavelength and peak intensity data are only rough guides since both are influenced by solvent effects as well as structural details of the molecule. In addition, conjugation between two or more chromophores

Chromophores are unsaturated organic functional groups that absorb in the ultraviolet or visible region.

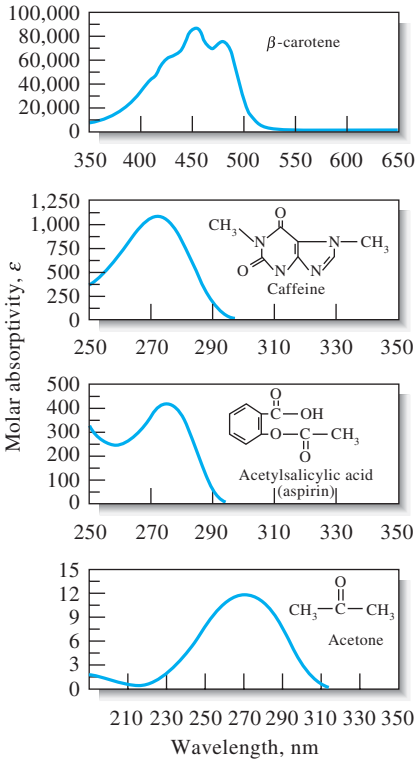

Figure 26-1 Absorption spectra for typical organic compounds.

TABLE 26-1
Absorption Characteristics of Some Common Organic Chromophores

Chromophore	Example	Solvent	λ_{max}, nm	ε_{max}
Alkene	$C_6H_{13}CH{=}CH_2$	*n*-Heptane	177	13,000
Conjugated alkene	$CH_2{=}CHCH{=}CH_2$	*n*-Heptane	217	21,000
Alkyne	$C_5H_{11}C{\equiv}C{-}CH_3$	*n*-Heptane	178	10,000
			196	2,000
			225	160
Carbonyl	$CH_3\overset{\overset{O}{\|}}{C}CH_3$	*n*-Hexane	186	1,000
			280	16
	$CH_3\overset{\overset{O}{\|}}{C}H$	*n*-Hexane	180	Large
			293	12
Carboxyl	$CH_3\overset{\overset{O}{\|}}{C}OH$	Ethanol	204	41
Amido	$CH_3\overset{\overset{O}{\|}}{C}NH_2$	Water	214	60
Azo	$CH_3N{=}NCH_3$	Ethanol	339	5
Nitro	CH_3NO_2	Isooctane	280	22
Nitroso	C_4H_9NO	Ethyl ether	300	100
			665	20
Nitrate	$C_2H_5ONO_2$	Dioxane	270	12
Aromatic	Benzene	*n*-Hexane	204	7,900
			256	200

tends to cause shifts in absorption maxima to longer wavelengths. Finally, it is often difficult to determine precisely an absorption maximum because vibrational effects broaden absorption bands in the ultraviolet and visible regions. Typical spectra for organic compounds are shown in **Figure 26-1**.

Saturated organic compounds containing such heteroatoms as oxygen, nitrogen, sulfur, or halogens have nonbonding electrons that can be excited by radiation in the 170- to 250-nm range. **Table 26-2** lists a few examples of such compounds. Some of these compounds, such as alcohols and ethers, are common solvents. Their absorption in this region prevents measuring absorption of analytes dissolved in these solvents at wavelengths shorter than 180 to 200 nm. Occasionally, absorption in this region is used for determining halogen and sulfur-bearing compounds.

TABLE 26-2
Absorption by Organic Compounds Containing Unsaturated Heteroatoms

Compound	λ_{max}, nm	ε_{max}
CH_3OH	167	1480
$(CH_3)_2O$	184	2520
CH_3Cl	173	200
CH_3I	258	365
$(CH_3)_2S$	229	140
$(CH_3)NH_2$	215	600
$(CH_3)_3N$	227	900

Absorption by Inorganic Species

In general, the ions and complexes of elements in the first two transition series absorb broad bands of visible radiation in at least one of their oxidation states. As a result, these compounds are colored (see, for example, **Figure 26-2**). Absorption occurs when electrons make transitions between filled and unfilled *d*-orbitals with energies that depend on the ligands bonded to the metal ions. The energy differences between these *d*-orbitals (and thus the position of the corresponding absorption maxima) depend on the position of the element in the periodic table, its oxidation state, and the nature of the ligand bonded to it.

Absorption spectra of ions of the lanthanide and actinide series differ substantially from those shown in Figure 26-2. The electrons responsible for absorption by these elements (4*f* and 5*f*, respectively) are shielded from external influences by electrons

that occupy orbitals with larger principal quantum numbers. As a result, the bands tend to be narrow and relatively unaffected by the species bonded by the outer electrons, as shown in **Figure 26-3**.

Charge-Transfer Absorption

Charge-transfer absorption is particularly important for quantitative analysis because molar absorptivities are unusually large ($\varepsilon > 10{,}000$ L mol^{1} cm^{1}), which leads to high sensitivity. Many inorganic and organic complexes exhibit this type of absorption and are therefore called charge-transfer complexes.

A **charge-transfer complex** consists of an electron-donor group bonded to an electron acceptor. When this product absorbs radiation, an electron from the donor is transferred to an orbital that is largely associated with the acceptor. The excited state is thus the product of a kind of internal oxidation/reduction process. This behavior differs from that of an organic chromophore in which the excited electron is in a molecular orbital that is shared by two or more atoms.

Familiar examples of charge-transfer complexes include the phenolic complex of iron(III), the 1,10-phenanthroline complex of iron(II), the iodide complex of molecular iodine, and the ferro/ferricyanide complex responsible for the color of Prussian blue. The red color of the iron(III)/thiocyanate complex is yet another example of charge-transfer absorption. Absorption of a photon results in the transfer of an electron from the thiocyanate ion to an orbital that is largely associated with the iron(III) ion. The product is an excited species involving predominantly iron(II) and the thiocyanate radical SCN. As with other types of electronic excitation, the electron in this complex normally returns to its original state after a brief period. Occasionally, however, an excited complex may dissociate and produce photochemical oxidation/reduction products. Three spectra of charge-transfer complexes are shown in **Figure 26-4**.

In most charge-transfer complexes containing a metal ion, the metal serves as the electron acceptor. Exceptions are the 1,10-phenanthroline complexes of iron(II) (see Section 38N-2) and copper(I), where the ligand is the acceptor and the metal ion the donor. A few additional examples of this type of complex are known.

26A-2 Qualitative Applications of Ultraviolet/ Visible Spectroscopy

Spectrophotometric measurements with ultraviolet radiation are useful for detecting chromophoric groups, such as those shown in Table 26-1.[2] Because large parts of even the most complex organic molecules are transparent to radiation longer than 180 nm, the appearance of one or more absorption bands in the region from 200 to 400 nm is clear indication of the presence of unsaturated groups or of atoms such as sulfur or halogens. Often, you can get an idea as to the identity of the absorbing groups by comparing the spectrum of an analyte with those of simple molecules containing various chromophoric groups.[3] Usually, however, ultraviolet spectra do

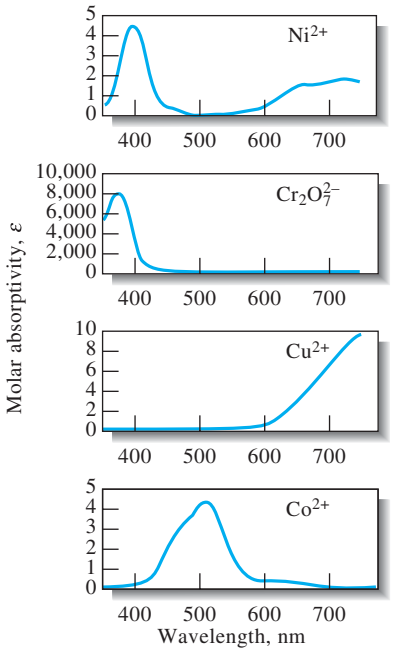

Figure 26-2 Absorption spectra of aqueous solutions of transition metal ions.

A **charge-transfer complex** is a strongly absorbing species that is made up of an electron-donating species that is bonded to an electron-accepting species.

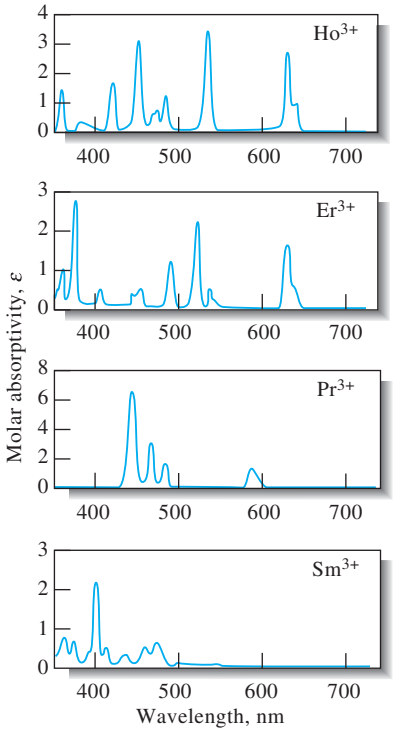

Figure 26-3 Absorption spectra of aqueous solutions of rare earth ions.

[2] For a detailed discussion of ultraviolet absorption spectroscopy in the identification of organic functional groups, see R. M. Silverstein and F. X. Webster, *Spectrometric Identification of Organic Compounds,* 6th ed., Ch. 7, New York: Wiley, 1998.

[3] H. H. Perkampus, *UV-VIS Atlas of Organic Compounds,* 2nd ed., Weinheim, Germany: Wiley-VCH, 1992. In addition, in the past, several organizations have published catalogs of spectra that may still be useful, including American Petroleum Institute, Ultraviolet Spectral Data, A.P.I. Research Project 44, Pittsburgh: Carnegie Institute of Technology; *Sadtler Handbook of Ultraviolet Spectra.* Philadelphia: Sadtler Research Laboratories, 1979; American Society for Testing Materials, Committee E-13, Philadelphia.

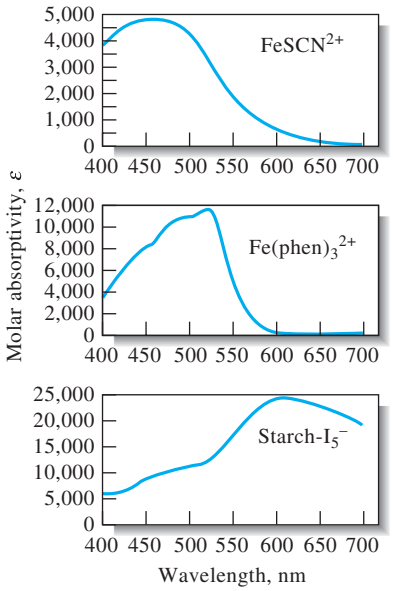

Figure 26-4 Absorption spectra of aqueous charge-transfer complexes.

not have sufficient fine structure to permit an analyte to be identified unambiguously. Thus, ultraviolet qualitative data must be supplemented with other physical or chemical evidence such as infrared, nuclear magnetic resonance, and mass spectra as well as solubility and melting- and boiling-point information.

Solvents

Ultraviolet spectra for qualitative analysis are usually measured using dilute solutions of the analyte. For volatile compounds, however, gas-phase spectra are often more useful than liquid-phase or solution spectra (for example, compare Figure 24-14a and 24-14b). Gas-phase spectra can often be obtained by allowing a drop or two of the pure liquid to evaporate and equilibrate with the atmosphere in a stoppered cuvette.

A solvent for ultraviolet/visible spectroscopy must be transparent in the region of the spectrum where the solute absorbs. The analyte must be sufficiently soluble in the solvent to give a well-defined analyte. In addition, we must consider possible interactions of the solvent with the absorbing species. For example, polar solvents, such as water, alcohols, esters, and ketones, tend to obliterate vibrational fine structure and should thus be avoided to preserve spectral detail. Spectra in nonpolar solvents, such as cyclohexane, often more closely approach gas-phase spectra (compare, for example, the three spectra in Figure 24-14). In addition, solvent polarity often influences the position of absorption maxima. For qualitative analysis, analyte spectra should thus be compared to spectra of known compounds taken in the same solvent.

Table 26-3 lists common solvents for studies in the ultraviolet and visible regions and their approximate lower wavelength limits. These limits strongly depend on the purity of the solvent. For example, ethanol and the hydrocarbon solvents are frequently contaminated with benzene, which absorbs below 280 nm.[4]

The Effect of Slit Width

Use small slit widths for qualitative studies to preserve maximum spectral detail. ❯

The effect of variation in slit width, and hence effective bandwidth, is illustrated by the spectra in **Figure 26-5**. The four traces show that peak heights and peak separation are distorted at wider bandwidths. To avoid this type of distortion, spectra for qualitative applications should be measured with the smallest slit widths that provide adequate signal-to-noise ratios.

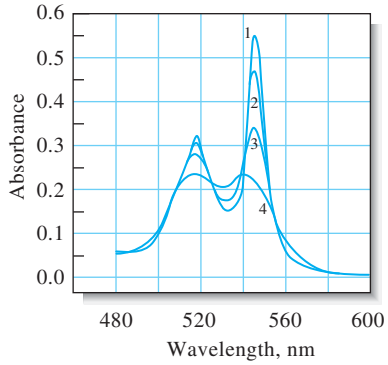

Figure 26-5 Spectra for reduced cytochrome *c* obtained with four spectral bandwidths: (1) 1 nm, (2) 5 nm, (3) 10 nm, and (4) 20 nm. At bandwidths < 1 nm, the noise on the absorption bands becomes pronounced. (Courtesy of Varian Instrument Division, Palo Alto, CA.)

TABLE 26-3
Solvents for the Ultraviolet and Visible Regions

Solvent	Lower Wavelength Limit, nm	Solvent	Lower Wavelength Limit, nm
Water	180	Carbon tetrachloride	260
Ethanol	220	Diethyl ether	210
Hexane	200	Acetone	330
Cyclohexane	200	Dioxane	320
		Cellosolve	320

[4]Most major suppliers of reagent chemicals in the United States offer spectrochemical grades of solvents. Spectral-grade solvents have been treated so as to remove absorbing impurities and meet or exceed the requirements set forth in *Reagent Chemicals, American Chemical Society Specifications,* 10th ed., Washington, DC: American Chemical Society, 2005, available online or in hard bound forms.

The Effect of Stray Radiation at the Wavelength Extremes of a Spectrophotometer

Previously, we demonstrated that stray radiation may lead to instrumental deviations from Beer's law (see Section 24C-3). Another undesirable effect of this type of radiation is that it occasionally causes false peaks to appear when a spectrophotometer is being operated at its wavelength extremes. **Figure 26-6** shows an example of such behavior. Curve *B* is the true spectrum for a solution of cerium(IV) produced with a research-quality spectrophotometer responsive down to 200 nm or less. Curve *A* was obtained for the same solution with an inexpensive instrument operated with a tungsten source designed for work in the visible region only. The false peak at about 360 nm is directly attributable to stray radiation, which was not absorbed because it was made up of wavelengths longer than 400 nm. Under most circumstances, such stray radiation has a negligible effect because its power is only a tiny fraction of the total power of the beam exiting from the monochromator. At wavelength settings below 380 nm, however, radiation from the monochromator is greatly attenuated as a result of absorption by glass optical components and cuvettes. In addition, both the output of the source and the transducer sensitivity fall off dramatically below 380 nm. These factors combine to cause a substantial fraction of the measured absorbance to be due to the stray radiation of wavelengths to which cerium(IV) is transparent. A false absorption maximum results. This same effect is sometimes observed with ultraviolet/visible instruments when attempts are made to measure absorbances at wavelengths lower than about 190 nm.

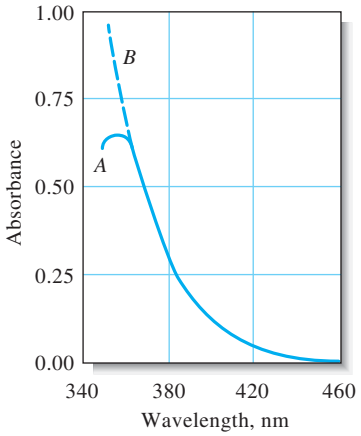

Figure 26-6 Spectra of cerium(IV) obtained with a spectrophotometer having glass optics (*A*) and quartz optics (*B*). The apparent absorption band in *A* occurs when stray radiation is transmitted at long wavelengths.

26A-3 Quantitative Applications

Ultraviolet and visible molecular absorption spectroscopy is one of the most useful tools available for quantitative analysis. The important characteristics of spectrophotometric and photometric methods are

- *Wide applicability.* A majority of inorganic, organic, and biochemical species absorb ultraviolet or visible radiation and are thus amenable to direct quantitative determination. Many nonabsorbing species can also be determined after chemical conversion to absorbing derivatives. Of the determinations performed in clinical laboratories, a large majority is based on ultraviolet and visible absorption spectroscopy.
- *High sensitivity.* Typical detection limits for absorption spectroscopy range from 10^{-4} to 10^{-5} M. This range can often be extended to 10^{-6} or even 10^{-7} M with procedural modifications.
- *Moderate to high selectivity.* Often a wavelength can be found at which the analyte alone absorbs. Furthermore, where overlapping absorption bands do occur, corrections based on additional measurements at other wavelengths sometimes eliminate the need for a separation step. When separations are required, spectrophotometry often provides the means for detecting the separated species (see Section 33A-5).
- *Good accuracy.* The relative errors in concentration encountered with a typical spectrophotometric or photometric procedure lie in the range from 1% to 5%. Such errors can often be decreased to a few tenths of a percent with special precautions.
- *Ease and convenience.* Spectrophotometric and photometric measurements are easily and rapidly performed with modern instruments. In addition, the methods lend themselves to automation quite nicely.

Scope

The applications of molecular absorption measurements are not only numerous but also touch on every area in which quantitative information is sought. You can get an idea of the scope of spectrophotometry by consulting specialized monographs on the subject.[5]

Applications to Absorbing Species. Table 26-1 (page 724) lists many common organic chromophores. Spectrophotometric determination of organic compounds containing one or more of these groups is thus potentially feasible. Many such applications can be found in the literature.

A number of inorganic species also absorb. We have noted that many ions of the transition metals are colored in solution and can thus be determined by spectrophotometric measurement. In addition, a number of other species show characteristic absorption bands, including nitrite, nitrate, and chromate ions, the oxides of nitrogen, the elemental halogens, and ozone.

Applications to Nonabsorbing Species. Many nonabsorbing analytes can be determined photometrically by causing them to react with chromophoric reagents to produce products that absorb strongly in the ultraviolet and visible regions. The successful application of these color-forming reagents usually requires that their reaction with the analyte be forced to near completion unless methods such as kinetic methods (see Chapter 30) are used.

Typical inorganic reagents include the following: thiocyanate ion for iron, cobalt, and molybdenum; hydrogen peroxide for titanium, vanadium, and chromium; and iodide ion for bismuth, palladium, and tellurium. Organic chelating reagents that form stable colored complexes with cations are even more important. Common examples include diethyldithiocarbamate for the determination of copper, diphenylthiocarbazone for lead, 1,10-phenanthroline for iron (see color plate 15), and dimethylglyoxime for nickel; **Figure 26-7** shows the color-forming reaction for the first two of these reagents. The structure of the 1,10-phenanthroline complex of iron(II) is shown on page 503, and the reaction of nickel with dimethylglyoxime to form a red precipitate is described on page 294 (see also color plate 7). In the application of the dimethylglyoxime reaction to the photometric determination of nickel, an aqueous solution of the cation is extracted with a solution of the chelating agent in an immiscible organic liquid. The absorbance of the resulting bright red organic layer serves as a measure of the concentration of the metal.

Other reagents are available that react with organic functional groups to produce colors that are useful for quantitative analysis. For example, the red color of the 1:1 complexes that form between low-molecular-mass aliphatic alcohols and cerium(IV) can be used for the quantitative estimation of these alcohols.

---

[5]M. L. Bishop, E. P Fody, and L. E. Schoeff, *Clinical Chemistry: Techniques, Principles, Correlations*, Part I, Ch. 5, Part II, Philadelphia: Lippincott, Williams, and Wilkins, 2009; O. Thomas, *UV-Visible Spectrophotometry of Water and Wasterwater*, Vol. 27, *Techniques and Instrumentation in Analytical Chemistry*, Amsterdam: Elsevier, 2007; S. Görög, *Ultraviolet-Visible Spectrophotometry in Pharmaceutical Analysis,* Boca Rotan, FL: CRC Press, 1995; H. Onishi, *Photometric Determination of Traces of Metals*, 4th ed., Parts IIA and IIB, New York: Wiley, 1986, 1989; *Colorimetric Determination of Nonmetals,* 2nd ed., D. F. Boltz, ed., New York: Interscience, 1978.

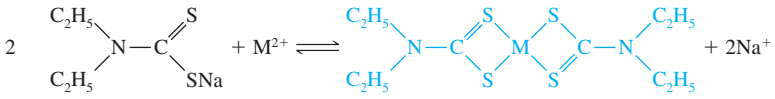

(a)

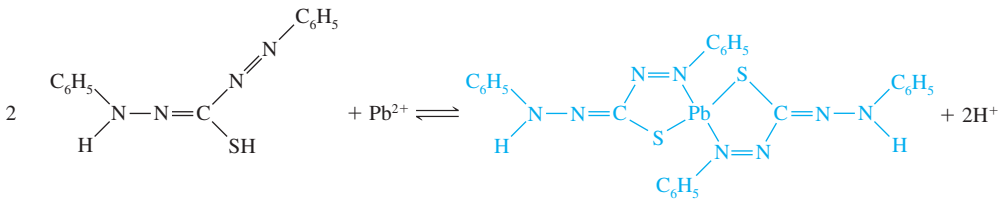

(b)

Figure 26-7 Typical chelating reagents for absorption spectrophotometry. (a) Diethyldithiocarbamate. (b) Diphenylthiocarbazone.

Procedural Details

A first step in any photometric or spectrophotometric analysis is the development of conditions that yield a reproducible relationship (preferably linear) between absorbance and analyte concentration.

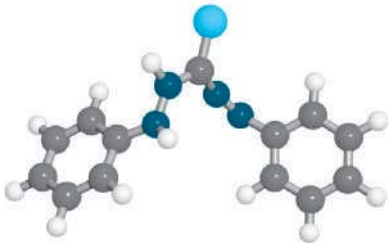

Molecular model of diphenylthiocarbazone.

Absorption spectra are affected by such variables as temperature, pH, electrolyte concentration, and the presence of interferences.

Wavelength Selection. In order to realize maximum sensitivity, spectrophotometric absorbance measurements are usually made at the wavelength of maximum absorption because the change in absorbance per unit of concentration is greatest at this point. In addition, the absorption curve is often flat at a maximum, leading to good adherence to Beer's law (see Figure 24-17) and less uncertainty from failure to reproduce precisely the wavelength setting of the instrument.

Variables That Influence Absorption. Common variables that influence the absorption spectrum of a substance include the nature of the solvent, the pH of the solution, the temperature, high electrolyte concentrations, and the presence of interfering substances. The effects of these variables must be known and conditions for the determination chosen such that the absorbance will not be materially affected by small, uncontrolled variations.

The Relationship between Absorbance and Concentration. The calibration standards for a photometric or a spectrophotometric method should approximate as closely as possible the overall composition of the actual samples and should encompass a reasonable range of analyte concentrations. A calibration curve of absorbance versus the concentrations of several standards is usually obtained to evaluate the relationship. It is seldom, if ever, safe to assume that Beer's law holds and to use only a single standard to determine the molar absorptivity. Unless there is no other choice, it is never a good idea to base the results of a determination solely on a literature value for the molar absorptivity. In cases where matrix effects are a problem, the standard addition method may improve results by providing compensation for some of these effects.

The Standard Addition Method. Ideally, the composition of calibration standards should approximate the composition of the samples to be analyzed. This is true not only for the analyte concentration but for the concentrations of the other species in the sample matrix. Approximating the sample composition should minimize the effects of various components of the sample on the measured absorbance. For example, the absorbance of many colored complexes of metal ions is decreased in the presence of sulfate and phosphate ions because of the tendency of these anions to

form colorless complexes with metal ions. As a result, the color formation reaction is often less complete, and the sample absorbance is lowered. The matrix effect of sulfate and phosphate can often be counteracted by introducing into the standards amounts of the two species that approximate the amounts found in the samples. Unfortunately, when complex materials such as soils, minerals, and plant ash are being analyzed, preparing standards that match the samples is often impossible or extremely difficult. When this is the case, the standard addition method can be helpful in counteracting matrix effects.

The standard addition method can take several forms as discussed in Section 8D-3; the single-point method was described in Example 8-8.[6] The multiple-additions method is often chosen for photometric or spectrophotometric analyses, and this method is described here. In the multiple additions technique, several increments of a standard solution are added to sample aliquots of the same size. Each solution is then diluted to a fixed volume before measuring its absorbance. When the amount of sample is limited, standard additions can be carried out by successive addition of increments of the standard to a single measured aliquot of the unknown. The measurements are made on the original solution and after each addition of standard analyte.

Assume that several identical aliquots V_x of the unknown solution with a concentration c_x are transferred to volumetric flasks having a volume V_t. To each of these flasks is added a variable volume V_s mL of a standard solution of the analyte having a known concentration c_s. The color development reagents are then added, and each solution is diluted to volume. If the chemical system follows Beer's law, the absorbance of the solutions is described by

$$A_s = \frac{\varepsilon b V_s c_s}{V_t} + \frac{\varepsilon b V_x c_x}{V_t}$$

$$= kV_s c_s + kV_x c_x \tag{26-1}$$

where k is a constant equal to $\varepsilon b/V_t$. A plot of A_s as a function of V_s should yield a straight line of the form

$$A_s = mV_s + b$$

where the slope m and the intercept b are given by

$$m = kc_s$$

and

$$b = kV_x c_x$$

Least-squares analysis (see Section 8D-2) of the data can be used to determine m and b. The unknown concentration c_x can then be calculated from the ratio of these two quantities and the known values of V_x and V_s. Thus,

$$\frac{m}{b} = \frac{kc_s}{kV_x c_x}$$

which rearranges to

$$c_x = \frac{bc_s}{mV_x} \tag{26-2}$$

If we assume that the uncertainties in c_s, V_s, and V_t are negligible with respect to those in m and b, the standard deviation in c_x can be estimated. It follows then

[6]See M. Bader, *J. Chem. Educ.*, **1980**, *57*, 703, **DOI**: 10.1021/ed057p703.

that the relative variance of the result $(s_c/c_x)^2$ is the sum of the relative variances of m and b, that is,

$$\left(\frac{s_c}{c_x}\right)^2 = \left(\frac{s_m}{m}\right)^2 + \left(\frac{s_b}{b}\right)^2$$

where s_m and s_b are the standard deviations of the slope and intercept, respectively. By taking the square root of this equation, we can solve for the standard deviation in concentration, s_c:

$$s_c = c_x\sqrt{\left(\frac{s_m}{m}\right)^2 + \left(\frac{s_b}{b}\right)^2} \qquad (26\text{-}3)$$

EXAMPLE 26-1

Ten-millimeter aliquots of a natural water sample were pipetted into 50.00 mL volumetric flasks. Exactly 0.00, 5.00, 10.00, 15.00, and 20.00 mL of a standard solution containing 11.1 ppm of Fe^{3+} were added to each, followed by an excess of thiocyanate ion to give the red complex $Fe(SCN)^{2+}$. After dilution to volume, absorbances for the five solutions, measured with a photometer equipped with a green filter, were found to be 0.240, 0.437, 0.621, 0.809, and 1.009, respectively (0.982-cm cells). (a) What was the concentration of Fe^{3+} in the water sample? (b) Calculate the standard deviation of the slope, the intercept, and the concentration of Fe.

Solution

(a) In this problem, $c_s = 11.1$ ppm, $V_x = 10.00$ mL, and $V_t = 50.00$ mL. A plot of the data, shown in **Figure 26-8**, demonstrates that Beer's law is obeyed. To obtain the equation for the line in Figure 26-8, the procedure illustrated in Example 8-4 (pages 174–175) is followed. The result is $m = 0.03820$, and $b = 0.2412$. Thus,

$$A_s = 0.03820V_s + 0.2412$$

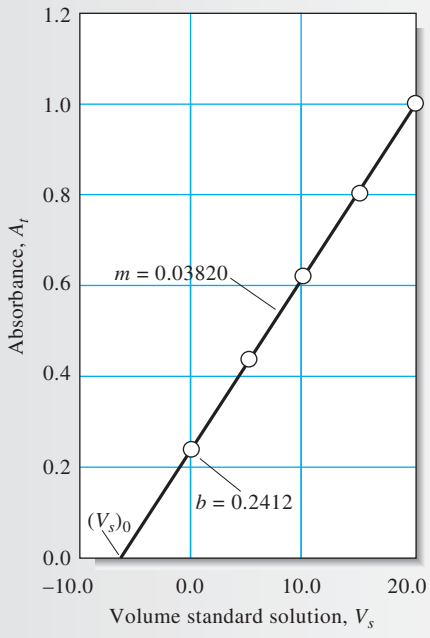

Figure 26-8 Plot of data for standard addition determination of Fe^{3+} as the $Fe(SCN)^{2+}$ complex.

(*continued*)

Substituting into Equation 26-2 gives

$$c_x = \frac{(0.2412)(11.1 \text{ ppm } Fe^{3+})}{(0.03820 \text{ mL}^{-1})(10.00 \text{ mL})} = 7.01 \text{ ppm } Fe^{3+}$$

(b) Equations 8-16 and 8-17 give the standard deviation of the slope and the intercept. That is, $s_m = 3.07 \times 10^{-4}$, and $s_b = 3.76 \times 10^{-3}$.
Substituting into Equation 26-3 gives

$$s_c = 7.01 \text{ ppm } Fe^{3+} \sqrt{\left(\frac{3.07 \times 10^{-4}}{0.03820}\right)^2 + \left(\frac{3.76 \times 10^{-3}}{0.2412}\right)^2}$$

$$= 0.12 \text{ ppm } Fe^{3+}$$

In the interest of saving time or sample, it is possible to perform a standard addition analysis using only two increments of sample. In that case, a single addition of V_s mL of standard is added to one of the two samples, and we can write

$$A_1 = \varepsilon b c_x$$

$$A_2 = \frac{\varepsilon b V_x c_x}{V_t} + \frac{\varepsilon b V_s c_s}{V_t}$$

where A_1 and A_2 are absorbances of the sample and the sample plus standard, respectively, and V_t is $V_x + V_s$. If we solve the first equation for εb, substitute into the second equation, and solve for c_x, we find

$$c_x = \frac{A_1 c_s V_s}{A_2 V_t - A_1 V_x} \tag{26-4}$$

Single-point standard additions methods are inherently more risky than multiple-point methods. There is no check on linearity with single-point methods, and results depend strongly on the reliability of one measurement.

Spreadsheet Summary In Chapter 12 of *Applications of Microsoft® Excel in Analytical Chemistry,* 2nd ed., we investigate the multiple standard additions method for determining solution concentration. Conventional and weighted linear regression methods are also used to determine concentrations and standard deviations.

EXAMPLE 26-2

The single-point standard addition method was used in the determination of phosphate by the molybdenum blue method. A 2.00-mL urine specimen was treated with molybdenum blue reagents to produce a species absorbing at 820 nm, after which the sample was diluted to 100 mL. A 25.00-mL aliquot of this solution gave an absorbance of 0.428 (solution 1). Addition of 1.00 mL of a solution containing 0.0500 mg of phosphate to a second 25.0-mL aliquot gave an absorbance of 0.517 (solution 2). Use these data to calculate the mass of phosphate in milligrams per millimeter of the specimen.

Solution

We substitute into Equation 26-4 and obtain

$$c_x = \frac{A_1 c_s V_s}{A_2 V_t - A_1 V_x} = \frac{(0.428)(0.0500 \text{ mg } PO_4^{3-}/\cancel{\text{mL}})(1.00 \cancel{\text{mL}})}{(0.517)(26.00 \text{ mL}) - (0.428)(25.00 \text{ mL})}$$

$$= 0.0780 \text{ mg } PO_4^{3-}/\text{mL}$$

This is the concentration of the diluted sample. To obtain the concentration of the original urine sample, we need to multiply by 100.00/2.00. Thus,

$$\text{concentration of phosphate} = 0.0780 \frac{\text{mg}}{\text{mL}} \times \frac{100.00 \cancel{\text{mL}}}{2.00 \cancel{\text{mL}}}$$

$$= 0.390 \text{ mg/mL}$$

Analysis of Mixtures. The total absorbance of a solution at any given wavelength is equal to the sum of the absorbances of the individual components in the solution (Equation 24-14). This relationship makes it possible in principle to determine the concentrations of the individual components of a mixture even if their spectra overlap completely. For example, **Figure 26-9** shows the spectrum of a solution containing a mixture of species M and species N as well as absorption spectra for the individual components. It is apparent that there is no wavelength where the absorbance is due to just one of these components. To analyze the mixture, molar absorptivities for M and N are first determined at wavelengths λ_1 and λ_2. The concentrations of the standard solutions of M and N should be such that Beer's law is obeyed over an absorbance range that encompasses the absorbance of the sample. As shown in Figure 26-9, wavelengths should be selected so that the molar absorptivities of the two components differ significantly. Thus, at λ_1, the molar absorptivity of component M is much larger than that for component N. The reverse is true for λ_2. To complete the analysis, the absorbance of the mixture is determined at the same two wavelengths. From the known molar absorptivities and path length, the following equations hold

$$A_1 = \varepsilon_{M_1} b c_M + \varepsilon_{N_1} b c_N \quad (26\text{-}5)$$

$$A_2 = \varepsilon_{M_2} b c_M + \varepsilon_{N_2} b c_N \quad (26\text{-}6)$$

where the subscript 1 indicates measurement at λ_1, and the subscript 2 indicates measurement a λ_2. With the known values of ε and b, Equations 26-5 and 26-6 are two equations in two unknowns (c_M and c_N) and can be solved as demonstrated in Example 26-3.

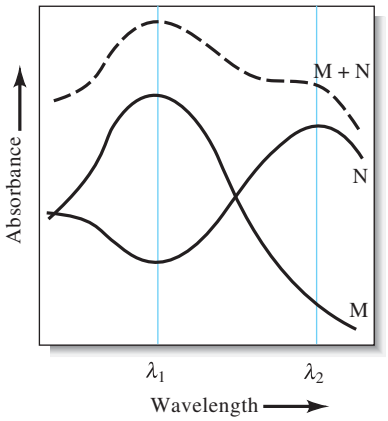

Figure 26-9 Absorption spectrum of a two-component mixture (M + N), with spectra of the individual components M and N.

EXAMPLE 26-3

Palladium(II) and gold(III) can be determined simultaneously by reaction with methiomeprazine ($C_{19}H_{24}N_2S_2$). The absorption maximum for the Pd complex occurs at 480 nm, while that for the Au complex is at 635 nm. Molar absorptivity data at these wavelengths are as follows:

(*continued*)

	ε, L mol^{-1} cm^{-1}	
	480 nm	**635 nm**
Pd complex	3.55×10^3	5.64×10^2
Au complex	2.96×10^3	1.45×10^4

A 25.0-mL sample was treated with an excess of methiomeprazine and subsequently diluted to 50.0 mL. Calculate the molar concentrations of Pd(II), c_{Pd}, and Au(III), c_{Au}, in the sample if the diluted solution had an absorbance of 0.533 at 480 nm and 0.590 at 635 nm when measured in a 1.00-cm cell.

Solution

At 480 nm from Equation 26-5,

$$A_{480} = \varepsilon_{Pd(480)} b c_{Pd} + \varepsilon_{Au(480)} b c_{Au}$$

$$0.533 = (3.55 \times 10^3\ M^{-1}\ \cancel{cm^{-1}})(1.00\ \cancel{cm}) c_{Pd} + (2.96 \times 10^3\ M^{-1} \cancel{cm^{-1}})(1.00\ \cancel{cm}) c_{Au}$$

or

$$c_{Pd} = \frac{0.533 - 2.96 \times 10^3\ M^{-1} c_{Au}}{3.55 \times 10^3\ M^{-1}}$$

At 635 nm from Equation 26-6,

$$A_{635} = \varepsilon_{Pd(635)} b c_{Pd} + \varepsilon_{Au(635)} b c_{Au}$$

$$0.590 = (5.64 \times 10^2\ M^{-1}\ \cancel{cm^{-1}})(1.00\ \cancel{cm}) c_{Pd} + (1.45 \times 10^4\ M^{-1}\ \cancel{cm^{-1}})(1.00\ \cancel{cm}) c_{Au}$$

Substitution for c_{Pd} in this expression gives

$$0.590 = \frac{(5.64 \times 10^2\ M^{-1})(0.533 - 2.96 \times 10^3\ M^{-1} c_{Au})}{3.55 \times 10^3\ M^{-1}} + (1.45 \times 10^4\ M^{-1}) c_{Au}$$

$$= 0.0847 - (4.70 \times 10^2\ M^{-1}) c_{Au} + (1.45 \times 10^4\ M^{-1}) c_{Au}$$

$$c_{Au} = \frac{(0.590 - 0.0847)}{(1.45 \times 10^4\ M^{-1} - 4.70 \times 10^2\ M^{-1})} = 3.60 \times 10^{-5}\ M$$

and

$$c_{Pd} = \frac{0.533 - (2.96 \times 10^3\ \cancel{M^{-1}})(3.60 \times 10^{-5}\ M)}{3.55 \times 10^3\ \cancel{M^{-1}}} = 1.20 \times 10^{-4}\ M$$

Since solutions were diluted twofold, the concentrations of Pd(II) and Au(III) in the original sample were 7.20×10^{-5} M and 2.40×10^{-4} M, respectively.

Mixtures containing more than two absorbing species can be analyzed, in principle at least, if one additional absorbance measurement is made for each extra component. The uncertainties in the resulting data become greater, however, as the number of measurements increases. Some computerized spectrophotometers are capable of minimizing these uncertainties by overdetermining the system. These instruments use many more data points than unknowns and effectively match the entire spectrum of the unknown as closely as possible by calculating synthetic spectra for various concentrations of the components. The calculated spectra are then added, and the sum is compared with the

spectrum of the analyte solution until a close match is found. The spectra for standard solutions of each component of the mixture are acquired and stored in computer memory prior to making measurements on the analyte mixture.

Spreadsheet Summary In Chapter 12 of *Applications of Microsoft® Excel in Analytical Chemistry*, 2nd ed., we use spreadsheet methods to determine concentrations of mixtures of analytes. Solutions to sets of simultaneous equations are evaluated using iterative techniques, the method of determinants, and matrix manipulations.

The Effect of Instrumental Uncertainties[7]

The accuracy and precision of spectrophotometric analyses are often limited by the indeterminate error, or noise, associated with the instrument. As pointed out in Chapter 25, a spectrophotometric absorbance measurement entails three steps: setting or measuring 0% T, setting or measuring 100% T, and measuring the % T of the sample. The random errors associated with each of these steps combine to give a net random error for the final value obtained for T. The relationship between the noise encountered in the measurement of T and the resulting *concentration uncertainty* can be derived by writing Beer's law in the form

In the context of this discussion, **noise** refers to random variations in the instrument output due to electrical fluctuations and also variables such as the temperature of the solution, the position of the cell in the light beam, and the output of the source. With older instruments, the way the operator reads the meter can also result in a random variation.

$$c = -\frac{1}{\varepsilon \mathrm{b}} \log T = \frac{-0.434}{\varepsilon b} \ln T$$

Taking the partial derivative of this equation while holding εb constant leads to the expression

$$\partial c = \frac{-0.434}{\varepsilon b T} \partial T$$

where ∂c can be interpreted as the uncertainty in c that results from the noise (or uncertainty) in T. Dividing this equation by the previous one gives

$$\frac{\partial c}{c} = \frac{0.434}{\log T}\left(\frac{\partial T}{T}\right) \qquad (26\text{-}7)$$

where $\partial T/T$ is the relative random error in T attributable to the noise in the three measurement steps, and $\partial c/c$ is the resulting relative random concentration error.

The best and most useful measure of the random error ∂T is the standard deviation σ_T, which may be measured conveniently for a given instrument by making 20 or more replicate transmittance measurements of an absorbing solution. Substituting σ_T and σ_c for the corresponding differential quantities in Equation 26-7 leads to

$$\frac{\sigma_c}{c} = \frac{0.434}{\log T}\left(\frac{\sigma_T}{T}\right) \qquad (26\text{-}8)$$

where σ_T/T is the relative standard deviation in transmittance and σ_c/c is the resulting relative standard deviation in concentration.

Equation 26-8 shows that the uncertainty in a photometric concentration measurement varies in a complex way with the magnitude of the transmittance. The situation is even more complicated than suggested by the equation, however, because

[7]For further reading, see J. D. Ingle, Jr., and S. R. Crouch, *Spectrochemical Analysis*, Ch. 5, Englewood Cliffs, NJ: Prentice Hall, 1988; J. Galbán, S. de Marcos, I. Sanz, C. Ubide, and J.Zuriarrain. *Anal. Chem.*, **2007**, *79*, 4763, **DOI:** 10.1021/ac071933h.

TABLE 26-4

Categories of Instrumental Indeterminate Errors in Transmittance Measurements

Category	Sources	Effect of T on Relative Standard Deviation in Concentration
$\sigma_T = k_1$	Readout resolution, thermal detector noise, dark current, and amplifier noise	$\frac{\sigma_c}{c} = \frac{0.434}{\log T}\left(\frac{k_1}{T}\right)$ (26-9)
$\sigma_T = k_2\sqrt{T^2 + T}$	Photon detector shot noise	$\frac{\sigma_c}{c} = \frac{0.434}{\log T} \times k_2\sqrt{1 + \frac{1}{T}}$ (26-10)
$\sigma_T = k_3 T$	Cell positioning uncertainty, fluctuations in source intensity	$\frac{\sigma_c}{c} = \frac{0.434}{\log T} \times k_3$ (26-11)

Note: σ_T is the standard deviation of the transmittance, σ_c/c is the relative standard deviation in concentration, T is transmittance, and k_1, k_2, and k_3 are constants for a given instrument.

Uncertainties in spectrophotometric concentration measurements depend on the magnitude of the transmittance (absorbance) in a complex way. The uncertainties can be independent of T, proportional to $\sqrt{T^2 + T}$, or proportional to T.

the uncertainty σ_T is, under many circumstances, also dependent on T. In a detailed theoretical and experimental study, Rothman, Crouch, and Ingle[8] described several sources of instrumental random errors and showed the net effect of these errors on the precision of concentration measurements. The errors fall into three categories: those for which the magnitude of σ_T is (1) independent of T, (2) proportional to $\sqrt{T^2 + T}$, and (3) proportional to T. Table 26-4 summarizes information about these sources of uncertainty. When the three relationships for σ_T in the first column are substituted into Equation 26-8, we obtain three equations for the relative standard deviation in concentration σ_c/c. These derived equations are shown in the third column of Table 26-4.

Concentration Errors When $\sigma_T = k_1$. For many photometers and spectrophotometers, the standard deviation in the measurement of T is constant and independent of the magnitude of T. We often see this type of random error in direct-reading instruments with analog meter readouts, which have somewhat limited resolution. The size of a typical scale is such that a reading cannot be reproduced to better than a few tenths of a percent of the full-scale reading, and the magnitude of this uncertainty is the same from one end of the scale to the other. For typical inexpensive instruments, we find standard deviations of about 0.003 ($\sigma_T = \pm 0.003$).

EXAMPLE 26-4

A spectrophotometric analysis was performed with an instrument that exhibited an absolute standard deviation of ±0.003 throughout its transmittance range. Find the relative standard deviation in concentration if the analyte solution has an absorbance of (a) 1.000 and (b) 2.000.

Solution

(a) To convert absorbance to transmittance, we write

$$\log T = -A = -1.000$$

$$T = \text{antilog}(-1.000) = 0.100$$

[8] L. D. Rothman, S. R. Crouch, and J. D. Ingle, Jr., *Anal. Chem.*, **1975,** *47,* 1226, **DOI:** 10.1021/ac60358a029.

For this instrument, $\sigma_T = k_1 = \pm 0.003$ (see first entry in Table 26-4). Substituting this value and $T = 0.100$ into Equation 26-8 yields

$$\frac{\sigma_c}{c} = \frac{0.434}{\log 0.100}\left(\frac{\pm 0.003}{0.100}\right) = \pm 0.013 \quad (1.3\%)$$

(b) At $A = 2.000$, $T = \text{antilog}(-2.000) = 0.010$

$$\frac{\sigma_c}{c} = \frac{0.434}{\log 0.010}\left(\frac{\pm 0.003}{0.010}\right) = \pm 0.065 \quad (6.5\%)$$

The data plotted as curve *A* in **Figure 26-10** were obtained from calculations similar to those in Example 26-4. Note that the relative standard deviation in concentration passes through a minimum at an absorbance of about 0.5 and rises rapidly when the absorbance is less than about 0.1 or greater than approximately 1.5.

Figure 26-11a is a plot of the relative standard deviation for experimentally determined concentrations as a function of absorbance. It was obtained with a spectrophotometer similar to the one shown in Figure 25-19 but with an old-fashioned analog panel meter rather than a digital readout. The striking similarity between this curve and curve *A* in Figure 26-10 indicates that the instrument studied is affected by an absolute indeterminate error in transmittance of about ±0.003 and that this error is independent of transmittance. The source of this uncertainty is probably the limited resolution of the manual transmittance scale. A digital readout with sufficient resolution, such as that shown in Figure 25-19, is less susceptible to this type of error.

Many infrared spectrophotometers also exhibit an indeterminate error that is independent of transmittance. The source of the error in these instruments lies in the thermal detector. Fluctuations in the output of this type of transducer are independent of the output; indeed, fluctuations are observed even in the absence of radiation. An experimental plot of data from an infrared spectrophotometer is similar in appearance to Figure 26-11a. The curve is displaced upward, however, because of the greater standard deviation characteristic of infrared measurements.

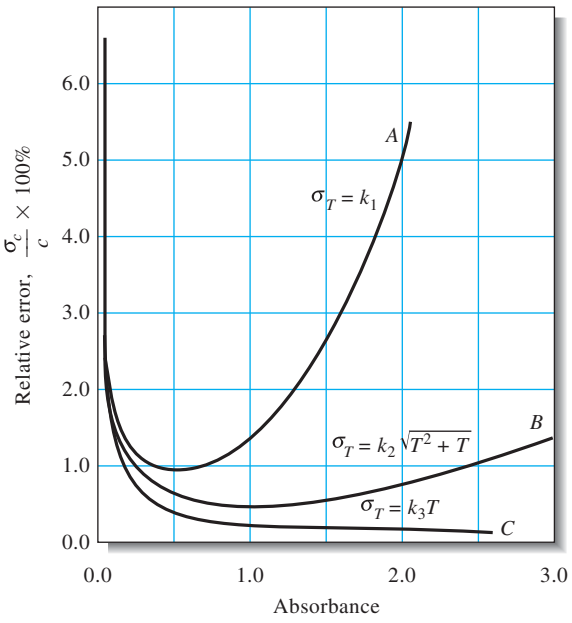

Figure 26-10 Error curves for various categories of instrumental uncertainties.

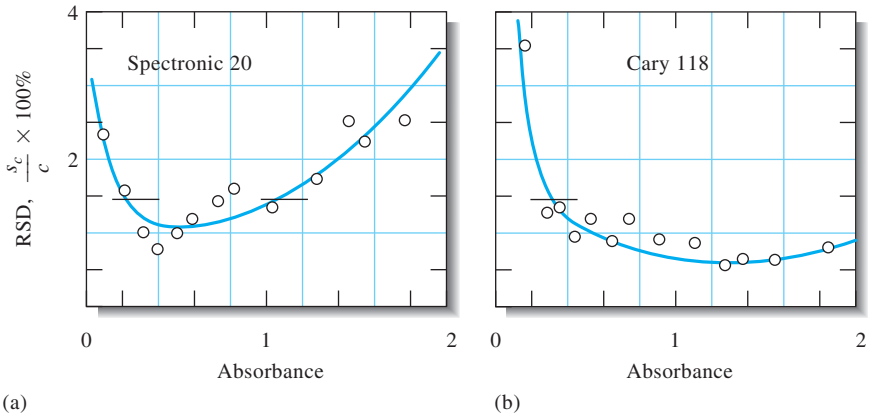

Figure 26-11 Experimental curves relating relative concentration uncertainties to absorbance for two spectrophotometers. Data obtained with (a) a Spectronic 20, a low-cost instrument (see Figure 25-19), and (b) a Cary 118, a research-quality instrument. (W. E. Harris and B. Kratochvil, An *Introduction to Chemical Analysis*, p. 384. Philadelphia: Saunders College Publishing, 1981. Reprinted by permission of the authors.)

Concentration Errors When $\sigma_T = k_2\sqrt{T^2 + T}$. This type of random uncertainty is characteristic of the highest-quality spectrophotometers. It has its origin in the shot noise that causes the output of photomultipliers and phototubes to fluctuate randomly about a mean value. Equation 26-10 in Table 26-4 describes the effect of shot noise on the relative standard deviation of concentration measurements. A plot of this relationship appears as curve *B* in Figure 26-10. We calculated these data assuming that $k_2 = \pm 0.003$, a value that is typical for high-quality spectrophotometers.

Figure 26-11b shows an analogous plot of experimental data obtained with a high-quality research-type ultraviolet/visible spectrophotometer. Note that, in contrast to the less expensive instrument, absorbances of 2.0 or greater can be measured here without serious deterioration in the quality of the data.

Concentration Errors When $\sigma_T = k_3 T$. Substituting $\sigma_T = k_3 T$ into Equation 26-8 reveals that the relative standard deviation in concentration from this type of uncertainty is inversely proportional to the logarithm of the transmittance (Equation 26-11 in Table 26-4). Curve *C* in Figure 26-10, which is a plot of Equation 25-11, reveals that this type of uncertainty is important at low absorbances (high transmittances) but approaches zero at high absorbances.

At low absorbances, the precision obtained with high-quality double-beam instruments is often described by Equation 26-11. The source of this behavior is failure to position cells reproducibly with respect to the beam during replicate measurements. This position dependence is probably the result of small imperfections in the cell windows, which cause reflective losses and transparency to differ from one area of the window to another.

It is possible to evaluate Equation 26-11 by comparing the precision of absorbance measurements made in the usual way with measurements in which the cells are left undisturbed at all times with replicate solutions being introduced with a syringe. Experiments of this kind with a high-quality spectrophotometer yielded a value of 0.013 for k_3.[9] Curve *C* in Figure 26-10 was obtained by substituting this numerical value into Equation 26-11. Cell positioning errors affect all types of spectrophotometric measurements in which cells are repositioned between measurements.

Fluctuations in source intensity also yield standard deviations that are described by Equation 26-11. This type of behavior sometimes occurs in inexpensive single-beam instruments that have unstable power supplies and in infrared instruments.

[9]L. D. Rothman, S. R. Crouch, and J. D. Ingle, Jr., *Anal. Chem.,* **1975,** *47,* 1226, **DOI:** 10.1021/ac60358a029.

Spreadsheet Summary In Chapter 12 of *Applications of Microsoft® Excel in Analytical Chemistry*, 2nd ed., we explore errors in spectrophotometric measurements by simulating error curves such as those shown in Figures 26-10 and 26-11.

26A-4 Photometric and Spectrophotometric Titrations

Photometric and spectrophotometric measurements are useful for locating the equivalence points of titrations.[10] This application of absorption measurements requires that one or more of the reactants or products absorb radiation or that an absorbing indicator be added to the analyte solution.

Titration Curves

A photometric titration curve is a plot of absorbance (corrected for volume change) as a function of titrant volume. If conditions are chosen properly, the curve consists of two straight-line regions with different slopes, one occurring prior to the equivalence point of the titration and the other located well beyond the equivalence-point region. The end point is taken as the intersection of extrapolated linear portions of the two lines.

Figure 26-12 shows typical photometric titration curves. Figure 26-12a is the curve for the titration of a nonabsorbing species with an absorbing titrant that reacts with the titrant to form a nonabsorbing product. An example is the titration of thiosulfate ion with triiodide ion. The titration curve for the formation of an absorbing product from nonabsorbing reactants is shown in Figure 26-12b. An example is the titration of iodide ion with a standard solution of iodate ion to form triiodide. The remaining figures illustrate the curves obtained with various combinations of absorbing analytes, titrants, and products.

To obtain titration curves with linear portions that can be extrapolated, the absorbing system(s) must obey Beer's law. In addition, absorbances must be corrected for volume changes by multiplying the observed absorbance by $(V + v)/V$, where V is the original volume of the solution and v is the volume of added titrant. In some cases, adequate end points can be obtained even for systems in which Beer's law is not strictly obeyed. An abrupt change in the slope of the titration curve signals the location of the end-point volume.

Instrumentation

Photometric titrations are usually performed with a spectrophotometer or a photometer that has been modified so that the titration vessel is held stationary in the light path. After the instrument is set to a suitable wavelength or an appropriate filter is inserted, the 0% T adjustment is made in the usual way. With radiation passing through the analyte solution to the detector, the instrument is then adjusted to a convenient absorbance reading by varying the source intensity or the detector sensitivity. It is not usually necessary to measure the true absorbance since relative values are adequate for end-point detection. Titration data are then collected without changing the instrument settings. The power of the radiation source and the response of the detector must remain constant during a photometric titration. Cylindrical containers are often used in photometric titrations, and it is important to avoid moving the cell

[10] For further information, see J. B. Headridge, *Photometric Titrations,* New York: Pergamon Press, 1961.

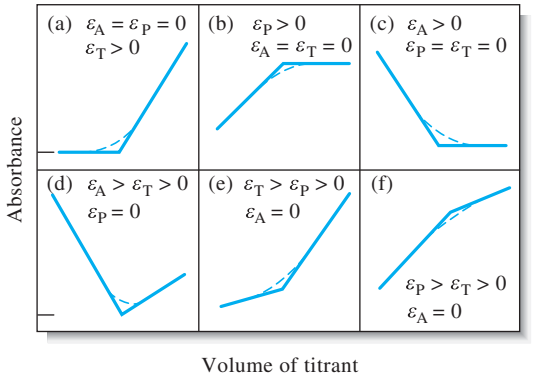

Figure 26-12 Typical photometric titration curves. Molar absorptivities of the substance titrated, the product, and the titrant are ε_s, ε_p, and ε_t, respectively.

so that the path length remains constant. Both filter photometers and spectrophotometers have been used for photometric titrations.

Applications of Photometric Titrations

Photometric titrations are often more accurate than direct photometric determinations. ›

Photometric titrations often provide more accurate results than a direct photometric determination because the data from several measurements are used to determine the end point.

Furthermore, the presence of other absorbing species may not interfere since only a change in absorbance is being measured.

An advantage of end points determined from linear-segment photometric titration curves is that the experimental data are collected well away from the equivalence-point region where the absorbance changes gradually. Consequently, the equilibrium constant for the reaction need not be as large as that required for a sigmoidal titration curve that depends on observations near the equivalence point (for example, potentiometric or indicator end points). For the same reason, more dilute solutions may be titrated using photometric detection.

The photometric end point has been applied to many types of reactions. For example, most standard oxidizing agents have characteristic absorption spectra and thus produce photometrically detectable end points. Although standard acids or bases do not absorb, the introduction of acid/base indicators permits photometric neutralization titrations. The photometric end point has also been used to great advantage in titrations with EDTA and other complexing agents. **Figure 26-13** illustrates the application of this technique to the successive titration of bismuth(III) and copper(II). At 745 nm, the cations, the reagent, and the bismuth complex formed do not absorb but the copper complex does. Thus, during the first segment of the titration when the bismuth-EDTA complex is being formed ($K_f = 6.3 \times 10^{22}$), the solution exhibits no absorbance until essentially all the bismuth has been titrated. With the first formation of the copper complex ($K_f = 6.3 \times 10^{18}$), an increase in absorbance occurs. The increase continues until the copper equivalence point is reached. Further additions of titrant cause no additional absorbance change. Two well-defined end points result as shown in Figure 26-13.

The photometric end point has also been adapted to precipitation titrations. The suspended solid product causes a decrease in the radiant power of the light source by scattering from the particles of the precipitate. The equivalence point occurs when the precipitate stops forming, and the amount of light reaching the detector becomes constant. This type of end-point detection is called **turbidimetry** because the amount of light reaching the detector is a measure of the **turbidity** of the solution.

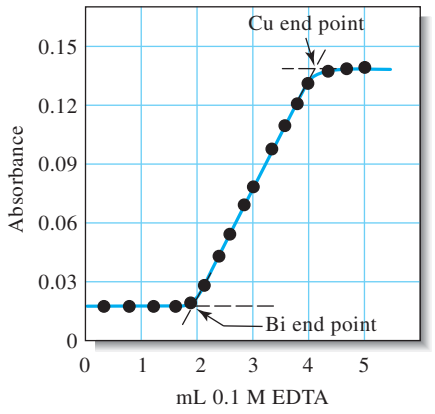

Figure 26-13 Photometric titration curve at 745 nm for 100 mL of a solution that was 2.0×10^{-3} M in Bi^{3+} and Cu^{2+}. (Reprinted with permission from A. L. Underwood, *Anal. Chem.*, **1954**, 26, 1322, **DOI**: 10.1021/ac60092a017. Copyright 1954 by the American Chemical Society.)

Spreadsheet Summary In Chapter 12 of *Applications of Microsoft® Excel in Analytical Chemistry*, 2nd ed., methods for treating data from spectrophotometric titrations are explored. We analyze titration data using least-squares procedures and use the resulting parameters to compute the concentration of the analyte.

26A-5 Spectrophotometric Studies of Complex Ions

The composition of a complex in solution can be determined without actually isolating the complex as a pure compound.

Spectrophotometry is a valuable tool for determining the composition of complex ions in solution and for determining their formation constants. The power of the technique lies in the fact that quantitative absorption measurements can be performed without disturbing the equilibria under consideration. Although in many spectrophotometric studies of systems of complexes, a reactant or a product absorbs, nonabsorbing systems can also be investigated successfully. For example, the composition and formation constant for a complex of iron(II) and a nonabsorbing ligand may often be determined by measuring the absorbance decreases that occur when solutions of the absorbing iron(II) complex of 1,10-phenanthroline are mixed with various amounts of the nonabsorbing ligand. The success of this approach depends on the well-known values of the formation constant ($K_f = 2 \times 10^{21}$) and the composition of the 1,10-phenanthroline (3:1) complex of iron(II).

The three most common techniques used for complex-ion studies are (1) the method of continuous variations, (2) the mole-ratio method, and (3) the slope-ratio method. We illustrate these methods for metal ion-ligand complexes, but the principles apply to other types.

The Method of Continuous Variations

In the method of continuous variations, cation and ligand solutions with identical analytical concentrations are mixed in such a way that the total volume and the total moles of reactants in each mixture are constant but the mole ratio of reactants varies systematically (for example, 1:9, 8:2, 7:3, and so forth). The absorbance of each solution is then measured at a suitable wavelength and corrected for any absorbance the mixture might exhibit if no reaction had occurred. The corrected absorbance is plotted against the volume fraction of one reactant, that is, $V_M/(V_M + V_L)$, where V_M is the volume of the cation solution and V_L is the volume of the ligand solution. A typical continuous-variations plot is shown in **Figure 26-14**. A maximum (or minimum if the complex absorbs less than the reactants) occurs at a volume ratio V_M/V_L, corresponding to the combining ratio of metal ion and ligand in the complex. In Figure 26-14,

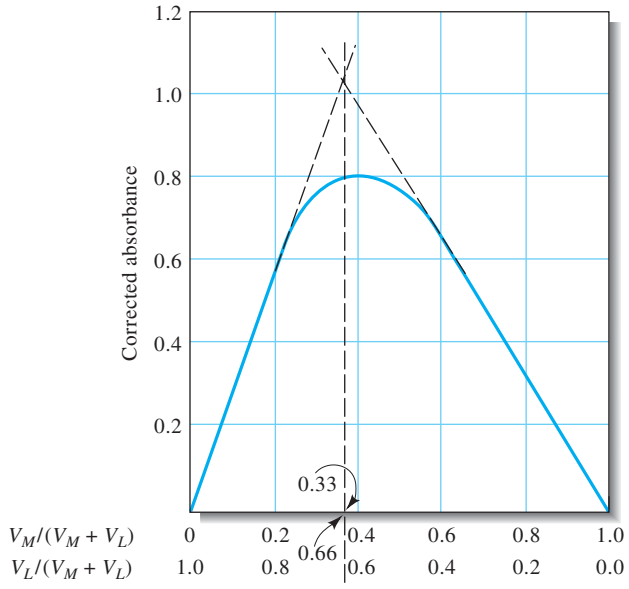

Figure 26-14 Continuous-variation plot for the 1:2 complex ML_2.

$V_M/(V_M + V_L)$ is 0.33, and $V_L/(V_M + V_L)$ is 0.66; thus, V_M/V_L is 0.33/0.66, suggesting that the complex has the formula ML_2.

The curvature of the experimental lines in Figure 26-14 is the result of incompleteness of the complex-formation reaction. A formation constant for the complex can be evaluated from measurements of the deviations from the theoretical straight lines, which represent the curve that would result if the reaction between the ligand and the metal proceeded to completion.

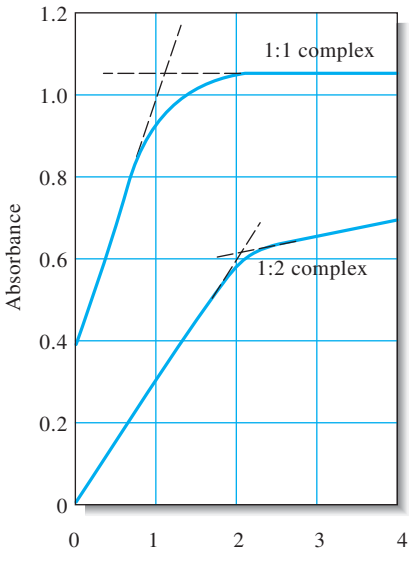

Figure 26-15 Mole-ratio plots for a 1:1 and a 1:2 complex. The 1:2 complex is the more stable of the two complexes as indicated by closeness of the experimental curve to the extrapolated lines. The closer the curve is to the extrapolated lines, the larger the formation constant of the complex; the larger the deviation from the straight lines, the smaller the formation constant of the complex.

The Mole-Ratio Method

In the mole-ratio method, a series of solutions is prepared in which the analytical concentration of one reactant (usually the metal ion) is held constant while that of the other is varied. A plot of absorbance versus mole ratio of the reactants is then prepared. If the formation constant is reasonably favorable, two straight lines of different slopes that intersect at a mole ratio that corresponds to the combining ratio in the complex are obtained. Typical mole-ratio plots are shown in **Figure 26-15**. Notice that the ligand of the 1:2 complex absorbs at the wavelength selected so that the slope beyond the equivalence point is greater than zero. We deduce that the uncomplexed cation of the 1:1 complex absorbs because the initial point has an absorbance greater than zero.

Formation constants can be evaluated from the data in the curved portion of mole-ratio plots where the reaction is least complete.

EXAMPLE 26-5

Derive equations to calculate the equilibrium concentrations of all the species in the 1:2 complex-formation reaction illustrated in Figure 26-15.

Derivation

Two mass-balance expressions based on the preparatory data can be written. Thus, for the reaction

$$M + 2L \rightleftharpoons ML_2$$

we can write

$$c_M = [M] + [ML_2]$$

$$c_L = [L] + 2[ML_2]$$

where c_M and c_L are the molar concentrations of M and L before reaction occurs. For 1-cm cells, the absorbance of the solution is

$$A = \varepsilon_M[M] + \varepsilon_L[L] + \varepsilon_{ML_2}(ML_2)$$

From the mole-ratio plot, we see that $\varepsilon_M = 0$. Values for ε_{ML} and ε_{ML_2} can be obtained from the two straight-line portions of the curve. With one or more measurements of A in the curved region of the plot, sufficient data are available to calculate the three equilibrium concentrations and thus the formation constant.

A mole-ratio plot may reveal the stepwise formation of two or more complexes as successive slope changes if the complexes have different molar absorptivities and their formation constants are sufficiently different from each other.

The Slope-Ratio Method

The slope-ratio approach is particularly useful for weak complexes but is applicable only to systems in which a single complex is formed. The method assumes (1) that the complex-formation reaction can be forced to completion by a large excess of either reactant, (2) that Beer's law is followed under these circumstances, and (3) that only the complex absorbs at the wavelength chosen.

Consider the reaction in which the complex M_xL_y is formed by the reaction of x moles of the cation M with y moles of a ligand L:

$$xM + yL \rightleftharpoons M_xL_y$$

Mass-balance expressions for this system are

$$c_M = [M] + x[M_xL_y]$$

$$c_L = [L] + y[M_xL_y]$$

where c_M and c_L are the molar analytical concentrations of the two reactants. We now assume that, at very high analytical concentrations of L, the equilibrium is shifted far to the right and $[M] \ll x[M_xL_y]$. Under this condition, the first mass-balance expression simplifies to

$$c_M = x[M_xL_y]$$

If the system obeys Beer's law,

$$A_1 = \varepsilon b[M_xL_y] = \varepsilon b c_M/x$$

where ε is the molar absorptivity of M_xL_y and b is the path length. A plot of absorbance as a function of c_M is linear when there is sufficient L present to justify the assumption that $[M] \ll x[M_xL_y]$. The slope of this plot is $\varepsilon b/x$.

When c_M is made very large, we assume that $[L] \ll y[M_xL_y]$, and the second mass-balance equation reduces to

$$c_L = y[M_xL_y]$$

and

$$A_2 = \varepsilon b[M_xL_y] = \varepsilon b c_L/y$$

Again, if our assumptions are valid, we find that a plot of A versus c_L is linear at high concentrations of M. The slope of this line is $\varepsilon b/y$.

The ratio of the slopes of the two straight lines gives the combining ratio between M and L:

$$\frac{\varepsilon b/x}{\varepsilon b/y} = \frac{y}{x}$$

Spreadsheet Summary In Chapter 12 of *Applications of Microsoft® Excel in Analytical Chemistry*, 2nd ed., we investigate the method of continuous variations using the slope and intercept functions and learn how to produce inset plots.

26B AUTOMATED PHOTOMETRIC AND SPECTROPHOTOMETRIC METHODS

The first fully automated instrument for chemical analysis (the Technicon AutoAnalyzer®) appeared on the market in 1957. This instrument was designed to fulfill the needs of clinical laboratories where blood and urine samples are routinely analyzed for a dozen or more chemical species. The number of such analyses demanded by modern medicine is enormous, so it is necessary to keep their cost at a reasonable level. These two considerations motivated the development of analytical systems that perform several analyses simultaneously with a minimum input of human labor. The use of automatic instruments has spread from clinical laboratories to laboratories for the control of industrial processes and the routine determination of a wide spectrum of species in air, water, soils, and pharmaceutical and agricultural products. In the majority of these applications, the measurement step in the analyses is accomplished by photometry, spectrophotometry, or fluorometry.

In Section 8C, we described various automated sample handling techniques including discrete and continuous flow methods. In this section, we explore the instrumentation and two applications of flow-injection analysis (FIA) with photometric detection.

26B-1 Instrumentation

Figure 26-16a is a flow diagram of the simplest of all flow-injection systems. In this example, a colorimetric reagent for chloride ion is pumped by a peristaltic pump directly into a valve that permits injection of samples into the flowing stream. The sample and reagent then pass through a 50-cm reactor coil where the reagent mixes with the sample plug and produces a colored product by the sequence of reaction

$$Hg(SCN)_2(aq) + 2Cl^- \rightleftharpoons HgCl_2(aq) + 2SCN^-$$

$$Fe^{3+} + SCN^- \rightleftharpoons \underset{\text{red}}{Fe(SCN)^{2+}}$$

From the reactor coil, the solution passes into a flow-through photometer equipped with a 480-nm interference filter for absorbance measurement.

The signal output from this system for a series of standards containing from 5 to 75 ppm of chloride is shown in Figure 26-16b. Notice that four injections of each standard were made to demonstrate the reproducibility of the system. The two

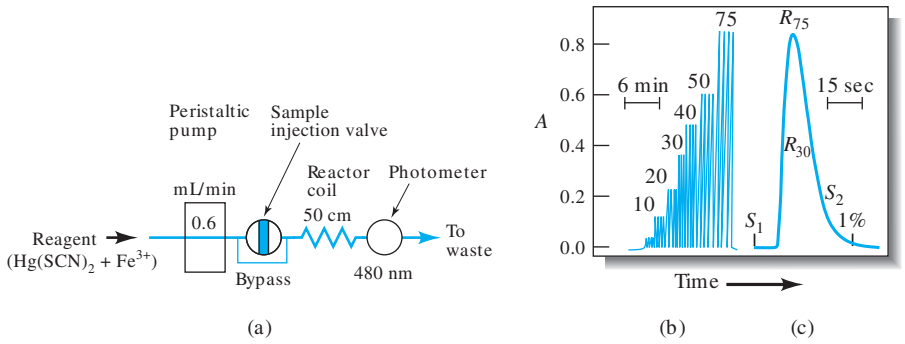

Figure 26-16 Flow-injection determination of chloride: (a) Flow diagram. (b) Recorder readout for quadruplicate runs on standards containing 5 to 75 ppm of chloride ion. (c) Fast scan of two of the standards to demonstrate the low analyte carryover (less than 1%) from run to run. Notice that the point marked 1% corresponds to where the response would just begin for a sample injected at time S_2. (Reprinted with permission from E. H. Hansen and J. Ruzicka, *J. Chem. Educ.*, **1979**, 56, 677, **DOI**: 10.1021/ ed056p677. Copyright by the American Chemical Society.)

curves in Figure 26-16c are high-speed recorder scans of one of the samples containing 30 ppm (R_{30}) and another containing 75 ppm (R_{75}) chloride. These curves demonstrate that cross-contamination between successive samples is minimal in this unsegmented stream. Thus, less than 1% of the first analyte is present in the flow cell after 28 s, the time of the next injection (S_2). This system has been successfully used for the routine determination of chloride ion in brackish and waste waters as well as in serum samples.

Sample and Reagent Transport System

Normally, the solution in a flow-injection analysis is pumped through flexible tubing in the system by a peristaltic pump, a device in which a fluid (liquid or gas) is squeezed through plastic tubing by rollers. **Figure 26-17** illustrates the operating principle of the peristaltic pump. The spring-loaded cam, or band, pinches the tubing against two or more of the rollers at all times, thus forcing a continuous flow of fluid through the tubing. These pumps generally have 8 to 10 rollers, arranged in a circular configuration so that half are squeezing the tube at any instant. This design leads to a flow that is relatively pulse free. The flow rate is controlled by the speed of the motor, which should be greater than 30 rpm, and the inside diameter of the tube. A wide variety of tube sizes (i.d. = 0.25 to 4 mm) are available commercially that permit flow rates as small as 0.0005 mL/min and as great as 40 mL/min. The rollers of typical commercial peristaltic pumps are long enough so that several reagent and sample streams can be pumped simultaneously. Syringe pumps and electroosmosis are also used to induce flow in flow-injection systems. Flow-injection systems have been miniaturized through the use of fused silica capillaries (i.d. 25-100 μm) or through **lab-on-a-chip** technology (see Feature 8-1).

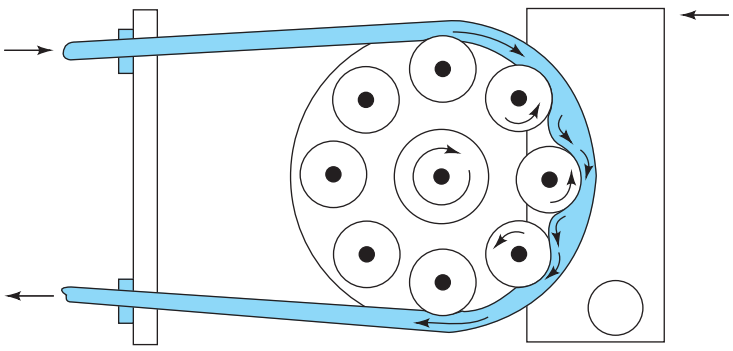

Figure 26-17 Diagram showing one channel of a peristaltic pump. Several additional tubes may be located under the one shown (below the plane of the diagram) to carry multiple channels of reagent or sample. (Reprinted from B. Karl- berg and G. E. Pacey, *Flow Injection Analysis. A Practical Guide*, New York: Elsevier, 1989, p. 34 with permission from Elsevier.)

Sample Injectors and Detectors

Sample sizes for flow-injection analysis range from 5 to 200 μL, with 10 to 30 μL being typical for most applications. For a successful determination, it is important to inject the sample solution rapidly as a plug, or pulse, of liquid; in addition, the injections must not disturb the flow of the carrier stream. The most useful and convenient injector systems are based on sampling loops similar to those used in chromatography (see, for example, Figure 33-6). The method of operation of a sampling loop is illustrated in Figure 26-16a. With the valve of the loop in the position shown, reagents flow through the bypass. When a sample has been injected into the loop and the valve turned 90 deg, the sample enters the flow as a single, well-defined zone. For all practical purposes, flow through the bypass ceases with the valve in this position because the diameter of the sample loop is significantly greater than that of the bypass tubing.

Flow-injection analyzers can be fairly simple, consisting of a pump, an injection valve, plastic tubing, and a detector. Filter photometers and spectrophotometers are the most common detectors.

The most common detectors in flow-injection analysis are spectrophotometers, photometers, and fluorometers. Electrochemical systems, refractometers, atomic emission, and atomic absorption spectrometers have also been used.

Advanced Flow-Injection Techniques[11]

Flow-injection methods have been used to accomplish separations, titrations, and kinetic methods. In addition, several variations of flow injection have been shown to be useful. These include flow reversal FIA, sequential injection FIA, and lab-on-a-valve technology.

Separations by dialysis, by liquid/liquid extraction, and by gaseous diffusion can be accomplished automatically with flow-injection systems.

26B-2 A Typical Application of Flow-Injection Analysis

Figure 26-18 illustrates a flow-injection system designed for the automatic spectrophotometric determination of caffeine in acetyl salicylic acid drug preparations after extraction of the caffeine into chloroform. The chloroform solvent, after cooling in an ice bath to minimize evaporation, is mixed with the alkaline sample stream in a T-tube (see lower insert). After passing through the 2-m extraction coil, the mixture enters a T-tube separator, which is differentially pumped so that about 35% of the organic phase containing the caffeine passes into the flow cell, the other 65% accompanying the aqueous solution containing the rest of the sample to waste. In order to avoid contaminating the flow cell with water, Teflon fibers, which are not wetted by water, are twisted into a thread and inserted in the inlet to the T-tube in such a way as to form a smooth downward bend. The chloroform flow then follows this bend to the photometer cell where the caffeine concentration is determined based on its absorption peak at 275 nm. The output of the photometer is similar in appearance to that shown in Figure 26-16b.

26C INFRARED ABSORPTION SPECTROSCOPY

Infrared spectroscopy is a powerful tool for identifying pure organic and inorganic compounds because, with the exception of a few homonuclear molecules such as O_2, N_2, and Cl_2, all molecular species absorb infrared radiation. In addition, with the exception of chiral molecules in the crystalline state, every molecular compound has a unique infrared absorption spectrum. Therefore, an exact match between the

[11] For more information on FIA methods, see D. A. Skoog, F. J. Holler, and S. R. Crouch, *Principles of Instrumental Analysis,* 6th ed., Belmont, CA: Brooks/Cole, 2007, pp. 933–41.

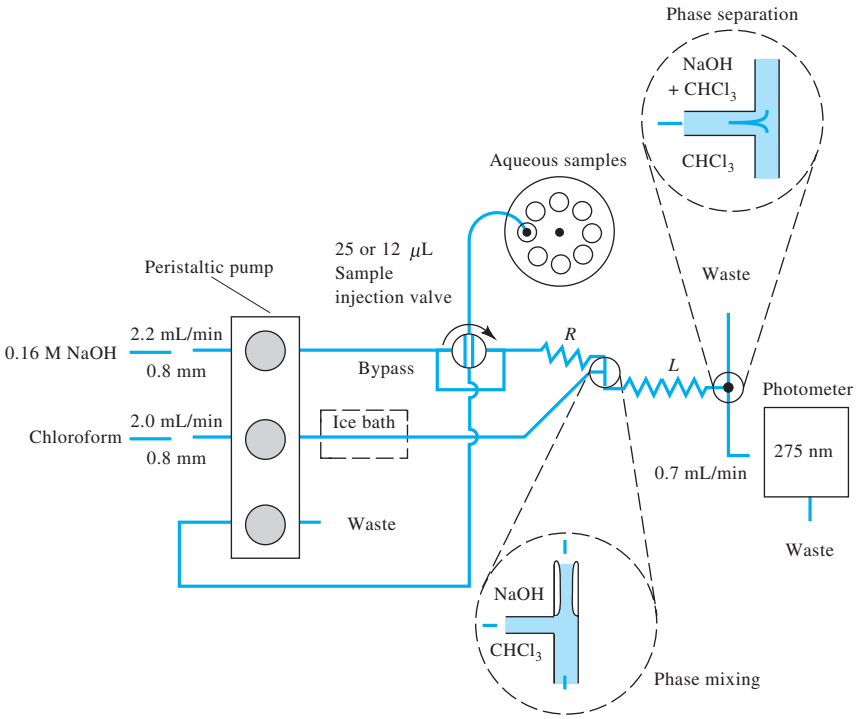

Figure 26-18 Flow-injection apparatus for the determination of caffeine in acetylsalicylic acid preparations. With the valve rotated at 90 deg, the flow in the bypass is essentially zero because of its small diameter. *R* and *L* are Teflon coils with 0.8-mm inside diameters; *L* has a length of 2 m, and the distance from the injection point through *R* to the mixing point is 0.15 m. (Reprinted from B. Karlberg and S. Thelander, *Anal. Chim. Acta*, **1978**, 98, 2, **DOI**: 10.1016/S0003-2670(01)83231-1 with permission from Elsevier.)

spectrum of a compound of known structure and the spectrum of an analyte unambiguously identifies the analyte.

Infrared spectroscopy is a less satisfactory tool for quantitative analyses than its ultraviolet and visible counterparts because of lower sensitivity and frequent deviations from Beer's law. Additionally, infrared absorbance measurements are considerably less precise. Nevertheless, in instances where modest precision is adequate, the unique nature of infrared spectra provides a degree of selectivity in a quantitative measurement that may offset these undesirable characteristics.[12]

26C-1 Infrared Absorption Spectra

The energy of infrared radiation can excite vibrational and rotational transitions, but it is insufficient to excite electronic transitions. As shown in **Figure 26-19**, infrared spectra exhibit narrow, closely spaced absorption peaks resulting from transitions among the various vibrational quantum levels. Variations in rotational levels may also give rise to a series of peaks for each vibrational state. With liquid or solid samples, however, rotation is often hindered or prevented, and the effects of these small energy differences are not detected. Thus, a typical infrared spectrum for a liquid, such as that in Figure 26-19, consists of a series of vibrational bands.

The number of ways a molecule can vibrate is related to the number of atoms, and thus the number of bonds, it contains. For even a simple molecule, the number of possible vibrations is large. For example, *n*-butanal ($CH_3CH_2CH_2CHO$) has 33 vibrational modes, most differing from each other in energy. Not all of these vibrations produce infrared peaks, but, as shown in Figure 26-19, the spectrum for *n*-butanal is relatively complex.

[12] For a detailed discussion of infrared spectroscopy, see N. B. Colthup, L. H. Daly, and S. E. Wiberley, *Introduction to Infrared and Raman Spectroscopy*, 3rd ed., New York: Academic Press, 1990.

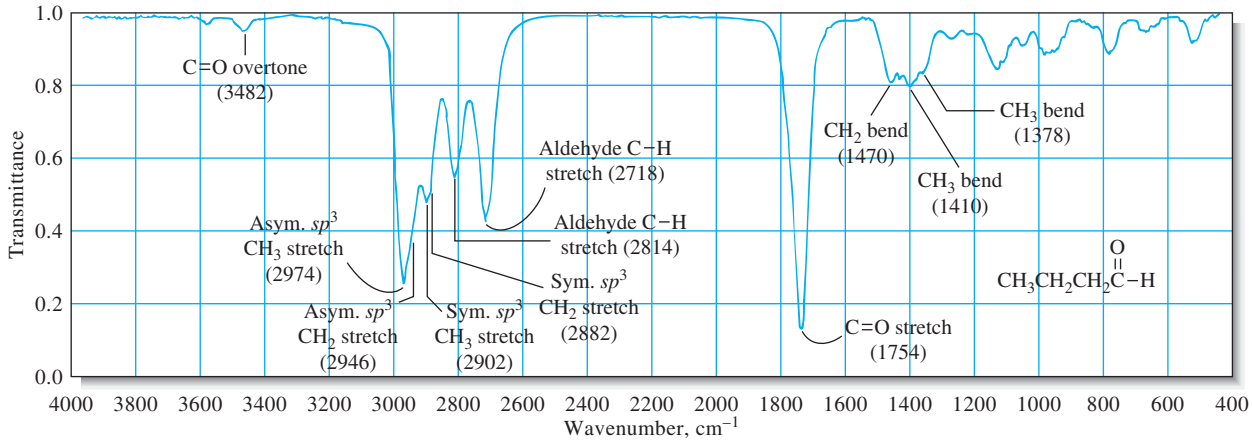

Figure 26-19 Infrared spectrum for *n*-butanal (*n*-butyraldehyde). The vertical scale is plotted as transmittance, as has been common practice in the past. The horizontal scale is linear in wavenumbers, which is proportional to frequency and thus energy. Most modern IR spectrometers are capable of providing data plotted as either transmittance or absorbance on the vertical axis and wavenumber or wavelength on the horizontal axis. IR spectra are usually plotted with frequency increasing from right to left, which is a historical artifact. Early IR spectrometers produced spectra with wavelength increasing from left to right, which led to an auxiliary frequency scale from right to left. Note that several of the bands have been labeled with assignments of the vibrations that produce the bands. Data from NIST Mass Spec Data Center, S. E. Stein, director, "Infrared Spectra," in NIST Chemistry WebBook, NIST Standard Reference Database Num- ber 69, P. J. Linstrom and W .G. Mallard, eds., Gaithersburg MD: National Institute of Standards and Technology, March 2003 (http:// webbook.nist.gov).

Molecular model of *n*-butanal.

Infrared absorption occurs not only with organic molecules but also with covalently bonded metal complexes, which are generally active in the longer-wavelength infrared region. Infrared studies have provided important information about complex metal ions.

26C-2 Instruments for Infrared Spectrometry

Three types of infrared instruments are found in modern laboratories; dispersive spectrometers (spectrophotometers), Fourier transform spectrometers, and filter photometers. The first two are used for obtaining complete spectra for qualitative identification, while filter photometers are designed for quantitative work. Fourier transform and filter instruments are nondispersive in the sense that neither uses a grating or prism to disperse radiation into its component wavelengths.[13]

Dispersive Instruments

With one difference, dispersive infrared instruments are similar in general design to the double-beam (in time) spectrophotometers shown in Figures 25-20c. The difference lies in the location of the cell compartment with respect to the monochromator. In ultraviolet/visible instruments, cells are always located between the monochromator and the detector in order to avoid photochemical decomposition, which may occur if samples are exposed to the full power of an ultraviolet or visible source. Infrared radiation, in contrast, is not sufficiently energetic to bring about photodecomposition; thus, the cell compartment can be located between the source and the monochromator. This arrangement is advantageous because any scattered radiation generated in the cell compartment is largely removed by the monochromator.

[13] For a discussion of the principles of Fourier transform spectroscopy, see D. A. Skoog, F. J. Holler, and S. R. Crouch, *Principles of Instrumental Analysis,* 6th ed., Belmont, CA: Brooks/Cole, 2007, pp. 439–47.

As shown in Section 25A, the components of infrared instruments differ considerably in detail from those in ultraviolet and visible instruments. Therefore, infrared sources are heated solids rather than deuterium or tungsten lamps, infrared gratings are much coarser than those required for ultraviolet/visible radiation, and infrared detectors respond to heat rather than photons. In addition, the optical components of infrared instruments are constructed from polished solids, such as sodium chloride or potassium bromide.

Fourier Transform Spectrometers

Fourier transform infrared (FTIR) spectrometers offer the advantages of high sensitivity, resolution, and speed of data acquisition (data for an entire spectrum can be obtained in 1 s or less). In the early days of FTIR, instruments were large, intricate, costly devices controlled by expensive laboratory computers. Since the 1980s, the instrumentation has evolved, and the price of spectrometers and computers have dropped dramatically. Today, FTIR spectrometers are commonplace, having replaced older, dispersive instruments in most laboratories.

The FTIR spectrometer is the most common type of IR spectrometer. The great majority of infrared instruments sold today are FTIR systems.

Fourier transform instruments contain no dispersing element, and all wavelengths are detected and measured simultaneously using a Michelson interferometer as we described in Feature 25-7. In order to separate wavelengths, it is necessary to modulate the source signal and pass it through the sample in such a way that it can be recorded as an **interferogram**. The interferogram is subsequently decoded by Fourier transformation, a mathematical operation that is conveniently carried out by the computer, which is now an integral part of all spectrometers. Although the detailed mathematical theory of Fourier transform measurements is beyond the scope of this book, the qualitative treatment presented in Feature 25-7 and in Feature 26-1 should give you an idea of how the IR signal is collected and how spectra are extracted from the data.

An **interferogram** is a recording of the signal produced by a Michelson interferometer. The signal is processed by a mathematical process known as the Fourier transform to produce an IR spectrum.

Figure 26-20 is a photo of a typical benchtop FTIR spectrometer. A personal computer is needed for data acquisition, analysis, and presentation. The instrument is relatively inexpensive (ca. $10,000), has a resolution better than 0.8 cm^{-1}, and achieves a signal-to-noise ratio of 8000 for a five-second measurement. The measured spectrum appears on the computer screen where the included software allows many different display options (%T, A, zoom, peak height, and peak area). Various processing tools, such as baseline correction, spectral subtraction, and spectral interpretation, are featured in the software package. A number of different sampling accessories allow gaseous, liquid, and solid samples to be measured and techniques such as attenuated total reflectance (ATR) to be implemented. Some benchtop FTIR spectrometers are self-contained with a built-in computer for data acquisition, analysis, and presentation. These instruments typically are less flexible in terms of software, display modes, and data storage than units with a separate computer.

A research-quality instrument may cost more than $50,000. It can have a resolution of 0.10 cm^{-1} or better and can exhibit a signal-to-noise ratio of 50,000 or greater for a one-minute measurement period. Research-grade spectrometers typically have multiple scanning ranges (27000 to 15 cm^{-1}) and a variety of scanning velocities. They have excellent wavenumber precision (0.01 cm^{-1}). Research-grade instruments can accommodate numerous sampling modes (solids, gases, liquids, polymers, attenuated total reflectance, diffuse reflectance, and microscope attachments, among others). Typically, a research-grade instrument will be connected to a separate computer, providing a number of advantages. Software and databases of spectra can be installed and used to process spectral data and to match measured spectra to known spectra in the database. In addition, a personal computer provides considerable flexibility for archiving data on CDs or DVDs, and if the computer is connected to a local area network, spectra may

Figure 26-20 Photo of a basic student-grade benchtop FTIR spectrometer. A separate laptop or desktop computer is required. Spectra are recorded in a few seconds and displayed on the computer screen for viewing and interpretation. (Courtesy of Thermo Fisher Scientific Inc)

be transmitted to colleagues or coworkers, and software or firmware upgrades may be conveniently downloaded and installed on the computer or in the spectrometer.

Filter Photometers

Infrared photometers designed to monitor the concentration of air pollutants, such as carbon monoxide, nitrobenzene, vinyl chloride, hydrogen cyanide, and pyridine, are often used to ensure compliance with regulations established by the Occupational Safety and Health Administration (OSHA). Interference filters, each designed for the determination of a specific pollutant, are available. These transmit narrow bands of radiation in the range of 3 to 14 μm. There are also nondispersive spectrometers for monitoring gas streams for a single component.[14]

26C-3 Qualitative Applications of Infrared Spectrometry

An infrared absorption spectrum, even one for a relatively simple compound, often contains a bewildering array of sharp peaks and minima. Peaks useful for the identification of functional groups are located in the shorter-wavelength region of the infrared (from about 2.5 to 8.5 μm), where the positions of the maxima are only slightly affected by the carbon skeleton of the molecule. This region of the spectrum thus abounds with information regarding the overall constitution of the molecule under investigation. **Table 26-5** gives the positions of characteristic maxima for some common functional groups.[15]

Identifying functional groups in a molecule is seldom sufficient to positively identify the compound, and the entire spectrum from 2.5 to 15 μm must be compared with that of known compounds. Collections of spectra are available for this purpose.[16]

---

[14] For more information, see D. A. Skoog, F. J. Holler, and S. R. Crouch, *Principles of Instrumental Analysis,* 6th ed., Belmont, CA: Brooks/Cole, 2007, pp. 447–48.

[15] For more detailed information, see R. M. Silverstein, F. X. Webster, and D. Kiemle, *Spectrometric Identification of Organic Compounds,* 7th ed., Ch. 2, New York: Wiley, 2005.

[16] See *Sadtler Standard Spectra*, Informatics/Sadtler Group, Bio-Rad Laboratories, Philadelphia, PA; C. J. Pouchert, *The Aldrich Library of Infrared Spectra,* 3rd ed., Milwaukee, WI: Aldrich Chemical, 1981; *NIST Chemistry WebBook*, NIST Standard Reference Database Number 69, Gaithersburg, MD: National Institute of Standards and Technology, 2008 (http://webbook.nist.gov).

FEATURE 26-1

Producing Spectra with an FTIR Spectrometer

In Feature 25-7, we described the basic operating principles of the Michelson interferometer and the function of the Fourier transform to produce a frequency spectrum from a measured interferogram. Figure 26F-1 shows an optical diagram for a Michelson interferometer similar to the one in the spectrometer depicted in Figure 26-20. The interferometer is actually two parallel interferometers, one to modulate the IR radiation from the source before it passes through the sample and a second to modulate the red light from the He-Ne laser to provide a reference signal for acquiring data from the IR detector. The output of the detector is digitized and stored in the memory of the instrument computer.

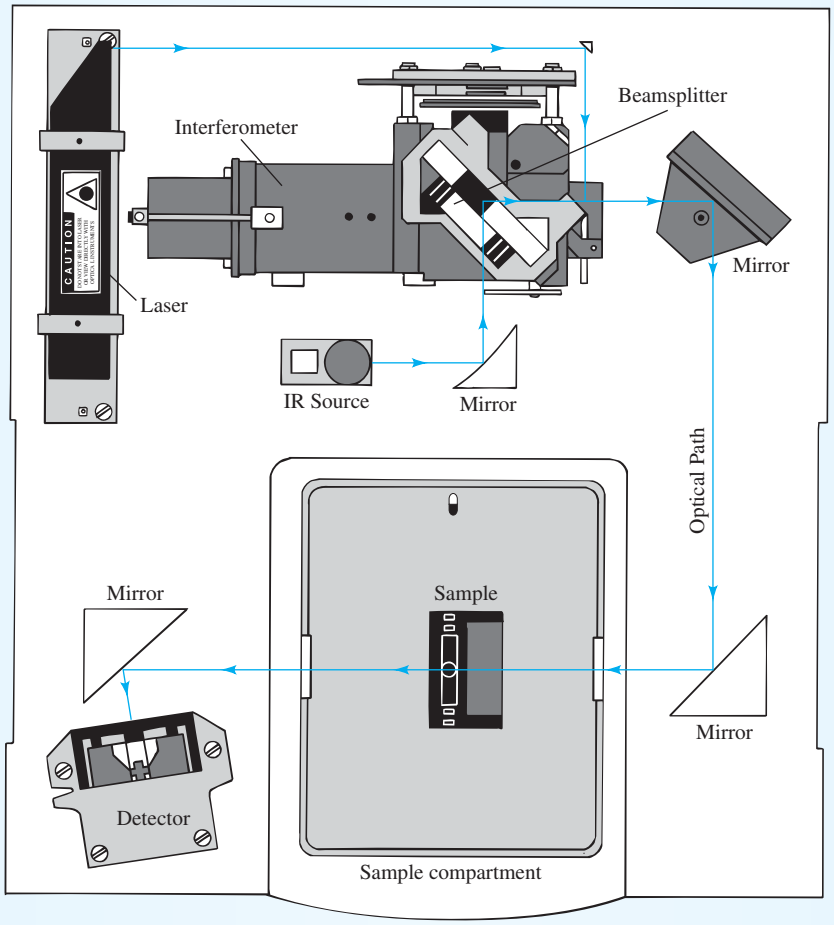

Figure 26F-1 Instrument diagram for a basic FTIR spectrometer. Radiation of all frequencies from the IR source are reflected into the interferometer where it is modulated by the moving mirror on the left. The modulated radiation is then reflected from the two mirrors on the right through the sample in the compartment at the bottom. After passing through the sample, the radiation falls on the detector. A data acquisition system attached to the detector records the signal and stores it in the memory of a computer as an interferogram. (Reprinted by permission of Thermo Fisher Scientific.)

The first step in producing an IR spectrum is to collect and store a reference interferogram with no sample in the sample cell. Then, the sample is placed in the cell, and a second interferogram is collected. Figure 26F-2a shows an interferogram collected using an FTIR spectrometer with methylene chloride, CH_2Cl_2, in the sample cell. The Fourier transform is then applied to the two interferograms to compute the IR spectra of the reference and the sample. The ratio of the two spectra can then be computed to produce an IR spectrum of the analyte such as the one illustrated in Figure 26F-2b.

(*continued*)

Notice that the methylene chloride IR spectrum exhibits little noise. Since a single interferogram can be scanned in only a second or two, many interferograms can be scanned in a relatively short time and summed in the memory of the computer. This process, which is often called **signal averaging**, reduces the noise on the resulting signal and improves the signal-to-noise ratio of the spectrum, as described in Feature 25-5 and illustrated in Figure 25F-4. This capability of noise reduction and speed coupled with Fellgett's advantage and Jacquinot's advantage (see Feature 25-7) makes the FTIR spectrometer a marvelous tool for a broad range of qualitative and quantitative analyses.

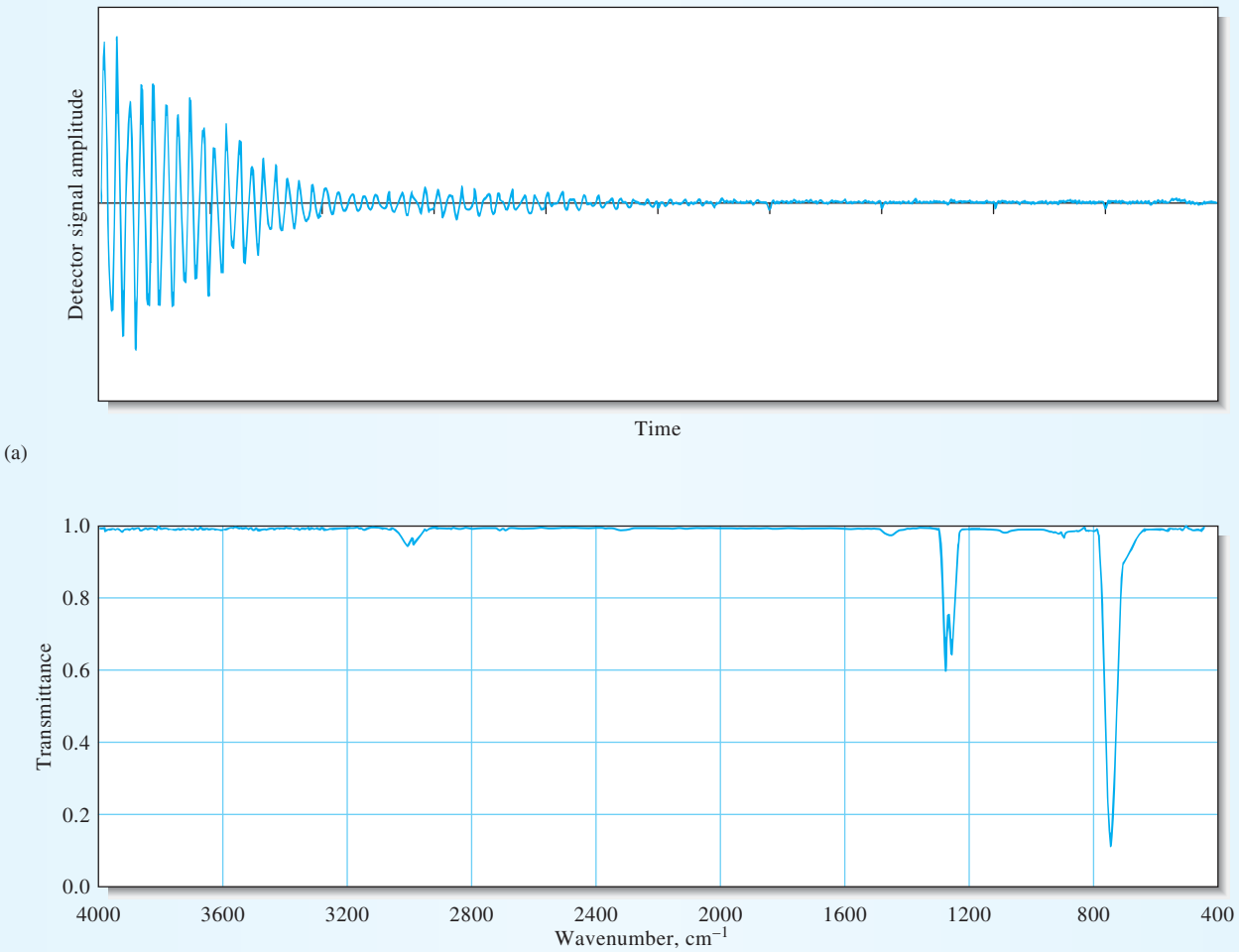

Figure 26F-2 (a) Interferogram obtained from a typical FTIR spectrometer for methylene chloride. The plot shows detector signal output as a function of time, or displacement of the moving mirror of the interferometer. (b) IR spectrum of methylene chloride produced by the Fourier transformation of the data in (a). Note that the Fourier transform takes signal intensity collected as a function of time and produces transmittance as a function of frequency after subtraction of a background interferogram and proper scaling.

26C-4 Quantitative Infrared Spectrometry

Quantitative infrared absorption methods differ somewhat from their ultraviolet and visible counterparts because of the greater complexity of the spectra, the narrowness of the absorption bands, and the capabilities of the instruments available for measurements in this spectral region.[17]

[17]For an extensive discussion of quantitative infrared analysis, see A. L. Smith, in *Treatise on Analytical Chemistry,* 2nd ed., P. J. Elving, E. J. Meehan, and I. M. Kolthoff, eds., Part I, Vol. 7, pp. 415–56, New York: Wiley, 1981.

TABLE 26-5

Some Characteristic Infrared Absorption Peaks

	Functional Group	Absorption Peaks	
		Wavenumber, cm^{-1}	Wavelength, μm
O—H	Aliphatic and aromatic	3600–3000	2.8–3.3
NH_2	Also secondary and tertiary	3600–3100	2.8–3.2
C—H	Aromatic	3150–3000	3.2–3.3
C—H	Aliphatic	3000–2850	3.3–3.5
C≡N	Nitrile	2400–2200	4.2–4.6
C≡C—	Alkyne	2260–2100	4.4–4.8
COOR	Ester	1750–1700	5.7–5.9
COOH	Carboxylic acid	1740–1670	5.7–6.0
C=O	Aldehydes and ketones	1740–1660	5.7–6.0
$CONH_2$	Amides	1720–1640	5.8–6.1
C=C—	Alkene	1670–1610	6.0–6.2
ϕ—O—R	Aromatic	1300–1180	7.7–8.5
R—O—R	Aliphatic	1160–1060	8.6–9.4

Absorbance Measurements

Using matched cuvettes for solvent and analyte is seldom practical for infrared measurements because it is difficult to obtain cells with identical transmission characteristics. Part of this difficulty results from degradation of the transparency of infrared cell windows (typically polished sodium chloride) with use due to attack by traces of moisture in the atmosphere and in samples. In addition, path lengths are hard to reproduce because infrared cells are often less than 1 mm thick. Such narrow cells are required to permit the transmission of measurable intensities of infrared radiation through pure samples or through very concentrated solutions of the analyte. Measurements on dilute analyte solutions, as is done in ultraviolet or visible spectroscopy, are usually difficult because there are few good solvents that transmit over appreciable regions of the IR spectrum.

For these reasons, a reference absorber is often dispensed with entirely in qualitative infrared work, and the intensity of the radiation passing through the sample is simply compared with that of the unobstructed beam; alternatively, a salt plate may be used as a reference. Either way, the resulting transmittance is often less than 100%, even in regions of the spectrum where the sample is totally transparent.

Applications of Quantitative Infrared Spectroscopy

Infrared spectrophotometry offers the potential for determining an unusually large number of substances because nearly all molecular species absorb in the IR region. Moreover, the uniqueness of an IR spectrum provides a degree of specificity that is matched or exceeded by relatively few other analytical methods. This specificity has particular application to the analysis of mixtures of closely related organic compounds.

The recent proliferation of government regulations on atmospheric contaminants has demanded the development of sensitive, rapid, and highly specific methods for a variety of chemical compounds. IR absorption procedures appear to meet this need better than any other single analytical tool.

Table 26-6 illustrates the variety of atmospheric pollutants that can be determined with a simple, portable filter photometer equipped with a separate interference filter for each analyte species. Of the more than 400 chemicals for which maximum tolerable limits have been set by OSHA, half or more have absorption characteristics that make

TABLE 26-6

Examples of Infrared Vapor Analysis for OSHA Compliance*

Compound	Allowable Exposure, ppm†	Wavelength, μm	Minimum Detectable Concentration, ppm‡
Carbon disulfide	4	4.54	0.5
Chloroprene	10	11.4	4
Diborane	0.1	3.9	0.05
Ethylenediamine	10	13.0	0.4
Hydrogen cyanide	4.7§	3.04	0.4
Methyl mercaptan	0.5	3.38	0.4
Nitrobenzene	1	11.8	0.2
Pyridine	5	14.2	0.2
Sulfur dioxide	2	8.6	0.5
Vinyl chloride	1	10.9	0.3

*Courtesy of The Foxboro Company, Foxboro, MA 02035.
†1992–1993 OSHA exposure limits for 8-hr weighted average.
‡For 20.25-m cell.
§Short-term exposure limit:15-min time-weighted average that shall not be exceeded at any time during the work day.

them amenable to determination by infrared photometry or spectrophotometry. With so many compounds absorbing, overlapping peaks are quite common. In spite of this potential disadvantage, the method provides a moderately high degree of selectivity.

WEB WORKS

Locate the *NIST Chemistry WebBook* on the web, and perform a search for 1,3-dimethyl benzene. What data are available for this compound on the NIST site? Click on the link to the IR spectrum and notice that there are several versions of the spectrum. How are they alike, and how do they differ? Where did the spectra originate? Select the gas-phase 2-cm^{-1} resolution spectrum. Click on View Image of Digitized Spectrum and print a copy of the spectrum. Now, return to the IR spectrum and its links. Under gas phase, choose the highest resolution spectrum with boxcar apodization. Click on the desired resolution to load the spectrum. Note that this spectrum presents molar absorptivity versus wavenumber while the previous lower resolution spectrum shows transmittance versus wavenumber. What are the major spectral differences noted? Does the additional resolution give any extra information? How might the molar absorptivity spectrum be used for quantitative analysis? Try a few other compounds and compare the low resolution vapor-phase spectra to the high-resolution quantitative spectra.

QUESTIONS AND PROBLEMS

26-1. Describe the differences between the following pairs of terms and list any particular advantages of one over the other:
*(a) spectrophotometers and photometers.
(b) single-beam and double-beam instruments for absorbance measurements.
*(c) conventional and diode-array spectrophotometers.

26-2. What minimum requirement is needed to obtain reproducible results with a single-beam spectrophotometer?

***26-3.** What experimental variables must be controlled to assure reproducible absorbance data?

26-4. What is(are) advantage(s) of the multiple standard addition method over the single-point standard addition method?

***26-5.** The molar absorptivity for the complex formed between bismuth(III) and thiourea is 9.32×10^3 L cm^{-1} mol^{-1} at 470 nm. Calculate the range of permissible concentrations for the complex if the absorbance is to

be no less than 0.10 nor greater than 0.90 when the measurements are made in 1.00-cm cells.

26-6. The molar absorptivity for aqueous solutions of phenol at 211 nm is 6.17×10^3 L cm^{-1} mol^{-1}. Calculate the permissible range of phenol concentrations if the transmittance is to be less than 85% and greater than 7% when the measurements are made in 1.00-cm cells.

***26-7.** The logarithm of the molar absorptivity for acetone in ethanol is 2.75 at 366 nm. Calculate the range of acetone concentrations that can be used if the absorbance is to be greater than 0.100 and less than 2.000 with a 1.50-cm cell.

26-8. The logarithm of the molar absorptivity of phenol in aqueous solution is 3.812 at 211 nm. Calculate the range of phenol concentrations that can be used if the absorbance is to be greater than 0.150 and less than 1.500 with a 1.25-cm cell.

26-9. A photometer with a linear response to radiation gave a reading of 690 mV with a blank in the light path and 169 mV when the blank was replaced by an absorbing solution. Calculate

*(a) the transmittance and absorbance of the absorbing solution.

(b) the expected transmittance if the concentration of absorber is one half that of the original solution.

*(c) the transmittance to be expected if the light path through the original solution is doubled.

26-10. A portable photometer with a linear response to radiation registered 75.5 μA with a blank solution in the light path. Replacement of the blank with an absorbing solution yielded a response of 23.7 μA. Calculate

(a) the percent transmittance of the sample solution.

*(b) the absorbance of the sample solution.

(c) the transmittance to be expected for a solution in which the concentration of the absorber is one third that of the original sample solution.

*(d) the transmittance to be expected for a solution that has twice the concentration of the sample solution.

26-11. Sketch a photometric titration curve for the titration of Sn^{2+} with MnO_4^-. What color radiation should be used for this titration? Explain.

26-12. Iron(III) reacts with thiocyanate ion (SCN) to form the red complex, $Fe(SCN)^{2+}$. Sketch a photometric titration curve for Fe(III) with thiocyanate ion when a photometer with a green filter is used to collect data. Why is a green filter used?

***26-13.** Ethylenediaminetetraacetic acid displaces bismuth(III) from its thiourea complex:

$$Bi(tu)_6^{3+} + H_2Y^{2-} \rightarrow BiY^- + 6tu + 2H^+$$

where tu is the thiourea molecule, $(NH_2)_2CS$. Predict the shape of a photometric titration curve based on this process, given that the Bi(III)/thiourea complex is the only species in the system that absorbs at 465 nm, the wavelength selected for the titration.

26-14. The accompanying data (1.00-cm cells) were obtained for the spectrophotometric titration of 10.00 mL of Pd(II) with M Nitroso R (O. W. Rollins and M. M. Oldham, *Anal. Chem.,* **1971,** *43,* 262, **DOI:** 10.1021/ac60297a026):

Volume of Nitroso R, mL	A500
0	0
1.00	0.147
2.00	0.271
3.00	0.375
4.00	0.371
5.00	0.347
6.00	0.325
7.00	0.306
8.00	0.289

Calculate the concentration of the Pd(II) solution, given that the ligand-to-cation ratio in the colored product is 2:1.

26-15. A 4.97-g petroleum specimen was decomposed by wet ashing and subsequently diluted to 500 mL in a volumetric flask. Cobalt was determined by treating 25.00-mL aliquots of this diluted solution as follows:

Reagent Volume			
Co(II), 3.00 ppm	Ligand	H_2O	Absorbance
0.00	20.00	5.00	0.398
5.00	20.00	0.00	0.510

Assume that the Co(II)/ligand chelate obeys Beer's law and calculate the percentage of cobalt in the original sample.

***26-16.** Iron(III) forms a complex with thiocyanate ion that has the formula $Fe(SCN)^{2+}$. The complex has an absorption maximum at 580 nm. A specimen of well water was assayed according to the scheme below. Calculate the concentration of iron in parts per million.

	Volumes, mL					
Sample	Sample Volume	Oxidizing Reagent	Fe(II) 2.75 ppm	KSCN 0.050 M	H_2O	Absorbance, 580 nm (1.00-cm cells)
1	50.00	5.00	5.00	20.00	20.00	0.549
2	50.00	5.00	0.00	20.00	25.00	0.231

26-17. A. J. Mukhedkar and N. V. Deshpande (*Anal. Chem.*, **1963**, *35*, 47, **DOI:** 10.1021/ac60194a014) report on a simultaneous determination for cobalt and nickel based on absorption by their 8-quinolinol complexes. Molar absorptivities (L mol^{-1} cm^{-1}) are $\varepsilon_{Co} = 3529$ and $\varepsilon_{Ni} = 3228$ at 365 nm and $\varepsilon_{Co} = 428.9$ and $\varepsilon_{Ni} = 0$ at 700 nm. Calculate the concentration of nickel and cobalt in each of the following solutions (1.00-cm cells):

Solution	A_{365}	A_{700}
1	0.617	0.0235
2	0.755	0.0714
3	0.920	0.0945
4	0.592	0.0147
5	0.685	0.0540

***26-18.** Molar absorptivity data for the cobalt and nickel complexes with 2,3-quinoxalinedithiol are $\varepsilon_{Co} = 36{,}400$ and $\varepsilon_{Ni} = 5520$ at 510 nm and $\varepsilon_{Co} = 1240$ and $\varepsilon_{Ni} = 17{,}500$ at 656 nm. A 0.425-g sample was dissolved and diluted to 50.0 mL. A 25.0-mL aliquot was treated to eliminate interferences; after addition of 2,3-quinoxalinedithiol, the volume was adjusted to 50.0 mL. This solution had an absorbance of 0.446 at 510 nm and 0.326 at 656 nm in a 1.00-cm cell. Calculate the concentration in parts per million of cobalt and nickel in the sample.

26-19. The indicator HIn has an acid dissociation constant of 4.80×10^{-6} at ordinary temperatures. The accompanying absorbance data are for 8.00×10^{-5} M solutions of the indicator measured in 1.00-cm cells in strongly acidic and strongly alkaline media:

	Absorbance	
λ, nm	pH 1.00	pH 13.00
420	0.535	0.050
445	0.657	0.068
450	0.658	0.076
455	0.656	0.085
470	0.614	0.116
510	0.353	0.223
550	0.119	0.324
570	0.068	0.352
585	0.044	0.360
595	0.032	0.361
610	0.019	0.355
650	0.014	0.284

Estimate the wavelength at which absorption by the indicator becomes independent of pH (that is, the isosbestic point).

26-20. Calculate the absorbance (1.00-cm cells) at 450 nm of a solution in which the total molar concentration of the indicator described in Problem 26-19 is 8.00×10^{-5} M and the pH is *(a) 4.92, (b) 5.46, *(c) 5.93, and (d) 6.16.

***26-21.** What is the absorbance at 595 nm (1.00-cm cells) of a solution that is 1.25×10^{-4} M in the indicator of Problem 26-19 and has a pH of (a) 5.30, (b) 5.70, and (c) 6.10?

26-22. Several buffer solutions were made 1.00×10^{-4} M in the indicator of Problem 26-19. Absorbance data (1.00-cm cells) are

Solution	A_{450}	A_{595}
*A	0.344	0.310
B	0.508	0.212
*C	0.653	0.136
D	0.220	0.380

Calculate the pH of each solution.

26-23. Construct an absorption spectrum for an 7.00×10^{-5} M solution of the indicator of Problem 26-19 when measurements are made with 1.00-cm cells and

(a) $\dfrac{[HIn]}{[In^-]} = 3$

(b) $\dfrac{[HIn]}{[In^-]} = 1$

(c) $\dfrac{[HIn]}{[In^-]} = \dfrac{1}{3}$

26-24. Solutions of P and Q individually obey Beer's law over a large concentration range. Spectral data for these species in 1.00-cm cells are

	Absorbance	
λ, nm	8.55×10^{-5} M P	2.37×10^{-4} M Q
400	0.078	0.500
420	0.087	0.592
440	0.096	0.599
460	0.102	0.590
480	0.106	0.564
500	0.110	0.515
520	0.113	0.433
540	0.116	0.343
580	0.170	0.170
600	0.264	0.100
620	0.326	0.055
640	0.359	0.030
660	0.373	0.030
680	0.370	0.035
700	0.346	0.063

(a) Plot an absorption spectrum for a solution that is 6.45×10^{-5} M in P and 3.21×10^{-4} M in Q.

(b) Calculate the absorbance (1.00-cm cells) at 440 nm of a solution that is 3.86×10^{-5} M in P and 5.37×10^{-4} M in Q.

(c) Calculate the absorbance (1.00-cm cells) at 620 nm of a solution that is 1.89×10^{-4} M in P and 6.84×10^{-4} M in Q.

26-25. Use the data in Problem 26-24 to calculate the molar concentration of P and Q in each of the following solutions:

	A_{440}	A_{620}
*(a)	0.357	0.803
(b)	0.830	0.448
*(c)	0.248	0.333
(d)	0.910	0.338
*(e)	0.480	0.825
(f)	0.194	0.315

26-26. A standard solution was put through appropriate dilutions to give the concentrations of iron shown in the accompanying table. The iron(II)-1,10,phenanthroline complex was then formed in 25.0-mL aliquots of these solutions, following which each was diluted to 50.0 mL (see color plate 15). The absorbances in the table (1.00-cm cells) were recorded at 510 nm.

Fe(II) Concentration in Original Solution, ppm	A_{510}
4.00	0.160
10.0	0.390
16.0	0.630
24.0	0.950
32.0	1.260
40.0	1.580

(a) Plot a calibration curve from these data.
*(b) Use the method of least squares to find an equation relating absorbance and the concentration of iron(II).
*(c) Calculate the standard deviation of the slope and intercept.

26-27. The method developed in Problem 26-26 was used for the routine determination of iron in 25.0-mL aliquots of ground water. Express the concentration (as ppm Fe) in samples that yielded the accompanying absorbance data (1.00-cm cell). Calculate the relative standard deviation of the result. Repeat the calculation assuming the absorbance data are means of three measurements.
(a) 0.143
(b) 0.675
(c) 0.068
(d) 1.009
(e) 1.512
(f) 0.546

***26-28.** The sodium salt of 2-quinizarinsulfonic acid (NaQ) forms a complex with Al^{3+} that absorbs strongly at 560 nm.[18] The data collected on this system are shown in the accompanying table. (a) Find the formula of the complex from the data. In all solutions, $c_{Al} = 3.7 \times 10^{-5}$ M, and all measurements were made in 1.00-cm cells. (b) Find the molar absorptivity of the complex.

c_Q, M	A_{560}
1.00×10^{-5}	0.131
2.00×10^{-5}	0.265
3.00×10^{-5}	0.396
4.00×10^{-5}	0.468
5.00×10^{-5}	0.487
6.00×10^{-5}	0.498
8.00×10^{-5}	0.499
1.00×10^{-4}	0.500

26-29. The accompanying data were obtained in a slope-ratio investigation of the complex formed between Ni^{2+} and 1-cyclopentene-1-dithiocarboxylic acid (CDA). The measurements were made at 530 nm in 1.00-cm cells.

$c_{CDA} = 1.00 \times 10^{-3}$ M	
c_{Ni}, M	A_{530}
5.00×10^{-6}	0.051
1.20×10^{-5}	0.123
3.50×10^{-5}	0.359
5.00×10^{-5}	0.514
6.00×10^{-5}	0.616
7.00×10^{-5}	0.719

$c_{Ni} = 1.00 \times 10^{-3}$ M	
c_{CDA}, M	A_{530}
9.00×10^{-6}	0.031
1.50×10^{-5}	0.051
2.70×10^{-5}	0.092
4.00×10^{-5}	0.137
6.00×10^{-5}	0.205
7.00×10^{-5}	0.240

(a) Determine the formula of the complex. Use linear least squares to analyze the data.
(b) Find the molar absorptivity of the complex and its uncertainty.

***26-30.** The accompanying absorption data were recorded at 390 nm in 1.00-cm cells for a continuous-variation study of the colored product formed between Cd^{2+} and the complexing reagent R.

	Reagent Volumes, mL		
Solution	$c_{Cd} = 1.25 \times 10^{-4}$ M	$c_R = 1.25 \times 10^{-4}$ M	A_{390}
0	10.00	0.00	0.000
1	9.00	1.00	0.174
2	8.00	2.00	0.353
3	7.00	3.00	0.530
4	6.00	4.00	0.672
5	5.00	5.00	0.723
6	4.00	6.00	0.673
7	3.00	7.00	0.537
8	2.00	8.00	0.358
9	1.00	9.00	0.180
10	0.00	10.00	0.000

(a) Find the ligand-to-metal ratio in the product.

[18] E. G. Owens and J. H. Yoe, *Anal. Chem.*, **1959**, *31*, 384, **DOI:** 10.1021/ac60147a016.

(b) Calculate an average value for the molar absorptivity of the complex and its uncertainty. Assume that in the linear portions of the plot the metal is completely complexed.
(c) Calculate K_f for the complex using the stoichiometric ratio determined in (a) and the absorption data at the point of intersection of the two extrapolated lines.

26-31. Palladium(II) forms an intensely-colored complex at pH 3.5 with arsenazo III at 660 nm.[19] A meteorite was pulverized in a ball mill, and the resulting powder was digested with various strong mineral acids. The resulting solution was evaporated to dryness, dissolved in dilute hydrochloric acid, and separated from interferents by ion-exchange chromatography (see Section 33D). The resulting solution containing an unknown amount of Pd(II) was then diluted to 50.00 mL with pH 3.5 buffer. Ten-milliliter aliquots of this analyte solution were then transferred to six 50-mL volumetric flasks. A standard solution was then prepared that was 1.00×10^{-5} M in Pd(II). Volumes of the standard solution shown in the table were then pipetted into the volumetric flasks along with 10.00 mL of 0.01 M arsenazo III. Each solution was then diluted to 50.00 mL, and the absorbance of each solution was measured at 660 nm in 1.00-cm cells.

Volume Standard Solution, mL	A_{660}
0.00	0.209
5.00	0.329
10.00	0.455
15.00	0.581
20.00	0.707
25.00	0.833

(a) Enter the data into a spreadsheet and construct a standard additions plot.
(b) Determine the slope and intercept of the line.
(c) Determine the standard deviation of the slope and of the intercept.
(d) Calculate the concentration of Pd(II) in the analyte solution.
(e) Find the standard deviation of the measured concentration.

26-32. Mercury(II) forms a 1:1 complex with triphenyltetrazolium chloride (TTC) that exhibits an absorption maximum at 255 nm.[20] The mercury(II) in a soil sample was extracted into an organic solvent containing an excess of TTC, and the resulting solution was diluted to 100.0 mL in a volumetric flask. Five-milliliter aliquots of the analyte solution were then transferred to six 25-mL volumetric flasks. A standard solution was then prepared that was 5.00×10^{-6} M in Hg(II). Volumes of the standard solution shown in the table were then pipetted into the volumetric flasks, and each solution was then diluted to 25.00 mL. The absorbance of each solution was measured at 255 nm in 1.00-cm quartz cells.

Volume Standard Solution, mL	A_{255}
0.00	0.582
2.00	0.689
4.00	0.767
6.00	0.869
8.00	1.009
10.00	1.127

(a) Enter the data into a spreadsheet, and construct a standard-additions plot.
(b) Determine the slope and intercept of the line.
(c) Determine the standard deviation of the slope and of the intercept.
(d) Calculate the concentration of Hg(II) in the analyte solution.
(e) Find the standard deviation of the measured concentration.

***26-33.** Estimate the frequencies of the absorption maxima in the IR spectrum of methylene chloride shown in Figure 26F-2. From these frequencies, assign molecular vibrations of methylene chloride to each of the bands. Notice that some of the group frequencies that you will need are not listed in Table 26-5, so you will have to look elsewhere.

26-34. Challenge Problem: (a) Show that the overall formation constant for the complex ML_n is

$$K_f = \frac{\left(\frac{A}{A_{extr}}\right)c}{\left[c_M - \left(\frac{A}{A_{extr}}\right)c\right]\left[c_L - n\left(\frac{A}{A_{extr}}\right)c\right]^n}$$

where A is the experimental absorbance at a given value on the x-axis in a continuous variations plot, A_{extr} is the absorbance determined from the extrapolated lines corresponding to the same point on the x-axis, c_M is the molar analytical concentration of the ligand, c_L is the molar analytical concentration of the metal, and n is the ligand-to-metal ratio in the complex.[21]
(b) Under what assumptions is the equation valid?
(c) What is c?
(d) Discuss the implications of the occurrence of the maximum in a continuous variations plot at a value of less than 0.5.

[19] J. G. Sen Gupta, *Anal. Chem.*, **1967**, *39*, 18, **DOI:** 10.1021/ac60245a029.
[20] M. Kamburova, *Talanta.*, **1993**, *40*(5), 719, **DOI**: 10.1016/0039-9140(93)80285-y
[21] J. Inczédy, *Analytical Applications of Complex Equilibria,* New York: Wiley, 1976.

CHAPTER 27

Molecular Fluorescence Spectroscopy

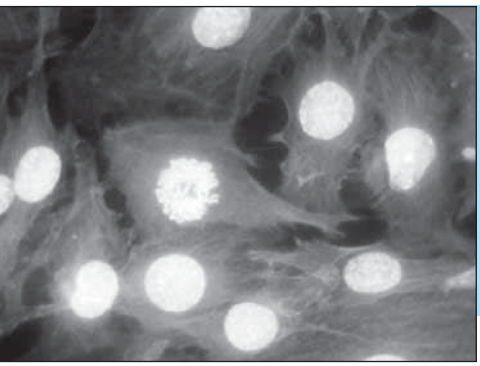

Dr. Gopal Murti/Science Photo Library/Photo Researchers, Inc.

The photograph is an immunofluorescent light micrograph of HeLa cancer cells. The cell in the center of the photo is in the prophase stage of mitotic cell division. The chromosomes have condensed before dividing to form two nuclei. The cells are stained to reveal actin microfilaments and microtubules of the cytoskeleton, which appear as the filamentary structures surrounding the cell nuclei. The nuclei of the cells are visualized by exposing the cells to structure-specific fluorescent antibodies, prepared by covalently attaching ordinary antibodies to fluorescent molecules. The antibodies collect in the nuclei so that when they are exposed to UV radiation, they glow as shown in the photo. Similar chemistry is used in the fluorescence immunoassay described in Feature 11-2.

Fluorescence is a photoluminescence process in which atoms or molecules are excited by absorption of electromagnetic radiation (recall Figure 24-6). The excited species then relax to the ground state, giving up their excess energy as photons. One of the most attractive features of molecular fluorescence is its inherent sensitivity, which is often one to three orders of magnitude better than absorption spectroscopy. In fact, single molecules of selected species have been detected by fluorescence spectroscopy under controlled conditions. Another advantage is the large linear concentration ranges of fluorescence methods, which are significantly broader than linear concentration ranges in absorption spectroscopy. Fluorescence methods are, however, less widely applicable than absorption methods because of the smaller number of chemical systems that show appreciable fluorescence. Fluorescence is also subject to many more environmental interference effects than absorption methods. We consider here some of the most important aspects of molecular fluorescence methods.[1]

27A THEORY OF MOLECULAR FLUORESCENCE

Molecular fluorescence is measured by exciting the sample at an absorption wavelength, also called the excitation wavelength, and measuring the emission at a longer wavelength called the emission or fluorescence wavelength. For example, the reduced form of the coenzyme nicontinamide adenine dinucleotide (NADH) absorbs radiation at 340 nm, and the molecule emits photoluminescence radiation with an emission maximum at 465 nm. Usually photoluminescence emission is measured at right angles to the incident beam to avoid measuring the incident radiation (recall Figure 25-1b). The short-lived emission that occurs is called **fluorescence**, while luminescence that is much longer lasting is called **phosphorescence**.

Fluorescence emission occurs in 10^{-5} s or less. In contrast, phosphorescence may last for several minutes or even hours. Fluorescence is much more widely used for chemical analysis than phosphorescence.

[1]For more information on molecular fluorescence spectroscopy, see J. R.. Lakowicz, *Principles of Fluorescence Spectroscopy*, New York: Springer, 2006.

27A-1 Relaxation Processes

Figure 27-1 shows a partial energy level diagram for a hypothetical molecular species. Three electronic energy states are shown, E_0, E_1, and E_2; the ground state is E_0, and the excited states are E_1 and E_2. Each of the electronic states is shown as having four excited vibrational levels. When this species is irradiated with a band of wavelengths λ_1 to λ_5 (see Figure 27-1a), the five vibrational levels of the first excited electronic state, E_1, are momentarily populated. Similarly, when the molecules are irradiated with a more energetic band made up of shorter wavelengths λ_1' to λ_5', the five vibrational levels of the higher energy electronic state E_2 become populated briefly.

Once the molecule is excited to E_1 or E_2, several processes can occur that cause the molecule to lose its excess energy. Two of the most important of these processes, **nonradiative relaxation** and **fluorescence emission**, are illustrated in Figure 27-1b and c.

The two most important nonradiative relaxation methods that compete with fluorescence are illustrated in Figure 27-1b. **Vibrational relaxation**, depicted by the short wavy arrows between vibrational energy levels, takes place during collisions between excited molecules and molecules of the solvent. Nonradiative relaxation between the lower vibrational levels of an excited electronic state and the higher vibrational levels of another electronic state can also occur. This type of relaxation, sometimes called **internal conversion**, is depicted by the two longer wavy arrows in Figure 27-1b. Internal conversion is much less efficient than vibrational relaxation so that the average lifetime of an electronic excited state is between 10^{-9} and 10^{-6} s. The exact mechanism by which these two relaxational processes occur is currently under study, but the net result is a tiny increase in the temperature of the medium.

Figure 27-1c illustrates the relaxation process that is desired: the fluorescence process. Fluorescence is almost always observed from the lowest-lying excited electronic state E_1 to the ground state E_0. Also, the fluorescence usually occurs only from the

Vibrational relaxation involves transfer of the excess energy of a vibrationally excited species to molecules of the solvent. This process takes place in less than 10^{-15} s and leaves the molecules in the lowest vibrational state of an electronic excited state.

Internal conversion is a type of relaxation that involves transfer of the excess energy of a species in the lowest vibrational level of an excited electronic state to solvent molecules and conversion of the excited species to a lower electronic state.

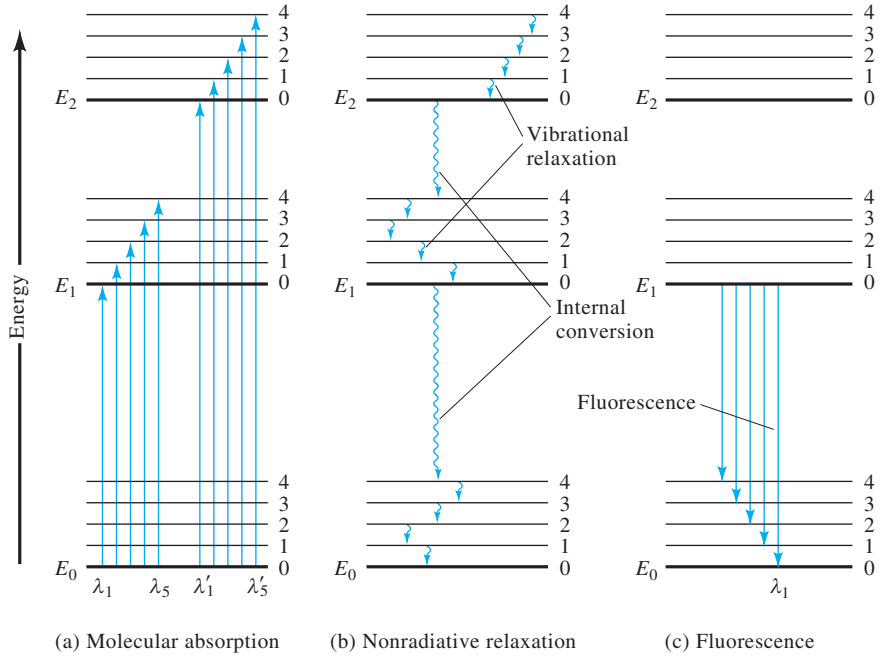

Figure 27-1 Energy level diagram shows some of the processes that occur during (a) absorption of incident radiation, (b) nonradiative relaxation, and (c) fluorescence emission by a molecular species. Absorption typically occurs in 10^{-15} s, while vibrational relaxation occurs in 10^{-11} to 10^{-10} s. Internal conversion between different electronic states is also very rapid (10^{-12} s), while fluorescence lifetimes are typically 10^{-10} to 10^{-5} s.

Fluorescence bands consist of a large number of closely spaced lines.

lowest vibrational level of E_1 to various vibrational levels of E_0, because the internal conversion and vibrational relaxation processes are very rapid compared to fluorescence. Hence, a fluorescence spectrum usually consists of only one band with many closely spaced lines that represent transitions from the lowest vibrational level of E_1 to the many different vibrational levels of E_0.

The line in Figure 27-1c that terminates the fluorescence band on the short-wavelength or high-energy side (λ_1) is identical in energy to the line labeled λ_1 in the absorption diagram in Figure 27-1a. Since fluorescence lines in this band originate in the lowest vibrational state of E_1, all of the other lines in the band are of lower energy or longer wavelength than the line corresponding to λ_1. Molecular fluorescence bands are mostly made up of lines that are longer in wavelength, higher in frequency, and thus lower in energy than the band of absorbed radiation responsible for their excitation. This shift to longer wavelength is called the **Stokes shift**.

Stokes-shifted fluorescence is longer in wavelength than the radiation that caused the excitation.

Relationship between Excitation Spectra and Fluorescence Spectra

Because the energy differences between vibrational states is about the same for both ground and excited states, the absorption, or **excitation spectrum**, and the fluorescence spectrum for a compound often appear as approximate mirror images of one another with overlap occurring near the origin transition (0 vibrational level of E_1 to 0 vibrational level of E_0). This effect is demonstrated by the spectra for anthracene shown in **Figure 27-2**. There are many exceptions to this mirror-image rule, particularly when the excited and ground states have different molecular geometries or when different fluorescence bands originate from different parts of the molecule.

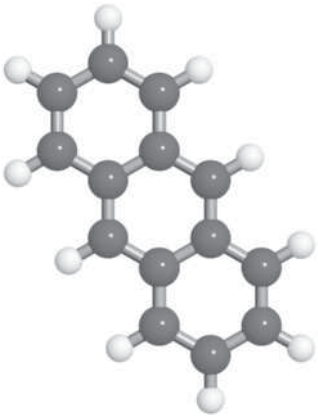

Molecular model of anthracene.

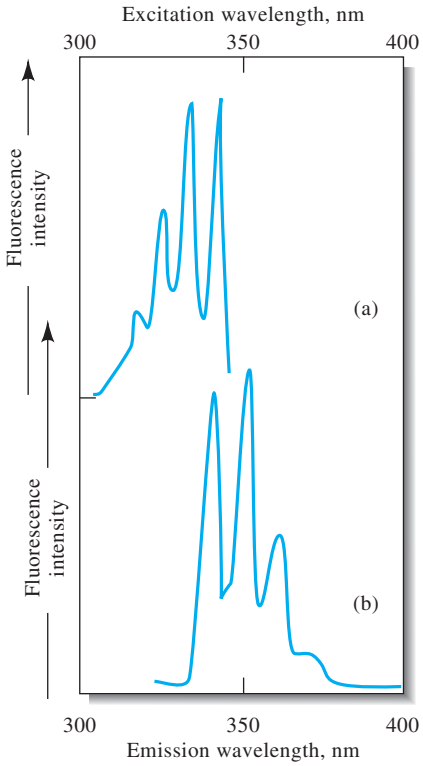

Figure 27-2 Fluorescence spectra for 1 ppm anthracene in alcohol: (a) excitation spectrum; (b) emission spectrum.

27A-2 Fluorescent Species

As shown in Figure 27-1, fluorescence is one of several mechanisms by which a molecule returns to the ground state after it has been excited by absorption of radiation. All absorbing molecules have the potential to fluoresce, but most compounds do not because their structure allows radiationless pathways for relaxation to occur *at a greater rate* than fluorescence emission. The **quantum yield** of molecular fluorescence is simply the ratio of the number of molecules that fluoresce to the total number of excited molecules, or the ratio of photons emitted to photons absorbed. Highly fluorescent molecules, such as fluorescein, have quantum efficiencies that approach unity under some conditions. Species that do not fluoresce or that show very weak fluorescence have quantum efficiencies that are essentially zero.

Quantum efficiency is described by the **quantum yield of fluorescence**, Φ_F.

$$\Phi_F = \frac{k_F}{k_F + k_{nr}}$$

where k_F is the first-order rate constant for fluorescence relaxation and k_{nr} is the rate constant for radiationless relaxation. See Chapter 30 for a discussion of rate constants.

Fluorescence and Structure

Compounds containing aromatic rings give the most intense and most useful molecular fluorescence emission. While certain aliphatic and alicyclic carbonyl compounds as well as highly conjugate double-bonded structures also fluoresce, there are very few of these compared to the number of fluorescent compounds containing aromatic systems.

Most unsubstituted aromatic hydrocarbons fluoresce in solution, with the quantum efficiency increasing with the number of rings and their degree of condensation. The simplest heterocyclics, such as pyridine, furan, thiophene, and pyrrole, do not exhibit molecular fluorescence (see **Figure 27-3**), but fused-ring structures containing these rings often do (see **Figure 27-4**). Substitution on an aromatic ring causes shifts in the wavelength of absorption maxima and corresponding changes in the fluorescence bands. In addition, substitution frequently affects the fluorescence efficiency. These effects are demonstrated by the data in the **Table 27-1**.

❮ Many unsubstituted aromatic compounds fluoresce.

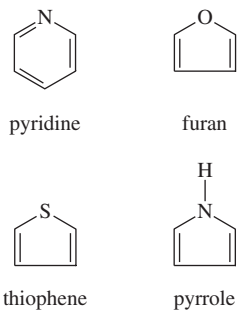

Figure 27-3 Typical aromatic molecules that do not fluoresce.

The Effect of Structural Rigidity

Experiments show that fluorescence is particularly favored in rigid molecules. For example, under similar measurement conditions, the quantum efficiency of fluorene is nearly 1.0 while that of biphenyl is about 0.2 (see **Figure 27-5**). The difference in behavior is a result of the increased rigidity provided by the bridging methylene group in fluorene. This rigidity lowers the rate of nonradiative relaxation to the point where relaxation by fluorescence has time to occur. There are many similar examples of this type of behavior. In addition, enhanced emission frequently results when fluorescing dyes are adsorbed on a solid surface. Once again, the added rigidity provided by the solid may account for the observed effect.

The influence of rigidity also explains the increase in fluorescence of certain organic chelating agents when they are complexed with a metal ion. For example, the fluorescence intensity of 8-hydroxyquinoline is much less than that of the zinc complex (see **Figure 27-6**).

❮ Rigid molecules or complexes are often fluorescent.

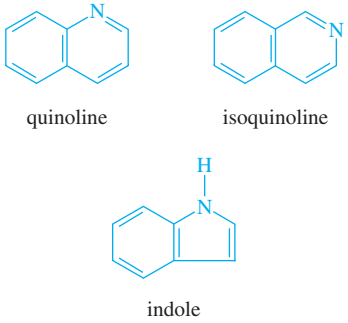

Figure 27-4 Typical aromatic compounds that fluoresce.

Temperature and Solvent Effects

In most molecules, the quantum efficiency of fluorescence decreases with increasing temperature because the increased frequency of collision at elevated temperatures increases the probability of collisional relaxation. A decrease in solvent viscosity leads to the same result.

TABLE 27-1

Effect of Substitution on the Fluorescence of Benzene Derivatives*

Compound	Relative Intensity of Fluorescence
Benzene	10
Toluene	17
Propylbenzene	17
Fluorobenzene	10
Chlorobenzene	7
Bromobenzene	5
Iodobenzene	0
Phenol	18
Phenolate ion	10
Anisole	20
Aniline	20
Anilinium ion	0
Benzoic acid	3
Benzonitrile	20
Nitrobenzene	0

*In ethanol solution. From W.West, Chemical Applications of Spetroscopy, Techniques of Organic Chemistry, Vol. IX, p. 730. New York: Interscience, 1956. Reprinted by permission of John Wiley & Sons.

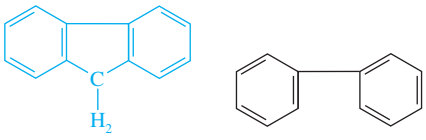

fluorene
Φ → 1

biphenyl
Φ → 0.2

Figure 27-5 Effect of molecular rigidity on quantum yield. The fluorine molecule is held rigid by the central ring, so fluorescence is enhanced. The planes of the two benzene rings in biphenyl can rotate relative to one another, so fluorescence is suppressed.

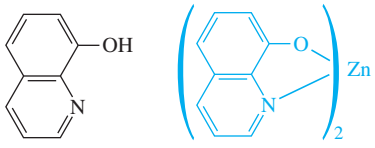

nonfluorescing

fluorescing

Figure 27-6 Effect of rigidity on quantum yield in complexes. Free 8-hydroxyquinoline molecules in solution are easily deactivated through collisions with solvent molecules and do not fluoresce. The rigidity of the Zn-8-hydroxyquinoline complex enhances fluorescence.

27B EFFECT OF CONCENTRATION ON FLUORESCENCE INTENSITY

The radiant power of fluorescence emitted F is proportional to the radiant power of the excitation beam absorbed by the system:

$$F = K'(P_0 - P) \tag{27-1}$$

where P_0 is the radiant power of the beam incident on the solution and P is its power after it passes through a length b of the medium. The constant K' depends on the quantum efficiency of the fluorescence. In order to relate F to the concentration c of the fluorescing particle, we write Beer's law in the form

$$\frac{P}{P_0} = 10^{-\varepsilon bc} \tag{27-2}$$

where ε is the molar absorptivity of the fluorescing species and εbc is the absorbance. By substituting Equation 27-2 into Equation 27-1, we obtain

$$F = K'P_0(1 - 10^{-\varepsilon bc}) \tag{27-3}$$

Expansion of the exponential term in Equation 27-3 leads to

$$F = K'P_0\left[2.3\varepsilon bc - \frac{(-2.3\varepsilon bc)^2}{2!} - \frac{(-2.3\varepsilon bc)^3}{3!} - \cdots\right] \tag{27-4}$$

When $\varepsilon bc = A < 0.05$, the first term inside the brackets, $2.3\varepsilon bc$, is much larger than subsequent terms, and we can write

$$F = 2.3K'\varepsilon bcP_0 \tag{27-5}$$

or when the incident power P_0 is constant,

$$F = Kc \tag{27-6}$$

Thus, a plot of the fluorescence power emitted versus the concentration of the emitting species should be linear at low concentrations. When c becomes large enough that the absorbance exceeds about 0.05 (or the transmittance is smaller than about 0.9), the relationship represented by Equation 27-6 become nonlinear, and F lies below an extrapolation of the linear plot. This effect is a result of **primary absorption** in which the incident beam is absorbed so strongly that fluorescence is no longer proportional to concentration as shown in the more complete Equation 27-4. At very high concentrations, F reaches a maximum and may even begin to decrease with increasing concentration because of **secondary absorption**. This phenomenon occurs because of absorption of the emitted radiation by other analyte molecules. A typical plot of F versus concentration is shown in Figure 27-7. Note that primary and secondary absorption effects, sometimes called **inner-filter effects**, can also occur because of absorption by nonanalyte molecules in the sample matrix.

27C FLUORESCENCE INSTRUMENTATION

There are several different types of fluorescence instruments. All follow the general block diagram of Figure 25-1b. Optical diagrams of typical instruments are shown in Figure 27-8. If the two wavelength selectors are both filters, the instrument is called a **fluorometer**. If both wavelength selectors are monochromators, the instrument is a **spectrofluorometer**. Some instruments are hybrids and use an excitation filter along with an emission monochromator. Fluorescence instruments can incorporate a double-beam design in order to compensate for changes in the source radiant power with time and wavelength. Instruments that correct for the source spectral distribution are called **corrected spectrofluorometers**.

Radiation sources for fluorescence are usually more powerful than typical absorption sources. In fluorescence, the radiant power emitted is directly proportional to the source intensity (Equation 27-5), but absorbance is essentially independent

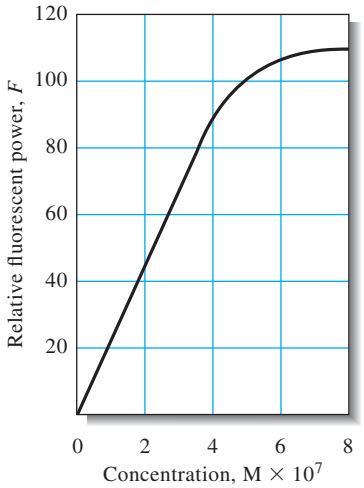

Figure 27-7 Calibration curve for the spectrofluorometric determination of tryptophan in soluble proteins from the lens of a mammalian eye.

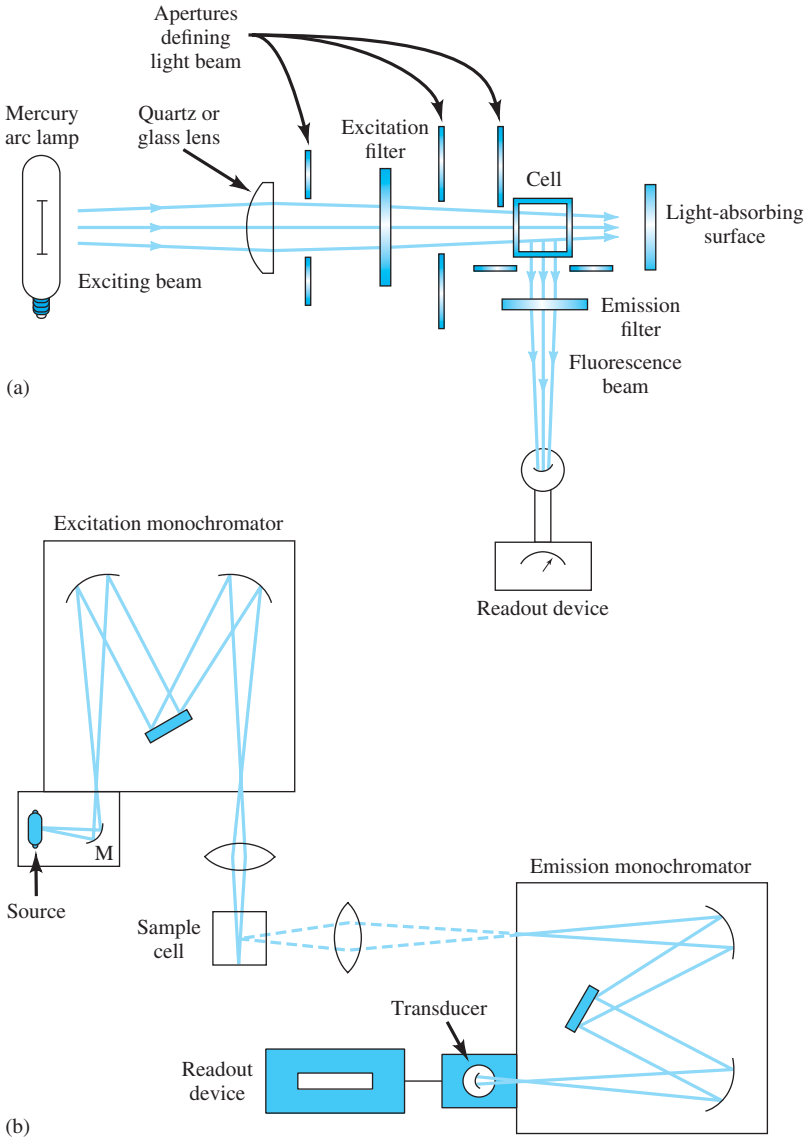

Figure 27-8 Typical fluorescence instruments. A filter fluorometer is shown in (a). Note that the emission is measured at right angles to the mercury arc lamp source. Fluorescence radiation is emitted in all directions, and the 90-deg geometry avoids the detector viewing the source. The spectrofluorometer (b) uses two grating monochromators and also views the emission at right angles. The two monochromators allow the scanning of excitation spectra (excitation wavelength scanned at a fixed emission wavelength), emission spectra (emission wavelength scanned at a fixed excitation wavelength), or synchronous spectra (both wavelengths scanned with a fixed wavelength offset between the two monochromators).

of source intensity because it is related to the ratio of radiant powers as shown in Equation 27-7.

$$c = kA = k \log \left(\frac{P_0}{P} \right) \tag{27-7}$$

Fluorescence methods are 10 to 1000 times more sensitive than absorption methods.

As a result of these different dependencies on source intensity, fluorescence methods are generally one to three orders of magnitude more sensitive than methods based on absorption. Mercury arc lamps, xenon arc lamps, xenon-mercury arc lamps, and lasers are typical fluorescence sources. Monochromators and transducers are typically similar to those used in absorption spectrophotometers. Photomultipliers are still widely used in high-sensitivity spectrofluorometers, but CCDs and photodiode arrays have become popular in recent years. The sophistication, performance characteristics, and cost of fluorometers and spectrofluorometers vary widely as with absorption spectrophotometers. Generally, fluorescence instruments are more expensive than absorption instruments of corresponding quality.

27D APPLICATIONS OF FLUORESCENCE METHODS

Fluorescence spectroscopy is not a major structural or qualitative analysis tool because molecules with subtle structural differences often have similar fluorescence spectra. Also, fluorescence bands in solution are relatively broad at room temperature. However, fluorescence has proved to be a valuable tool in oil spill identification. The source of an oil spill can often be identified by comparing the fluorescence emission spectrum of the spill sample to that of a suspected source. The vibrational structure of polycyclic hydrocarbons present in the oil makes this type of identification possible.

Fluorescence methods are used to study chemical equilibria and kinetics in much the same way as absorption spectrophotometry. Often, it is possible to study chemical reactions at lower concentrations because of the higher sensitivity of fluorescence methods. In many cases where fluorescence monitoring is not feasible, fluorescent probes or tags can be bound covalently to specific sites in molecules such as proteins, thus making them detectable via fluorescence. These tags can be used to provide information about energy transfer processes, the polarity of the protein, and the distances between reactive sites (see for example Feature 27-1).

Quantitative fluorescence methods have been developed for inorganic, organic, and biochemical species. Inorganic fluorescence methods can be divided into two classes: direct methods and indirect methods. Direct methods are based on the reaction of the analyte with a complexing agent to form a fluorescent complex. Indirect methods depend on the decrease in fluorescence, also called **quenching**, as a result of interaction of the analyte with a fluorescent reagent. Quenching methods are primarily used for the determination of anions and dissolved oxygen. Some fluorescence reagents for cations are shown in **Figure 27-9**.

Nonradiative relaxation of transition-metal chelates is so efficient that these species seldom fluoresce. It is worth noting that most transition metals absorb in the UV or visible region, while nontransition-metal ions do not. For this reason, fluorescence is often considered complementary to absorption for the determination of cations.

The number of applications of fluorescence methods to organic and biochemical problems is impressive. Among the compound types that can be determined by fluorescence are amino acids, proteins, coenzymes, vitamins, nucleic acids, alkaloids,

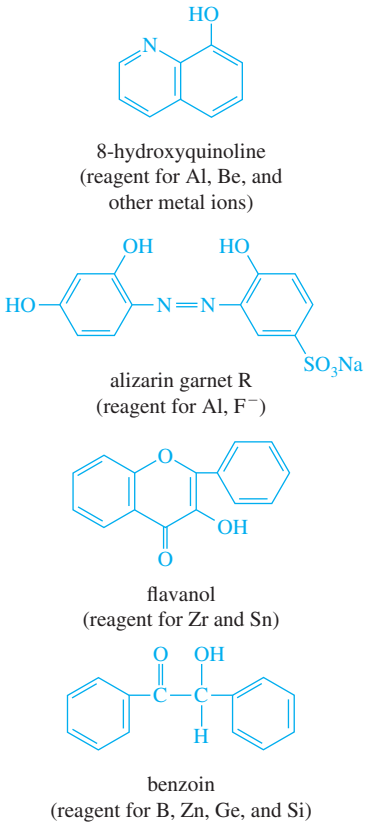

Figure 27-9 Some fluorometric chelating agents for metal cations. Alizarin garnet R can detect Al^{3+} at levels as low as 0.007 μg/mL. Detection of F^- with alizarin garnet R is based on quenching of the fluorescence of the Al^{3+} complex. Flavanol can detect Sn^{4+} at the 0.1-μg/mL level.

FEATURE 27-1

Use of Fluorescence Probes in Neurobiology: Probing the Enlightened

Fluorescent indicators have been widely used to probe biological events in individual cells. A particularly interesting probe is the so-called ion probe that changes its excitation or emission spectrum when it binds to specific ions such as Ca^{2+} or Na^{+}. These indicators can be used to record events that take place in different parts of individual neurons or to monitor simultaneously the activity of a collection of neurons. In neurobiology, for example, the dye Fura-2 has been used to monitor the free intracellular calcium concentration following some pharmacological or electrical stimulation. By following the fluorescence changes with time at specific sites in the neuron, researchers can determine when and where a calcium-dependent electrical event took place.

One cell that has been studied is the Purkinje neuron in the cerebellum, which is one of the largest in the central nervous system. When this cell is loaded with the Fura-2 fluorescent indicator, sharp changes in fluorescence can be measured that correspond to individual calcium action potentials. The changes are correlated to specific sites in the cell by means of fluorescence imaging techniques. **Figure 27F-1** shows the fluorescent image on the right along with fluorescence transients, recorded as the change in fluorescence relative to the steady fluorescence $\Delta F/F$, correlated with sodium action potential spikes. The interpretation of these kinds of patterns can have important implications in understanding the details of synaptic activity.

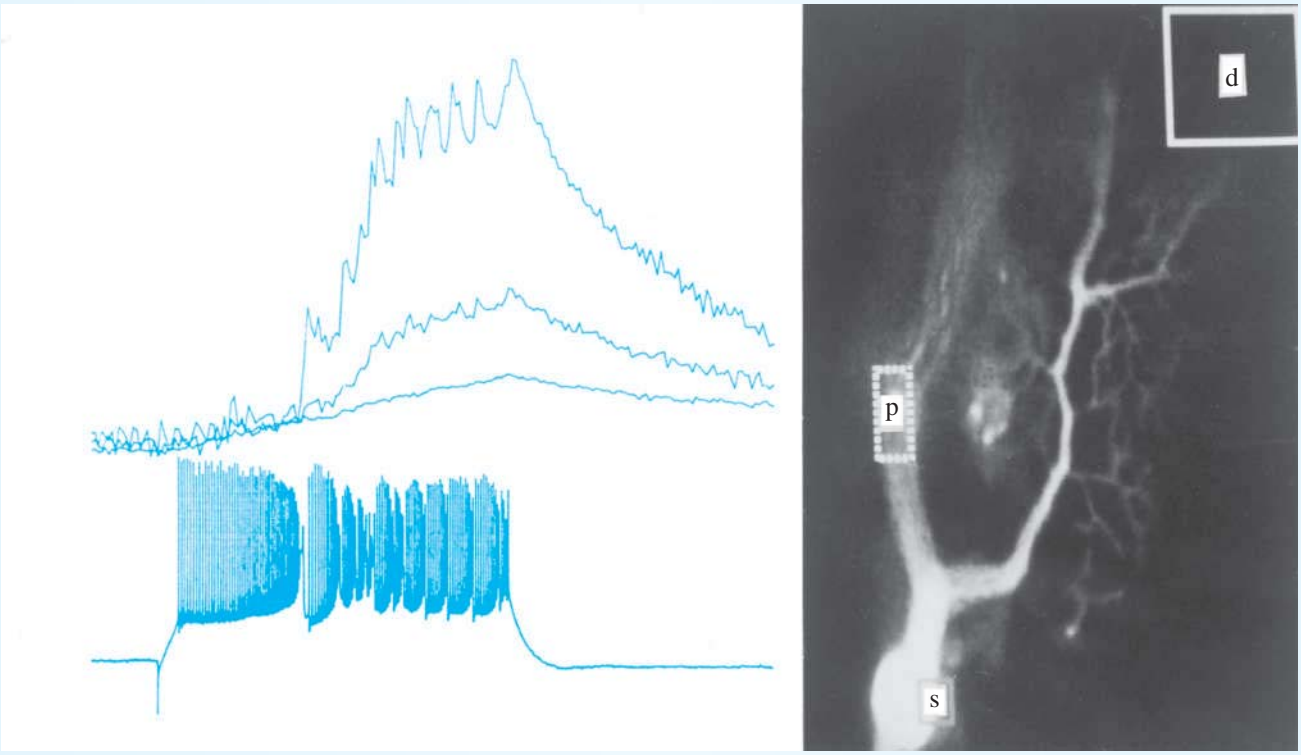

Figure 27F-1 Calcium transients in a cerebellar Purkinje cell. The image on the right is of the cell filled with a fluorescent dye that responds to the calcium concentration. Fluorescent transients are shown on the top left recorded at areas d, p, and s in the cell. The transients in region d correspond to the dendrite region of the cell. Specific calcium signals can be correlated to the action potentials shown on the bottom left. (From V. Lev-Ram, H. Mikayawa, N. Lasser-Ross, and W. N. Ross, *J. Neurophysiol.*, **1992**, *68*, 1167. With permission of the American Physiological Society.)

Some typical polycyclic aromatic hydrocarbons found in oil spills are chrysene, perylene, pyrene, fluorene, and 1,2-benzofluorene. Most of these compounds are carcinogenic.

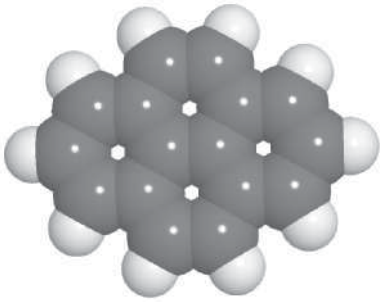

Molecular model of pyrene.

porphryins, steroids, flavonoids, and many metabolites.[2] Because of its sensitivity, fluorescence is widely used as a detection technique for liquid chromatographic methods (see Chapter 33), for flow analysis methods, and for electrophoresis. In addition to methods that are based on measurements of fluorescence intensity, there are many methods involving measurements of fluorescence lifetimes. Several instruments have been developed that provide microscopic images of specific species based on fluorescence lifetimes.[3]

27D-1 Methods for Inorganic Species

The most successful fluorometric reagents for the determination of cations are aromatic compounds having two or more donor functional groups that form chelates with the metal ion. A typical example is 8-hydroxyquinoline, the structure of which is given in Section 12C-3. A few other fluorometric reagents and their applications are found in **Table 27-2**. With most of these reagents, the cation is extracted into a solution of the reagent in an immiscible organic solvent, such as chloroform. The fluorescence of the organic solution is then measured. For a more complete summary of fluorometric methods for inorganic substances, see the handbook by Dean.[4]

27D-2 Methods for Organic and Biochemical Species

The number of applications of fluorometric methods to organic problems is impressive. Dean summarizes the most important of these methods in a table.[5] There are more than 200 entries under the heading "Fluorescence Spectroscopy of Some Organic Compounds," including such diverse compounds as adenine, anthranilic acid, aromatic polycyclic hydrocarbons, cysteine, guanine, isoniazid, naphthols, nerve gases sarin and tabun, proteins, salicylic acid, skatole, trypotophan, uric acid, and warfarin (Coumadin). Many medicinal agents that can be determined fluorometrically are listed, including adrenaline, morphine, penicillin, phenobarbital, procaine, reserpine, and lysergic acid diethylamide (LSD). The most important applications of

TABLE 27-2

Selected Fluorometric Methods for Inorganic Species*

		Wavelength, nm			
Ion	**Reagent**	**Absorption**	**Fluorescence**	**Sensitivity, μg/mL**	**Interference**
Al^{3+}	Alizarin garnet R	470	500	0.007	Be, Co, Cr, Cu, F^-, NO_3^-, Ni, PO_4^{3-}, Th, Zr
F^-	Al complex of Alizarin garnet R (quenching)	470	500	0.001	Be, Co, Cr, Cu, Fe, Ni, PO_4^{3-}, Th, Zr
$B_4O_7^{2-}$	Benzoin	370	450	0.04	Be, Sb
Cd^{2+}	2-(*o*-Hydroxyphenyl)-benzoxazole	365	Blue	2	NH_3
Li^+	8-Hydroxyquinoline	370	580	0.2	Mg
Sn^{4+}	Flavanol	400	470	0.1	F^-, PO_4^{3-}, Zr
Zn^{2+}	Benzoin	—	Green	10	B, Be, Sb, colored ions

* From L. Meites, ed., *Handbook of Analytical Chemistry*, New York: McGraw-Hill, 1963, pp. 6-178-6-181.

[2] See O. S. Wolfbeis, in *Molecular Luminescence Spectroscopy: Methods and Applications*, S. G. Schulman, ed., Part I, Ch. 3, New York: Wiley-Interscience, 1985.
[3] See J. R. Lakowicz, H. Szmacinski, K. Nowacyzk, K. Berndt, and M. L. Johnson, in *Fluorescence Spectroscopy: New Methods and Applications*, O. S. Wolfbeis, ed., Ch. 10, Berlin: Springer-Verlag, 1993.
[4] J. A. Dean, *Analytical Chemistry Handbook,* New York: McGraw-Hill, 1995, pp. 5.60–5.62.
[5] *Ibid.*, pp. 5.63–5.69.

fluorometry include the analysis of food products, pharmaceuticals, clinical samples, and natural products. The sensitivity and selectivity of molecular fluorescence make it a particularly valuable tool in these fields.

27E MOLECULAR PHOSPHORESCENCE SPECTROSCOPY

Phosphorescence is a photoluminescence phenomenon that is quite similar to fluorescence. To understand the difference between these two phenomena, we must consider electron spin and the difference between a **singlet state** and a **triplet state**. Ordinary molecules that are not free radicals exist in the ground state with their electron spins paired. A molecular electronic state in which all electron spins are paired is said to be a **singlet state**. The ground state of a free radical, on the other hand, is a **doublet state**, because the odd electron can assume two orientations in a magnetic field.

When one of a pair of electrons in a molecule is excited to a higher energy level, a singlet or a triplet state can be produced. In the excited singlet state, the spin of the promoted electron is still opposite that of the remaining electron. In the triplet state, however, the spins of the two electrons become unpaired and are thus parallel. These states can be represented as illustrated in Figure 27-10. The excited triplet state is less energetic than the corresponding excited singlet state.

Transitions from an excited singlet state to the ground singlet state produce molecular fluorescence. This singlet-singlet transition is highly probable, and thus, the lifetime of an excited singlet state is very short (10^{-5} s or less). On the other hand, transitions from an excited triplet state to the ground singlet state produce molecular phosphorescence. Because the triplet-singlet transition produces a change in electron spin, it is much less probable. As a result, the triplet state has a much longer lifetime (typically 10^{-4} to 10^{4} s).

The long lifetime of phosphorescence is also one of its drawbacks. Because the excited state is relatively long-lived, nonradiational processes have time to compete with phosphorescence for deactivation. Therefore, the efficiency of the phosphorescence process, as well as the corresponding phosphorescence intensity, is relatively low. To increase the efficiency, phosphorescence is commonly observed at low temperatures in rigid media, such as glasses. Another approach is to adsorb the analyte on a solid surface or enclose it in a molecular cavity (micelle or cyclodextrin cavity), which protects the fragile triplet state. This technique is known as **room temperature phosphorescence**.

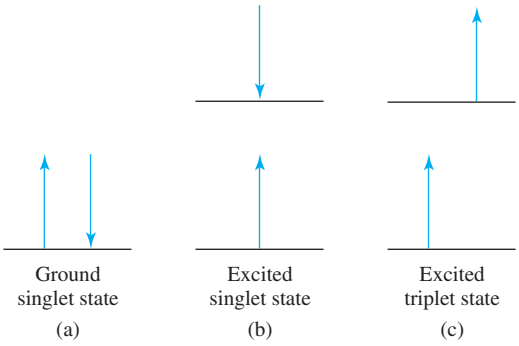

Figure 27-10 Electronic spin states of molecules. In (a), the ground electronic state is shown. In the lowest energy or ground state, the spins are always paired, and the state is a singlet state. In (b) and (c), excited electronic states are shown. If the spins remain paired in the excited state, the molecule is in an excited singlet state (b). If the spins become unpaired, the molecule is in an excited triplet state (c).

Phosphorescence materials and pigments, called **phosphors**, find many uses, including the markings of safety-related signs, such as highway exit and stop signs. Luminous watches contain a phosphor consisting of alkaline earth metal aluminates doped with rare earth elements, such as europium. Cathode-ray tubes, used in some oscilloscopes, computer monitors, and older television sets have solid-state phosphors coated on the screen, allowing actions of the electron beam to be visualized.

In room temperature phosphorescence, the triplet state of the analyte can be protected by being incorporated into a surfactant aggregate called a micelle. In aqueous solutions the aggregate has a nonpolar core due to repulsion of the polar head groups. The opposite occurs in nonpolar solvents. Cyclodextrin cavities are also used.

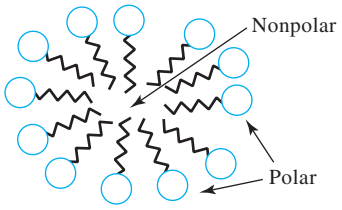

Micelle in aqueous solvent

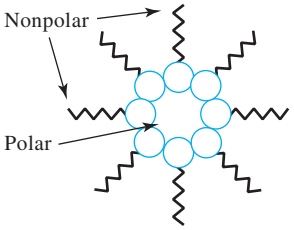

Micelle in nonaqueous solvent

Structure of micelles.

Because of its weak intensity, phosphorescence is much less widely applicable than fluorescence. However, molecular phosphorescence has been used for the determination of a variety of organic and biochemical species, including nucleic acids, amino acids, pyrine and pyrimidine, enzymes, polycyclic hydrocarbons, and pesticides. Many pharmaceutical compounds exhibit measurable phosphorescence signals. The instrumentation for phosphorescence is also somewhat more complex than that for fluorescence. Phosphorescence instruments usually discriminate phosphorescence from fluorescence by delaying the phosphorescence measurement until the fluorescence has decayed to nearly zero. Many fluorescence instruments have attachments, called **phosphoroscopes**, that allow the same instrument to be used for phosphorescence measurements.

27F CHEMILUMINESCENCE METHODS

Fireflies produce light by the phenomenon of bioluminescence. Different firefly species flash with different on-off cycle times. Fireflies mate only with their own species. The familiar bioluminescence reaction occurs when the firefly is looking for a mate.

Chemiluminescence is produced when a chemical reaction yields an electronically excited molecule, which emits light as it returns to the ground state. Chemiluminescence reactions occur in a number of biological systems, where the process is often termed, **bioluminescence**. Examples of species exhibiting bioluminescence include the firefly, the sea pansy, certain jellyfish, bacteria, protozoa, and crustacea.[6]

Several commercial analyzers for the determination of gases are based on chemiluminescence. Nitrous oxide (NO) can be determined by reaction with ozone (O_3). The reaction converts the NO to excited NO_2 with the subsequent emission of light.

One attractive feature of chemiluminescence for analytical uses is the very simple instrumentation required. Since no external source of radiation is needed for excitation, the instrument may consist of only a reaction vessel and a photomultiplier tube. Generally, no wavelength selection device is needed because the only source of radiation is the emission caused by the chemical reaction.

Chemiluminescence methods are known for their high sensitivities. Typical detection limits range from parts per million to parts per billion or lower. Applications include the determination of gases, such as oxides of nitrogen, ozone, and sulfur compounds; determination of inorganic species, such as hydrogen peroxide and some metal ions; immunoassay techniques; DNA probe assays; and polymerase chain reaction methods.[7]

WEB WORKS

One of the problems plaguing quantitative fluorescence measurements has been that of excessive absorption effects, often called inner-filter effects. Use a browser to find this interesting article, Q. Gu and J. E. Kenny, *Anal. Chem.*, **2009**, *81*, 420–26, **DOI:** 10.1021/ac801676j, which describes an approach for correcting fluorescence measurements for excessive absorption. (If your school does not subscribe to this online journal, find a hard copy in the school library.) Their correction method extends the range of linearity for fluorescence measurements to systems in which the absorbance is quite high. Discuss the model used by Gu and Kenny for their correction scheme. How does it differ from previous schemes that allowed corrections for absorbances up to $A \approx 2.0$? What were the major restrictions of these prior correction methods? What is the cell-shift method, and how can it be used for correcting fluorescence values? How does the Gu and Kenny approach allow corrections with common instrument geometries? How large can absorbances be in the Gu and Kenny scheme for linear fluorescence results to be obtained in the case of only a primary inner-filter effect and for both a primary- and a secondary-inner-filter effect?

[6]For more information on chemiluminescence and bioluminescence see O. Shimomura, *Bioluminescence: Chemical Principles and Methods,* Singapore: World Scientific Publishing, 2006; A. Roda, ed., *Chemiluminescence and Bioluminescence: Past, Present and Future,* London: Royal Society of Chemistry, 2010.

[7]See T. A. Nieman, in *Handbook of Instrumental Techniques for Analytical Chemistry*, F. A. Settle, ed., Ch. 27, Upper Saddle River, NJ: Prentice Hall, 1997.

QUESTIONS AND PROBLEMS

27-1. Briefly describe or define
- *(a) fluorescence.
- (b) vibrational relaxation.
- *(c) internal conversion.
- (d) phosphorescence.
- *(e) Stokes shift.
- (f) quantum yield.
- *(g) inner-filter effect.
- (h) excitation spectrum.

27-2. Why is spectrofluorometry potentially more sensitive than spectrophotometry?

27-3. Which compound in each of the pairs below would you expect to have a greater fluorescence quantum yield? Explain.

*(a)

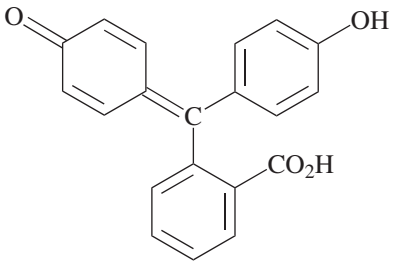

phenolphthalein

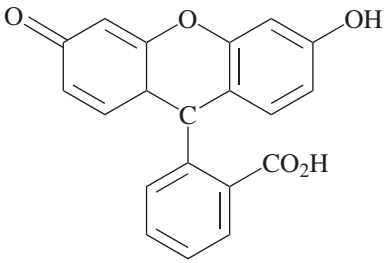

fluorescein

(b)

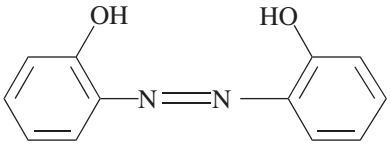

o,*o*′-dihydroxyazobenzene

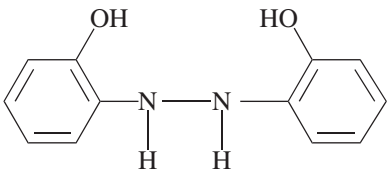

bis(*o*-hydroxyphenyl) hydrazine

27-4. Why do some absorbing compounds fluoresce while others do not?

***27-5.** Describe the characteristics of organic compounds that fluoresce.

27-6. Explain why molecular fluorescence often occurs at a longer wavelength than the exciting radiation.

***27-7.** Describe the components of a filter fluorometer and a spectrofluorometer.

27-8. Why are most fluorescence instruments double beam in design?

***27-9.** Why are fluorometers often more useful than spectrofluorometers for quantitative analysis?

27-10. The reduced form of nicotinamide adenine dinucleotide (NADH) is an important and highly fluorescent coenzyme. It has an absorption maximum of 340 nm and an emission maximum at 465 nm. Standard solutions of NADH gave the following fluorescence intensities:

Concn NADH, μmol/L	Relative Intensity
0.100	2.24
0.200	4.52
0.300	6.63
0.400	9.01
0.500	10.94
0.600	13.71
0.700	15.49
0.800	17.91

- (a) Construct a spreadsheet and use it to draw a calibration curve for NADH.
- *(b) Find the least-squares slope and intercept for the plot in (a).
- (c) Calculate the standard deviation of the slope and the standard deviation about regression for the curve.
- *(d) An unknown exhibits a relative fluorescence intensity of 11.34. Use the spreadsheet to calculate the concentration of NADH.
- *(e) Calculate the relative standard deviation for the result in part (d).
- (f) Calculate the relative standard deviation for the result in part (d) if the reading of 12.16 was the mean of three measurements.

27-11. The volumes of a 1.10 ppm standard solution of Zn^{2+} shown in the table below were pipetted into separatory funnels each containing 5.00 mL of an unknown zinc solution. Each was extracted with three 5-mL aliquots of CCl_4 containing an excess of 8-hydroxyquinoline. The extracts were then diluted to 25.0 mL, and their fluorescence measured with a fluorometer. The results were:

Volume Std Zn^{2+}, mL	Fluorometer Reading
0.000	6.12
4.00	11.16
8.00	15.68
12.00	20.64

- (a) Construct a working curve from the data.
- (b) Calculate a linear least-squares equation for the data.

(c) Calculate the standard deviation of the slope and the standard deviation about regression.
(d) Calculate the concentration of zinc in the sample.
(e) Calculate a standard deviation for the result in part (d).

*27-12. Quinine in a 1.664-g antimalarial tablet was dissolved in sufficient 0.10 M HCl to give 500 mL of solution. A 15.00-mL aliquot was then diluted to 100.0 mL with the acid. The fluorescence intensity for the diluted sample at 347.5 nm provided a reading of 288 on an arbitrary scale. A standard 100 ppm quinine solution registered 180 when measured under conditions identical to those for the diluted sample. Calculate the mass of quinine in milligrams in the tablet.

27-13. The determination in Problem 27-12 was modified to use the standard addition method. In this case, a 2.196-g tablet was dissolved in sufficient 0.10 M HCl to give 1.000 L. Dilution of a 20.00-mL aliquot to 100 mL produced a solution that gave a reading of 540 at 347.5 nm. A second 20.00-mL aliquot was mixed with 10.0 mL of 50 ppm quinine solution before dilution to 100 mL. The fluorescence intensity of this solution was 600. Calculate the concentration in parts per million of quinine in the tablet.

27-14. **Challenge Problem:** The following volumes of a standard 10.0 ppb F^- solution were added to four 10.00-mL aliquots of a water sample: 0.00, 1.00, 2.00, and 3.00 mL. Precisely 5.00 mL of a solution containing an excess of the strongly absorbing Al-acid Alizarin Garnet R complex was added to each of the four solutions, and they were each diluted to 50.0 mL. The fluorescence intensity of the four solutions were as follows:

V_s, mL	Meter reading
0.00	68.2
1.00	55.3
2.00	41.3
3.00	28.8

(a) Explain the chemistry of the analytical method.
(b) Construct a plot of the data.
(c) Use the fact that the fluorescence decreases with increasing amounts of the F^- standard to derive a relationship like Equation 26-1 for multiple standard additions. Then use this relationship to obtain an equation for the unknown concentration c_x in terms of the slope and intercept of the standard additions plot, similar to Equation 26-2.
(d) Use linear least squares to find the equation for the line representing the relationship between the decrease in fluorescence and the volume of standard fluoride V_s.
(e) Calculate the standard deviation of the slope and intercept.
(f) Calculate the concentration of F^- in the sample in ppb.
(g) Calculate the standard deviation of the result in (e).

Electrochemical Methods

PART IV

CHAPTER 18

Introduction to Electrochemistry

© Norbert Wu/Minden Pictures/Corbis

From the earliest days of experimental science, workers such as Galvani, Volta, and Cavendish realized that electricity interacts in interesting and important ways with animal tissues. Electrical charge causes muscles to contract, for example. Perhaps more surprising is that a few animals such as the torpedo (shown in the photo) produce charge by physiological means. More than 50 billion nerve terminals in the torpedo's flat "wings" on its left and right sides rapidly emit acetylcholine on the bottom side of membranes housed in the wings. The acetylcholine causes sodium ions to surge through the membranes, producing a rapid separation of charge and a corresponding potential difference, or voltage, across the membrane.[1] The potential difference then generates an electric current of several amperes in the surrounding seawater that may be used to stun or kill prey, detect and ward off enemies, or navigate. Natural devices for separating charge and creating electrical potential difference are relatively rare, but humans have learned to separate charge mechanically, metallurgically, and chemically to create cells, batteries, and other useful charge storage devices.

We now turn our attention to several analytical methods that are based on oxidation/reduction reactions. These methods, which are described in Chapters 18 through 23, include oxidation/reduction titrimetry, potentiometry, coulometry, electrogravimetry, and voltammetry. In this chapter, we present the fundamentals of electrochemistry that are necessary for understanding the principles of these procedures.

18A CHARACTERIZING OXIDATION/REDUCTION REACTIONS

Oxidation/reduction reactions are sometimes called **redox** reactions.

In an **oxidation/reduction reaction** electrons are transferred from one reactant to another. An example is the oxidation of iron(II) ions by cerium(IV) ions. The reaction is described by the equation

$$Ce^{4+} + Fe^{2+} \rightleftharpoons Ce^{3+} + Fe^{3+} \qquad (18\text{-}1)$$

A **reducing agent** is an electron donor. An **oxidizing agent** is an electron acceptor.

In this reaction, an electron is transferred from Fe^{2+} to Ce^{4+} to form Ce^{3+} and Fe^{3+} ions. A substance that has a strong affinity for electrons, such as Ce^{4+}, is called an **oxidizing agent**, or an **oxidant**. A **reducing agent**, or **reductant**, is a species, such

[1] Y. Dunant and M. Israel, *Sci. Am.* **1985**, *252,* 58, **DOI**: 10.1038/scientificamerican0485-58.

as Fe^{2+}, that donates electrons to another species. To describe the chemical behavior represented by Equation 18-1, we say that Fe^{2+} is oxidized by Ce^{4+}; similarly, Ce^{4+} is reduced by Fe^{2+}.

We can split any oxidation/reduction equation into two half-reactions that show which species gains electrons and which loses them. For example, Equation 18-1 is the sum of the two half-reactions

$$Ce^{4+} + e^- \rightleftharpoons Ce^{3+} \qquad \text{(reduction of } Ce^{4+}\text{)}$$

$$Fe^{2+} \rightleftharpoons Fe^{3+} + e^- \qquad \text{(oxidation of } Fe^{2+}\text{)}$$

It is important to understand that while we can write an equation for a half-reaction in which electrons are consumed or generated, we cannot observe an isolated half-reaction experimentally because there must always be a second half-reaction that serves as a source of electrons or a recipient of electrons. In other words, an individual half-reaction is a theoretical concept.

The rules for balancing half-reactions (see Feature 18-1) are the same as those for other reaction types, that is, the number of atoms of each element as well as the net charge on each side of the equation must be the same. Thus, for the oxidation of Fe^{2+} by MnO_4^-, the half-reactions are

$$MnO_4^- + 5e^- + 8H^+ \rightleftharpoons Mn^{2+} + 4H_2O$$

$$5Fe^{2+} \rightleftharpoons 5Fe^{3+} + 5e^-$$

In the first half-reaction, the net charge on the left side is $(-1 - 5 + 8) = +2$, which is the same as the charge on the right. Note also that we have multiplied the second half-reaction by 5 so that the number of electrons lost by Fe^{2+} equals the number gained by MnO_4^-. We can then write a balanced net ionic equation for the overall reaction by adding the two half-reactions

$$MnO_4^- + 5Fe^{2+} + 8H^+ \rightleftharpoons Mn^{2+} + 5Fe^{3+} + 4H_2O$$

18A-1 Comparing Redox Reactions to Acid/Base Reactions

Oxidation/reduction reactions can be viewed in a way that is analogous to the Brønsted-Lowry concept of acid/base reactions (see Section 9A-2). In both, one or more charged particles are transferred from a donor to an acceptor—the particles

Recall that in the Brønsted/Lowry concept an acid/base reaction is described by the equation

$$acid_1 + base_2 \rightleftharpoons base_1 + acid_2$$

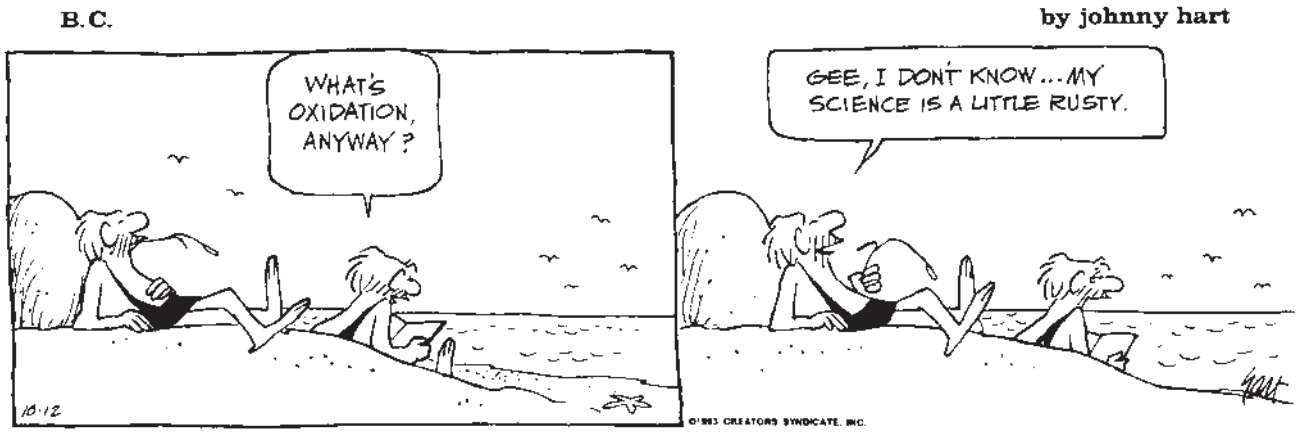

FEATURE 18-1

Balancing Redox Equations

Knowing how to balance oxidation/reduction reactions is essential to understanding all the concepts covered in this chapter. Although you probably remember this technique from your general chemistry course, we present a quick review to remind you of how the process works. For practice, we will complete and balance the following equation after adding H^+, OH^-, or H_2O as needed.

$$MnO_4^- + NO_2^- \rightleftharpoons Mn^{2+} + NO_3^-$$

First, we write and balance the two half-reactions. For MnO_4^-, we write

$$MnO_4^- \rightleftharpoons Mn^{2+}$$

To account for the 4 oxygen atoms on the left-hand side of the equation, we add $4H_2O$ on the right-hand side. Then, to balance the hydrogen atoms, we must provide $8H^+$ on the left:

$$MnO_4^- + 8H^+ \rightleftharpoons Mn^{2+} + 4H_2O$$

To balance the charge, we need to add 5 electrons to the left side of the equation. Thus,

$$MnO_4^- + 8H^+ + 5e^- \rightleftharpoons Mn^{2+} + 4H_2O$$

For the other half-reaction,

$$NO_2^- \rightleftharpoons NO_3^-$$

we add one H_2O to the left side of the equation to supply the needed oxygen and $2H^+$ on the right to balance hydrogen:

$$NO_2^- + H_2O \rightleftharpoons NO_3^- + 2H^+$$

Then, we add two electrons to the right-hand side to balance the charge:

$$NO_2^- + H_2O \rightleftharpoons NO_3^- + 2H^+ + 2e^-$$

Before combining the two equations, we must multiply the first by 2 and the second by 5 so that the number of electrons lost will be equal to the number of electrons gained. We then add the two half reactions to obtain

$$2MnO_4^- + 16H^+ + 10e^- + 5NO_2^- + 5H_2O \rightleftharpoons 2Mn^{2+} + 8H_2O + 5NO_3^- + 10H^+ + 10e^-$$

This equation rearranges to the balanced equation

$$2MnO_4^- + 6H^+ + 5NO_2^- \rightleftharpoons 2Mn^{2+} + 5NO_3^- + 3H_2O$$

being electrons in oxidation/reduction and protons in neutralization. When an acid donates a proton, it becomes a conjugate base that is capable of accepting a proton. By analogy, when a reducing agent donates an electron, it becomes an oxidizing agent that can then accept an electron. This product could be called a conjugate oxidant, but that terminology is seldom, if ever, used. With this idea in mind, we can write a generalized equation for a redox reaction as

$$A_{red} + B_{ox} \rightleftharpoons A_{ox} + B_{red} \qquad (18\text{-}2)$$

In this equation, B_{ox}, the oxidized form of species B, accepts electrons from A_{red} to form the new reductant, B_{red}. At the same time, reductant A_{red}, having given up electrons, becomes an oxidizing agent, A_{ox}. If we know from chemical evidence that the equilibrium in Equation 18-2 lies to the right, we can state that B_{ox} is a better electron acceptor (stronger oxidant) than A_{ox}. Likewise, A_{red} is a more effective electron donor (better reductant) than B_{red}.

Charles D. Winters

Figure 18-1 Photograph of a "silver tree" created by immersing a coil of copper wire in a solution of silver nitrate.

EXAMPLE 18-1

The following reactions are spontaneous and thus proceed to the right, as written:

$$2H^+ + Cd(s) \rightleftharpoons H_2 + Cd^{2+}$$
$$2Ag^+ + H_2(g) \rightleftharpoons 2Ag(s) + 2H^+$$
$$Cd^{2+} + Zn(s) \rightleftharpoons Cd(s) + Zn^{2+}$$

What can we deduce regarding the strengths of H^+, Ag^+, Cd^{2+}, and Zn^{2+} as electron acceptors (or oxidizing agents)?

Solution

The second reaction establishes that Ag^+ is a more effective electron acceptor than H^+; the first reaction demonstrates that H^+ is more effective than Cd^{2+}. Finally, the third equation shows that Cd^{2+} is more effective than Zn^{2+}. Thus, the order of oxidizing strength is $Ag^+ > H^+ > Cd^{2+} > Zn^{2+}$.

18A-2 Oxidation/Reduction Reactions in Electrochemical Cells

Many oxidation/reduction reactions can be carried out in either of two ways that are physically quite different. In one, the reaction is performed by bringing the oxidant and the reductant into direct contact in a suitable container. In the second, the reaction is carried out in an electrochemical cell in which the reactants do not come in direct contact with one another. A spectacular example of direct contact is the famous "silver tree" experiment in which a piece of copper is immersed in a silver nitrate solution (see **Figure 18-1**). Silver ions migrate to the metal and are reduced:

$$Ag^+ + e^- \rightleftharpoons Ag(s)$$

At the same time, an equivalent quantity of copper is oxidized:

$$Cu(s) \rightleftharpoons Cu^{2+} + 2e^-$$

For an interesting illustration of this reaction, immerse a piece of copper in a solution of silver nitrate. The result is the deposition of silver on the copper in the form of a "silver tree." See Figure 18-1 and color plate 10.

By multiplying the silver half-reaction by two and adding the reactions, we obtain a net ionic equation for the overall process:

$$2Ag^+ + Cu(s) \rightleftharpoons 2Ag(s) + Cu^{2+} \qquad (18\text{-}3)$$

A unique aspect of oxidation/reduction reactions is that the transfer of electrons—and thus an identical net reaction—can often be brought about in an **electrochemical cell** in which the oxidizing agent and the reducing agent are physically separated from one another. Figure 18-2a shows such an arrangement. Note that a **salt bridge** isolates the reactants but maintains electrical contact between the two halves of the cell. When a voltmeter of high internal resistance is connected as shown or the electrodes are not connected externally, the cell is said to be at **open circuit** and delivers the full cell potential. When the circuit is open, no net reaction occurs in the cell, although we shall show that the cell has the **potential** for doing work. The voltmeter measures the potential difference, or **voltage**, between the two electrodes at any instant. This voltage is a measure of the tendency of the cell reaction to proceed toward equilibrium.

Salt bridges are widely used in electrochemistry to prevent mixing of the contents of the two electrolyte solutions making up electrochemical cells. Normally, the two ends of the bridge are fitted with sintered glass disks or other porous materials to prevent liquid from siphoning from one part of the cell to the other.

In Figure 18-2b, the cell is connected so that electrons can pass through a low-resistance external circuit. The potential energy of the cell is now converted to electrical energy to light a lamp, run a motor, or do some other type of electrical work. In the cell in Figure 18-2b, metallic copper is oxidized at the left-hand electrode, silver ions are reduced at the right-hand electrode, and electrons flow through the external circuit to the silver electrode. As the reaction goes on, the cell potential, initially 0.412 V when the circuit is open, decreases continuously and approaches zero as the overall reaction approaches equilibrium. When the cell is at equilibrium, the forward reaction (left-to-right) occurs at the same rate as the reverse reaction (right-to-left), and the cell voltage is zero. A cell with zero voltage does not perform work, as anyone who has found a "dead" battery in a flashlight or in a laptop computer can attest.

When the $CuSO_4$ and $AgNO_3$ solutions are 0.0200 M, the cell has a potential of 0.412 V, as shown in Figure 18-2a.

When zero voltage is reached in the cell of Figure 18-2b, the concentrations of Cu(II) and Ag(I) ions will have values that satisfy the equilibrium-constant expression shown in Equation 18-4. At this point, no further net flow of electrons will occur. *It is important to recognize that the overall reaction and its position of equilibrium are totally independent of the way the reaction is carried out*, whether it is by direct reaction in a solution or by indirect reaction in an electrochemical cell.

The equilibrium-constant expression for the reaction shown in Equation 18-3 is

$$K_{eq} = \frac{[Cu^{2+}]}{[Ag^+]} = 4.1 \times 10^{15} \qquad (18\text{-}4)$$

This expression applies whether the reaction occurs directly between reactants or within an electrochemical cell.

At equilibrium, the two half reactions in a cell continue, but their rates are equal.

18B ELECTROCHEMICAL CELLS

We can study oxidation/reduction equilibria conveniently by measuring the potentials of electrochemical cells in which the two half-reactions making up the equilibrium are participants. For this reason, we must consider some characteristics of electrochemical cells.

The electrodes in some cells share a common electrolyte; these are known as **cells without liquid junction**. For an example of such a cell, see Figure 19-2 and Example 19-7.

An electrochemical cell consists of two conductors called **electrodes**, each of which is immersed in an electrolyte solution. In most of the cells that will be of interest to us, the solutions surrounding the two electrodes are different and must be separated to avoid direct reaction between the reactants. The most common way of avoiding mixing is to insert a salt bridge, such as that shown in Figure 18-2, between the solutions. Conduction of electricity from one electrolyte solution to the other then occurs by migration of potassium ions in the bridge in one direction and chloride ions in the other. However, direct contact between copper metal and silver ions is prevented.

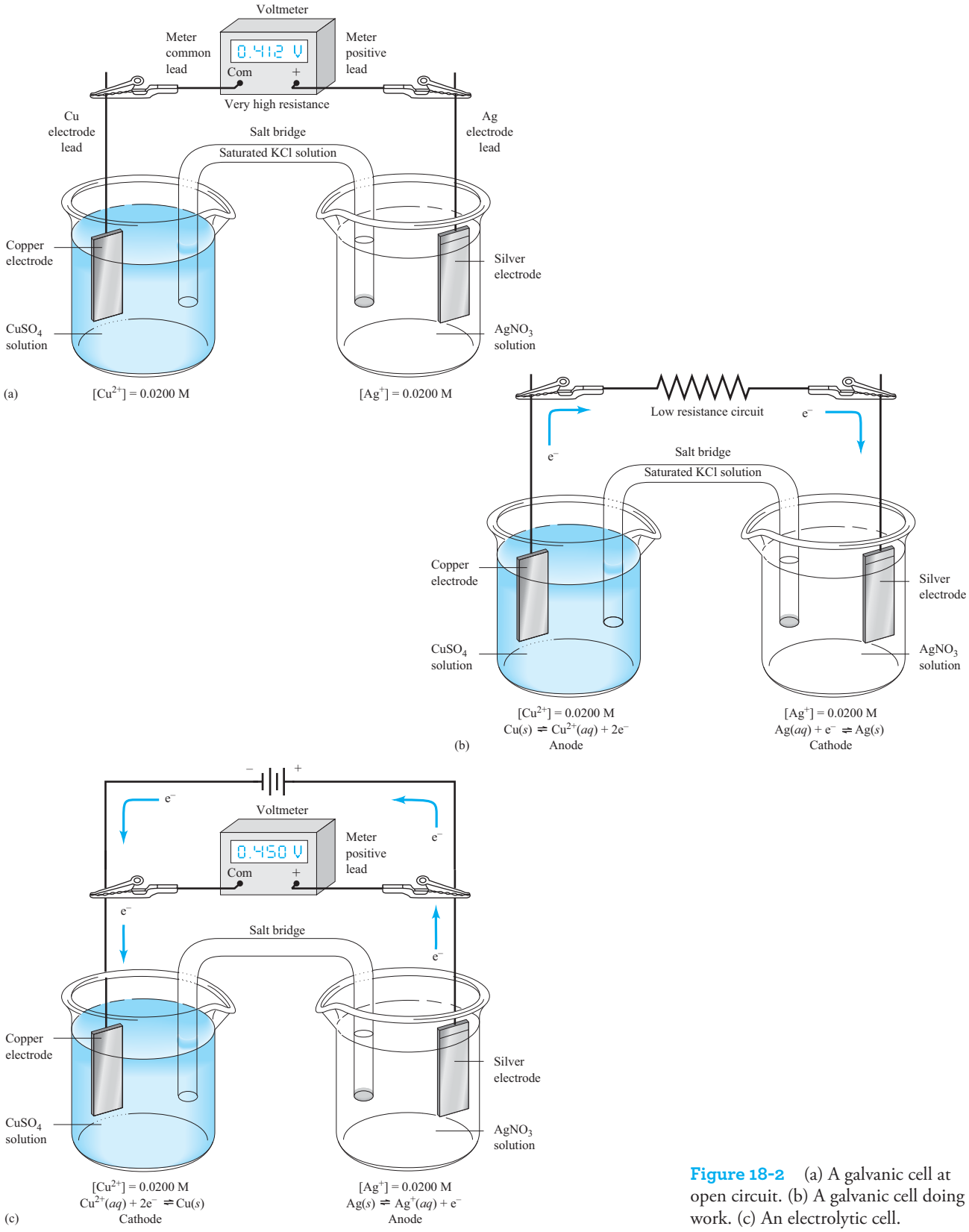

Figure 18-2 (a) A galvanic cell at open circuit. (b) A galvanic cell doing work. (c) An electrolytic cell.

18B-1 Cathodes and Anodes

A **cathode** is an electrode where reduction occurs. An **anode** is an electrode where oxidation occurs.

The **cathode** in an electrochemical cell is the electrode at which reduction occurs. The **anode** is the electrode at which an oxidation takes place.

Examples of typical cathodic reactions include

$$Ag^+ + e^- \rightleftharpoons Ag(s)$$

$$Fe^{3+} + e^- \rightleftharpoons Fe^{2+}$$

$$NO_3^- + 10H^+ + 8e^- \rightleftharpoons NH_4^+ + 3H_2O$$

The reaction $2H^+ + 2e^- \rightleftharpoons H_2(g)$ occurs at a cathode when an aqueous solution contains no other species that are more easily reduced than H^+.

We can force a desired reaction to occur by applying a suitable potential to an electrode made of an unreactive material such as platinum. Note that the reduction of NO_3^- in the third reaction reveals that anions can migrate to a cathode and be reduced.

Typical anodic reactions include

$$Cu(s) \rightleftharpoons Cu^{2+} + 2e^-$$

$$2Cl^- \rightleftharpoons Cl_2(g) + 2e^-$$

$$Fe^{2+} \rightleftharpoons Fe^{3+} + e^-$$

The Fe^{2+}/Fe^{3+} half-reaction may seem somewhat unusual because a cation rather than an anion migrates to the anode and gives up an electron. Oxidation of a cation at an anode or reduction of an anion at a cathode is a relatively common process.

The first reaction requires a copper anode, but the other two can be carried out at the surface of an inert platinum electrode.

18B-2 Types of Electrochemical Cells

Electrochemical cells are either galvanic or electrolytic. They can also be classified as reversible or irreversible.

Galvanic cells store electrical energy; **electrolytic cells** consume electricity.

Galvanic, or **voltaic**, **cells** store electrical energy. **Batteries** are usually made from several such cells connected in series to produce higher voltages than a single cell can produce. The reactions at the two electrodes in such cells tend to proceed spontaneously and produce a flow of electrons from the anode to the cathode via an external conductor. The cell shown in Figure 18-2a shows a galvanic cell that exhibits a potential of about 0.412 V when no current is being drawn from it. The silver electrode is positive with respect to the copper electrode in this cell. The copper electrode, which is negative with respect to the silver electrode, is a potential source of electrons to the external circuit when the cell is discharged. The cell in Figure 18-2b is the same galvanic cell, but now it is under discharge so that electrons move through the external circuit from the copper electrode to the silver electrode. While being discharged, the silver electrode is the *cathode* since the reduction of Ag^+ occurs here. The copper electrode is the *anode* since the oxidation of $Cu(s)$ occurs at this electrode. Galvanic cells operate spontaneously, and the net reaction during discharge is called the **spontaneous cell reaction**. For the cell of Figure 18-2b, the spontaneous cell reaction is that given by equation 18-3, that is, $2Ag^+ + Cu(s) \rightleftharpoons 2Ag(s) + Cu^{2+}$.

The reaction $2H_2O \rightleftharpoons O_2(g) + 4H^+ + 4e^-$ occurs at an anode when an aqueous solution contains no other species that are more easily oxidized than H_2O.

For both galvanic and electrolytic cells, remember that (1) reduction always takes place at the cathode, and (2) oxidation always takes place at the anode. The cathode in a galvanic cell becomes the anode, however, when the cell is operated as an electrolytic cell.

An **electrolytic cell**, in contrast to a voltaic cell, requires an external source of electrical energy for operation. The cell in Figure 18-2 can be operated as an electrolytic cell by connecting the positive terminal of an external voltage source with

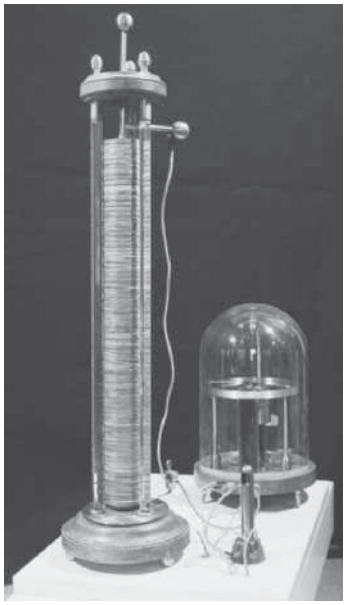

Alessandro Volta (1745–1827), Italian physicist, was the inventor of the first battery, the so-called voltaic pile (shown on the right). It consisted of alternating disks of copper and zinc separated by disks of cardboard soaked with salt solution. In honor of his many contributions to electrical science, the unit of potential difference, the volt, is named for Volta. In fact, in modern usage, we often call the quantity the voltage instead of potential difference.

a potential somewhat greater than 0.412 V to the silver electrode and the negative terminal of the source to the copper electrode, as shown in **Figure 18-2c**. Since the negative terminal of the external voltage source is electron rich, electrons flow from this terminal to the copper electrode, where reduction of Cu^{2+} to $Cu(s)$ occurs. The current is sustained by the oxidation of $Ag(s)$ to Ag^+ at the right-hand electrode, producing electrons that flow to the positive terminal of the voltage source. Note that in the electrolytic cell, the direction of the current is the reverse of that in the galvanic cell in Figure 18-2b, and the reactions at the electrodes are reversed as well. The silver electrode is forced to become the *anode*, while the copper electrode is forced to become the *cathode*. The net reaction that occurs when a voltage higher than the galvanic cell voltage is applied is the opposite of the spontaneous cell reaction. That is,

$$2Ag(s) + Cu^{2+} \rightleftharpoons 2Ag^+ + Cu(s)$$

The cell in Figure 18-2 is an example of a reversible cell, in which the direction of the electrochemical reaction is reversed when the direction of electron flow is changed. In an irreversible cell, changing the direction of current causes entirely different half-reactions to occur at one or both electrodes. The lead-acid storage battery in an automobile is a common example of a series of reversible cells. When an external charger or the generator charges the battery, its cells are electrolytic. When it is used to operate the headlights, the radio, or the ignition, its cells are galvanic.

In a **reversible cell**, reversing the current reverses the cell reaction. In an **irreversible cell**, reversing the current causes a different half-reaction to occur at one or both of the electrodes.

FEATURE 18-2

The Daniell Gravity Cell

The Daniell gravity cell was one of the earliest galvanic cells to find widespread practical application. It was used in the mid-1800s to power telegraphic communication systems. As shown in **Figure 18F-1** (also see color plate 11), the cathode was a piece of copper immersed in a saturated solution of copper sulfate. A much less dense solution of dilute zinc sulfate was layered on top of the copper sulfate, and a massive zinc electrode was located in this solution. The electrode reactions were

$$Zn(s) \rightleftharpoons Zn^{2+} + 2e^-$$
$$Cu^{2+} + 2e^- \rightleftharpoons Cu(s)$$

This cell develops an initial voltage of 1.18 V, which gradually decreases as the cell discharges.

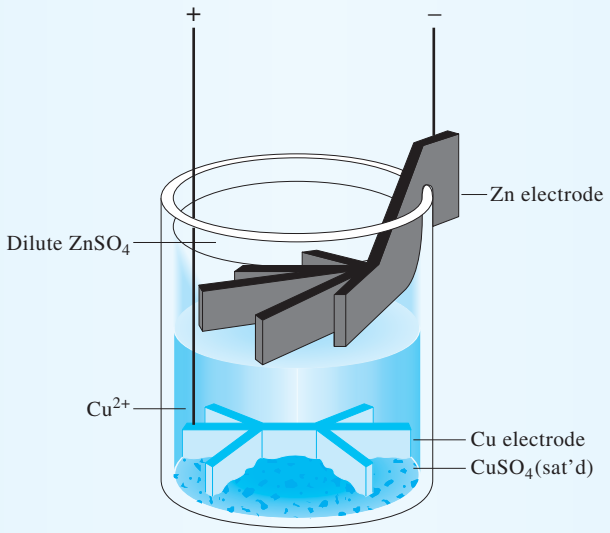

Figure 18F-1 A Daniell gravity cell.

18B-3 Representing Cells Schematically

Chemists frequently use a shorthand notation to describe electrochemical cells. The cell in Figure 18-2a, for example, is described by

$$Cu\,|\,Cu^{2+}(0.0200\ M)\,||\,Ag^+(0.0200\ M)\,|\,Ag \qquad (18\text{-}5)$$

By convention, a single vertical line indicates a phase boundary, or interface, at which a potential develops. For example, the first vertical line in this schematic indicates that a potential develops at the phase boundary between the copper electrode and the copper sulfate solution. The double vertical lines represent two-phase boundaries, one at each end of the salt bridge. There is a **liquid-junction potential** at each of these interfaces. The junction potential results from differences in the rates

at which the ions in the cell compartments and the salt bridge migrate across the interfaces. A liquid-junction potential can amount to as much as several hundredths of a volt but can be negligibly small if the electrolyte in the salt bridge has an anion and a cation that migrate at nearly the same rate. A saturated solution of potassium chloride, KCl, is the electrolyte that is most widely used. This electrolyte can reduce the junction potential to a few millivolts or less. For our purposes, we will neglect the contribution of liquid-junction potentials to the total potential of the cell. There are also several examples of cells that are without liquid junction and therefore do not require a salt bridge.

An alternative way of writing the cell shown in Figure 18-2a is

$$\text{Cu} \mid \text{CuSO}_4(0.0200\ \text{M}) \parallel \text{AgNO}_3(0.0200\ \text{M}) \mid \text{Ag}$$

In this description, the compounds used to prepare the cell are indicated rather than the active participants in the cell half-reactions.

18B-4 Currents in Electrochemical Cells

Figure 18-3 shows the movement of various charge carriers in a galvanic cell during discharge. The electrodes are connected with a wire so that the spontaneous cell reaction occurs. Charge is transported through such an electrochemical cell by three mechanisms:

1. Electrons carry the charge within the electrodes as well as the external conductor. Notice that by convention, current, which is normally indicated by the symbol I, is opposite in direction to electron flow.
2. Anions and cations are the charge carriers within the cell. At the left-hand electrode, copper is oxidized to copper ions, giving up electrons to the electrode. As shown in Figure 18-3, the copper ions formed move away from the copper electrode into the bulk of solution, while anions, such as sulfate and hydrogen sulfate ions, migrate toward the copper anode. Within the salt bridge, chloride ions migrate toward and into the copper compartment, and potassium ions move in the opposite direction. In the right-hand compartment, silver ions move toward the silver electrode where they are reduced to silver metal, and the nitrate ions move away from the electrode into the bulk of solution.
3. The ionic conduction of the solution is coupled to the electronic conduction in the electrodes by the reduction reaction at the cathode and the oxidation reaction at the anode.

In a cell, electricity is carried by the movement of ions. Both anions and cations contribute.

The phase boundary between an electrode and its solution is called an **interface**.

18C ELECTRODE POTENTIALS

The potential difference between the electrodes of the cell in **Figure 18-4a** is a measure of the tendency for the reaction

$$2\text{Ag}(s) + \text{Cu}^{2+} \rightleftharpoons 2\text{Ag}^{+} + \text{Cu}(s)$$

to proceed from a nonequilibrium state to the condition of equilibrium. The cell potential E_{cell} is related to the free energy of the reaction ΔG by

$$\Delta G = -nFE_{\text{cell}} \qquad (18\text{-}6)$$

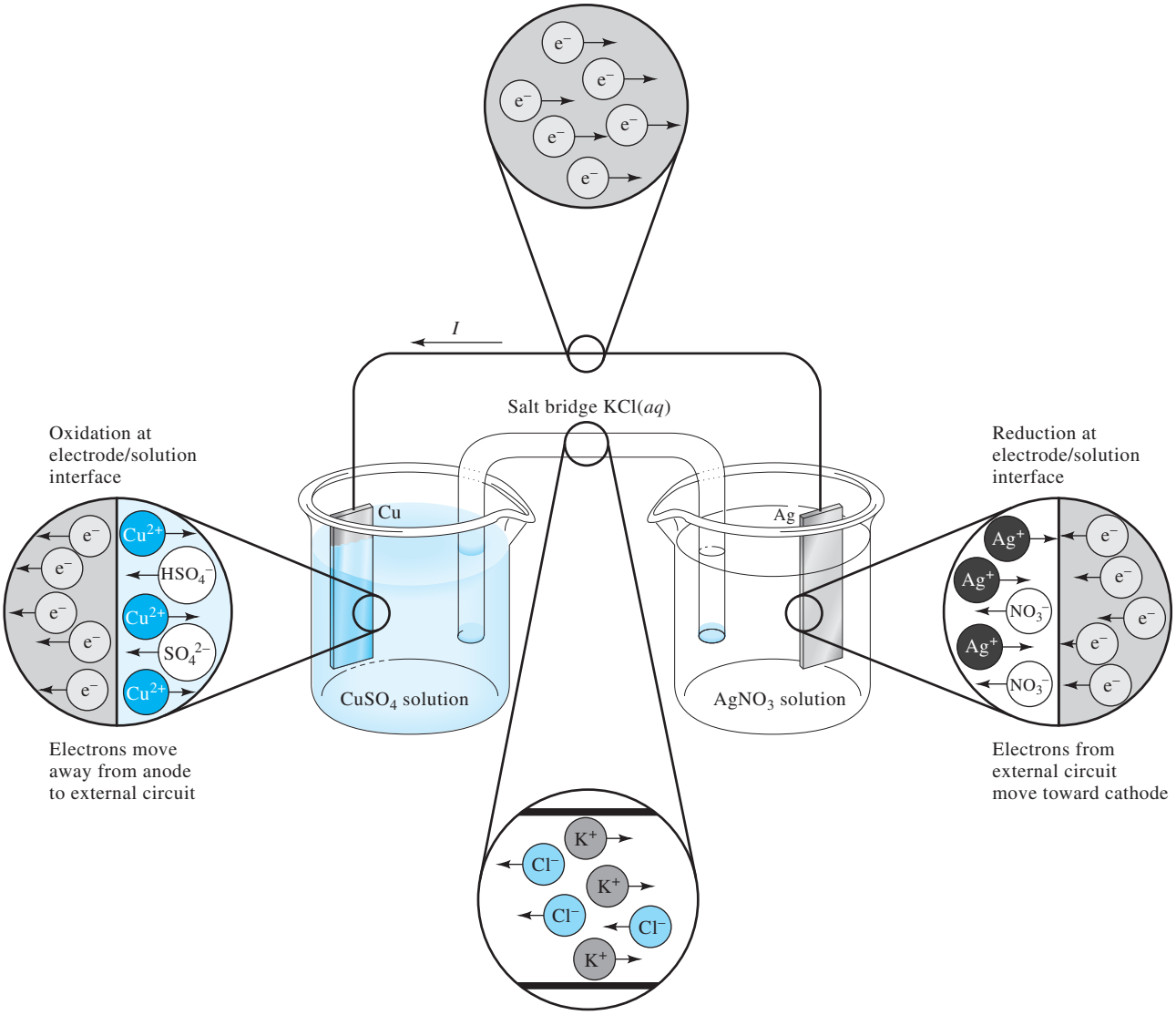

Figure 18-3 Movement of charge in a galvanic cell.

The **standard state** of a substance is a reference state that allows us to obtain relative values of such thermodynamic quantities as free energy, activity, enthalpy, and entropy. All substances are assigned unit activity in their standard states. For gases, the standard state has the properties of an ideal gas but at one atmosphere pressure. It is thus said to be a *hypothetical* state. For pure liquids and solvents, the standard states are *real* states and are the pure substances at a specified temperature and pressure. For solutes in dilute solution, the standard state is a hypothetical state that has the properties of an infinitely dilute solute but at unit concentration (molar or molal concentration, or mole fraction). The standard state of a solid is a real state and is the pure solid in its most stable crystalline form.

If the reactants and products are in their **standard states**, the resulting cell potential is called the **standard cell potential**. This latter quantity is related to the standard free energy change for the reaction and thus to the equilibrium constant by

$$\Delta G^0 = -nFE^0_{\text{cell}} = -RT \ln K_{\text{eq}} \tag{18-7}$$

where R is the gas constant and T is the absolute temperature.

18C-1 Sign Convention for Cell Potentials

When we consider a normal chemical reaction, we speak of the reaction occurring from reactants on the left side of the arrow to products on the right side. By the International Union of Pure and Applied Chemistry (IUPAC) sign convention, when

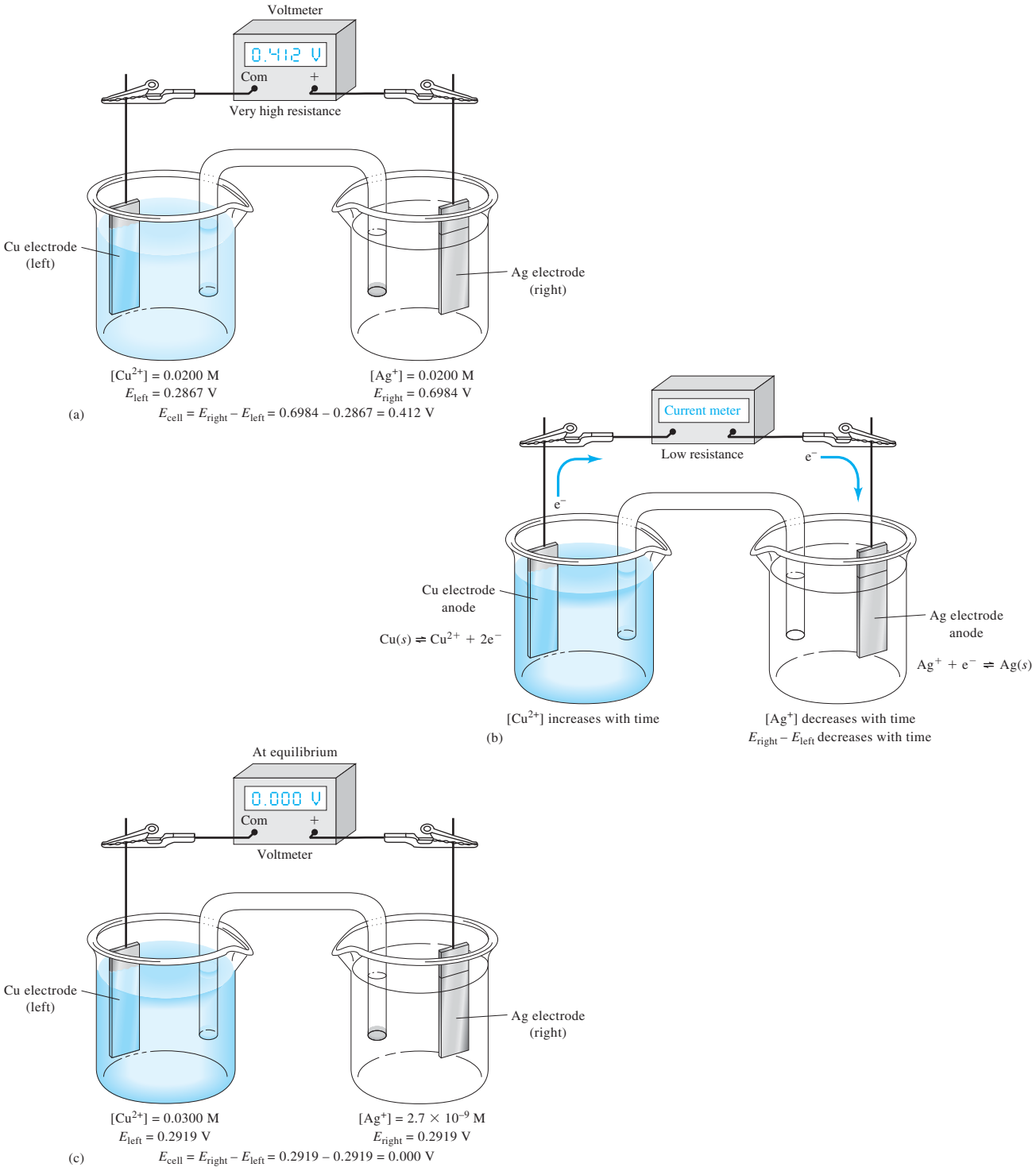

Figure 18-4 Change in cell potential after passage of current until equilibrium is reached. In (a), the high-resistance voltmeter prevents any significant electron flow, and the full open-circuit cell potential is measured. For the concentrations shown, this potential is +0.412 V. In (b), the voltmeter is replaced with a low-resistance current meter, and the cell discharges with time until eventually equilibrium is reached. In (c), after equilibrium is reached, the cell potential is again measured with a voltmeter and found to be 0.000 V. The concentrations in the cell are now those at equilibrium as shown.

we consider an electrochemical cell and its resulting potential, we consider the cell reaction to occur in a certain direction as well. The convention for cells is called the **plus right rule**. This rule implies that we always measure the cell potential by connecting the positive lead of the voltmeter to the right-hand electrode in the schematic or cell drawing (Ag electrode in Figure 18-4) and the common, or ground, lead of the voltmeter to the left-hand electrode (Cu electrode in Figure 18-4). If we always follow this convention, the value of E_{cell} is a measure of the tendency of the cell reaction to occur spontaneously in the direction written below from left to right.

$$Cu\,|\,Cu^{2+}(0.0200\ M)\ ||\ Ag^{+}(0.0200\ M)\,|\,Ag$$

That is, the direction of the overall process has Cu metal being oxidized to Cu^{2+} in the left-hand compartment and Ag^{+} being reduced to Ag metal in the right-hand compartment. In other words, the reaction being considered is

$$Cu(s) + 2Ag^{+} \rightleftharpoons Cu^{2+} + 2Ag(s).$$

Implications of the IUPAC Convention

The leads of voltmeters are color coded. The positive lead is red, and the common, or ground, lead is black.

There are several implications of the sign convention that may not be obvious. First, if the measured value of E_{cell} is positive, the right-hand electrode is positive with respect to the left-hand electrode, and the free energy change for the reaction in the direction being considered is negative according to Equation 18-6. Hence, the reaction in the direction being considered would occur spontaneously if the cell were short-circuited or connected to some device to perform work (e.g., light a lamp, power a radio, or start a car). On the other hand, if E_{cell} is negative, the right-hand electrode is negative with respect to the left-hand electrode, the free energy change is positive, and the reaction in the direction considered (oxidation on the left, reduction on the right) is *not* the spontaneous cell reaction. For our cell of Figure 18-4a, $E_{cell} = +0.412$ V, and the oxidation of Cu and reduction of Ag^{+} occur spontaneously when the cell is connected to a device and allowed to do so.

The IUPAC convention is consistent with the signs that the electrodes actually develop in a galvanic cell. That is, in the Cu/Ag cell shown in Figure 18-4, the Cu electrode becomes electron rich (negative) because of the tendency of Cu to be oxidized to Cu^{2+}, and the Ag electrode is electron deficient (positive) because of the tendency for Ag^{+} to be reduced to Ag. As the galvanic cell discharges spontaneously, the silver electrode is the cathode, while the copper electrode is the anode. Note that for the same cell written in the opposite direction

$$Ag\,|\,AgNO_3\ (0.0200\ M)\ ||\ CuSO_4\ (0.0200\ M)\,|\,Cu$$

the measured cell potential would be $E_{cell} = -0.412$ V, and the reaction considered is

$$2Ag(s) + Cu^{2+} \rightleftharpoons 2Ag^{+} + Cu(s)$$

This reaction is *not* the spontaneous cell reaction because E_{cell} is negative, and ΔG is thus positive. It does not matter to the cell which electrode is written in the schematic on the right and which is written on the left. The spontaneous cell reaction is *always*

$$Cu(s) + 2Ag^{+} \rightleftharpoons Cu^{2+} + 2Ag(s)$$

By convention, we just measure the cell in a standard manner and consider the cell reaction in a standard direction. Finally, we must emphasize that, no matter how we may write the cell schematic or arrange the cell in the laboratory, if we connect a wire or a low-resistance circuit to the cell, *the spontaneous cell reaction will occur.* The only way to achieve the reverse reaction is to connect an external voltage source and force the electrolytic reaction $2Ag(s) + Cu^{2+} \rightleftharpoons 2Ag^{+} + Cu(s)$ to occur.

Half-Cell Potentials

The potential of a cell such as that shown in Figure 18-4a is the difference between two half-cell or single-electrode potentials, one associated with the half-reaction at the right-hand electrode (E_{right}) and the other associated with the half-reaction at the left-hand electrode (E_{left}). According to the IUPAC sign convention, as long as the liquid-junction potential is negligible or there is no liquid junction, we may write the cell potential E_{cell} as

$$E_{cell} = E_{right} - E_{left} \tag{18-8}$$

Although we cannot determine absolute potentials of electrodes such as these (see Feature 18-3), we can easily determine relative electrode potentials. For example, if we replace the copper electrode in the cell in Figure 18-2 with a cadmium electrode immersed in a cadmium sulfate solution, the voltmeter reads about 0.7 V more positive than the original cell. Since the right-hand compartment remains unaltered, we conclude that the half-cell potential for cadmium is about 0.7 V less than that for copper (that is, cadmium is a stronger reductant than is copper). Substituting other electrodes while keeping one of the electrodes unchanged allows us to construct a table of relative electrode potentials, as discussed in Section 18C-3.

Discharging a Galvanic Cell

The galvanic cell of Figure 18-4a is in a nonequilibrium state because the very high resistance of the voltmeter prevents the cell from discharging significantly. So when we measure the cell potential, no reaction occurs, and what we measure is the tendency of the reaction to occur *if* we allowed it to proceed. For the Cu/Ag cell with the concentrations shown, the cell potential measured under open circuit conditions is +0.412 V, as previously noted. If we now allow the cell to discharge by replacing the voltmeter with a low-resistance current meter, as shown in **Figure 18-4b**, the spontaneous cell reaction occurs. The current, initially high, decreases exponentially with time (see **Figure 18-5**). As shown in **Figure 18-4c**, when equilibrium is reached, there is no net current in the cell, and the cell potential is 0.000 V. The copper ion concentration at equilibrium is then 0.0300 M, while the silver ion concentration falls to 2.7×10^{-9} M.

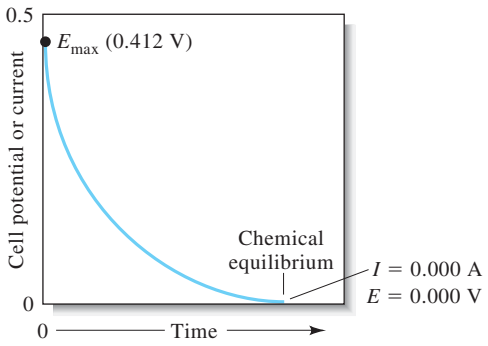

Figure 18-5 Cell potential in the galvanic cell of Figure 18-4b as a function of time. The cell current, which is directly related to the cell potential, also decreases with the same time behavior.

FEATURE 18-3

Why We Cannot Measure Absolute Electrode Potentials

Although it is not difficult to measure *relative* half-cell potentials, it is impossible to determine absolute half-cell potentials because all voltage-measuring devices measure only *differences* in potential. To measure the potential of an electrode, one contact of a voltmeter is connected to the electrode in question. The other contact from the meter must then be brought into electrical contact with the solution in the electrode compartment via another conductor. This second contact, however, inevitably creates a solid/solution interface that acts as a second half-cell when the potential is measured. Thus, an absolute half-cell potential is not obtained. What we do obtain is the difference between the half-cell potential of interest and a half-cell made up of the second contact and the solution.

Our inability to measure absolute half-cell potentials presents no real obstacle because relative half-cell potentials are just as useful provided they are all measured against the same reference half-cell. Relative potentials can be combined to give cell potentials. We can also use them to calculate equilibrium constants and generate titration curves.

18C-2 The Standard Hydrogen Reference Electrode

The standard hydrogen electrode is sometimes called the **normal hydrogen electrode (NHE)**.

For relative electrode potential data to be widely applicable and useful, we must have a generally agreed-upon reference half-cell against which all others are compared. Such an electrode must be easy to construct, reversible, and highly reproducible in its behavior. The **standard hydrogen electrode (SHE)** meets these specifications and has been used throughout the world for many years as a universal reference electrode. It is a typical **gas electrode**.

SHE is the abbreviation for standard hydrogen electrode.

Figure 18-6 shows the physical arrangement of a hydrogen electrode. The metal conductor is a piece of platinum that has been coated, or **platinized**, with finely divided platinum (platinum black) to increase its specific surface area. This electrode is immersed in an aqueous acid solution of known, constant hydrogen ion activity. The solution is kept saturated with hydrogen by bubbling the gas at constant pressure over the surface of the electrode. The platinum does not take part in the electrochemical reaction and serves only as the site where electrons are transferred. The half-reaction responsible for the potential that develops at this electrode is

Platinum black is a layer of finely divided platinum that is formed on the surface of a smooth platinum electrode by electrolytic deposition of the metal from a solution of chloroplatinic acid, H_2PtCl_6. The platinum black provides a large specific surface area of platinum at which the H^+/H_2 reaction can occur. Platinum black catalyzes the reaction shown in Equation 18-9. Remember that catalysts do not change the position of equilibrium but simply shorten the time it takes to reach equilibrium.

$$2H^+(aq) + 2e^- \rightleftharpoons H_2(g) \qquad (18\text{-}9)$$

The hydrogen electrode shown in Figure 18-6 can be represented schematically as

$$\text{Pt, } H_2(p = 1.00 \text{ atm}) \mid (H^+ = x \text{ M}) \parallel$$

The reaction shown as Equation 18-9 combines two equilibria:

$$2H^+ + 2e^- \rightleftharpoons H_2(aq)$$
$$H_2(aq) \rightleftharpoons H_2(g)$$

The continuous stream of gas at constant pressure provides the solution with a constant molecular hydrogen concentration.

In Figure 18-6, the hydrogen is specified as having a partial pressure of one atmosphere and the concentration of hydrogen ions in the solution is x M. The hydrogen electrode is reversible.

The potential of a hydrogen electrode depends on temperature and the activities of hydrogen ion and molecular hydrogen in the solution. The latter, in turn, is proportional to the pressure of the gas that is used to keep the solution saturated in hydrogen. For the SHE, the activity of hydrogen ions is specified as unity, and the partial pressure of the gas is specified as one atmosphere. *By convention, the potential*

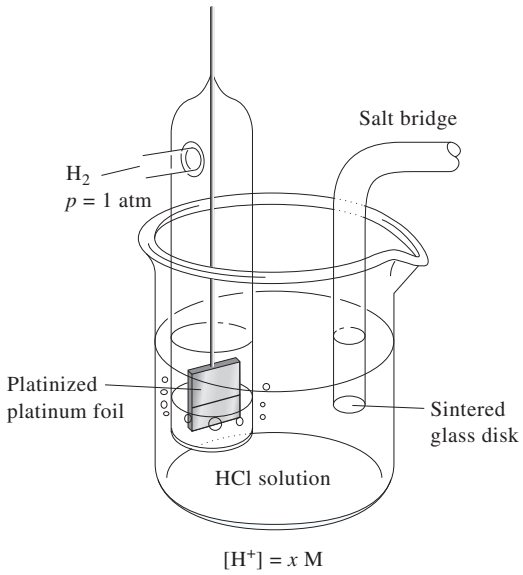

Figure 18-6 The hydrogen gas electrode.

of the standard hydrogen electrode is assigned a value of 0.000 V at all temperatures. As a consequence of this definition, any potential developed in a galvanic cell consisting of a standard hydrogen electrode and some other electrode is attributed entirely to the other electrode.

At $p_{H_2} = 1.00$ and $a_{H^+} = 1.00$, the potential of the hydrogen electrode is assigned a value of exactly 0.000 V at all temperatures.

Several other reference electrodes that are more convenient for routine measurements have been developed. Some of these are described in Section 21B.

18C-3 Electrode Potential and Standard Electrode Potential

An **electrode potential** is defined as the potential of a cell in which the electrode in question is the right-hand electrode and the standard hydrogen electrode is the left-hand electrode. So if we want to obtain the potential of a silver electrode in contact with a solution of Ag^+, we would construct a cell as shown in **Figure 18-7**. In this cell, the half-cell on the right consists of a strip of pure silver in contact with a solution containing silver ions; the electrode on the left is the standard hydrogen electrode. The cell potential is defined as in Equation 18-8. Because the left-hand electrode is the standard hydrogen electrode with a potential that has been assigned a value of 0.000 V, we can write

An electrode potential is the potential of a cell that has a standard hydrogen electrode as the left electrode (reference).

$$E_{cell} = E_{right} - E_{left} = E_{Ag} - E_{SHE} = E_{Ag} - 0.000 = E_{Ag}$$

where E_{Ag} is the potential of the silver electrode. Despite its name, an electrode potential is in fact the potential of an electrochemical cell which has a carefully defined reference electrode. Often, the potential of an electrode, such as the silver electrode in Figure 18-7, is referred to as E_{Ag} versus SHE to emphasize that it is the potential of a complete cell measured against the standard hydrogen electrode as a reference.

The **standard electrode potential**, $\boldsymbol{E^0}$, of a half-reaction is defined as its electrode potential when the activities of the reactants and products are all unity. For the cell in Figure 18-7, the E^0 value for the half reaction

$$Ag^+ + e^- \rightleftharpoons Ag(s)$$

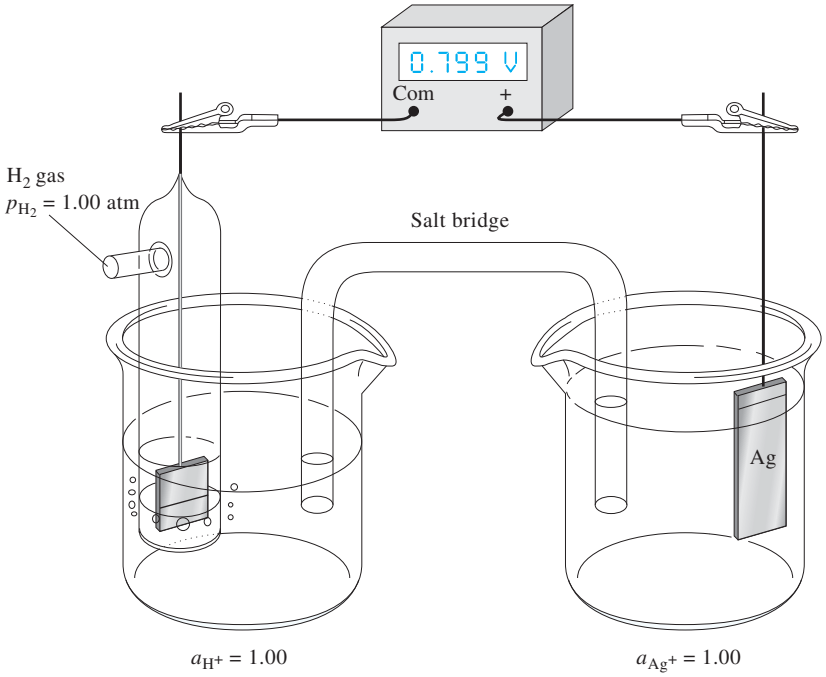

Figure 18-7 Measurement of the electrode potential for an Ag electrode. If the silver ion activity in the right-hand compartment is 1.00, the cell potential is the standard electrode potential of the Ag^+/Ag half-reaction.

can be obtained by measuring E_{cell} with the activity of Ag^+ equal to 1.00. In this case, the cell shown in Figure 18-7 can be represented schematically as

$$\text{Pt, } H_2(p = 1.00 \text{ atm}) \,|\, H^+(a_{H^+} = 1.00) \,||\, Ag^+(a_{Ag^+} = 1.00) \,|\, Ag$$

or alternatively as

$$\text{SHE} \,||\, Ag^+(a_{Ag^+} = 1.00) \,|\, Ag$$

This galvanic cell develops a potential of +0.799 V with the silver electrode on the right, that is, the spontaneous cell reaction is oxidation in the left-hand compartment and reduction in the right-hand compartment:

$$2Ag^+ + H_2(g) \rightleftharpoons 2Ag(s) + 2H^+$$

A metal ion/metal half-cell is sometimes called a **couple**.

Because the silver electrode is on the right and the reactants and products are in their standard states, the measured potential is by definition the standard electrode potential for the silver half-reaction, or the **silver couple**. Note that the silver electrode is positive with respect to the standard hydrogen electrode. Therefore, the standard electrode potential is given a positive sign, and we write

$$Ag^+ + e^- \rightleftharpoons Ag(s) \qquad E^0_{Ag^+/Ag} = +0.799 \text{ V}$$

Figure 18-8 illustrates a cell used to measure the standard electrode potential for the half-reaction

$$Cd^{2+} + 2e^- \rightleftharpoons Cd(s)$$

In contrast to the silver electrode, the cadmium electrode is negative with respect to the standard hydrogen electrode. Therefore, the standard electrode potential of

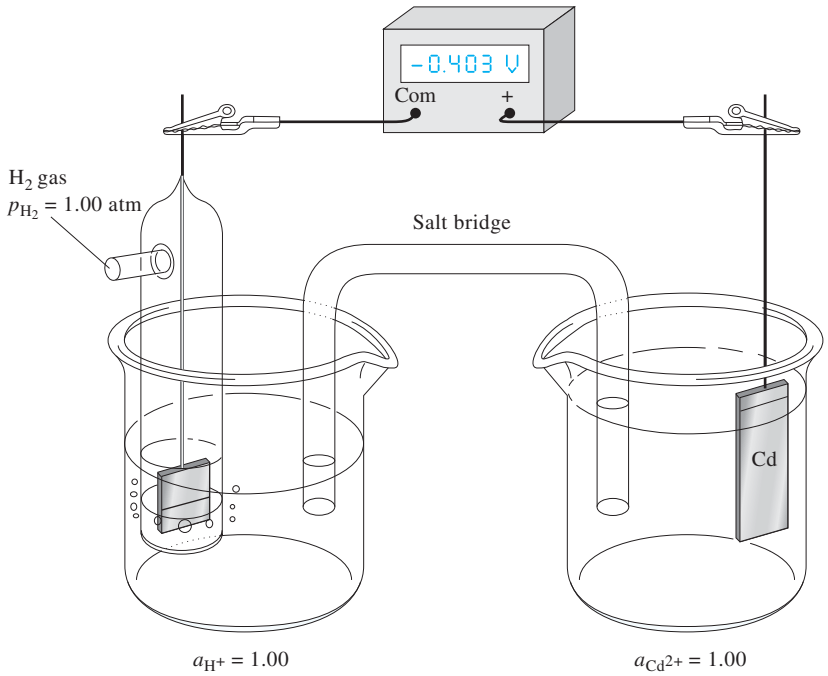

Figure 18-8 Measurement of the standard electrode potential for $Cd^{2+} + 2e^- \rightleftharpoons Cd(s)$.

the Cd/Cd^{2+} couple is *by convention* given a negative sign, and $E^0_{Cd^{2+}/Cd} = -0.403$ V. Because the cell potential is negative, the spontaneous cell reaction is not the reaction as written (that is, oxidation on the left and reduction on the right). Rather, the spontaneous reaction is in the opposite direction.

$$Cd(s) + 2H^+ \rightleftharpoons Cd^{2+} + H_2(g)$$

A zinc electrode immersed in a solution having a zinc ion activity of unity develops a potential of −0.763 V when it is the right-hand electrode paired with a standard hydrogen electrode on the left. Thus, we can write $E^0_{Zn^{2+}/Zn} = -0.763$ V.

The standard electrode potentials for the four half-cells just described can be arranged in the following order:

Half-Reaction	Standard Electrode Potential, V
$Ag^+ + e^- \rightleftharpoons Ag(s)$	+0.799
$2H^+ + 2e^- \rightleftharpoons H_2(g)$	0.000
$Cd^{2+} + 2e^- \rightleftharpoons Cd(s)$	−0.403
$Zn^{2+} + 2e^- \rightleftharpoons Zn(s)$	−0.763

The magnitudes of these electrode potentials indicate the relative strength of the four ionic species as electron acceptors (oxidizing agents), that is, in decreasing strength, $Ag^+ > H^+ > Cd^{2+} > Zn^{2+}$.

18C-4 Additional Implications of the IUPAC Sign Convention

The sign convention described in the previous section was adopted at the IUPAC meeting in Stockholm in 1953 and is now accepted internationally. Prior to this

An **electrode potential** is by definition a reduction potential. An oxidation potential is the potential for the half-reaction written in the opposite way. The sign of an oxidation potential is, therefore, opposite that for a reduction potential, but the magnitude is the same.

agreement, chemists did not always use the same convention, and this inconsistency was the cause of controversy and confusion in the development and routine use of electrochemistry.

Any sign convention must be based on expressing half-cell processes in a single way—either as oxidations or as reductions. According to the IUPAC convention, the term "*electrode potential*" (or, more exactly, "relative electrode potential") *is reserved exclusively to describe half-reactions written as reductions*. There is no objection to the use of the term "oxidation potential" to indicate a process written in the opposite sense, but it is not proper to refer to such a potential as an electrode potential.

The IUPAC sign convention is based on the actual sign of the half-cell of interest when it is part of a cell containing the standard hydrogen electrode as the other half-cell.

The sign of an electrode potential is determined by the sign of the half-cell in question when it is coupled to a standard hydrogen electrode. When the half-cell of interest exhibits a positive potential versus the SHE (see Figure 18-7), it will behave spontaneously as the cathode when the cell is discharging. When the half-cell of interest is negative versus the SHE (see Figure 18-8), it will behave spontaneously as the anode when the cell is discharging.

18C-5 Effect of Concentration on Electrode Potentials: The Nernst Equation

An electrode potential is a measure of the extent to which the concentrations of the species in a half-cell differ from their equilibrium values. For example, there is a greater tendency for the process

$$Ag^+ + e^- \rightleftharpoons Ag(s)$$

to occur in a concentrated solution of silver(I) than in a dilute solution of that ion. It follows that the magnitude of the electrode potential for this process must also become larger (more positive) as the silver ion concentration of a solution is increased. We now examine the quantitative relationship between concentration and electrode potential.

Consider the reversible half-reaction

$$aA + bB + \cdots + ne^- \rightleftharpoons cC + dD + \cdots \qquad (18\text{-}10)$$

where the capital letters represent formulas for the participating species (atoms, molecules, or ions), e^- represents the electrons, and the lower case italic letters indicate the number of moles of each species appearing in the half-reaction as it has been written. The electrode potential for this process is given by the equation

The meanings of the bracketed terms in Equations 18-11 and 18-12 are,

for a solute A [A] = molar concentration and
for a gas B [B] = p_B = partial pressure in atmospheres.
If one or more of the species appearing in Equation 18-11 is a pure liquid, pure solid, or the solvent present in excess, then no bracketed term for this species appears in the quotient because the activities of these are unity.

$$E = E^0 - \frac{RT}{nF} \ln \frac{[C]^c[D]^d \cdots}{[A]^a[B]^b \cdots} \qquad (18\text{-}11)$$

where

E^0 = the *standard electrode potential*, which is characteristic for each half-reaction
R = the ideal gas constant, 8.314 J K^{-1} mol^{-1}
T = temperature, K
n = number of moles of electrons that appears in the half-reaction for the electrode process as written
F = the faraday = 96,485 C (coulombs) per mole of electrons
ln = natural logarithm = 2.303 log

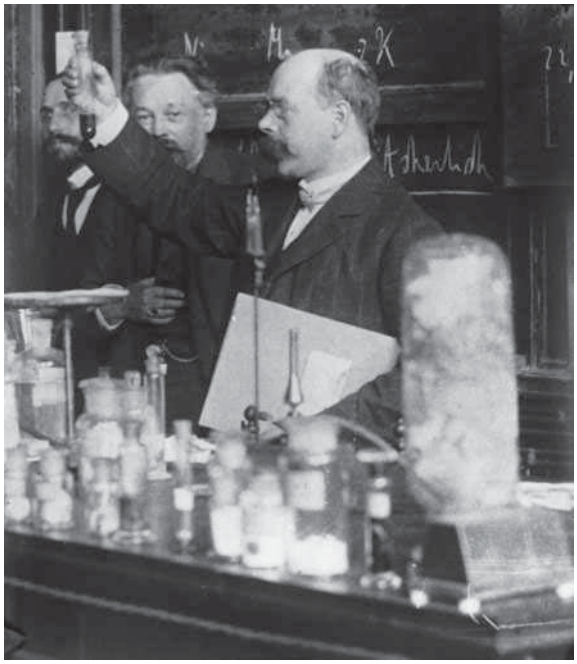

Walther Nernst (1864–1941) received the 1920 Nobel Prize in chemistry for his numerous contributions to the field of chemical thermodynamics. Nernst (right) is seen here in his laboratory in 1921.

If we substitute numerical values for the constants, convert to base 10 logarithms, and specify 25°C for the temperature, we get

$$E = E^0 - \frac{0.0592}{n} \log \frac{[C]^c[D]^d \cdots}{[A]^a[B]^b \cdots} \qquad (18\text{-}12)$$

Strictly speaking, the letters in brackets represent activities, but we will usually follow the practice of substituting molar concentrations for activities in most calculations. Thus, if some participating species A is a solute, [A] is the concentration of A in moles per liter. If A is a gas, [A] in Equation 18-12 is replaced by p_A, the partial pressure of A in atmospheres. If A is a pure liquid, a pure solid, or the solvent, its activity is unity, and no term for A is included in the equation. The rationale for these assumptions is the same as that described in Section 9B-2, which deals with equilibrium-constant expressions. Equation 18-12 is known as the Nernst equation in honor of the German chemist Walther Nernst, who was responsible for its development.

EXAMPLE 18-2

Typical half-cell reactions and their corresponding Nernst expressions follow.

(1) $Zn^{2+} + 2e^- \rightleftharpoons Zn(s)$ $\qquad E = E^0 - \frac{0.0592}{2} \log \frac{1}{[Zn^{2+}]}$

No term for elemental zinc is included in the logarithmic term because it is a pure second phase (solid). Thus, the electrode potential varies linearly with the logarithm of the reciprocal of the zinc ion concentration.

(2) $Fe^{3+} + e^- \rightleftharpoons Fe^{2+}(s)$ $\qquad E = E^0 - \frac{0.0592}{1} \log \frac{[Fe^{2+}]}{[Fe^{3+}]}$

The potential for this couple can be measured with an inert metallic electrode immersed in a solution containing both iron species. The potential depends on the logarithm of the ratio between the molar concentrations of these ions.

(3) $2H^+ + 2e^- \rightleftharpoons H_2(g)$ $\qquad E = E^0 - \dfrac{0.0592}{2} \log \dfrac{p_{H_2}}{[H^+]^2}$

In this example, p_{H_2} is the partial pressure of hydrogen (in atmospheres) at the surface of the electrode. Usually, its value will be the same as atmospheric pressure.

(4) $MnO_4^- + 5e^- + 8H^+ \rightleftharpoons Mn^{2+} + 4H_2O$

$$E = E^0 - \frac{0.0592}{5} \log \frac{[Mn^{2+}]}{[MnO_4^-][H^+]^8}$$

In this situation, the potential depends not only on the concentrations of the manganese species but also on the pH of the solution.

The Nernst expression in part (5) of Example 18-2 requires an excess of solid AgCl so that the solution is saturated with the compound at all times.

(5) $AgCl(s) + e^- \rightleftharpoons Ag(s) + Cl^-$ $\qquad E = E^0 - \dfrac{0.0592}{1} \log [Cl^-]$

This half-reaction describes the behavior of a silver electrode immersed in a chloride solution that is *saturated* with AgCl. To ensure this condition, an excess of the solid AgCl must always be present. Note that this electrode reaction is the sum of the following two reactions:

$$AgCl(s) \rightleftharpoons Ag^+ + Cl^-$$
$$Ag^+ + e^- \rightleftharpoons Ag(s)$$

Note also that the electrode potential is independent of the amount of AgCl present as long as there is at least some present to keep the solution saturated.

18C-6 The Standard Electrode Potential, E°

The **standard electrode potential** for a half-reaction, E^0, is defined as the electrode potential when all reactants and products of a half-reaction are at unit activity.

When we look carefully at Equations 18-11 and 18-12, we see that the constant E^0 is the electrode potential whenever the concentration quotient (actually, the activity quotient) has a value of 1. This constant is by definition the standard electrode potential for the half-reaction. Note that the quotient is always equal to 1 when the activities of the reactants and products of a half-reaction are unity.

The standard electrode potential is an important physical constant that provides quantitative information regarding the driving force for a half-cell reaction.[2] The important characteristics of these constants are the following:

1. The standard electrode potential is a relative quantity in the sense that it is the potential of an electrochemical cell in which the reference electrode (left-hand electrode) is the standard hydrogen electrode, whose potential has been assigned a value of 0.000 V.
2. The standard electrode potential for a half-reaction refers exclusively to a reduction reaction, that is, it is a relative reduction potential.
3. The standard electrode potential measures the relative force tending to drive the half-reaction from a state in which the reactants and products are at unit activity to a state in which the reactants and products are at their equilibrium activities relative to the standard hydrogen electrode.

[2] For further reading on standard electrode potentials, see R. G. Bates, in *Treatise on Analytical Chemistry*, 2nd ed., I. M. Kolthoff and P. J. Elving, eds., Part I, Vol. 1, Ch. 13, New York: Wiley, 1978.

4. The standard electrode potential is independent of the number of moles of reactant and product shown in the balanced half-reaction. Thus, the standard electrode potential for the half-reaction

$$Fe^{3+} + e^- \rightleftharpoons Fe^{2+} \qquad E^0 = +0.771 \text{ V}$$

does not change if we choose to write the reaction as

$$5Fe^{3+} + 5e^- \rightleftharpoons 5Fe^{2+} \qquad E^0 = +0.771 \text{ V}$$

Note, however, that the Nernst equation must be consistent with the half-reaction as written. For the first case, it will be

$$E = 0.771 - \frac{0.0592}{1} \log \frac{[Fe^{2+}]}{[Fe^{3+}]}$$

and for the second

$$E = 0.771 - \frac{0.0592}{5} \log \frac{[Fe^{2+}]^5}{[Fe^{3+}]^5} = 0.771 - \frac{0.0592}{5} \log \left(\frac{[Fe^{2+}]}{[Fe^{3+}]} \right)^5$$

$$= 0.771 - \frac{5 \times 0.0592}{5} \log \frac{[Fe^{2+}]}{[Fe^{3+}]}$$

Note that the two log terms have identical values, that is,

$$\frac{0.0592}{1} \log \frac{[Fe^{2+}]}{[Fe^{3+}]} = \frac{0.0592}{5} \log \frac{[Fe^{2+}]^5}{[Fe^{3+}]^5} = \frac{0.0592}{5} \log \left(\frac{[Fe^{2+}]}{[Fe^{3+}]} \right)^5$$

5. A positive electrode potential indicates that the half-reaction in question is spontaneous with respect to the standard hydrogen electrode half-reaction. In other words, the oxidant in the half-reaction is a stronger oxidant than is hydrogen ion. A negative sign indicates just the opposite.
6. The standard electrode potential for a half-reaction is temperature dependent.

Standard electrode potential data are available for an enormous number of half-reactions. Many have been determined directly from electrochemical measurements. Others have been computed from equilibrium studies of oxidation/reduction systems and from thermochemical data associated with such reactions. **Table 18-1** contains standard electrode potential data for several half-reactions that we will be considering in the pages that follow. A more extensive listing is found in Appendix 5.[3]

Table 18-1 and Appendix 5 illustrate the two common ways for tabulating standard potential data. In Table 18-1, potentials are listed in decreasing numerical order. As a consequence, the species in the upper left part are the most effective electron acceptors, as evidenced by their large positive values. They are therefore the strongest oxidizing agents. As we proceed down the left side of such a table, each succeeding species is less effective as an electron acceptor than the one above it. The half-cell reactions at the bottom of the table have little or no tendency to take place as they are written. On the other hand, they do tend to occur in the opposite sense. The most effective reducing agents, then, are those species that appear in the lower right portion of the table.

[3] Comprehensive sources for standard electrode potentials include A. J. Bard, R. Parsons, and J. Jordan, eds., *Standard Electrode Potentials in Aqueous Solution*, New York: Dekker, 1985; G. Milazzo, S. Caroli, and V. K. Sharma, *Tables of Standard Electrode Potentials,* New York: Wiley-Interscience, 1978; M. S. Antelman and F. J. Harris, *Chemical Electrode Potentials,* New York: Plenum Press, 1982. Some compilations are arranged alphabetically by element; others are tabulated according to the value of E^0.

Based on the E° values in Table 18-1 for Fe^{3+} and I_3^-, which species would you expect to predominate in a solution produced by mixing iron(III) and iodide ions? See color plate 12.

TABLE 18-1

Standard Electrode Potentials*

Reaction	E^0 at 25°C, V
$Cl_2(g) + 2e^- \rightleftharpoons 2Cl^-$	+1.359
$O_2(g) + 4H^+ + 4e^- \rightleftharpoons 2H_2O$	+1.229
$Br_2(aq) + 2e^- \rightleftharpoons 2Br^-$	+1.087
$Br_2(l) + 2e^- \rightleftharpoons 2Br^-$	+1.065
$Ag^+ + e^- \rightleftharpoons Ag(s)$	+0.799
$Fe^{3+} + e^- \rightleftharpoons Fe^{2+}$	+0.771
$I_3^- + 2e^- \rightleftharpoons 3I^-$	+0.536
$Cu^{2+} + 2e^- \rightleftharpoons Cu(s)$	+0.337
$UO_2^{2+} + 4H^+ + 2e^- \rightleftharpoons U^{4+} + 2H_2O$	+0.334
$Hg_2Cl_2(s) + 2e^- \rightleftharpoons 2Hg(l) + 2Cl^-$	+0.268
$AgCl(s) + e^- \rightleftharpoons Ag(s) + Cl^-$	+0.222
$Ag(S_2O_3)_2^{3-} + e^- \rightleftharpoons Ag(s) + 2S_2O_3^{2-}$	+0.017
$2H^+ + 2e^- \rightleftharpoons H_2(g)$	**0.000**
$AgI(s) + e^- \rightleftharpoons Ag(s) + I^-$	−0.151
$PbSO_4 + 2e^- \rightleftharpoons Pb(s) + SO_4^{2-}$	−0.350
$Cd^{2+} + 2e^- \rightleftharpoons Cd(s)$	−0.403
$Zn^{2+} + 2e^- \rightleftharpoons Zn(s)$	−0.763

*See Appendix 5 for a more extensive list.

FEATURE 18-4

Sign Conventions in the Older Literature

Reference works, particularly those published before 1953, often contain tabulations of electrode potentials that are not in accord with the IUPAC recommendations. For example, in a classic source of standard-potential data compiled by Latimer,[4] one finds

$$Zn(s) \rightleftharpoons Zn^{2+} + 2e^- \qquad E = +0.76\ V$$

$$Cu(s) \rightleftharpoons Cu^{2+} + 2e^- \qquad E = +0.34\ V$$

To convert these oxidation potentials to electrode potentials as defined by the IUPAC convention, we must mentally (1) express the half-reactions as reductions and (2) change the signs of the potentials.

The sign convention used in a tabulation of electrode potentials may not be explicitly stated. This information can be deduced, however, by noting the direction and sign of the potential for a familiar half-reaction. If the sign agrees with the IUPAC convention, the table can be used as is. If not, the signs of all of the data must be reversed. For example, the reaction

$$O_2(g) + 4H^+ + 4e^- \rightleftharpoons 2H_2O \qquad E = +1.229\ V$$

occurs spontaneously with respect to the standard hydrogen electrode and thus carries a positive sign. If the potential for this half-reaction is negative in a table, it and all the other potentials should be multiplied by −1.

[4]W. M. Latimer, *The Oxidation States of the Elements and Their Potentials in Aqueous Solutions,* 2nd ed. Englewood Cliffs, NJ: Prentice-Hall, 1952.

Compilations of electrode-potential data, such as that shown in Table 18-1, provide chemists with qualitative insights into the extent and direction of electron-transfer reactions. For example, the standard potential for silver(I) (+0.799 V) is more positive than that for copper(II) (+0.337 V). We therefore conclude that a piece of copper immersed in a silver(I) solution will cause the reduction of that ion and the oxidation of the copper. On the other hand, we would expect no reaction if we place a piece of silver in a copper(II) solution.

In contrast to the data in Table 18-1, standard potentials in Appendix 5 are arranged alphabetically by element to make it easier to locate data for a given electrode reaction.

Systems Involving Precipitates or Complex Ions

In Table 18-1, we find several entries involving Ag(I) including

$$Ag^+ + e^- \rightleftharpoons Ag(s) \qquad E^0_{Ag^+/Ag} = +0.799\ V$$

$$AgCl(s) + e^- \rightleftharpoons Ag(s) + Cl^- \qquad E^0_{AgCl/Ag} = +0.222\ V$$

$$Ag(S_2O_3)_2^{3-} + e^- \rightleftharpoons Ag(s) + 2S_2O_3^{2-} \qquad E^0_{Ag(S_2O_3)_2^{3-}/Ag} = +0.017\ V$$

Each gives the potential of a silver electrode in a different environment. Let us see how the three potentials are related.

The Nernst expression for the first half-reaction is

$$E = E^0_{Ag^+/Ag} - \frac{0.0592}{1} \log \frac{1}{[Ag^+]}$$

If we replace $[Ag^+]$ with $K_{sp}/[Cl^-]$, we obtain

$$E = E^0_{Ag^+/Ag} - \frac{0.0592}{1} \log \frac{[Cl^-]}{K_{sp}} = E^0_{Ag^+/Ag} + 0.0592 \log K_{sp} - 0.0592 \log [Cl^-]$$

By definition, the standard potential for the second half-reaction is the potential where $[Cl^-] = 1.00$. That is, when $[Cl^-] = 1.00$, $E = E^0_{AgCl/Ag}$. Substituting these values gives

$$E^0_{AgCl/Ag} = E^0_{Ag^+/Ag} - 0.0592 \log 1.82 \times 10^{-10} - 0.0592 \log (1.00)$$

$$= 0.799 + (-0.577) - 0.000 = 0.222\ V$$

Figure 18-9 shows the measurement of the standard electrode potential for the Ag/AgCl electrode.

If we proceed in the same way, we can obtain an expression for the standard electrode potential for the reduction of the thiosulfate complex of silver ion depicted in the third equilibrium shown at the start of this section. In this case, the standard potential is given by

$$E^0_{Ag(S_2O_3)_2^{3-}/Ag} = E^0_{Ag^+/Ag} - 0.0592 \log \beta_2 \qquad (18\text{-}13)$$

CHALLENGE: Derive Equation 18-13.

where β_2 is the formation constant for the complex. That is,

$$\beta_2 = \frac{[Ag(S_2O_3)_2^{3-}]}{[Ag^+][S_2O_3^{2-}]^2}$$

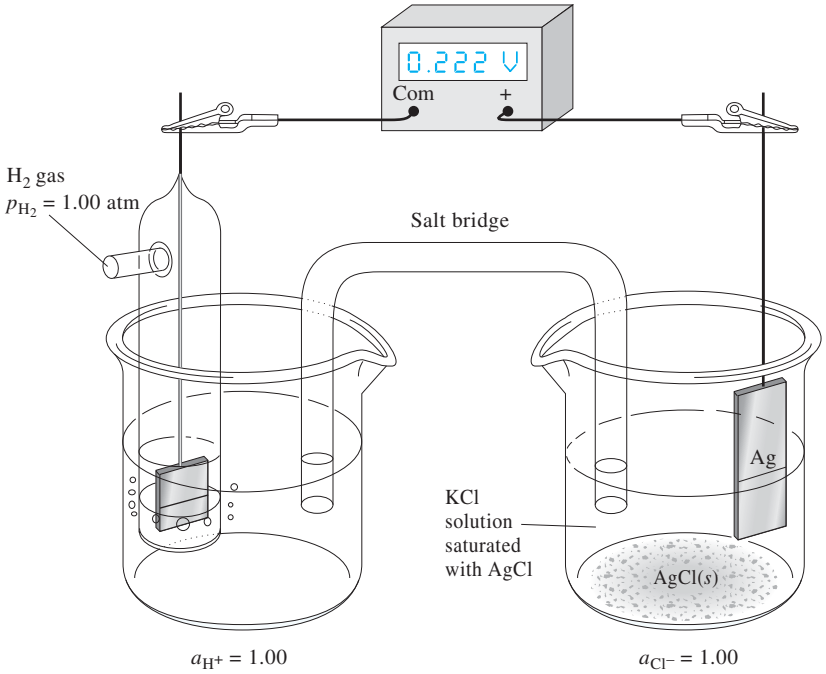

Figure 18-9 Measurement of the standard electrode potential for an Ag/AgCl electrode.

EXAMPLE 18-3

Calculate the electrode potential of a silver electrode immersed in a 0.0500 M solution of NaCl using (a) $E^\circ_{Ag^+/Ag} = 0.799$ V and (b) $E^\circ_{AgCl/Ag} = 0.222$ V.

Solution

(a) $Ag^+ + e^- \rightleftharpoons Ag(s)$ $\qquad E^0_{Ag^+/Ag} = +0.799$ V

The Ag^+ concentration of this solution is given by

$$[Ag^+] = \frac{K_{sp}}{[Cl^-]} = \frac{1.82 \times 10^{-10}}{0.0500} = 3.64 \times 10^{-9}\ M$$

Substituting into the Nernst expression gives

$$E = 0.799 - 0.0592 \log \frac{1}{3.64 \times 10^{-9}} = 0.299\ V$$

(b) We may write this last equation as

$$E = 0.222 - 0.0592 \log [Cl^-] = 0.222 - 0.0592 \log 0.0500$$
$$= 0.299$$

FEATURE 18-5

Why Are There Two Electrode Potentials for Br_2 in Table 18-1?

In Table 18-1, we find the following data for Br_2:

$$Br_2(aq) + 2e^- \rightleftharpoons 2Br^- \qquad E^0 = +1.087\ V$$
$$Br_2(l) + 2e^- \rightleftharpoons 2Br^- \qquad E^0 = +1.065\ V$$

The second standard potential applies only to a solution that is saturated with Br_2 and not to undersaturated solutions. You should use 1.065 V to calculate the electrode potential of a 0.0100 M solution of KBr that is saturated with Br_2 and in contact with an excess of the liquid. In such a case,

$$E = 1.065 - \frac{0.0592}{2}\log[Br^-]^2 = 1.065 - \frac{0.0592}{2}\log(0.0100)^2$$

$$= 1.065 - \frac{0.0592}{2} \times (-4.00) = 1.183\ V$$

In this calculation, no term for Br_2 appears in the logarithmic term because it is a pure liquid present in excess (unit activity). The standard electrode potential shown in the first entry for $Br_2(aq)$ is hypothetical because the solubility of Br_2 at 25°C is only about 0.18 M. Thus, the recorded value of 1.087 V is based on a system that—in terms of our definition of E^0—cannot be realized experimentally. Nevertheless, the hypothetical potential does permit us to calculate electrode potentials for solutions that are undersaturated in Br_2. For example, if we wish to calculate the electrode potential for a solution that was 0.0100 M in KBr and 0.00100 M in Br_2, we would write

$$E = 1.087 - \frac{0.0592}{2}\log\frac{[Br^-]^2}{[Br_2(aq)]} = 1.087 - \frac{0.0592}{2}\log\frac{(0.0100)^2}{0.00100}$$

$$= 1.087 - \frac{0.0592}{2}\log 0.100 = 1.117\ V$$

18C-7 Limitations to the Use of Standard Electrode Potentials

We will use standard electrode potentials throughout the rest of this text to calculate cell potentials and equilibrium constants for redox reactions as well as to calculate data for redox titration curves. You should be aware that such calculations sometimes lead to results that are significantly different from those you would obtain in the laboratory. There are two main sources of these differences: (1) the necessity of using concentrations in place of activities in the Nernst equation and (2) failure to take into account other equilibria such as dissociation, association, complex formation, and solvolysis. Measurement of electrode potentials can allow us to investigate these equilibria and determine their equilibrium constants, however.

Use of Concentrations Instead of Activities

Most analytical oxidation/reduction reactions are carried out in solutions that have such high ionic strengths that activity coefficients cannot be obtained via the Debye-Hückel equation (see Equation 10-5, Section 10B-2). Significant errors may result, however, if concentrations are used in the Nernst equation rather than activities. For example, the standard potential for the half-reaction

$$Fe^{3+} + e^- \rightleftharpoons Fe^{2+} \qquad E^0 = +0.771\ V$$

is +0.771 V. When the potential of a platinum electrode immersed in a solution that is 10^{-4} M in iron(III) ion, iron(II) ion, and perchloric acid is measured against a standard hydrogen electrode, a reading of close to +0.77 V is obtained, as predicted by theory. If, however, perchloric acid is added to this mixture until the acid

concentration is 0.1 M, the potential is found to decrease to about +0.75 V. This difference is attributable to the fact that the activity coefficient of iron(III) is considerably smaller than that of iron(II) (0.4 versus 0.18) at the high ionic strength of the 0.1 M perchloric acid medium (see Table 10-2 page 242). As a consequence, the ratio of activities of the two species ($[Fe^{2+}]/[Fe^{3+}]$) in the Nernst equation is greater than unity, a condition that leads to a decrease in the electrode potential. In 1 M $HClO_4$, the electrode potential is even smaller (≈ 0.73 V).

Effect of Other Equilibria

The following further complicate application of standard electrode potential data to many systems of interest in analytical chemistry: association, dissociation, complex formation, and solvolysis equilibria of the species that appear in the Nernst equation. These phenomena can be taken into account only if their existence is known and appropriate equilibrium constants are available. More often than not, neither of these requirements is met and significant discrepancies arise. For example, the presence of 1 M hydrochloric acid in the iron(II)/iron(III) mixture we have just discussed leads to a measured potential of +0.70 V, while in 1 M sulfuric acid, a potential of +0.68 V is observed, and in a 2 M phosphoric acid, the potential is +0.46 V. In each of these cases, the iron(II)/iron(III) activity ratio is larger because the complexes of iron(III) with chloride, sulfate, and phosphate ions are more stable than those of iron(II). In these cases, the ratio of the species concentrations, $[Fe^{2+}]/[Fe^{3+}]$, in the Nernst equation is greater than unity, and the measured potential is less than the standard potential. If formation constants for these complexes were available, it would be possible to make appropriate corrections. Unfortunately, such data are often not available, or if they are, they are not very reliable.

Formal Potentials

A **formal potential** is the electrode potential when the ratio of **analytical concentrations** of reactants and products of a half-reaction are exactly 1.00 and the molar concentrations of any other solutes are specified. To distinguish the formal potential from the standard electrode potential a prime symbol is added to E^0.

Formal potentials are empirical potentials that compensate for the types of activity and competing equilibria effects that we have just described. The formal potential $E^{0'}$ of a system is the potential of the half-cell with respect to the standard hydrogen electrode measured under conditions such that the ratio of analytical concentrations of reactants and products as they appear in the Nernst equation is exactly unity and the concentrations of other species in the system are all carefully specified. For example, the formal potential for the half-reaction

$$Ag^+ + e^- \rightleftharpoons Ag(s) \qquad E^{0'} = 0.792 \text{ V in 1 M } HClO_4$$

could be obtained by measuring the potential of the cell shown in **Figure 18-10**. Here, the right-hand electrode is a silver electrode immersed in a solution that is 1.00 M in $AgNO_3$ and 1.00 M in $HClO_4$. The reference electrode on the left is a standard hydrogen electrode. This cell has a potential of +0.792 V, which is the formal potential of the Ag^+/Ag couple in 1.00 M $HClO_4$. Note that the standard potential for this couple is +0.799 V.

Formal potentials for many half-reactions are listed in Appendix 5. Note that there are large differences between the formal and standard potentials for some half-reactions. For example, the formal potential for

$$Fe(CN)_6^{3-} + e^- \rightleftharpoons Fe(CN)_6^{4-} \qquad E^0 = +0.36 \text{ V}$$

is 0.72 V in 1 M perchloric or sulfuric acids, which is 0.36 V greater than the standard electrode potential for the half-reaction. The reason for this difference is that in the presence of high concentrations of hydrogen ion, hexacyanoferrate(II) ions ($Fe(CN)_6^{4-}$), and hexacyanoferrate(III) ions ($Fe(CN)_6^{3-}$) combine with one or more protons to form hydrogen hexacyanoferrate(II) and hydrogen hexacyanoferrate(III)

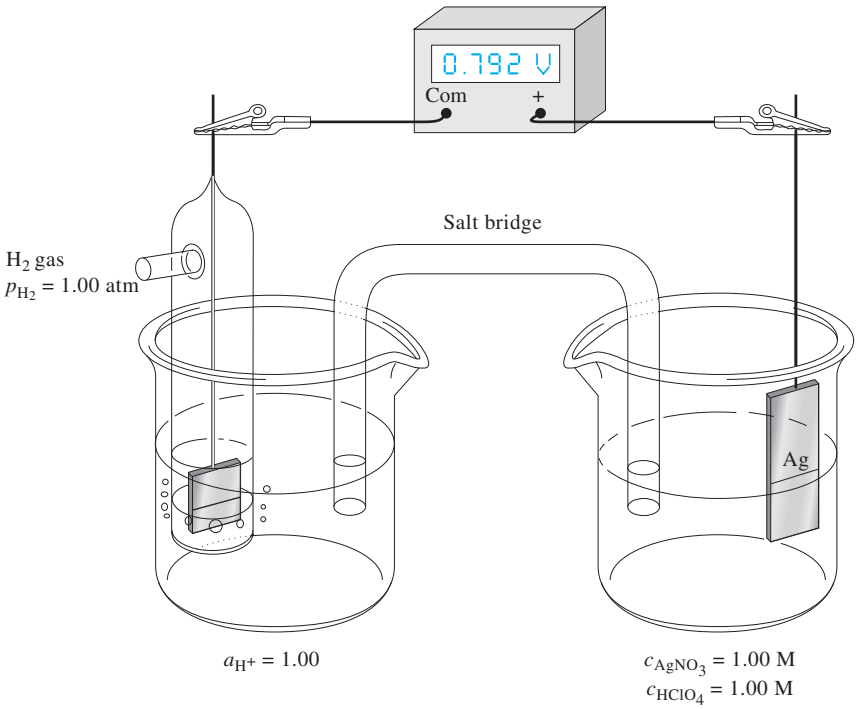

Figure 18-10 Measurement of the formal potential of the Ag^+/Ag couple in 1 M $HClO_4$.

acid species. Because $H_4Fe(CN)_6$ is a weaker acid than $H_3Fe(CN)_6$, the ratio of the species concentrations, $[Fe(CN)_6^{4-}]/[Fe(CN)_6^{3-}]$, in the Nernst equation is less than 1, and the observed potentials are greater.

Substitution of formal potentials for standard electrode potentials in the Nernst equation yields better agreement between calculated and experimental results—provided, of course, that the electrolyte concentration of the solution approximates that for which the formal potential is applicable. Not surprisingly, attempts to apply formal potentials to systems that differ substantially in type and in concentration of electrolyte can result in errors that are larger than those associated with the use of standard electrode potentials. In this text, we use whichever is the more appropriate.

Spreadsheet Summary In the first exercise in Chapter 10 of *Applications of Microsoft® Excel in Analytical Chemistry*, 2nd ed., a spreadsheet is developed to calculate electrode potentials as a function of the ratio of reductant-to-oxidant concentration ([R]/[O]) for the case of two soluble species. Plots of E versus [R]/[O] and E versus log([R]/[O]) are made, and the slopes and intercepts determined. The spreadsheet is modified for metal/metal ion systems.

WEB WORKS

Fuel cells have been used to provide electrical power for spacecraft since the 1960s. In recent years, fuel cell technology has begun to mature, and batteries made up of fuel cells will soon be or are now available for small-scale power generation and electric automobiles. Use a search engine to find the Fuel Cells 2000 website. Locate an article that explains the operation of the hydrogen fuel cell. Describe the proton-exchange membrane and explain its role in the hydrogen fuel cell. Discuss the advantages of the hydrogen fuel cell over other electrical energy storage devices such as lead-acid batteries, lithium-hydride batteries, and so forth. What are its disadvantages? What are the some of the reasons why this technology has not rapidly replaced current energy technologies?

QUESTIONS AND PROBLEMS

NOTE: Numerical data are molar analytical concentrations where the full formula of a species is provided. Molar equilibrium concentrations are supplied for species displayed as ions.

18-1. Briefly describe or define
- *(a) oxidation.
- (b) reducing agent.
- *(c) salt bridge.
- (d) liquid junction.
- *(e) Nernst equation.

18-2. Briefly describe or define
- *(a) electrode potential.
- (b) formal potential.
- *(c) standard electrode potential.
- (d) liquid-junction potential.
- (e) oxidation potential.

18-3. Make a clear distinction between
- *(a) oxidation and oxidizing agent.
- (b) an electrolytic cell and a galvanic cell.
- *(c) the cathode of an electrochemical cell and the right-hand electrode.
- (d) a reversible electrochemical cell and an irreversible electrochemical cell.
- *(e) the standard electrode potential and formal potential.

***18-4.** The following entries are found in a table of standard electrode potentials:

$$I_2(s) + 2e^- \rightleftharpoons 2I^- \qquad E^0 = 0.5355\ V$$
$$I_2(aq) + 2e^- \rightleftharpoons 2I^- \qquad E^0 = 0.615\ V$$

What is the significance of the difference between these two standard potentials?

***18-5.** Why is it necessary to bubble hydrogen through the electrolyte in a hydrogen electrode?

18-6. The standard electrode potential for the reduction of Ni^{2+} to Ni is −0.25 V. Would the potential of a nickel electrode immersed in a 1.00 M NaOH solution saturated with $Ni(OH)_2$ be more negative than $E^0_{Ni^{2+}/Ni}$ or less? Explain.

18-7. Write balanced net ionic equations for the following reactions. Supply H^+ and/or H_2O as needed to obtain balance.
- *(a) $Fe^{3+} + Sn^{2+} \rightarrow Fe^{2+} + Sn^{4+}$
- (b) $Cr(s) + Ag^+ \rightarrow Cr^{3+} + Ag(s)$
- *(c) $NO_3^- + Cu(s) \rightarrow NO_2(g) + Cu^{2+}$
- (d) $MnO_4^- + H_2SO_3 \rightarrow Mn^{2+} + SO_4^{2-}$
- *(e) $Ti^{3+} + Fe(CN)_6^{3-} \rightarrow TiO^{2+} + Fe(CN)_6^{4-}$
- (f) $H_2O_2 + Ce^{4+} \rightarrow O_2(g) + Ce^{3+}$
- *(g) $Ag(s) + I^- + Sn^{4+} \rightarrow AgI(s) + Sn^{2+}$
- (h) $UO_2^{2+} + Zn(s) \rightarrow U^{4+} + Zn^{2+}$
- *(i) $HNO_2 + MnO_4^- \rightarrow NO_3^- + Mn^{2+}$
- (j) $HN_2NNH_2 + IO_3^- + Cl^- \rightarrow N_2(g) + ICl_2^-$

***18-8.** Identify the oxidizing agent and the reducing agent on the left side of each equation in Problem 18-7; write a balanced equation for each half-reaction.

18-9. Write balanced net ionic equations for the following reactions. Supply H^+ and/or H_2O as needed to obtain balance.
- *(a) $MnO_4^- + VO^{2+} \rightarrow Mn^{2+} + V(OH)_4^+$
- (b) $I_2 + H_2S(g) \rightarrow I^- + S(s)$
- *(c) $Cr_2O_7^{2-} + U^{4+} \rightarrow Cr^{3+} + UO_2^{2+}$
- (d) $Cl^- + MnO_2(s) \rightarrow Cl_2(g) + Mn^{2+}$
- *(e) $IO_3^- + I^- \rightarrow I_2(aq)$
- (f) $IO_3^- + I^- + Cl^- \rightarrow ICl_2^-$
- *(g) $HPO_3^{2-} + MnO_4^- + OH^- \rightarrow PO_4^{3-} + MnO_4^{2-}$
- (h) $SCN^- + BrO_3^- \rightarrow Br^- + SO_4^{2-} + HCN$
- *(i) $V^{2+} + V(OH)_4^+ \rightarrow VO^{2+}$
- (j) $MnO_4^- + Mn^{2+} + OH^- \rightarrow MnO_2(s)$

18-10. Identify the oxidizing agent and the reducing agent on the left side of each equation in Problem 18-9; write a balanced equation for each half-reaction.

***18-11.** Consider the following oxidation/reduction reactions:

$$AgBr(s) + V^{2+} \rightarrow Ag(s) + V^{3+} + Br^-$$
$$Tl^{3+} + 2Fe(CN)_6^{4-} \rightarrow Tl^+ + 2Fe(CN)_6^{3-}$$
$$2V^{3+} + Zn(s) \rightarrow 2V^{2+} + Zn^{2+}$$
$$Fe(CN)_6^{3-} + Ag(s) + Br^- \rightarrow Fe(CN)_6^{4-} + AgBr(s)$$
$$S_2O_8^{2-} + Tl^+ \rightarrow 2SO_4^{2-} + Tl^{3+}$$

- (a) Write each net process in terms of two balanced half-reactions.
- (b) Express each half-reaction as a reduction.
- (c) Arrange the half-reactions in (b) in order of decreasing effectiveness as electron acceptors.

18-12. Consider the following oxidation/reduction reactions:

$$2H^+ + Sn(s) \rightarrow H_2(g) + Sn^{2+}$$
$$Ag^+ + Fe^{2+} \rightarrow Ag(s) + Fe^{3+}$$
$$Sn^{4+} + H_2(g) \rightarrow Sn^{2+} + 2H^+$$
$$2Fe^{3+} + Sn^{2+} \rightarrow 2Fe^{2+} + Sn^{4+}$$
$$Sn^{2+} + Co(s) \rightarrow Sn(s) + Co^{2+}$$

- (a) Write each net process in terms of two balanced half-reactions.
- (b) Express each half-reaction as a reduction.
- (c) Arrange the half-reactions in (b) in order of decreasing effectiveness as electron acceptors.

***18-13.** Calculate the potential of a copper electrode immersed in
- (a) 0.0380 M $Cu(NO_3)_2$.
- (b) 0.0650 M in NaCl and saturated with CuCl.
- (c) 0.0350 M in NaOH and saturated with $Cu(OH)_2$.
- (d) 0.0375 M in $Cu(NH_3)_4^{2+}$ and 0.108 M in NH_3 (β_4 for $Cu(NH_3)_4^{2+}$ is 5.62×10^{11}).

(e) a solution in which the molar analytical concentration of $Cu(NO_3)_2$ is 3.90×10^{-3} M, that for H_2Y^{2-} is 3.90×10^{-2} M (Y = EDTA), and the pH is fixed at 4.00.

18-14. Calculate the potential of a zinc electrode immersed in
(a) 0.0500 M $Zn(NO_3)_2$.
(b) 0.0200 M in NaOH and saturated with $Zn(OH)_2$.
(c) 0.0150 M in $Zn(NH_3)_4^{2+}$ and 0.350 M in NH_3—β_4 for $Zn(NH_3)_4^{2+}$ is 7.76×10^8.
(d) a solution in which the molar analytical concentration of $Zn(NO_3)_2$ is 4.00×10^{-3}, that for H_2Y^{2-} is 0.0550 M, and the pH is fixed at 9.00.

18-15. Use activities to calculate the electrode potential of a hydrogen electrode in which the electrolyte is 0.0100 M HCl and the activity of H_2 is 1.00 atm.

***18-16.** Calculate the potential of a platinum electrode immersed in a solution that is
(a) 0.0160 M in K_2PtCl_4 and 0.2450 M in KCl.
(b) 0.0650 M in $Sn(SO_4)_2$ and 3.5×10^{-3} M in $SnSO_4$.
(c) buffered to a pH of 6.50 and saturated with $H_2(g)$ at 1.00 atm.
(d) 0.0255 M in $VOSO_4$, 0.0686 M in $V_2(SO_4)_3$, and 0.100 M in $HClO_4$.
(e) prepared by mixing 25.00 mL of 0.0918 M $SnCl_2$ with an equal volume of 0.1568 M $FeCl_3$.
(f) prepared by mixing 25.00 mL of 0.0832 M $V(OH)_4^+$ with 50.00 mL of 0.01087 M $V_2(SO_4)_3$ and has a pH of 1.00.

18-17. Calculate the potential of a platinum electrode immersed in a solution that is
(a) 0.0613 M in $K_4Fe(CN)_6$ and 0.00669 M in $K_3Fe(CN)_6$.
(b) 0.0400 M in $FeSO_4$ and 0.00915 M in $Fe_2(SO_4)_3$.
(c) buffered to a pH of 5.55 and saturated with H_2 at 1.00 atm.
(d) 0.1015 M in $V(OH)_4^+$, 0.0799 M in VO^{2+}, and 0.0800 M in $HClO_4$.
(e) prepared by mixing 50.00 mL of 0.0607 M $Ce(SO_4)_2$ with an equal volume of 0.100 M $FeCl_2$ (assume solutions were 1.00 M in H_2SO_4 and use formal potentials).
(f) prepared by mixing 25.00 mL of 0.0832 M $V_2(SO_4)_3$ with 50.00 mL of 0.00628 M $V(OH)_4^+$ and has a pH of 1.00.

***18-18.** If the following half-cells are the right-hand electrode in a galvanic cell with a standard hydrogen electrode on the left, calculate the cell potential. If the cell were shorted, indicate whether the electrodes shown would act as an anode or a cathode.
(a) $Ni|Ni^{2+}(0.0883\ M)$
(b) $Ag|AgI(sat'd), KI(0.0898\ M)$
(c) $Pt|O_2(780\ torr), HCl(2.50 \times 10^{-4}\ M)$
(d) $Pt|Sn^{2+}(0.0893\ M), Sn^{4+}(0.215\ M)$
(e) $Ag|Ag(S_2O_3)_2^{3-}(0.00891\ M), Na_2S_2O_3(0.1035\ M)$

18-19. The following half-cells are on the left and coupled with the standard hydrogen electrode on the right to form a galvanic cell. Calculate the cell potential. Indicate which electrode would be the cathode if each cell were short circuited.
(a) $Cu|Cu^{2+}(0.0805\ M)$
(b) $Cu|CuI(sat'd), KI(0.0993\ M)$
(c) $Pt, H_2(0.914\ atm)|HCl(1.00 \times 10^{-4}\ M)$
(d) $Pt|Fe^{3+}(0.0886\ M), Fe^{2+}(0.1420\ M)$
(e) $Ag|Ag(CN)_2^-\ (0.0778\ M), KCN(0.0651\ M)$

***18-20.** The solubility-product constant for Ag_2SO_3 is 1.5×10^{-14}. Calculate E^0 for the process

$$Ag_2SO_3(s) + 2e^- \rightleftharpoons 2Ag + SO_3^{2-}$$

18-21. The solubility-product constant for $Ni_2P_2O_7$ is 1.7×10^{-13}. Calculate E^0 for the process

$$Ni_2P_2O_7(s) + 4e^- \rightleftharpoons 2Ni(s) + P_2O_7^{4-}$$

***18-22.** The solubility-product constant for Tl_2S is 6×10^{-22}. Calculate E^0 for the reaction

$$Tl_2S(s) + 2e^- \rightleftharpoons 2Tl(s) + S^{2-}$$

18-23. The solubility product for $Pb_3(AsO_4)_2$ is 4.1×10^{-36}. Calculate E^0 for the reaction

$$Pb_2(AsO_4)_2(s) + 6e^- \rightleftharpoons 3Pb(s) + 2AsO_4^{2-}$$

***18-24.** Compute E^0 for the process

$$ZnY^{2-} + 2e^- \rightleftharpoons Zn(s) + Y^{4-}$$

where Y^{4-} is the completely deprotonated anion of EDTA. The formation constant for ZnY^{2-} is 3.2×10^{16}.

***18-25.** Given the formation constants

$$Fe^{3+} + Y^{4-} \rightleftharpoons FeY^- \quad K_f = 1.3 \times 10^{25}$$
$$Fe^{2+} + Y^{4-} \rightleftharpoons FeY^{2-} \quad K_f = 2.1 \times 10^{14}$$

calculate E^0 for the process

$$FeY^- + e^- \rightleftharpoons FeY^{2-}$$

18-26. Calculate E^0 for the process

$$Cu(NH_3)_4^{2+} + e^- \rightleftharpoons Cu(NH_3)_2^+ + 2\,NH_3$$

given that

$$Cu^+ + 2NH_3 \rightleftharpoons Cu(NH_3)_2^+ \quad \beta_2 = 7.2 \times 10^{10}$$
$$Cu^{2+} + 4NH_3 \rightleftharpoons Cu(NH_3)_4^{2+} \quad \beta_4 = 5.62 \times 10^{11}$$

18-27. For a $Pt|Fe^{3+}, Fe^{2+}$ half-cell, find the potential for the following ratios of $[Fe^{3+}]/[Fe^{2+}]$: 0.001, 0.0025, 0.005, 0.0075, 0.010, 0.025, 0.050, 0.075, 0.100, 0.250, 0.500, 0.750, 1.00, 1.250, 1.50, 1.75, 2.50, 5.00, 10.00, 25.00, 75.00, and 100.00.

18-28. For a $Pt|Ce^{4+}, Ce^{3+}$ half-cell, find the potential for the same ratios of $[Ce^{4+}]/[Ce^{3+}]$ as given in Problem 18-27 for $[Fe^{3+}]/[Fe^{2+}]$.

18-29. Plot the half-cell potential versus concentration ratio for the half-cells of Problems 18-27 and 18-28. How

would the plot look if potential were plotted against log(concentration ratio)?

18-30. **Challenge Problem**: At one time, the standard hydrogen electrode was used for measuring pH.

(a) Sketch a diagram of an electrochemical cell that could be used to measure pH and label all parts of the diagram. Use the SHE for both half-cells.

(b) Derive an equation that gives the potential of the cell in terms of the hydronium ion concentration $[H_3O^+]$ in both half-cells.

(c) One half-cell should contain a solution of known hydronium ion concentration, and the other should contain the unknown solution. Solve the equation in (b) for the pH of the solution in the unknown half-cell.

(d) Modify your resulting equation to account for activity coefficients and express the result in terms of $pa_H = -\log a_H$, the negative logarithm of the hydronium ion activity.

(e) Describe the circumstances under which you would expect the cell to provide accurate measurements of pa_H.

(f) Could your cell be used to make practical absolute measurements of pa_H or would you have to calibrate your cell with solutions of known pa_H? Explain your answer in detail.

(g) How (or where) could you obtain solutions of known pa_H?

(h) Discuss the practical problems that you might encounter in using your cell for making pH measurements.

(i) Klopsteg[5] discusses how to make hydrogen electrode measurements. In Figure 2 of his paper, he suggests using a slide rule, a segment of which is shown here, to convert hydronium ion concentrations to pH and vice versa.

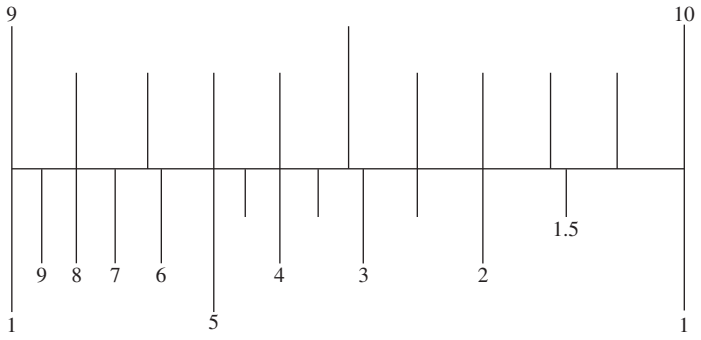

pH slide rule.

Explain the principles of operation of this slide rule and describe how it works. What reading would you obtain from the slide rule for a hydronium ion concentration of 3.56×10^{-4} M? How many significant figures are there in the resulting pH? What is the hydronium ion concentration of a solution of pH = 9.85?

[5] P. E. Klopsteg, *Ind. Eng. Chem,* **1922**, *14*(5), 399, **DOI:** 10.1021/ie50149a011.

Potentiometry

CHAPTER 21

The research vessel *Meteor*, shown in the photo, is owned by the Federal Republic of Germany through the Ministry of Research and Technology and is operated by the German Research Foundation. It is used by a multinational group of chemical oceanographers to collect data in an effort to better understand the changing chemical composition of the earth's atmosphere and oceans. For example, during April, 2012, a group from the Uni Bjerknes Centre and the Bjerknes Centre for Climate Research in Bergen, Norway, were aboard *Meteor* in the North Atlantic Ocean west of Norway performing measurements related to the oceanic cycling of carbon as well as measurements estimating the flux of oxygen directly involved in biological activity. An important observation in these experiments is the total alkalinity of sea water, which is determined by potentiometric titration, a method that is discussed in this chapter.

Potentiometric methods of analysis are based on measuring the potential of electrochemical cells without drawing appreciable current. For nearly a century, potentiometric techniques have been used for locating end points in titrations. In more recent methods, ion concentrations are measured directly from the potential of ion-selective membrane electrodes. These electrodes are relatively free from interferences and provide a rapid, convenient, and nondestructive means for quantitatively determining numerous important anions and cations.[1]

Analysts make more potentiometric measurements than perhaps any other type of chemical instrumental measurement. The number of potentiometric measurements made on a daily basis is staggering. Manufacturers measure the pH of many consumer products, clinical laboratories determine blood gases as important indicators of disease states, industrial and municipal effluents are monitored continuously to determine pH and concentrations of pollutants, and oceanographers determine carbon dioxide and other related variables in seawater. Potentiometric measurements are also used in fundamental studies to determine thermodynamic equilibrium constants, such as K_a, K_b, and K_{sp}. These examples are but a few of the many thousands of applications of potentiometric measurements.

The equipment for potentiometric methods is simple and inexpensive and includes a reference electrode, an indicator electrode, and a potential-measuring device. The principles of operation and design of each of these components are described in the initial sections of this chapter. Following these discussions, we investigate analytical applications of potentiometric measurements.

[1]R. S. Hutchins and L. G. Bachas, in *Handbook of Instrumental Techniques for Analytical Chemistry*, F. A. Settle, ed., Ch. 38, pp. 727–48, Upper Saddle River, NJ: Prentice-Hall, 1997.

21A GENERAL PRINCIPLES

In Feature 18-3, we showed that absolute values for individual half-cell potentials cannot be determined in the laboratory, that is, only relative cell potentials can be measured experimentally. **Figure 21-1** shows a typical cell for potentiometric analysis. This cell can be represented as

$$\underbrace{\text{reference electrode}}_{E_{ref}}\,|\,\underbrace{\text{salt bridge}}_{E_j}\,|\,\text{analyte solution}\,|\,\underbrace{\text{indicator electrode}}_{E_{ind}}$$

A **reference electrode** is a half-cell having a known electrode potential that remains constant at constant temperature and is independent of the composition of the analyte solution.

An **indicator electrode** has a potential that varies in a known way with variations in the concentration of an analyte.

The **reference electrode** in this diagram is a half-cell with an accurately known electrode potential, E_{ref}, that is independent of the concentration of the analyte or any other ions in the solution under study. It can be a standard hydrogen electrode but seldom is because a standard hydrogen electrode is somewhat troublesome to maintain and use. By convention, the reference electrode is always treated as the left-hand electrode in potentiometric measurements. The **indicator electrode**, which is immersed in a solution of the analyte, develops a potential, E_{ind}, that depends on the activity of the analyte. Most indicator electrodes used in potentiometry are selective in their responses. The third component of a potentiometric cell is a salt bridge that prevents the components of the analyte solution from mixing with those of the reference electrode. As noted in Chapter 18, a potential develops across the liquid junctions at each end of the salt bridge. These two potentials tend to cancel one another if the mobilities of the cation and the anion in the bridge solution are approximately the same. Potassium chloride is a nearly ideal electrolyte for the salt bridge because the mobilities of the K^+ ion and the Cl^- ion are nearly equal. The net potential across the salt bridge, E_j, is thereby reduced to a few millivolts or less. For most electroanalytical methods, the junction potential is small enough to be neglected. In the potentiometric methods discussed in this chapter, however, the junction potential and its uncertainty can be factors that limit the measurement accuracy and precision.

As shown in Figure 21-1, reference electrodes are *always* treated as the left-hand electrode. This practice, which we adopt throughout this text, is consistent with the International Union of Pure and Applied Chemistry (IUPAC) convention for electrode potentials, discussed in Section 18C-4, in which the reference is the standard hydrogen electrode and is the electrode on the left in a cell diagram.

A hydrogen electrode is seldom used as a reference electrode for day-to-day potentiometric measurements because it is inconvenient to use and maintain and is also a fire hazard.

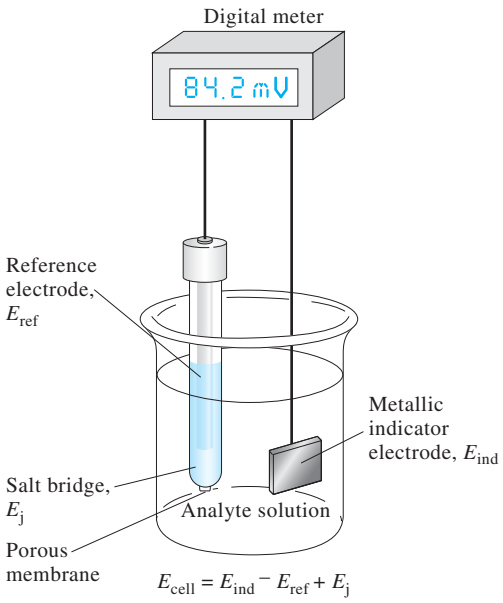

Figure 21-1 A cell for potentiometric determinations.

The potential of the cell we have just considered is given by the equation

$$E_{cell} = E_{ind} - E_{ref} + E_j \qquad (21\text{-}1)$$

The first term in this equation, E_{ind}, contains the information that we are looking for—the concentration of the analyte. To make a potentiometric determination of an analyte then, we must measure a cell potential, correct this potential for the reference and junction potentials, and compute the analyte concentration from the indicator electrode potential. Strictly, the potential of a galvanic cell is related to the activity of the analyte. Only through proper calibration of the electrode system with solutions of known concentration can we determine the concentration of the analyte.

In the sections that follow, we discuss the nature and origin of the three potentials shown on the right side of Equation 21-1.

21B REFERENCE ELECTRODES

The ideal reference electrode has a potential that is accurately known, constant, and completely insensitive to the composition of the analyte solution. In addition, this electrode should be rugged, easy to assemble, and should maintain a constant potential while passing minimal currents.

21B-1 Calomel Reference Electrodes

Calomel reference electrodes consist of mercury in contact with a solution that is saturated with mercury(I) chloride (calomel) and that also contains a known concentration of potassium chloride. Calomel half-cells can be represented as follows:

$$Hg|Hg_2Cl_2(\text{sat'd}), KCl(x\ M)\|$$

where x represents the molar concentration of potassium chloride in the solution. The electrode potential for this half-cell is determined by the reaction

$$Hg_2Cl_2(s) + 2e^- \rightleftharpoons 2Hg(l) + 2Cl^-(aq)$$

and depends on the chloride concentration. Thus, the KCl concentration must be specified in describing the electrode.

The "saturated" in a saturated calomel electrode refers to the KCl concentration and not the calomel concentration. All calomel electrodes are saturated with Hg_2Cl_2 (calomel).

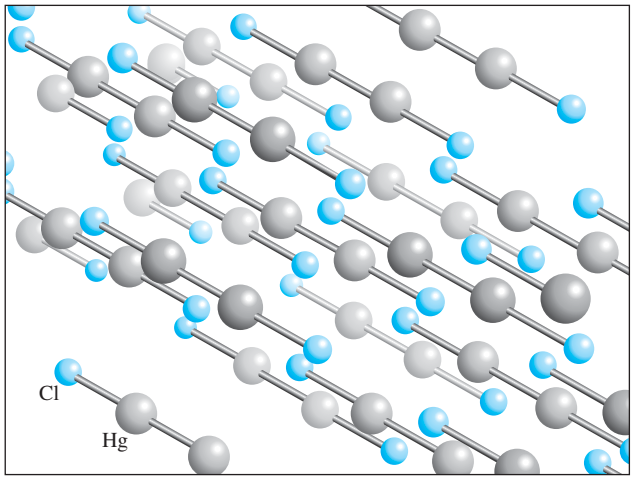

The crystal structure of calomel, Hg_2Cl_2, which has a limited solubility in water ($K_{sp} = 1.8 \times 10^{-18}$ at 25°C). Notice the Hg—Hg bond in the structure. There is considerable evidence that a similar type of bonding occurs in aqueous solution, and so mercury(I) is represented as Hg_2^{2+}.

TABLE 21-1

Formal Electrode Potentials for Reference Electrodes as a Function of Composition and Temperature

	Potential versus SHE, V				
Temperature, °C	**0.1 M Calomel***	**3.5 M Calomel†**	**Sat'd Calomel***	**3.5 M Ag/AgCl†**	**Sat'd Ag/AgCl†**
15	0.3362	0.254	0.2511	0.212	0.209
20	0.3359	0.252	0.2479	0.208	0.204
25	0.3356	0.250	0.2444	0.205	0.199
30	0.3351	0.248	0.2411	0.201	0.194
35	0.3344	0.246	0.2376	0.197	0.189

*From R. G. Bates, in *Treatise on Analytical Chemistry*, 2nd ed., I. M. Kolthoff and P. J. Elving, eds., Part I, Vol. 1, p. 793, New York: Wiley, 1978.
†From D. T. Sawyer, A. Sobkowiak, and J. L. Roberts, Jr., *Electrochemistry for Chemists*, New York: Wiley, 1995, p. 192.

A salt bridge is easily constructed by filling a U-tube with a conducting gel prepared by heating about 5 g of agar in 100 mL of an aqueous solution containing about 35 g of potassium chloride. When the liquid cools, it sets up into a gel that is a good conductor but prevents the two solutions at the ends of the tube from mixing. If either of the ions in potassium chloride interfere with the measurement process, ammonium nitrate may be used as the electrolyte in salt bridges.

Agar, which is available as translucent flakes, is a heteropolysaccharide that is extracted from certain East Indian seaweed. Solutions of agar in hot water set to a gel when they are cooled.

Table 21-1 lists the compositions and formal electrode potentials for the three most common calomel electrodes. Note that each solution is saturated with mercury(I) chloride (calomel) and that the cells differ only with respect to the potassium chloride concentration. Several convenient calomel electrodes, such as the electrode illustrated in **Figure 21-2**, are available commercially. The H-shape body of the electrode is made of glass of dimensions shown in the diagram. The right arm of the electrode contains a platinum electrical contact, a small quantity of mercury/mercury(I) chloride paste in saturated potassium chloride, and a few crystals of KCl. The tube is filled with saturated KCl to act as a salt bridge (see Section 18B-2) through a piece of porous Vycor ("thirsty glass") sealed in the end of the left arm. This type of junction has a relatively high resistance (2000 to 3000 Ω) and a limited current-carrying capacity, but contamination of the analyte solution due to leakage of potassium chloride is minimal. Other configurations of SCEs are available with much lower resistance and better electrical contact to the analyte solution, but they tend to leak small amounts of saturated potassium chloride into the sample. Because of concerns with mercury contamination, SCEs are less common than they once were, but for some applications, they are superior to Ag-AgCl reference electrodes, which are described next.

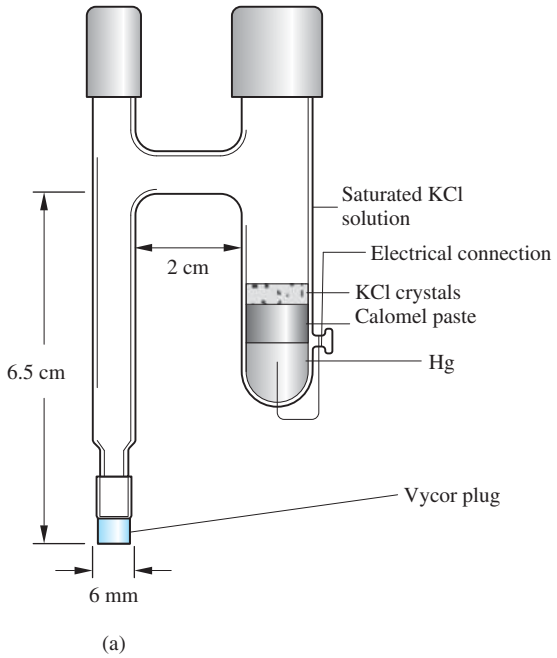

(a)

Figure 21-2 Diagram of a typical commercial saturated calomel electrode. (Reprinted with permission of Bioanalytical Systems, W. Lafayette, IN.)

21B-2 Silver/Silver Chloride Reference Electrodes

The most widely marketed reference electrode system consists of a silver electrode immersed in a solution of potassium chloride that has been saturated with silver chloride:

$$\text{Ag}|\text{AgCl(sat'd)}, \text{KCl(sat'd)}\|$$

The electrode potential is determined by the half-reaction

$$\text{AgCl}(s) + e^- \rightleftharpoons \text{Ag}(s) + \text{Cl}^-$$

Normally, this electrode is prepared with either a saturated or a 3.5 M potassium chloride solution; potentials for these electrodes are given in Table 21-1. **Figure 21-3** shows a commercial model of this electrode, which is little more than a piece of glass tubing that has a narrow opening at the bottom connected to a Vycor plug for making contact with the analyte solution. The tube contains a silver wire coated with a layer of silver chloride that is immersed in a potassium chloride solution saturated with silver chloride.

Silver–silver chloride electrodes have the advantage that they can be used at temperatures greater than 60°C, while calomel electrodes cannot. On the other hand, mercury(II) ions react with fewer sample components than do silver ions (which can react with proteins, for example). Such reactions can lead to plugging of the junction between the electrode and the analyte solution.

At 25°C, the potential of the saturated calomel electrode versus the standard hydrogen electrode is 0.244 V. For the saturated silver/silver chloride electrode, it is 0.199 V.

21C LIQUID-JUNCTION POTENTIALS

When two electrolyte solutions of different composition are in contact with one another, there is a potential difference across the interface. This junction potential is the result of an unequal distribution of cations and anions across the boundary due

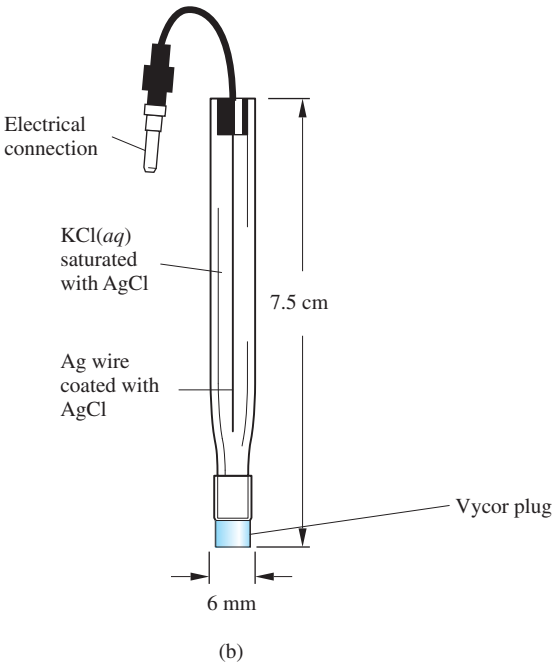

Figure 21-3 Diagram of a silver/silver chloride electrode showing the parts of the electrode that produce the reference electrode potential, E_{ref}, and the junction potential, E_j. (Reprinted with permission of Bioanalytical Systems, W. Lafayette, IN.)

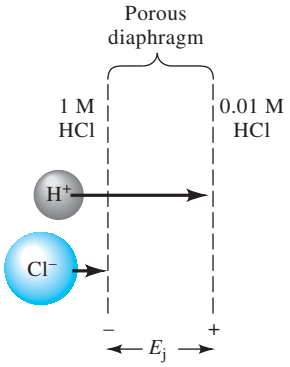

Figure 21-4 Schematic representation of a liquid junction, showing the source of the junction potential, E_j. The lengths of the arrows correspond to the relative mobilities of the ions.

to differences in the rates at which these species diffuse. **Figure 21-4** shows a very simple liquid junction consisting of a 1 M hydrochloric acid solution that is in contact with a solution that is 0.01 M in that acid. An inert porous barrier, such as a fritted glass plate, prevents the two solutions from mixing. The liquid junction may be represented as

$$\text{HCl}(1\text{ M})|\text{HCl}(0.01\text{ M})$$

Both hydrogen ions and chloride ions tend to diffuse across this boundary from the more concentrated to the more dilute solution, that is, left to right. The driving force for each ion is proportional to the activity difference between the two solutions. In the present example, hydrogen ions are substantially more mobile than chloride ions. Thus, hydrogen ions diffuse more rapidly than chloride ions, and as shown in the Figure 21-4, a separation of charge results. The more dilute side of the boundary becomes positively charged because of the more rapid diffusion of hydrogen ions. The concentrated side, therefore, acquires a negative charge from the excess of slower-moving chloride ions. The charge developed tends to counteract the differences in diffusion rates of the two ions so that a condition of equilibrium is attained rapidly. The potential difference resulting from this charge separation may be several hundredths of a volt.

The junction potential across a typical KCl salt bridge is a few millivolts. ❯

The magnitude of the liquid-junction potential can be minimized by placing a salt bridge between the two solutions. The salt bridge is most effective if the mobilities of the negative and positive ions in the bridge are nearly equal and if their concentrations are large. A saturated solution of potassium chloride is good from both standpoints. The junction potential with such a bridge is typically a few millivolts.

21D INDICATOR ELECTRODES

The results of potentiometric determinations are the activities of analytes in contrast to most analytical methods that give the concentrations of analytes. Recall that the activity of a species a_X is related to the molar concentration of X by Equation 10-2

$$a_X = \gamma_X[X]$$

where γ_X is the activity coefficient of X, a parameter that varies with the ionic strength of the solution. Because potentiometric data are dependent on activities, it will not be necessary in most cases to make the usual approximation that $a_X \approx [X]$ in this chapter. ❯

An ideal indicator electrode responds rapidly and reproducibly to changes in the concentration of an analyte ion (or group of analyte ions). Although no indicator electrode is absolutely specific in its response, a few are now available that are remarkably selective. Indicator electrodes are of three types: metallic, membrane, and ion-sensitive field effect transistors.

21D-1 Metallic Indicator Electrodes

It is convenient to classify metallic indicator electrodes as **electrodes of the first kind**, **electrodes of the second kind**, and **inert redox electrodes**.

Electrodes of the First Kind

An electrode of the first kind is a pure metal electrode that is in direct equilibrium with its cation in the solution. A single reaction is involved. For example, the equilibrium between a copper and its cation Cu^{2+} is

$$Cu^{2+}(aq) + 2e^- \rightleftharpoons Cu(s)$$

for which

$$E_{ind} = E^0_{Cu} - \frac{0.0592}{2}\log\frac{1}{a_{Cu^{2+}}} = E^0_{Cu} + \frac{0.0592}{2}\log a_{Cu^{2+}} \qquad (21\text{-}2)$$

where E_{ind} is the electrode potential of the metal electrode and $a_{Cu^{2+}}$ is the activity of the ion (or in dilute solution, approximately its molar concentration, $[Cu^{2+}]$).

We often express the electrode potential of the indicator electrode in terms of the p-function of the cation ($pX = -\log a_{Cu^{2+}}$). Thus, substituting this definition of pCu into Equation 21-2 gives

$$E_{ind} = E^0_{Cu} + \frac{0.0592}{2}\log a_{Cu^{2+}} = E^0_{Cu} - \frac{0.0592}{2}pCu$$

A general expression for any metal and its cation is

$$E_{ind} = E^0_{X^{n+}/X} + \frac{0.0592}{n}\log a_{X^{n+}} = E^0_{X^{n+}/X} - \frac{0.0592}{n}pX \qquad (21\text{-}3)$$

This function is plotted in **Figure 21-5**.

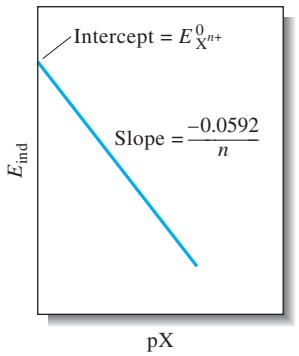

Figure 21-5 A plot of Equation 21-3 for an electrode of the first kind.

Electrode systems of the first kind are not widely used for potentiometric determinations for several reasons. For one, metallic indicator electrodes are not very selective and respond not only to their own cations but also to other more easily reduced cations. For example, a copper electrode cannot be used for the determination of copper(II) ions in the presence of silver(I) ions because the electrode potential is also a function of the Ag^+ concentration. In addition, many metal electrodes, such as zinc and cadmium, can only be used in neutral or basic solutions because they dissolve in the presence of acids. Third, other metals are so easily oxidized that they can be used only when analyte solutions are deaerated to remove oxygen. Finally, certain harder metals, such as iron, chromium, cobalt, and nickel, do not provide reproducible potentials. For these electrodes, plots of E_{ind} versus pX yield slopes that differ significantly and irregularly from the theoretical ($-0.0592/n$). For these reasons, the only electrode systems of the first kind that have been used in potentiometry are Ag/Ag^+ and Hg/Hg^{2+} in neutral solutions and Cu/Cu^{2+}, Zn/Zn^{2+}, Cd/Cd^{2+}, Bi/Bi^{3+}, Tl/Tl^+, and Pb/Pb^{2+} in deaerated solutions.

Electrodes of the Second Kind

Metals not only serve as indicator electrodes for their own cations but also respond to the activities of anions that form sparingly soluble precipitates or stable complexes with such cations. The potential of a silver electrode, for example, correlates reproducibly with the activity of chloride ion in a solution saturated with silver chloride. In this situation, the electrode reaction can be written as

$$AgCl(s) + e^- \rightleftharpoons Ag(s) + Cl^-(aq) \qquad E^0_{AgCl/Ag} = 0.222\ V$$

The Nernst expression for this process at 25°C is

$$E_{ind} = E^0_{AgCl/Ag} - 0.0592\log a_{Cl^-} = E^0_{AgCl/Ag} + 0.0592\ pCl \qquad (21\text{-}4)$$

Equation 21-4 shows that the potential of a silver electrode is proportional to pCl, the negative logarithm of the chloride ion activity. Thus, in a solution saturated with silver chloride, a silver electrode can serve as an indicator electrode of the second kind for chloride ion. Note that the sign of the log term for an electrode of this type is opposite that for an electrode of the first kind (see Equation 21-3). A plot of the potential of the silver electrode versus pCl is shown in **Figure 21-6**.

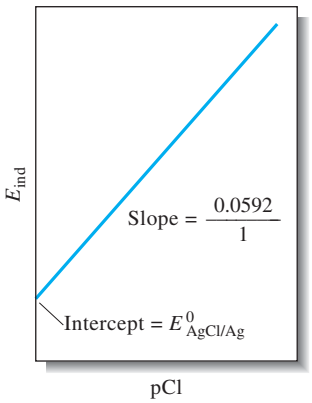

Figure 21-6 A plot of Equation 21-4 for an electrode of the second kind for Cl^-.

Inert Metallic Electrodes for Redox Systems

As noted in Chapter 18, several relatively inert conductors respond to redox systems. Such materials as platinum, gold, palladium, and carbon can be used to monitor redox systems. For example, the potential of a platinum electrode immersed in a solution containing cerium(III) and cerium(IV) is

$$E_{\text{ind}} = E^0_{Ce^{4+}/Ce^{3+}} - 0.0592 \log \frac{a_{Ce^{3+}}}{a_{Ce^{4+}}}$$

A platinum electrode is a convenient indicator electrode for titrations involving standard cerium(IV) solutions.

21D-2 Membrane Indicator Electrodes[2]

For nearly a century, the most convenient method for determining pH has involved measurement of the potential that appears across a thin glass membrane that separates two solutions with different hydrogen ion concentrations. The phenomenon on which the measurement is based was first reported in 1906 and by now has been extensively studied by many investigators. As a result, the sensitivity and selectivity of glass membranes toward hydrogen ions are reasonably well understood. Furthermore, this understanding has led to the development of other types of membranes that respond selectively to many other ions.

Membrane electrodes are sometimes called **p-ion electrodes** because the data obtained from them are usually presented as p-functions, such as pH, pCa, or pNO_3. In this section, we consider several types of p-ion membranes.

It is important to note at the outset of this discussion that membrane electrodes are fundamentally different from metal electrodes both in design and in principle. We shall use the glass electrode for pH measurements to illustrate these differences.

21D-3 The Glass Electrode for Measuring pH

Figure 21-7a shows a typical *cell* for measuring pH. The cell consists of a glass indicator electrode and a saturated calomel reference electrode immersed in the solution of unknown pH. The indicator electrode consists of a thin pH-sensitive glass membrane sealed onto one end of a heavy-walled glass or plastic tube. A small volume of dilute hydrochloric acid saturated with silver chloride is contained in the tube. The inner solution in some electrodes is a buffer containing chloride ion. A silver wire in this solution forms a silver/silver chloride reference electrode, which is connected to one of the terminals of a potential-measuring device. The calomel electrode is connected to the other terminal.

The membrane of a typical glass electrode (with a thickness of 0.03 to 0.1 mm) has an electrical resistance of 50 to 500 MΩ.

Figure 21-7a and the representation of this cell in **Figure 21-8** show that a glass-electrode system contains two reference electrodes: the external calomel electrode and the internal silver/silver chloride electrode. While the internal reference electrode is a part of the glass electrode, it is not the pH-sensing element. *It is the thin glass membrane bulb at the tip of the electrode that responds to pH*. At first, it may seem unusual that an insulator like glass (see margin note) can be used to detect ions, but keep in mind that whenever there is a charge imbalance across any material, there is an

[2]Some suggested sources for additional information on this topic are R. S. Hutchins and L. G. Bachas, in *Handbook of Instrumental Techniques for Analytical Chemistry,* F. A. Settle, ed., Upper Saddle River, NJ: Prentice-Hall, 1997; A. Evans, *Potentiometry and Ion-Selective Electrodes*, New York: Wiley, 1987; J. Koryta, *Ions, Electrodes, and Membranes*, 2nd ed., New York: Wiley, 1991.

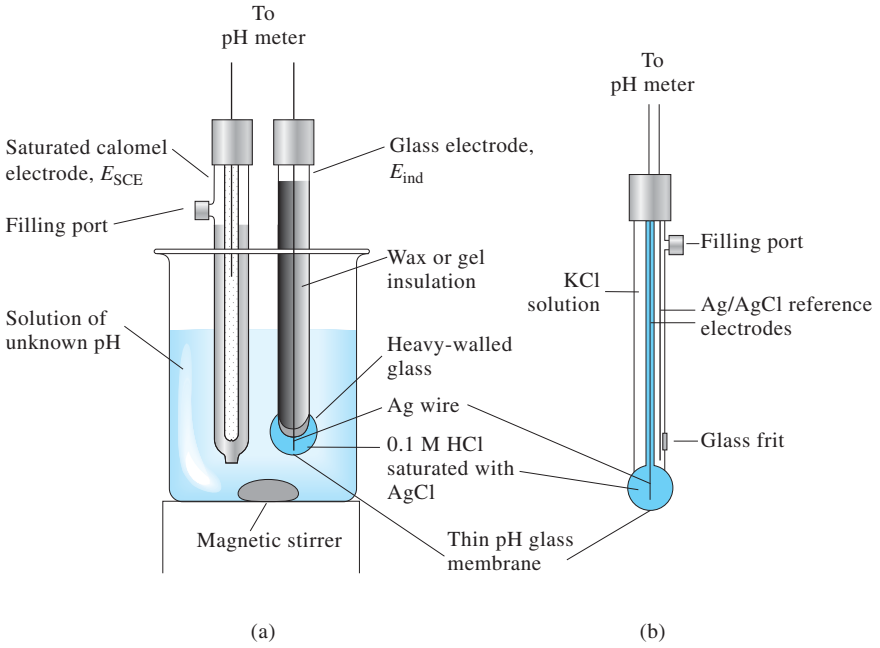

Figure 21-7 Typical electrode system for measuring pH. (a) Glass electrode (indicator) and SCE (reference) immersed in a solution of unknown pH. (b) Combination probe consisting of both an indicator glass electrode and a silver/silver chloride reference. A second silver/silver chloride electrode serves as the internal reference for the glass electrode. The two electrodes are arranged concentrically with the internal reference in the center and the external reference outside. The reference makes contact with the analyte solution through the glass frit or other suitable porous medium. Combination probes are the most common configuration of glass electrode and reference for measuring pH.

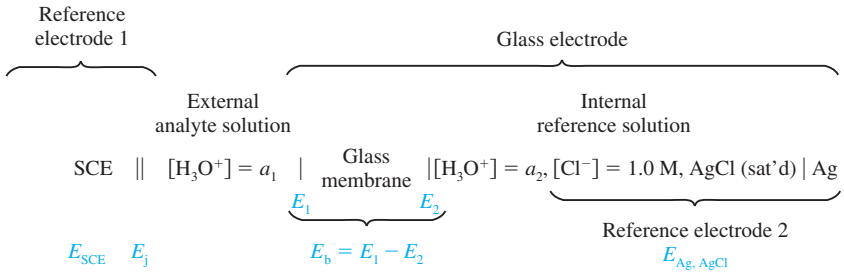

Figure 21-8 Diagram of glass/calomel cell for the measurement of pH. E_{SCE} is the potential of the reference electrode, E_j is the junction potential, a_1 is the activity of hydronium ions in the analyte solution, E_1 and E_2 are the potentials on either side of the glass membrane, E_b is the boundary potential, and a_2 is the activity of hydronium ion in the internal reference solution.

electrical potential difference across the material. In the case of the glass electrode, the concentration (and the activity) of protons inside the membrane is constant. The concentration outside the membrane is determined by the activity of hydrogen ions in the analyte solution. This concentration difference produces the potential difference that we measure with a pH meter. Notice that the internal and external reference electrodes are just the means of making electrical contact with the two sides of the glass membrane and that their potentials are essentially constant except for the junction potential, which depends to a small extent on the composition of the analyte solution. The potentials of the two reference electrodes depend on the electrochemical characteristics of their respective redox couples, but the potential across the glass membrane depends on the physicochemical characteristics of the glass and its response to ionic concentrations on both sides of the membrane. To understand how the glass electrode works, we must explore the mechanism of the creation of the charge differential across the membrane that produces the membrane potential. In the next few sections, we investigate this mechanism and the important characteristics of these membranes.

In Figure 21-7b, we see the most common configuration for measuring pH with a glass electrode. In this arrangement, the glass electrode and its Ag/AgCl internal reference electrode are positioned in the center of a cylindrical probe. Surrounding the glass electrode is the external reference electrode, which is most often of the Ag/AgCl type. The presence of the external reference electrode is not as obvious as in the dual-probe arrangement of Figure 21-7a, but the single-probe, or combination, variety is

much more convenient and can be made much smaller than the dual system. The pH-sensitive glass membrane is attached to the tip of the electrode. These glass pH electrodes are manufactured in many different physical shapes and sizes (5 cm to 5 μm) to suit a broad range of laboratory and industrial applications.

The Composition and Structure of Glass Membranes

Much research has been devoted to the effects of glass composition on the sensitivity of membranes to protons and other cations, and a number of formulations are now used for the manufacture of electrodes. Corning 015 glass, which has been widely used for membranes, consists of approximately 22% Na_2O, 6% CaO, and 72% SiO_2. Membranes made from this glass exhibit excellent specificity to hydrogen ions up to a pH of about 9. At higher pH values, however, the glass becomes somewhat responsive to sodium as well as to other singly charged cations. Other glass formulations are now in use in which sodium and calcium ions are replaced to various degree by barium and lithium ions. These membranes have superior selectivity and lifetime.

As shown in **Figure 21-9**, a silicate glass used for membranes consists of an infinite three-dimensional network of groups in which each silicon atom is bonded to four oxygen atoms and each oxygen atom is shared by two silicon atoms. Within the empty spaces (interstices) inside this structure are enough cations to balance the negative charge of the silicate groups. Singly charged cations, such as sodium and lithium, can move around in the lattice and are responsible for electrical conduction within the membrane.

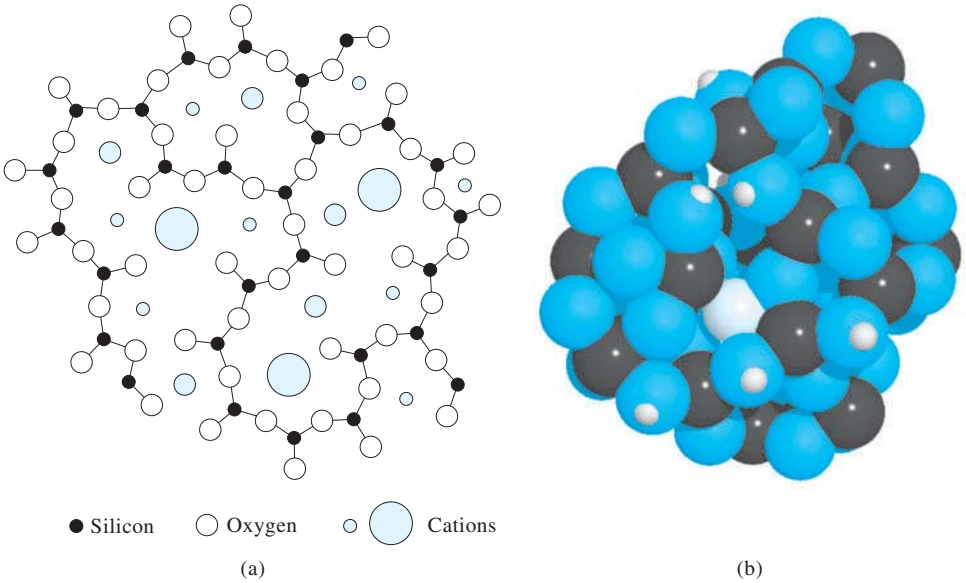

Figure 21-9 (a) Cross-sectional view of a silicate glass structure. In addition to the three Si—O bond shown, each silicon is bonded to an additional oxygen atom, either above or below the plane of the paper. (Reprinted (adapted) with permission from G. A. Perley, *Anal. Chem.*, **1949**, *21*, 395, **DOI**: 10.1021/ac60027a013. Copyright 1949 American Chemical Society.) (b) Model showing three-dimensional structure of amorphous silica with Na^+ ion (large dark green) and several H^+ ions (small dark green) incorporated. Note that the Na^+ ion is surrounded by a cage of oxygen atoms and that each proton in the amorphous lattice is attached to an oxygen. The cavities in the structure, the small size, and the high mobility of the proton ensure that protons can migrate deep into the surface of the silica. Other cations and water molecules may be incorporated into the interstices of the structure as well.

The two surfaces of a glass membrane must be hydrated before it will function as a pH electrode. Nonhygroscopic glasses show no pH function. Even hygroscopic glasses lose their pH sensitivity after dehydration by storage over a desiccant. The effect is reversible, however, and the response of a glass electrode can be restored by soaking it in water.

Glasses that absorb water are said to be **hygroscopic**.

The hydration of a pH-sensitive glass membrane involves an ion-exchange reaction between singly charged cations in the interstices of the glass lattice and hydrogen ions from the solution. The process involves +1 cations exclusively because +2 and +3 cations are too strongly held within the silicate structure to exchange with ions in the solution. The ion-exchange reaction can then be written as

$$\underset{\text{soln}}{H^+} + \underset{\text{glass}}{Na^+Gl^-} \rightleftharpoons \underset{\text{soln}}{Na^+} + \underset{\text{glass}}{H^+Gl^-} \qquad (21\text{-}5)$$

Oxygen atoms attached to only one silicon atom are the negatively charged Gl^- sites shown in this equation. The equilibrium constant for this process is so large that the surfaces of a hydrated glass membrane normally consist entirely of silicic acid (H^+Gl^-). There is an exception to this situation in highly alkaline media, where the hydrogen ion concentration is extremely small and the sodium ion concentration is large. Under this condition, a significant fraction of the sites are occupied by sodium ions.

Membrane Potentials

The lower part of Figure 21-8 shows four potentials that develop in a cell when pH is being determined with a glass electrode. Two of these potentials, $E_{Ag,AgCl}$ and E_{SCE}, are reference electrode potentials that are constant. There is a third potential, the junction potential, E_j, across the salt bridge that separates the calomel electrode from the analyte solution. This junction and its associated potential are found in all cells used to make potentiometric measurements of ion concentration. The fourth, and most important, potential shown in Figure 21-8 is the **boundary potential**, E_b, *which varies with the pH of the analyte solution*. The two reference electrodes simply provide electrical contacts with the solutions so that changes in the boundary potential can be measured.

The Boundary Potential

Figure 21-8 shows that the boundary potential is determined by potentials, E_1 and E_2, which appear at the two *surfaces* of the glass membrane. The source of these two potentials is the charge that accumulates as a consequence of the reactions

$$\underset{\text{glass}_1}{H^+Gl^-}(s) \rightleftharpoons \underset{\text{soln}_1}{H^+}(aq) + \underset{\text{glass}_1}{Gl^-}(s) \qquad (21\text{-}6)$$

$$\underset{\text{glass}_2}{H^+Gl^-}(s) \rightleftharpoons \underset{\text{soln}_2}{H^+}(aq) + \underset{\text{glass}_2}{Gl^-}(s) \qquad (21\text{-}7)$$

where subscript 1 refers to the interface between the exterior of the glass and the analyte solution and subscript 2 refers to the interface between the internal solution and the interior of the glass. These two reactions cause the two glass surfaces to be negatively charged with respect to the solutions with which they are in contact. These negative charges at the surfaces produce the two potentials E_1 and E_2 shown in Figure 21-8. The hydrogen ion concentrations in the solutions on the two sides of the membrane control the positions of the equilibria of Equations 21-7 and 21-8 that in turn determine E_1 and E_2. When the positions of the two equilibria differ, the surface where the greater dissociation has occurred is negative with respect to the

other surface. The resulting difference in potential between the two surfaces of the glass is the boundary potential, which is related to the activities of hydrogen ions in each of the solutions by the Nernst-like equation

$$E_b = E_1 - E_2 = 0.0592 \log \frac{a_1}{a_2} \tag{21-8}$$

where a_1 is the activity of the analyte solution and a_2 is that of the internal solution. For a glass pH electrode, the hydrogen ion activity of the internal solution, a_2, is held constant so that Equation 21-8 simplifies to

$$E_b = L' + 0.0592 \log a_1 = L' - 0.0592 \text{ pH} \tag{21-9}$$

where

$$L' = -0.0592 \log a_2$$

The boundary potential is then a measure of the hydrogen ion activity (pH) of the external solution.

The significance of the potentials and the potential differences shown in Equation 21-8 is illustrated by the potential profiles shown in **Figure 21-10**. The profiles are plotted across the membrane from the analyte solution on the left

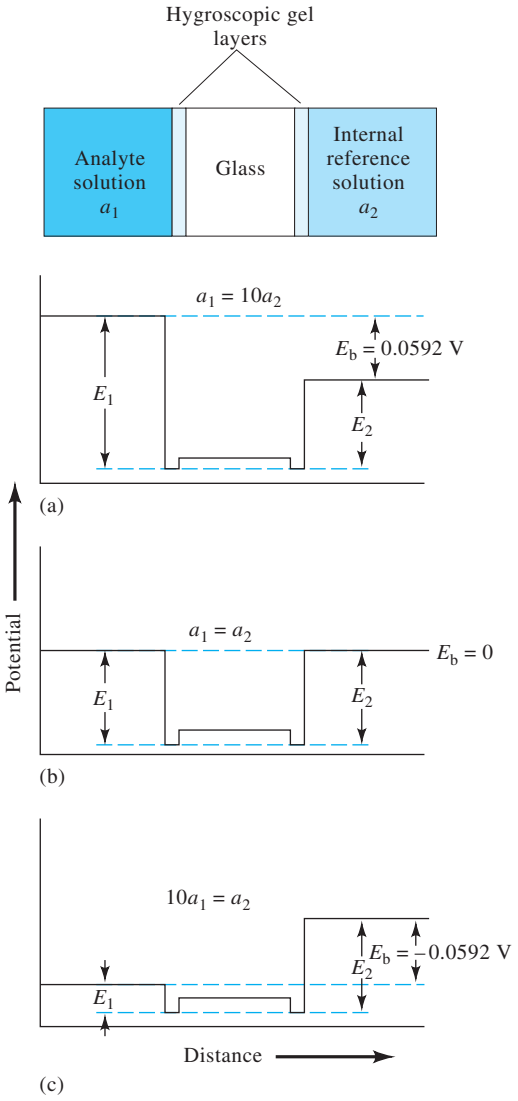

Figure 21-10 Potential profile across a glass membrane from the analyte solution to the internal reference solution. The reference electrode potentials are not shown.

through the membrane to the internal solution on the right. The important thing to note about these profiles is that regardless of the absolute potential inside the hygroscopic layers or the glass, the boundary potential is determined by the *difference* in potential on either side of the glass membrane that is in turn determined by the proton activity on each side of the membrane.

The Asymmetry Potential

When identical solutions and reference electrodes are placed on the two sides of a glass membrane, the boundary potential should in principle be zero. Frequently, however, we find a small asymmetry potential that changes gradually with time.

The sources of the asymmetry potential are obscure but undoubtedly include such causes as differences in strain on the two surfaces of the membrane created during manufacture, mechanical abrasion on the outer surface during use, and chemical etching of the outer surface. To eliminate the bias caused by the asymmetry potential, all membrane electrodes must be calibrated against one or more standard analyte solutions. Calibrations should be carried out at least daily and more often when the electrode is heavily used.

The Glass Electrode Potential

The potential of a glass indicator electrode, E_{ind}, has three components: (1) the boundary potential, given by Equation 21-8; (2) the potential of the internal Ag/AgCl reference electrode; and (3) the small asymmetry potential, E_{asy}, which changes slowly with time. In equation form, we may write

$$E_{ind} = E_b + E_{Ag/AgCl} + E_{asy}$$

Substitution of Equation 21-9 for E_b gives

$$E_{ind} = L' + 0.0592 \log a_1 + E_{Ag/AgCI} + E_{asy}$$

or

$$E_{ind} = L + 0.0592 \log a_1 = L - 0.0592\ \text{pH} \qquad (21\text{-}10)$$

where L is a combination of the three constant terms. Compare Equations 21-10 and 21-3. Although these two equations are similar in form and both potentials are produced by separation of charge, remember that *the mechanisms of charge separation that result in these expressions are considerably different*.

The Alkaline Error

In basic solutions, glass electrodes respond to the concentration of both hydrogen ion and alkali metal ions. The magnitude of the resulting alkaline error for four different glass membranes is shown in **Figure 21-11** (curves *C* to *F*). These curves refer to solutions in which the sodium ion concentration was held constant at 1 M while the pH was varied. Note that the error ($pH_{read} - pH_{true}$) is negative (that is, the measured pH values are lower than the true values), suggesting that the electrode is responding to sodium ions as well as to protons. This observation is confirmed by data obtained for solutions containing different sodium ion concentrations. Thus, at pH 12, the electrode with a Corning 015 membrane (curve *C* in Figure 21-11) registered a pH of 11.3 when immersed in a solution having a sodium ion concentration of 1 M but 11.7 in a solution that was 0.1 M in this ion. All singly charged cations induce an alkaline error whose magnitude depends on both the cation in question and the composition of the glass membrane.

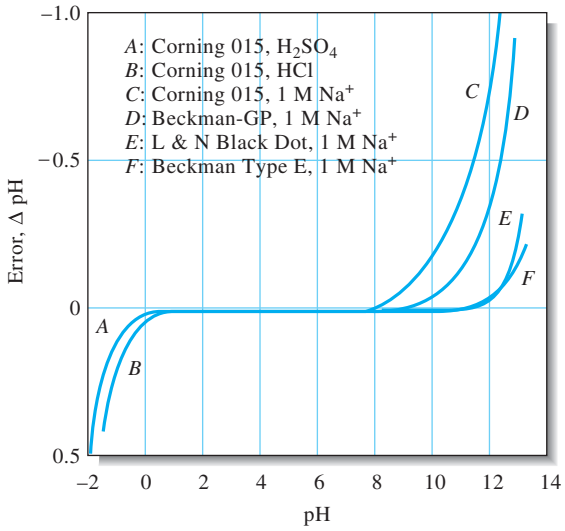

Figure 21-11 Acid and alkaline errors for selected glass electrodes at 25°C. (R.G. Bates, *Determination of pH*, 2nd ed., p.265. New York: Wiley, 1973. Reprinted by permission of the author's estate.)

The alkaline error can be satisfactorily explained by assuming an exchange equilibrium between the hydrogen ions on the glass surface and the cations in solution. This process is simply the reverse of that shown in Equation 21-5:

$$\underset{\text{glass}}{H^+Gl^-} + \underset{\text{soln}}{B^+} \rightleftharpoons \underset{\text{glass}}{B^+Gl^-} + \underset{\text{soln}}{H^+}$$

where B^+ represents some singly charged cation, such as sodium ion.

The equilibrium constant for this reaction is

$$K_{ex} = \frac{a_1 b_1'}{a_1' b_1} \tag{21-11}$$

In Equation 21-11, b_1 represents the activity of some singly charged cation such as Na^+ or K^+.

where a_1 and b_1 represent the activities of H^+ and B^+ in solution and a_1' and b_1' are the activities of these ions on the glass surface. Equation 21-11 can be rearranged to give ratio of the activities B^+ to H^+ on the glass surface:

$$\frac{b_1'}{a_1'} = K_{ex}\frac{b_1}{a_1}$$

For the glasses used for pH electrodes, K_{ex} is typically so small that the activity ratio b_1'/a_1' is minuscule. The situation differs in strongly alkaline media, however. For example, b_1'/a_1' for an electrode immersed in a pH 11 solution that is 1 M in sodium ions (see Figure 21-11) is $10^{11} \times K_{ex}$. Under these conditions, the activity of the sodium ions relative to that of the hydrogen ions becomes so large that the electrode responds to both species.

Describing Selectivity

The effect of an alkali metal ion on the potential across a membrane can be accounted for by inserting an additional term in Equation 21-9 to give

$$E_b = L' + 0.0592 \log (a_1 + k_{H,B} b_1) \tag{21-12}$$

The **selectivity coefficient** is a measure of the response of an ion-selective electrode to other ions.

where $k_{H,B}$ is the **selectivity coefficient** for the electrode. Equation 21-12 applies not only to glass indicator electrodes for hydrogen ion but also to all other types

of membrane electrodes. Selectivity coefficients range from zero (no interference) to values greater than unity. Thus, if an electrode for ion A responds 20 times more strongly to ion B than to ion A, $k_{H,B}$ has a value of 20. If the response of the electrode to ion C is 0.001 of its response to A (a much more desirable situation), $k_{H,B}$ is 0.001.[3]

The product $k_{H,B}b_1$ for a glass pH electrode is usually small relative to a_1 provided that the pH is less than 9; under these conditions, Equation 21-12 simplifies to Equation 21-9. At high pH values and at high concentrations of a singly charged ion, however, the second term in Equation 21-12 assumes a more important role in determining E_b, and an alkaline error is encountered. For electrodes specifically designed for work in highly alkaline media (curve *E* in Figure 21-11), the magnitude of $k_{H,B}b_1$ is appreciably smaller than for ordinary glass electrodes.

The Acid Error

As shown in Figure 21-11, the typical glass electrode exhibits an error, opposite in sign to the alkaline error, in solution of pH less than about 0.5. The negative error ($pH_{read} - pH_{true}$) indicates that pH readings tend to be too high in this region. The magnitude of the error depends on a variety of factors and is generally not very reproducible. All the causes of the acid error are not well understood, but one source is a saturation effect that occurs when all the surface sites on the glass are occupied with H^+ ions. Under these conditions, the electrode no longer responds to further increases in the H^+ concentration, and the pH readings are too high.

21D-4 Glass Electrodes for Other Cations

The alkaline error in early glass electrodes led to investigations concerning the effect of glass composition on the magnitude of this error. One consequence has been the development of glasses for which the alkaline error is negligible below about pH 12 (see curves *E* and *F*, Figure 21-11). Other studies have discovered glass compositions that permit the determination of cations other than hydrogen. Incorporation of Al_2O_3 or B_2O_3 in the glass has the desired effect. Glass electrodes that permit the direct potentiometric measurement of such singly charged species as Na^+, K^+, NH_4^+, Rb^+, Cs^+, Li^+, and Ag^+ have been developed. Some of these glasses are reasonably selective toward particular singly charged cations. Glass electrodes for Na^+, Li^+, NH_4^+, and total concentration of univalent cations are now available from commercial sources.

21D-5 Liquid-Membrane Electrodes

The potential of liquid-membrane electrodes develops across the interface between the solution containing the analyte and a liquid-ion exchanger that selectively bonds with the analyte ion. These electrodes have been developed for the direct potentiometric measurement of numerous polyvalent cations as well as certain anions.

Figure 21-12 is a schematic of a liquid-membrane electrode for calcium. It consists of a conducting membrane that selectively binds calcium ions, an internal solution containing a fixed concentration of calcium chloride, and a silver electrode that is coated with silver chloride to form an internal reference electrode. Notice the similarities between the liquid-membrane electrode and the glass electrode, as shown in

[3]For tables of selectivity coefficients for a variety of membranes and ionic species, see Y. Umezawa, *CRC Handbook of Ion Selective Electrodes: Selectivity Coefficients*, Boca Raton, FL: CRC Press, 1990.

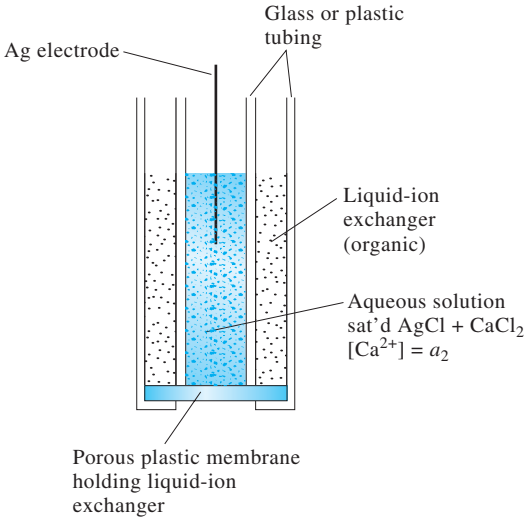

Figure 21-12 Diagram of a liquid-membrane electrode for Ca^{2+}.

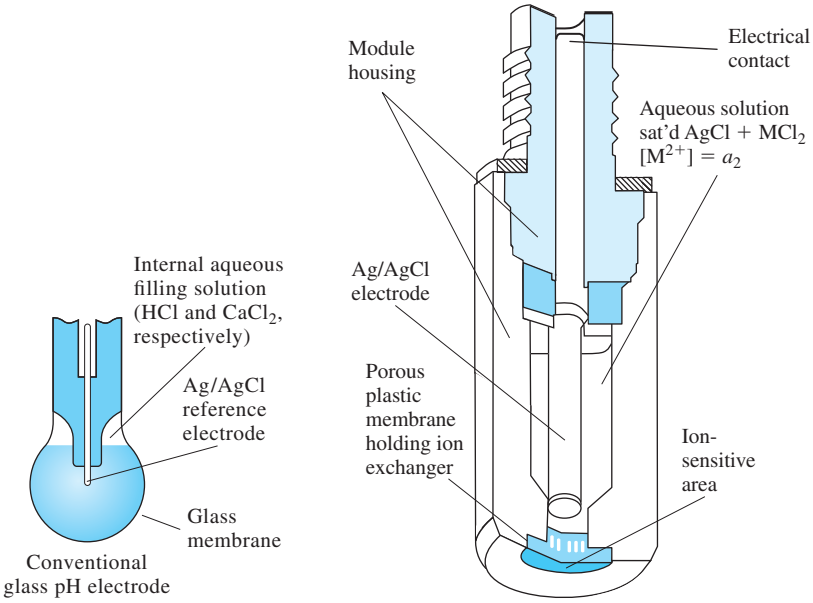

Figure 21-13 Comparison of a liquid-membrane calcium ion electrode with a glass pH electrode. (Courtesy of Thermo Orion, Beverly, MA.)

Figure 21-13. The active membrane ingredient is an ion exchanger that consists of a calcium dialkyl phosphate that is nearly insoluble in water. In the electrode shown in Figures 21-12 and 21-13, the ion exchanger is dissolved in an immiscible organic liquid that is forced by gravity into the pores of a hydrophobic porous disk. This disk then serves as the membrane that separates the internal solution from the analyte solution. In a more recent design, the ion exchanger is immobilized in a tough polyvinyl chloride gel attached to the end of a tube that holds the internal solution and reference electrode (see Figure 21-13, right). In either design, a dissociation equilibrium develops at each membrane interface that is analogous to Equations 21-6 and 21-7:

Hydrophobia means fear of water. The hydrophobic disk is porous toward organic liquids but repels water.

$$\underset{\text{organic}}{[(RO)_2POO]_2Ca} \rightleftharpoons \underset{\text{organic}}{2(RO)_2POO^-} + \underset{\text{aqueous}}{Ca^{2+}}$$

where R is a high-molecular-mass aliphatic group. As with the glass electrode, a potential develops across the membrane when the extent of dissociation of the ion exchanger dissociation at one surface differs from that at the other surface.

This potential is a result of differences in the calcium ion activity of the internal and external solutions. The relationship between the membrane potential and the calcium ion activities is given by an equation that is similar to Equation 21-8:

$$E_b = E_1 - E_2 = \frac{0.0592}{2} \log \frac{a_1}{a_2} \qquad (21\text{-}13)$$

where a_1 and a_2 are the activities of calcium ion in the external analyte and internal standard solutions, respectively. Since the calcium ion activity of the internal solution is constant,

$$E_b = N + \frac{0.0592}{2} \log a_1 = N - \frac{0.0592}{2} \text{pCa} \qquad (21\text{-}14)$$

where N is a constant (compare Equations 21-14 and 21-9). Note that, because calcium is divalent, the value of n in the denominator of the coefficient of the logarithmic term is 2.

The sensitivity of the liquid-membrane electrode for calcium ion is reported to be 50 times greater than for magnesium ion and 1000 times greater than for sodium or potassium ions. Calcium ion activities as low as 5×10^{-7} M can be measured. Performance of the electrode is independent of pH in the range between 5.5 and 11. At lower pH levels, hydrogen ions undoubtedly replace some of the calcium ions on the exchanger; the electrode then becomes sensitive to pH as well as to pCa.

The calcium ion liquid-membrane electrode is a valuable tool for physiological investigations because this ion plays important roles in such processes as nerve conduction, bone formation, muscle contraction, cardiac expansion and contraction, renal tubular function, and perhaps hypertension. Most of these processes are more influenced by the activity than the concentration of the calcium ion; activity, of course, is the parameter measured by the membrane electrode. Therefore, the calcium ion electrode as well as the potassium ion electrode and others are important tools in studying physiological processes.

A liquid-membrane electrode specific for potassium ion is also of great value for physiologists because the transport of neural signals appears to involve movement of this ion across nerve membranes. Investigation of this process requires an electrode that can detect small concentrations of potassium ion in media that contain much larger concentrations of sodium ion. Several liquid-membrane electrodes show promise in meeting this requirement. One is based on the antibiotic valinomycin, a cyclic ether that has a strong affinity for potassium ion. Of equal importance is the observation that a liquid membrane consisting of valinomycin in diphenyl ether is about 10^4 times as responsive to potassium ion as to sodium ion.[4] **Figure 21-14** is a photomicrograph of a tiny electrode used for determining the potassium content of a single cell.

Table 21-2 lists some liquid-membrane electrodes available from commercial sources. The anion-sensitive electrodes listed make use of a solution containing an anion-exchange resin in an organic solvent. Liquid-membrane electrodes in which the exchange liquid is held in a polyvinyl chloride gel have been developed for Ca^{2+}, K^+, NO_3^-, and BF_4^-. These have the appearance of crystalline electrodes, which are considered in the following section. A homemade liquid-membrane ion-selective electrode is described in Feature 21-1.

[4]M. S. Frant and J. W. Ross, Jr., *Science*, **1970**, *167*, 987, **DOI**: 10.1126/science.167.3920.987.

Ion-selective microelectrodes can be used to make measurements of ion activities within a living organism.

Figure 21-14 Photograph of a potassium liquid ion exchanger microelectrode with 125 μm of ion exchanger inside the tip. The magnification of the original photo was 400×. (Reprinted with permission from *Anal. Chem.*, March **1971**, *43*(*3*), 89A-93A. Copyright 1971 American Chemical Society.)

TABLE 21-2

Characteristics of Liquid-Membrane Electrodes*

Analyte Ion	Concentration Range, M†	Major Interferences‡
NH_4^+	10^0 to 5×10^{-7}	<1 H^+, 5×10^{-1} Li^+, 8×10^{-2}, Na^+, 6×10^{-4} K^+, 5×10^{-2} Cs^+, >1 Mg^{2+}, >1 Ca^{2+}, >1 Sr^{2+}, >0.5 Sr^{2+}, 1×10^{-2} Zn^{2+}
Cd^{2+}	10^0 to 5×10^{-7}	Hg^{2+} and Ag^+ (poisons electrode at $>10^{-7}$ M), Fe^{3+} (at $>0.1[Cd^{2+}]$, Pb^{2+} (at $>[Cd^{2+}]$), Cu^{2+} (possible)
Ca^{2+}	10^0 to 5×10^{-7}	10^{-5} Pb^{2+}; 4×10^{-3} Hg^{2+}, H^+, 6×10^{-3} Sr^{2+}; 2×10^{-2} Fe^{2+}; 4×10^{-2} Cu^{2+}; 5×10^{-2} Ni^{2+}; 0.2 NH_3; 0.2 Na^+; 0.3 $Tris^+$; 0.3 Li^+; 0.4 K^+; 0.7 Ba^{2+}; 1.0 Zn^{2+}; 1.0 Mg^{2+}
Cl^-	10^0 to 5×10^{-6}	Maximum allowable ratio of interferent to $[Cl^-]$: OH^- 80, Br^- 3×10^{-3}; I^- 5×10^{-7}, S^{2-} 10^{-6}, CN^- 2×10^{-7}, NH_3 0.12, $S_2O_3^{2-}$ 0.01
BF_4^-	10^0 to 7×10^{-6}	5×10^{-7} ClO_4^-; 5×10^{-6} I^-; 5×10^{-5} ClO_3^-; 5×10^{-4} CN^-; 10^{-3} Br^-; 10^{-3} NO_2^-; 5×10^{-3} NO_3^-; 3×10^{-3} HCO_3^-, 5×10^{-2} Cl^-; 8×10^{-2} $H_2PO_4^-$, HPO_4^{2-}, PO_4^{3-}; 0.2 OAc^-; 0.6 F^-; 1.0 SO_4^{2-}
NO_3^-	10^0 to 7×10^{-6}	10^{-7} ClO_4^-; 5×10^{-6}; I^-; 5×10^{-5} ClO_3^-; 10^{-4} CN^-; 7×10^{-4} Br^-; 10^{-3} HS^-; 10^{-2} HCO_3^-, 2×10^{-2} CO_3^{2-}; 3×10^{-2} Cl^-; 5×10^{-2} $H_2PO_4^-$, HPO_4^{2-}, PO_4^{3-}; 0.2 OAc^-; 0.6 F^-; 1.0 SO_4^{2-}
NO_2^-	1.4×10^{-6} to 3.6×10^{-6}	7×10^{-1} salicylate, 2×10^{-3} I^-, 10^{-1} Br^-, 3×10^{-1} ClO_3^-, 2×10^{-1} acetate, 2×10^{-1} HCO_3^-, 2×10^{-1} NO_3^-, 2×10^{-1} SO_4^{2-}, 1×10^{-1} Cl^-, 1×10^{-1} ClO_4^-, 1×10^{-1} F^-
ClO_4^-	10^0 to 7×10^{-6}	2×10^{-3} I^-; 2×10^{-2} ClO_3^-; 4×10^{-2} CN^-, Br^-; 5×10^{-2} NO_2^-, NO_3^-; 2 HCO_3^-, CO_3^{2-}; Cl^-, $H_2PO_4^-$, HPO_4^{2-}, PO_4^{3-}, OAc^-, F^-, SO_4^{2-}
K^+	10^0 to 1×10^{-6}	3×10^{-4} Cs^+; 6×10^{-3} NH_4^+, Tl^+; 10^{-2} H^+; 1.0 Ag^+, $Tris^+$; 2.0 Li^+, Na^+
Water hardness ($Ca^{2+}+Mg^{2+}$)	10^{-3} to 6×10^{-6}	3×10^{-5} Cu^{2+}, Zn^{2+}; 10^{-4} Ni^{2+}; 4×10^{-4} Sr^{2+}; 6×10^{-5} Fe^{2+}; 6×10^{-4} Ba^{2+}; 3×10^{-2} Na^+; 0.1 K^+

All electrodes are the plastic-membrane type. All values are selectivity coefficients unless otherwise noted.
†From product catalog, Boston, MA: Thermo Orion, 2006.
‡From product instruction manuals, Boston, MA: Thermo Orion, 2003.

FEATURE 21-1

An Easily Constructed Liquid-Membrane Ion-Selective Electrode

You can make a liquid-membrane ion-selective electrode with glassware and chemicals available in most laboratories.[5] All you need are a pH meter, a pair of reference electrodes, a fritted-glass filter crucible or tube, trimethylchlorosilane, and a liquid ion exchanger.

First, cut the filter crucible (or alternatively, a fritted tube), as shown in Figure 21F-1. Carefully clean and dry the crucible and then draw a small amount of trimethylchlorosilane into the frit. This coating makes the glass in the frit hydrophobic. Rinse the frit with water, dry, and apply a commercial liquid ion exchanger to it. After a minute, remove the excess exchanger. Add a few milliliters of a 10^{-2} M solution of the ion of interest to the crucible, insert a reference electrode into the solution, and voilá, you have a very nice ion-selective electrode. The exact details of washing, drying, and preparing the electrode are provided in the original article.

Connect the ion-selective electrode and the second reference electrode to the pH meter, as shown in Figure 21F-1. Prepare a series of standard solutions of the ion of interest, measure the cell potential for each concentration, plot a working curve of

[5]See T. K. Christopoulus and E. P. Diamandis, *J. Chem. Educ.*, **1988**, *65*, 648, **DOI**: 10.1021/ed065p648.

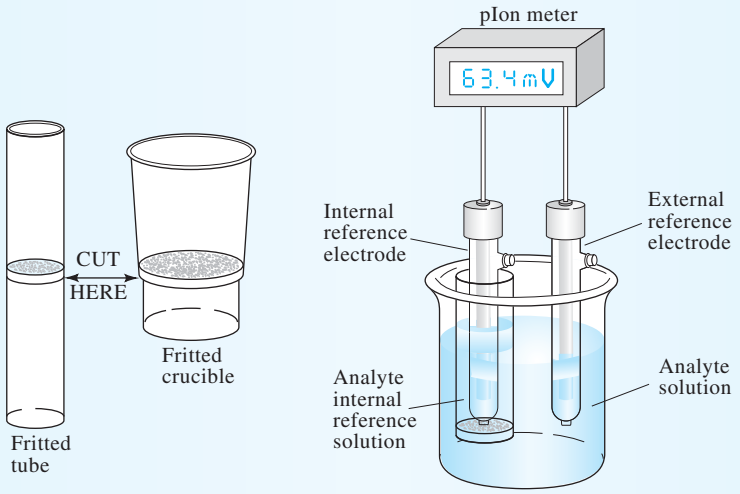

Figure 21F-1 A homemade liquid-membrane electrode.

E_{cell} versus log c, and perform a least-squares analysis on the data (see Chapter 8). Compare the slope of the line with the theoretical slope of (0.0592 V)/n. Measure the potential for an unknown solution of the ion and calculate the concentration from the least-squares parameters.

21D-6 Crystalline-Membrane Electrodes

Considerable work has been devoted to the development of solid membranes that are selective toward anions in the same way that some glasses respond to cations. We have seen that anionic sites on a glass surface account for the selectivity of a membrane toward certain cations. By analogy, a membrane with cationic sites might be expected to respond selectively toward anions.

Membranes prepared from cast pellets of silver halides have been used successfully in electrodes for the selective determination of chloride, bromide, and iodide ions. In addition, an electrode based on a polycrystalline Ag_2S membrane is offered by one manufacturer for the determination of sulfide ion. In both types of membranes, silver ions are sufficiently mobile to conduct electricity through the solid medium. Mixtures of PbS, CdS, and CuS with Ag_2S provide membranes that are selective for Pb^{2+}, Cd^{2+}, and Cu^{2+}, respectively. Silver ion must be present in these membranes to conduct electricity because divalent ions are immobile in crystals. The potential that develops across crystalline solid-state electrodes is described by a relationship similar to Equation 21-9.

A crystalline electrode for fluoride ion is available from commercial sources. The membrane consists of a slice of a single crystal of lanthanum fluoride that has been doped with europium(II) fluoride to improve its conductivity. The membrane, supported between a reference solution and the solution to be measured, shows a theoretical response to changes in fluoride ion activity from 10^0 to 10^{-6} M. The electrode is selective for fluoride ion over other common anions by several orders of magnitude; only hydroxide ion appears to offer serious interference.

Some solid-state electrodes available from commercial sources are listed in **Table 21-3**.

TABLE 21-3

Characteristics of Solid-State Crystalline Electrodes*

Analyte Ion	Concentration Range, M	Major Interferences
Br^-	10^0 to 5×10^{-6}	CN^-, I^-, S^{2-}
Cd^{2+}	10^{-1} to 1×10^{-7}	Fe^{2+}, Pb^{2+}, Hg^{2+}, Ag^+, Cu^{2+}
Cl^-	10^0 to 5×10^{-5}	CN^-, I^-, Br^-, S^{2-}, OH^-, NH_3
Cu^{2+}	10^{-1} to 1×10^{-8}	Hg^{2+}, Ag^+, Cd^{2+}
CN^-	10^{-2} to 1×10^{-6}	S^{2-}, I^-
F^-	Sat'd to 1×10^{-6}	OH^-
I^-	10^0 to 5×10^{-8}	CN^-
Pb^{2+}	10^{-1} to 1×10^{-6}	Hg^{2+}, Ag^+, Cu^{2+}
Ag^+/S^{2-}	Ag^+: 10^0 to 1×10^{-7} S^{2-}: 10^0 to 1×10^{-7}	Hg^{2+}
SCN^-	10^0 to 5×10^{-6}	I^-, Br^-, CN^-, S^{2-}

*From *Orion Guide to Ion Analysis,* Boston, MA: Thermo Orion, 1992.

21D-7 Ion-Sensitive Field Effect Transistors (ISFETs)

The **field effect transistor**, or the **metal oxide field effect transistor (MOSFET)**, is a tiny solid-state semiconductor device that is widely used in computers and other electronic circuits as a switch to control current flow in circuits. One of the problems in using this type of device in electronic circuits has been its pronounced sensitivity to ionic surface impurities, and a great deal of money and effort has been expended by the electronic industry in minimizing or eliminating this sensitivity in order to produce stable transistors.

Scientists have exploited the sensitivities of MOSFETs to surface ionic impurities for the selective potentiometric determination of various ions. These studies have led to the development of a number of different **ion-sensitive field effect transistors** termed **ISFETs**. The theory of their selective ion sensitivity is well understood and is described in Feature 21-2.[6]

ISFETs stands for ion-sensitive field effect transistors.

ISFETs offer a number of significant advantages over membrane electrodes including ruggedness, small size, inertness toward harsh environments, rapid response, and low electrical impedance. In contrast to membrane electrodes,

FEATURE 21-2

The Structure and Performance of Ion-Sensitive Field Effect Transistors

The metal oxide field effect transistor (MOSFET) is a solid-state semiconductor device that is used widely for switching signals in computers and many other types of electronic circuits. **Figure 21F-2** shows a cross-sectional diagram (a) and a circuit symbol (b) for an *n*-channel enhancement mode MOSFET. Modern semiconductor fabrication techniques are used to construct the MOSFET on the surface of a piece of *p*-type semiconductor called the substrate. For a discussion of the characteristics of *p*-type and *n*-type semiconductors, refer to the paragraphs on silicon photodiodes in Section 25A-4. As shown in Figure 21F-2a, two islands of *n*-type semiconductors are formed on the surface of the *p*-type substrate, and the surface is then covered by insulating SiO_2. The last step in the fabrication process is the deposition of metallic

[6]For a detailed explanation of the theory of ISFETs, see J. Janata, *Principles of Chemical Sensors,* 2nd ed., New York: Plenum, 2009, pp. 156–167.

conductors that are used to connect the MOSFET to external circuits. There are a total of four such connections to the drain, the gate, the source, and the substrate as shown in the figure.

The area on the surface of the *p*-type material between the drain and source is called the channel (see the dark shaded area in Figure 21F-2a). Note that the channel is separated from the gate connection by an insulating layer of SiO_2. When an electrical potential is applied between the gate and the source, the electrical conductivity of the channel is enhanced by a factor that is related to the size of the applied potential.

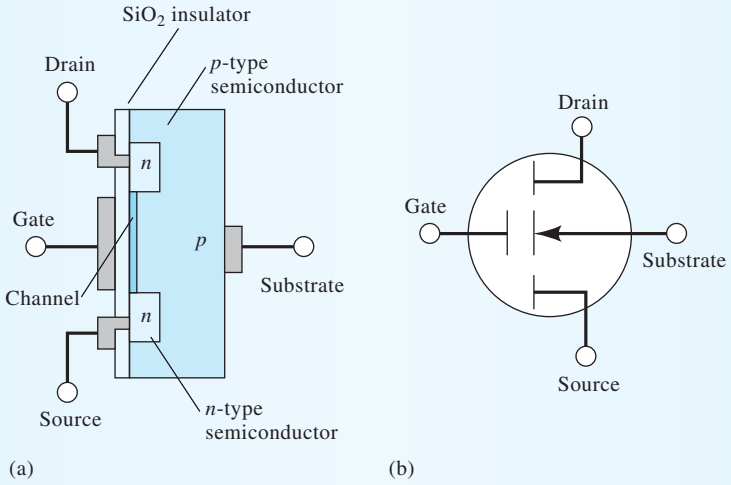

Figure 21F-2 A metal oxide field effect transistor (MOSFET). (a) Cross-sectional diagram. (b) Circuit symbol.

The **ion-sensitive field effect transistor**, or **ISFET**, is very similar in construction and function to an *n*-channel enhancement mode MOSFET. The ISFET differs only in that variation in the concentration of the ions of interest provides the variable gate voltage to control the conductivity of the channel. As shown in **Figure 21F-3**, instead of the usual metallic contact, the face of the ISFET is covered with an insulating layer of silicon nitride. The analytical solution, containing hydronium ions in this example, is in contact with this insulating layer and with a reference electrode. The surface of the gate insulator functions very much like the surface of a glass electrode. Protons from the hydronium ions in the test solution are absorbed by available microscopic sites on the silicon nitride. Any change in the hydronium ion concentration (or activity) of the solution results in a change in the concentration of adsorbed protons. The change in concentration of adsorbed protons then gives rise to a changing electrochemical potential between the gate and the source that in turn changes the conductivity of the channel of the ISFET. The conductivity of the channel can be monitored electronically to provide a signal that is proportional to the logarithm of the activity of hydronium ion in the solution. Note that the entire ISFET except the gate insulator is coated with a polymeric encapsulant to insulate all electrical connections from the analyte solution.

The ion-sensitive surface of the ISFET is naturally sensitive to pH changes, but the device may be modified so that it becomes sensitive to other species by coating the silicon nitride gate insulator with a polymer containing molecules that tend to form complexes with species other than hydronium ion. Furthermore, several ISFETs

(*continued*)

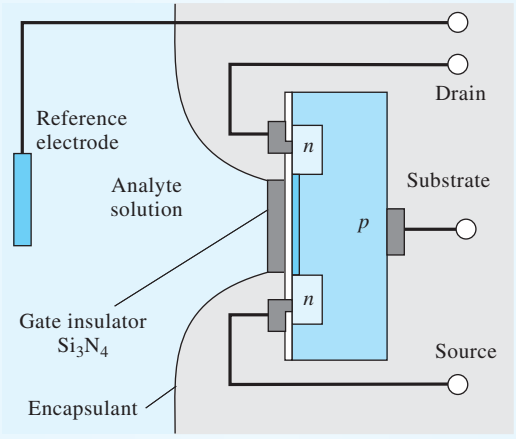

Figure 21F-3 An ion-sensitive field effect transistor (ISFET) for measuring pH.

may be fabricated on the same substrate so that multiple measurements may be made at the same time. All of the ISFETs may detect the same species to enhance accuracy and reliability, or each ISFET may be coated with a different polymer so that measurements of several different species may be made. Their small size (about 1 to 2 mm^2), rapid response time relative to glass electrodes, and ruggedness suggest that ISFETs may be the ion detectors of the future for many applications.

ISFETs do not require hydration before use and can be stored indefinitely in the dry state. Despite these many advantages, no ISFET-specific ion electrodes appeared on the market until the early 1990s, over 20 years after their invention. The reason for this delay is that manufacturers were unable to develop the technology of encapsulating the devices to give a product that did not exhibit drift and instability. Several companies now produce ISFETs for the determination of pH, but as of the writing of this text, these electrodes are certainly not as routinely used as the glass pH electrode.

21D-8 Gas-Sensing Probes

A **gas-sensing probe** is a galvanic *cell* whose potential is related to the concentration of a gas in a solution. In instrument brochures, these devices are often called gas-sensing electrodes, which is a misnomer as discussed later in this section.

Figure 21-15 illustrates the essential features of a potentiometric gas-sensing probe, which consists of a tube containing a reference electrode, a specific ion electrode, and an electrolyte solution. A thin, replaceable, gas-permeable membrane attached to one end of the tube serves as a barrier between the internal and analyte solutions. As can be seen from Figure 21-15, this device is a complete electrochemical cell and is more properly referred to as a probe rather than an electrode, a term that is frequently encountered in advertisements by instrument manufacturers. Gas-sensing probes are used widely for determining dissolved gases in water and other solvents.

Membrane Composition

A *microporous membrane* is fabricated from a hydrophobic polymer. As the name implies, the membrane is highly porous (the average pore size is less than 1 μm) and allows the free passage of gases; at the same time, the water-repellent polymer prevents

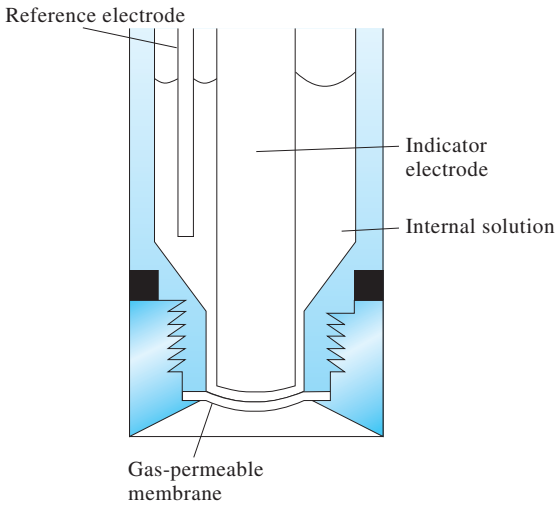

Figure 21-15 Diagram of a gas-sensing probe.

water and solute ions from entering the pores. The thickness of the membrane is about 0.1 mm.

The Mechanism of Response

Using carbon dioxide as an example, we can represent the transfer of gas to the internal solution in Figure 21-15 by the following set of equations:

$$\underset{\text{analyte solution}}{CO_2(aq)} \rightleftharpoons \underset{\text{membrane pores}}{CO_2(g)}$$

$$\underset{\text{membrane pores}}{CO_2(g)} \rightleftharpoons \underset{\text{internal solution}}{CO_2(aq)}$$

$$\underset{\text{internal solution}}{CO_2(aq)} + 2H_2O \rightleftharpoons \underset{\text{internal solution}}{HCO_3^-} + H_3O^+$$

The last equilibrium causes the pH of the internal surface film to change. This change is then detected by the internal glass/calomel electrode system. A description of the overall process is obtained by adding the equations for the three equilibria to give

$$\underset{\text{analyte solution}}{CO_2(aq)} + 2H_2O \rightleftharpoons \underset{\text{internal solution}}{HCO_3^-} + H_3O^+$$

The thermodynamic equilibrium constant K for this overall reaction is

$$K = \frac{(a_{H_3O^+})_{int}(a_{HCO_3^-})_{int}}{(a_{CO_2})_{ext}}$$

For a neutral species such as CO_2, $a_{CO_2} = [CO_2(aq)]$ so that

$$K = \frac{(a_{H_3O^+})_{int}(a_{HCO_3^-})_{int}}{[CO_2(aq)]_{ext}}$$

where $[CO_2(aq)]_{ext}$ is the molar concentration of the gas in the analyte solution. For the measured cell potential to vary linearly with the logarithm of the carbon dioxide concentration of the external solution, the hydrogen carbonate activity of the internal solution must be sufficiently large that it is not altered significantly by the carbon

dioxide entering from the external solution. Assuming then that $(a_{HCO_3^-})_{int}$ is constant, we can rearrange the previous equations to

$$\frac{(a_{H_3O^+})_{int}}{[CO_2(aq)]_{ext}} = \frac{K}{(a_{HCO_3^-})_{int}} = K_g$$

If we allow a_1 to be the hydrogen ion activity of the internal solution, we rearrange this equation to give

$$(a_{H_3O^+})_{int} = a_1 = K_g[CO_2(aq)]_{ext} \tag{21-15}$$

By substituting Equation 21-15 into Equation 21-10, we find

$$\begin{aligned} E_{ind} &= L + 0.0592 \log a_1 = L + 0.0592 \log K_g[CO_2(aq)]_{ext} \\ &= L + 0.0592 \log K_g + 0.0592 \log [CO_2(aq)]_{ext} \end{aligned}$$

Combining the two constant terms to give a new constant L' leads to

$$E_{ind} = L' + 0.0592 \log [CO_2(aq)]_{ext} \tag{21-16}$$

Finally, since

$$E_{cell} = E_{ind} - E_{ref}$$

then

$$E_{cell} = L' + 0.0592 \log [CO_2(aq)]_{ext} - E_{ref} \tag{21-17}$$

or

$$E_{cell} = L'' + 0.0592 \log [CO_2(aq)]_{ext}$$

where

$$L'' = L + 0.0592 \log K_g - E_{ref}$$

Thus, the potential between the glass electrode and the reference electrode in the internal solution is determined by the CO_2 concentration in the external solution. Note that no electrode comes in direct contact with the analyte solution. Therefore, these devices are gas-sensing cells, or probes, rather than gas-sensing electrodes. Nevertheless, they continue to be called electrodes is some literature and many advertising brochures.

Although sold as gas-sensing electrodes, these devices are complete electrochemical cells and should be called gas-sensing probes.

The only species that interfere are other dissolved gases that permeate the membrane and then affect the pH of the internal solution. The specificity of gas probes depends only on the permeability of the gas membrane. Gas-sensing cells for CO_2, NO_2, H_2S, SO_2, HF, HCN, and NH_3 are now available from commercial sources.

FEATURE 21-3

Point-of-Care Testing: Blood Gases, and Blood Electrolytes with Portable Instrumentation

Modern medicine relies heavily on analytical measurements for diagnosis and treatment in emergency rooms, operating rooms, and intensive care units. Prompt reporting of blood gas values, blood electrolyte concentrations, and other variables is especially important to physicians in these areas. In critical life-and-death situations, there is seldom sufficient time to transport blood samples to the clinical laboratory, perform required analyses, and transmit the results back to the bedside. In this feature, we describe an automated blood gas and electrolyte monitor, designed

specifically to analyze blood samples at the bedside.[7] The iSTAT® Portable Clinical Analyzer, shown in **Figure 21F-4**, is a handheld device that can measure a variety of important clinical analytes such as potassium, sodium, pH, pCO_2, pO_2, and hematocrit (see margin note). In addition, the computer-based analyzer calculates bicarbonate, total carbon dioxide, base excess, O_2 saturation, and hemoglobin in whole blood. In a study of the performance of the iSTAT system in a neonatal and pediatric intensive care unit, the results shown in the following table were obtained.[8] The results were judged to be sufficiently reliable and cost effective to substitute for similar measurements made in a traditional remote clinical laboratory.

Hematocrit (Hct) is the ratio of the volume of red blood cells to the total volume of a blood sample expressed as a percent.

Most of the analytes (pCO_2, Na^+, K^+, Ca^{2+}, and pH) are determined by potentiometric measurements using membrane-based ion-selective electrode technology. The hematocrit is measured by electrolytic conductivity detection and pO_2 is determined with a Clark voltammetric sensor (see Section 23C-4). Other results are calculated from these data.

The central component of the monitor is the single-use disposable electrochemical i-STAT sensor array, depicted in **Figure 21F-5**. The individual microfabricated sensor electrodes are located on chips along a narrow flow channel, as shown in the figure. Each new sensor array is automatically calibrated prior to the measurement step.

Analyte	Range	Precision, %RSD	Resolution
pO_2	5–800 mm Hg	3.5	1 mm Hg
pCO_2	5–130 mm Hg	1.5	0.1 mm Hg
Na^+	100–180 mmol/L	0.4	1 mmol/L
K^+	2.0–9.0 mmol/L	1.2	0.1 mmol/L
Ca^{2+}	0.25–2.50 mmol/L	1.1	0.01 mmol/L
pH	6.5–8.0	0.07	0.001

Figure 21F-4 Photo of iSTAT 1 portable clinical analyzer. (Courtesy of Abbott Point of Care, Inc., Princeton, NJ.)

(*continued*)

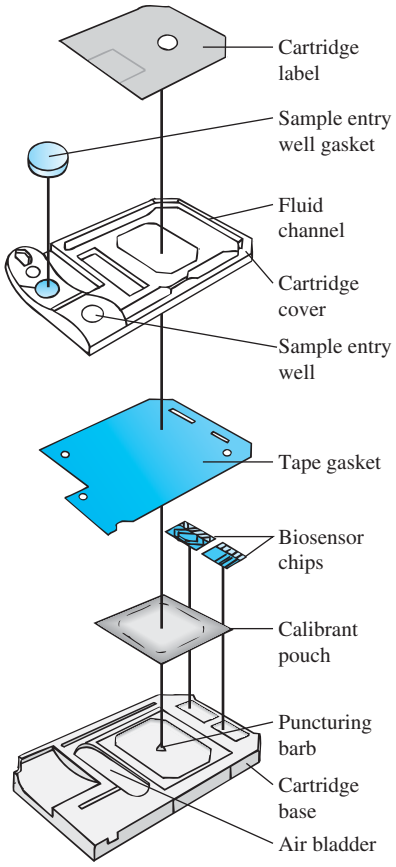

Figure 21F-5 Exploded view of iSTAT sensor array cartridge. (Abbott Point of Care, Prinston, NJ. Reprinted by permission.)

[7]Abbott Point of Care, Inc., Princeton, NJ 08540.

[8]J. N. Murthy, J. M. Hicks, and S. J. Soldin, *Clin. Biochem.*, **1997**, *30,* 385.

A blood sample withdrawn from the patient is deposited into the sample entry well, and the cartridge is inserted into the iSTAT analyzer. The calibrant pouch, which contains a standard buffered solution of the analytes, is punctured by the iSTAT analyzer and compressed to force the calibrant through the flow channel across the surface of the sensor array. When the calibration step is complete, the analyzer compresses the air bladder, which forces the blood sample through the flow channel to expel the calibrant solution to waste and bring the blood into contact with the sensor array. Electrochemical measurements are then made, results are calculated, and the data are presented on the liquid crystal display of the analyzer. The results are stored in the memory of the analyzer and may be transmitted wirelessly to the hospital laboratory data management system for permanent storage and retrieval.

This feature shows how modern ion-selective electrode technology coupled with computer control of the measurement process and data reporting can be used to provide rapid, essential measurements of analyte concentrations in whole blood at a patient's bedside.

21E INSTRUMENTS FOR MEASURING CELL POTENTIAL

Most cells containing a membrane electrode have very high electrical resistance (as much as 10^8 ohms or more). In order to measure potentials of such high-resistance circuits accurately, it is necessary that the voltmeter have an electrical resistance that is several orders of magnitude greater than the resistance of the cell being measured. If the meter resistance is too low, current is drawn from the cell, which has the effect of lowering its output potential, thus creating a negative *loading error*. When the meter and the cell have the same resistance a relative error of −50% results. When this ratio is 10, the error is about −9%. When it is 1000, the error is less than 0.1% relative.

FEATURE 21-4

The Loading Error in Potential Measurements

When we measure voltages in electrical circuits, the meter becomes a part of the circuit, perturbs the measurement process, and produces a **loading error** in the measurement. This situation is not unique to potential measurements. In fact, it is a basic example of a general limitation to any physical measurement. In other words, the process of measurement inevitably disturbs the system of interest so that the quantity actually measured differs from its value prior to the measurement. This type of error can never be completely eliminated, but it can often be reduced to an insignificant level.

The size of the loading error in potential measurements depends on the ratio of the internal resistance of the meter to the resistance of the circuit being studied. The percent relative loading error, E_r, associated with the measured potential, V_M, in Figure 21F-6 is given by

$$E_r = \frac{V_M - V_x}{V_x} \times 100\%$$

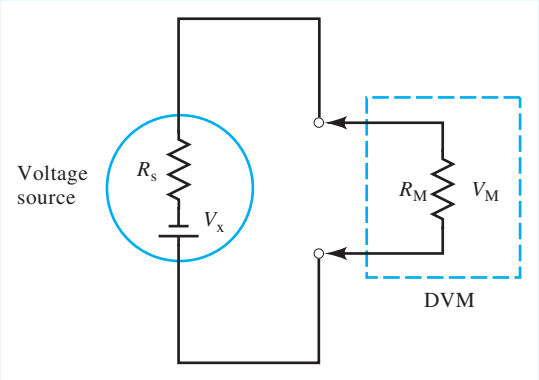

Figure 21F-6 Measurement of output V_x from a potential source with a digital voltmeter.

where V_x is the true voltage of the power source. The voltage drop across the resistance of the meter is given by

$$V_M = V_x \frac{R_M}{R_M + R_s}$$

Substituting this equation into the previous one and rearranging gives

$$E_r = \frac{-R_s}{R_M + R_s} \times 100\%$$

Note in this equation that the relative loading error becomes smaller as the meter resistance, R_M, becomes larger relative to the source resistance R_s. Table 21F-1 illustrates this effect. Digital voltmeters offer the great advantage of having huge internal resistances (10^{11} to 10^{12} ohms), thus avoiding loading errors except in circuits having load resistances greater than about 10^9 ohms.

TABLE 21F-1

Effect of Meter Resistance on the Accuracy of Potential Measurements

Meter Resistance R_M, Ω	Resistance of Source R_s, Ω	R_M/R_s	Relative Error, %
10	20	0.50	−67
50	20	2.5	−29
500	20	25	−3.8
1.0×10^3	20	50	−2.0
1.0×10^4	20	500	−0.2

Numerous high-resistance, direct-reading digital voltmeters with internal resistances of $> 10^{11}$ ohms are now on the market. These meters are commonly called **pH meters** but could more properly be referred to **as pIon meters** or **ion meters** since they are frequently used for the measurement of concentrations of other ions as well. A photo of a typical pH meter is shown in Figure 21-16.

Figure 21-16 Photo of a typical benchtop pH meter. (Courtesy of Mettler Toledo, Inc., Columbus, OH.)

FEATURE 21-5

Operational Amplifier Voltage Measurements

One of the most important developments in chemical instrumentation over the last three decades has been the advent of compact, inexpensive, versatile integrated-circuit amplifiers (op amps).[9] These devices allow us to make potential measurements on high-resistance cells, such as those that contain a glass electrode, without drawing appreciable current. Even a small current (10^{-7}–10^{-10} A) in a glass electrode produces a large error in the measured voltage due to loading (see Feature 21-4) and electrode polarization (see Chapter 22). One of the most important uses for op amps is to isolate voltage sources from their measurement circuits. The basic **voltage follower**, which permits this type of measurement, is shown in **Figure 21F-7a**. This circuit has two important characteristics. The output voltage, E_{out}, is equal to the input voltage, E_{in}, and the input current, I_i, is essentially zero (10^{-7}–10^{-10} A).

A practical application of this circuit is in measuring cell potentials. We simply connect the cell to the op amp input, as shown in **Figure 21F-7b**, and we connect the output of the op amp to a digital voltmeter to measure the voltage. Modern op amps are nearly ideal voltage-measurement devices and are incorporated in most ion meters and pH meters to monitor high-resistance indicator electrodes with minimal error.

Modern ion meters are digital, and some are capable of a precision on the order of 0.001 to 0.005 pH unit. Seldom is it possible to measure pH with a comparable degree of *accuracy*. Inaccuracies of ±0.02 to ±0.03 pH unit are typical.

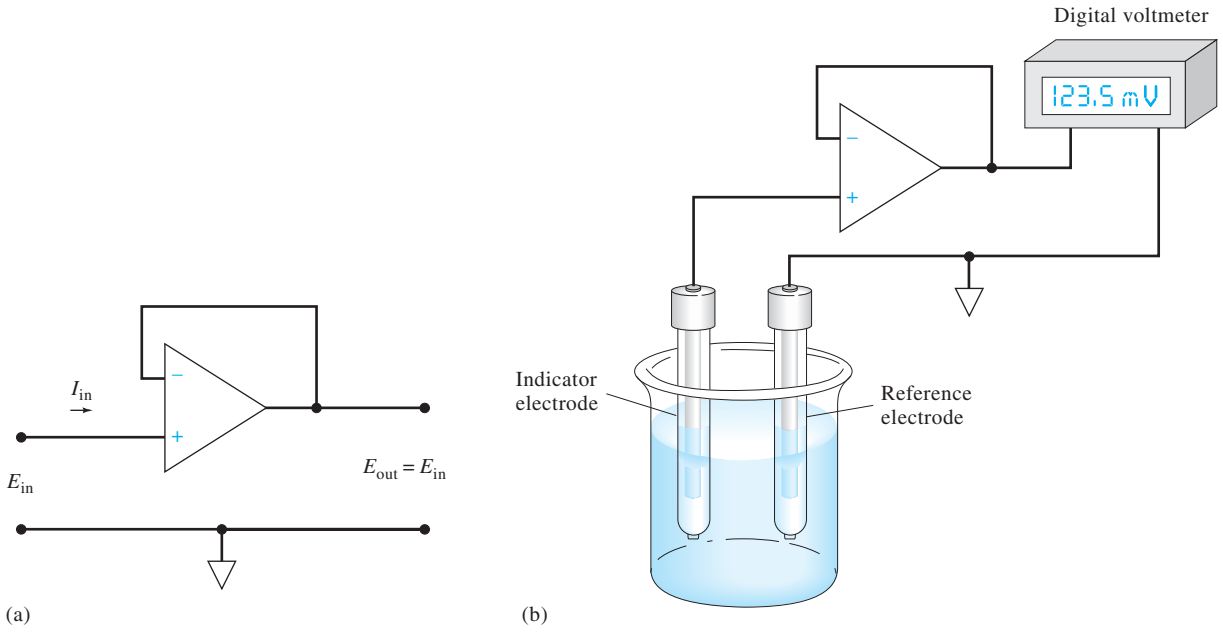

Figure 21F-7 (a) A voltage-follower operational amplifier. (b) Typical arrangement for potentiometric measurements with a membrane electrode.

[9]For a detailed description of op amp circuits, see H. V. Malmstadt, C. G. Enke, and S. R. Crouch, *Microcomputers and Electronic Instrumentation: Making the Right Connections*, Ch. 5, Washington, DC: American Chemical Society, 1994.

21F DIRECT POTENTIOMETRY

Direct potentiometric measurements provide a rapid and convenient method for determining the activity of a variety of cations and anions. The technique requires only a comparison of the potential developed in a cell containing the indicator electrode in the analyte solution with its potential when immersed in one or more standard solutions of known analyte concentration. If the response of the electrode is specific for the analyte, as it often is, no preliminary separation steps are required. Direct potentiometric measurements are also readily adapted to applications requiring continuous and automatic recording of analytical data.

21F-1 Equations Governing Direct Potentiometry

The sign convention for potentiometry is consistent with the convention described in Chapter 18 for standard electrode potential. In this convention, the indicator electrode is always treated as the right-hand electrode and the reference electrode as the left-hand electrode. For direct potentiometric measurements, the potential of a cell can then be expressed in terms of the potentials developed by the indicator electrode, the reference electrode, and a junction potential, as described in Section 21A:

$$E_{cell} = E_{ind} - E_{ref} + E_j \tag{21-18}$$

In Section 21D, we described the response of various types of indicator electrodes to analyte activities. For the cation X^{n+} at 25°C, the electrode response takes the general *Nernstian* form

$$E_{ind} = L - \frac{0.0592}{n}\,pX = L + \frac{0.0592}{n}\log a_X \tag{21-19}$$

where L is a constant and a_X is the activity of the cation. For metallic indicator electrodes, L is usually the standard electrode potential; for membrane electrodes, L is the summation of several constants, including the time-dependent asymmetry potential of uncertain magnitude.

Substitution of Equation 21-19 into Equation 21-18 yields with rearrangement

$$pX = -\log a_X = -\left[\frac{E_{cell} - (E_j - E_{ref} + L)}{0.0592/n}\right] \tag{21-20}$$

The constant terms in parentheses can be combined to give a new constant K.

$$pX = -\log a_X = -\frac{(E_{cell} - K)}{0.0592/n} = -\frac{n(E_{cell} - K)}{0.0592} \tag{21-21}$$

For an anion A^{n-}, the sign of Equation 21-21 is reversed:

$$pA = \frac{(E_{cell} - K)}{0.0592/n} = \frac{n(E_{cell} - K)}{0.0592} \tag{21-22}$$

All direct potentiometric methods are based on Equation 21-21 or 21-22. The difference in sign in the two equations has a subtle but important consequence in the

way that ion-selective electrodes are connected to pH meters and pIon meters. When the two equations are solved for E_{cell}, we find that for cations

$$E_{cell} = K - \frac{0.0592}{n} \text{pX} \tag{21-23}$$

and for anions

$$E_{cell} = K + \frac{0.0592}{n} \text{pA} \tag{21-24}$$

Equation 21-23 shows that, for a cation-selective electrode, an increase in pX results in a *decrease* in E_{cell}. Thus, when a high-resistance voltmeter is connected to the cell in the usual way, with the indicator electrode attached to the positive terminal, the meter reading decreases as pX increases. Another way of saying this is that, as the concentration (and activity) of the cation X increases, $\text{pX} = -\log [\text{X}]$ decreases, and E_{cell} increases. Notice that the sense of these changes is exactly the opposite of our sense of how pH meter readings change with increasing hydronium ion concentration. To eliminate this reversal from our sense of the pH scale, instrument manufacturers generally reverse the leads so that cation-sensitive electrodes such as glass electrodes are connected to the negative terminal of the voltage measuring device. Meter readings then increase with increases of pX, and as a result, they decrease with increasing concentration of the cation.

Anion-selective electrodes, on the other hand, are connected to the positive terminal of the meter so that increases in pA also yield larger readings. This sign-reversal conundrum is often confusing so that it is always a good idea to look carefully at the consequences of Equations 21-23 and 21-24 rationalize the output of the instrument with changes in concentration of the analyte anion or cation and corresponding changes in pX or pA.

21F-2 The Electrode-Calibration Method

The electrode-calibration method is also referred to as the method of external standards, which is described in some detail in Section 8D-2.

As we have seen from our discussions in Section 21D, the constant K in Equations 21-21 and 21-22 is made up of several constants, at least one of which, the junction potential, cannot be measured directly or calculated from theory without assumptions. Thus, before these equations can be used for the determination of pX or pA, K must be evaluated experimentally with a standard solution of the analyte.

In the electrode-calibration method, K in Equations 21-21 and 21-22 is determined by measuring E_{cell} for one or more standard solutions of known pX or pA. The assumption is then made that K is unchanged when the standard is replaced by the analyte solution. The calibration is normally performed at the time pX or pA for the unknown is determined. With membrane electrodes, recalibration may be required if measurements extend over several hours because of slow changes in the asymmetry potential.

The electrode-calibration method offers the advantages of simplicity, speed, and applicability to the continuous monitoring of pX or pA. It suffers, however, from a somewhat limited accuracy because of uncertainties in junction potentials.

Inherent Error in the Electrode-Calibration Procedure

A serious disadvantage of the electrode-calibration method is the inherent error that results from the assumption that K in Equations 21-21 and 21-22 remains constant after calibration. This assumption can seldom, if ever, be exactly true because the

electrolyte composition of the unknown almost inevitably differs from that of the solution used for calibration. The junction potential term contained in K varies slightly as a consequence, even when a salt bridge is used. This error is frequently on the order of 1 mV or more. Unfortunately, because of the nature of the potential/activity relationship, such an uncertainty has an amplified effect on the inherent accuracy of the analysis.

The magnitude of the error in analyte concentration can be estimated by differentiating Equation 21-21 while assuming E_{cell} constant.

$$-\log_{10} e \frac{da_x}{a_x} = -0.434 \frac{da_x}{a_x} = -\frac{dK}{0.0592/n}$$

$$\frac{da_x}{a_x} = \frac{ndK}{0.0257} = 38.9\, ndK$$

When we replace da_x and dK with finite increments and multiply both sides of the equation by 100%, we obtain

$$\text{percent relative error} = \frac{\Delta a_x}{a_x} \times 100\% = 38.9 n\Delta K \times 100\%$$
$$= 3.89 \times 10^3 n\Delta K\% \approx 4000 n\Delta K\%$$

The quantity $\Delta a_x/a_x$ is the relative error in a_x associated with an absolute uncertainty ΔK in K. If, for example, ΔK is ± 0.001 V, a relative error in activity of about $\pm 4n\%$ can be expected. *It is important to appreciate that this error is characteristic of all measurements involving cells that contain a salt bridge and that this error cannot be eliminated by even the most careful measurements of cell potentials or the most sensitive and precise measuring devices.*

Activity versus Concentration

Electrode response is related to analyte activity rather than analyte concentration. We are usually interested in concentration, however, and the determination of this quantity from a potentiometric measurement requires activity coefficient data. Activity coefficients are seldom available because the ionic strength of the solution either is unknown or else is so large that the Debye-Hückel equation is not applicable.

The difference between activity and concentration is illustrated by **Figure 21-17** in which the response of a calcium ion electrode is plotted against a logarithmic

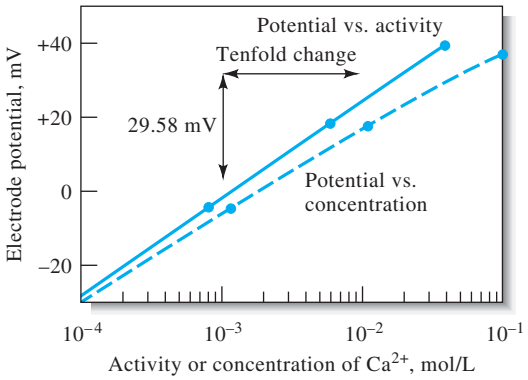

Figure 21-17 Response of a liquid-membrane electrode to variations in the concentration and activity of calcium ion. (Courtesy of Thermo Electron Corp., Beverly, MA.)

function of calcium chloride concentration. The nonlinearity is due to the increase in ionic strength—and the consequent decrease in the activity of calcium ion—with increasing electrolyte concentration. The upper curve is obtained when these concentrations are converted to activities. This straight line has the theoretical slope of 0.0296 (0.0592/2).

Activity coefficients for singly charged species are less affected by changes in ionic strength than are the coefficients for ions with multiple charges. Thus, the effect shown in Figure 21-17 is less pronounced for electrodes that respond to H^+, Na^+, and other univalent ions.

Many chemical reactions of physiological importance depend on the activity of metal ions rather than their concentration.

In potentiometric pH measurements, the pH of the standard buffer used for calibration is generally based on the activity of hydrogen ions. Therefore, the results are also on an activity scale. If the unknown sample has a high ionic strength, the hydrogen ion *concentration* will differ appreciably from the activity measured.

An obvious way to convert potentiometric measurements from activity to concentration is to make use of an empirical calibration curve, such as the lower plot in Figure 21-17. For this approach to be successful, it is necessary to make the ionic composition of the standards essentially the same as that of the analyte solution. Matching the ionic strength of standards to that of samples is often difficult, particularly for samples that are chemically complex.

A total ionic strength adjustment buffer (TISAB) is used to control the ionic strength and the pH of samples and standards, in ion-selective electrode measurements.

Where electrolyte concentrations are not too great, it is often useful to swamp both samples and standards with a measured excess of an inert electrolyte. The added effect of the electrolyte from the sample matrix becomes negligible under these circumstances, and the empirical calibration curve yields results in terms of concentration. This approach has been used, for example, in the potentiometric determination of fluoride ion in drinking water. Both samples and standards are diluted with a solution that contains sodium chloride, an acetate buffer, and a citrate buffer; the diluent is sufficiently concentrated so that the samples and standards have essentially identical ionic strengths. This method provides a rapid means for measuring fluoride concentrations in the part-per-million range with an accuracy of about 5% relative.

21F-3 The Standard Addition Method

The standard addition method (see Section 8D-3) involves determining the potential of the electrode system before and after a measured volume of a standard has been added to a known volume of the analyte solution. Multiple additions can also be made. Often, an excess of an electrolyte is introduced into the analyte solution to prevent any major shift in ionic strength that might accompany the addition of standard. It is also necessary to assume that the junction potential remains constant during the two measurements.

EXAMPLE 21-1

A cell consisting of a saturated calomel electrode and a lead ion electrode developed a potential of −0.4706 V when immersed in 50.00 mL of a sample. A 5.00-mL addition of standard 0.02000 M lead solution caused the potential to shift to −0.4490 V. Calculate the molar concentration of lead in the sample.

Solution

We shall assume that the activity of Pb^{2+} is approximately equal to $[Pb^{2+}]$ and apply Equation 21-21. Thus,

$$pPb = -\log [Pb^{2+}] = -\frac{E'_{cell} - K}{0.0592/2}$$

where E'_{cell} is the initial measured potential (−0.4706 V).

After the standard solution is added, the potential becomes E''_{cell} (−0.4490 V), and

$$-\log \frac{50.00 \times [Pb^{2+}] + 5.00 \times 0.0200}{50.00 + 5.00} = -\frac{E''_{cell} - K}{0.0592/2}$$

$$-\log(0.9091[Pb^{2+}] + 1.818 \times 10^{-3}) = -\frac{E''_{cell} - K}{0.0592/2}$$

Subtracting this equation from the first leads to

$$-\log \frac{[Pb^{2+}]}{0.09091[Pb^{2+}] + 1.818 \times 10^{-3}} = \frac{2(E''_{cell} - E'_{cell})}{0.0592}$$

$$= \frac{2[-0.4490 - (-0.4706)]}{0.0592}$$

$$= 0.7297$$

$$\frac{[Pb^{2+}]}{0.09091[Pb^{2+}] + 1.818 \times 10^{-3}} = \text{antilog}(-0.7297) = 0.1863$$

$$[Pb^{2+}] = 3.45 \times 10^{-4}\ M$$

21F-4 Potentiometric pH Measurement with the Glass Electrode[10]

The glass electrode is unquestionably the most important indicator electrode for hydrogen ion. It is convenient to use and subject to few of the interferences that affect other pH-sensing electrodes.

The glass/calomel electrode system is a remarkably versatile tool for the measurement of pH under many conditions. It can be used without interference in solutions containing strong oxidants, strong reductants, proteins, and gases; the pH of viscous or even semisolid fluids can be determined. Electrodes for special applications are available. Included among these electrodes are small ones for pH measurements in one drop (or less) of solution, in a tooth cavity, or in the sweat on the skin; microelectrodes that permit the measurement of pH inside a living cell; rugged electrodes for insertion in a flowing liquid stream to provide a continuous monitoring of pH; and small electrodes that can be swallowed to measure the acidity of the stomach contents (the calomel electrode is kept in the mouth).

Errors Affecting pH Measurements

The ubiquity of the pH meter and the general applicability of the glass electrode tend to lull the chemist into the attitude that any measurement obtained with such

[10]For a detailed discussion of potentiometric pH measurements, see R. G. Bates, *Determination of pH*, 2nd ed., New York: Wiley, 1973.

equipment is surely correct. The reader must be alert to the fact that there are distinct limitations to the electrode, some of which were discussed in earlier sections:

1. *The alkaline error*. The ordinary glass electrode becomes somewhat sensitive to alkali metal ions and gives low readings at pH values greater than 9.
2. *The acid error*. Values registered by the glass electrode tend to be somewhat high when the pH is less than about 0.5.
3. *Dehydration*. Dehydration may cause erratic electrode performance.
4. *Errors in low ionic strength solutions*. It has been found that significant errors (as much as 1 or 2 pH units) may occur when the pH of samples of low ionic strength, such as lake or stream water, is measured with a glass/calomel electrode system.[11] The prime source of such errors has been shown to be nonreproducible junction potentials, which apparently result from partial clogging of the fritted plug or porous fiber that is used to restrict the flow of liquid from the salt bridge into the analyte solution. To overcome this problem, free diffusion junctions of various types have been designed, one of which is produced commercially.
5. *Variation in junction potential*. A fundamental source of uncertainty for which a correction cannot be applied is the junction-potential variation resulting from differences in the composition of the standard and the unknown solution.
6. *Error in the pH of the standard buffer*. Any inaccuracies in the preparation of the buffer used for calibration or any changes in its composition during storage cause an error in subsequent pH measurements. The action of bacteria on organic buffer components is a common cause for deterioration.

Particular care must be taken in measuring the pH of approximately neutral unbuffered solutions, such as samples from lakes and streams.

The Operational Definition of pH

Perhaps the most common analytical instrumental technique is the measurement of pH.

The utility of pH as a measure of the acidity and alkalinity of aqueous media, the wide availability of commercial glass electrodes, and the relatively recent proliferation of inexpensive solid-state pH meters have made the potentiometric measurement of pH perhaps the most common analytical technique in all of science. It is thus extremely important that pH be defined in a manner that is easily duplicated at various times and in various laboratories throughout the world. To meet this requirement, it is necessary to define pH in operational terms, that is, by the way the measurement is made. Only then will the pH measured by one worker be the same as that by another.

By definition, pH is what you measure with a glass electrode and a pH meter. It is approximately equal to the theoretical definition of $pH = -\log a_{H^+}$.

The operational definition of pH is endorsed by the National Institute of Standards and Technology (NIST), similar organizations in other countries, and the IUPAC. It is based on the direct calibration of the meter with carefully prescribed standard buffers followed by potentiometric determination of the pH of unknown solutions.

Consider, for example, one of the glass/reference electrode pairs of Figure 21-7. When these electrodes are immersed in a standard buffer, Equation 21-21 applies, and we can write

$$pH_S = \frac{E_S - K}{0.0592}$$

[11] See W. Davison and C. Woof, *Anal. Chem.*, **1985**, *57*, 2567, **DOI**: 10.1021/ac00290a031; T. R. Harbinson and W. Davison, *Anal. Chem.*, **1987**, *59*, 2450, **DOI**: 10.1021/ac00147a002.

where E_S is the cell potential when the electrodes are immersed in the buffer. Similarly, if the cell potential is E_U when the electrodes are immersed in a solution of unknown pH, we have

$$pH_U = -\frac{E_U - K}{0.0592}$$

By subtracting the first equation from the second and solving for pH_U, we find

$$pH_U = pH_S - \frac{(E_U - E_S)}{0.0592} \qquad (21\text{-}25)$$

Equation 21-25 has been adopted throughout the world as the *operational definition of pH*.

An operational definition of a quantity defines the quantity in terms of how it is measured.

Workers at the NIST and elsewhere have used cells without liquid junctions to study primary-standard buffers extensively. Some of the properties of these buffers are discussed in detail elsewhere.[12] Note that the NIST buffers are described by their molal concentrations (mol solute/kg solvent) for accuracy and precision of preparation. For general use, the buffers can be prepared from relatively inexpensive laboratory reagents; for careful work, however, certified buffers can be purchased from the NIST.

It should be emphasized that the strength of the operational definition of pH is that it provides a coherent scale for the determination of acidity or alkalinity. However, measured pH values cannot be expected to yield a detailed picture of solution composition that is entirely consistent with solution theory. This uncertainty stems from our fundamental inability to measure single ion activities, that is, the operational definition of pH does not yield the exact pH as defined by the equation

$$pH = -\log \gamma_{H^+}[H^+]$$

21G POTENTIOMETRIC TITRATIONS

In a **potentiometric titration**, we measure the potential of a suitable indicator electrode as a function of titrant volume. The information provided by a potentiometric titration is different from the data obtained in a direct potentiometric measurement. For example, the direct measurement of 0.100 M solutions of hydrochloric and acetic acids yields two substantially different hydrogen ion concentrations because the weak acid is only partially dissociated. In contrast, the potentiometric titration of equal volumes of the two acids would require the same amount of standard base because both solutes have the same number of titratable protons.

Potentiometric titrations provide data that are more reliable than data from titrations that use chemical indicators and are particularly useful with colored or turbid solutions and for detecting the presence of unsuspected species. Potentiometric titrations have been automated in a variety of different ways, and commercial titrators are available from a number of manufacturers. Manual potentiometric titrations, on the other hand, suffer from the disadvantage of being more time consuming than those involving indicators.

[12]R. G. Bates, *Determination of pH*, 2nd ed., Ch. 4., New York: Wiley, 1973.

Automatic *titrators* for carrying out potentiometric titrations are available from several manufacturers. The operator of the instrument simply adds the sample to the titration vessel and pushes a button to initiate, the titration. The instrument adds titrant, records the potential versus volume data, and analyzes the data to determine the concentration of the unknown solution. A photo of such a device is shown on the opening page of Chapter 14.

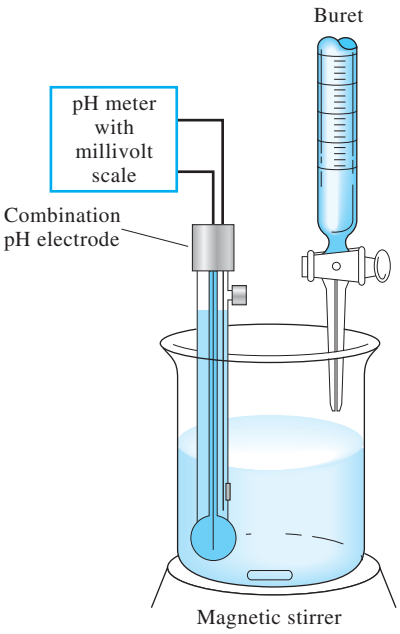

Figure 21-18 Apparatus for a potentiometric titration.

Potentiometric titrations offer additional advantages over direct potentiometry. Because the measurement is based on the titrant volume that causes a rapid *change* in potential near the equivalence point, potentiometric titrations are not dependent on measuring absolute values of E_{cell}. This characteristic makes the titration relatively free from junction potential uncertainties because the junction potential remains approximately constant during the titration. Titration results, instead, depend most heavily on having a titrant of accurately known concentration. The potentiometric instrument merely signals the end point and thus behaves in an identical fashion to a chemical indicator. Problems with electrodes fouling or not displaying Nernstian response are not nearly as serious when the electrode system is used to monitor a titration. Likewise, the reference electrode potential does not need to be known accurately in a potentiometric titration. Another advantage of a titration is that the result is analyte concentration even though the electrode responds to activity. For this reason, ionic strength effects are not important in the titration procedure.

Figure 21-18 illustrate a typical apparatus for performing a manual potentiometric titration. The operator measures and records the cell potential (in units of millivolts or pH, as appropriate) after each addition of reagent. The titrant is added in large increments early in the titration and in smaller and smaller increments as the end point is approached (as indicated by larger changes in cell potential per unit volume).

21G-1 Detecting the End Point

Several methods can be used to determine the end point of a potentiometric titration. In the most straightforward approach, a direct plot or other recording is made of cell potential as a function of reagent volume. In **Figure 21-19a**, we plot the data of **Table 21-4** and visually estimate the inflection point in the steeply rising portion of the curve and take it as the end point.

TABLE 21-4

Potentiometric Titration Data for 2.433 mmol of Chloride with 0.1000 M Silver Nitrate

Volume $AgNO_3$, mL	E vs. SCE, V	$\Delta E/\Delta V$, V/mL	$\Delta^2 E/\Delta V^2$, V^2/mL^2
5.00	0.062		
15.00	0.085	0.002	
20.00	0.107	0.004	
22.00	0.123	0.008	
23.00	0.138	0.015	
23.50	0.146	0.016	
23.80	0.161	0.050	
24.00	0.174	0.065	
24.10	0.183	0.09	
24.20	0.194	0.11	2.8
24.30	0.233	0.39	4.4
24.40	0.316	0.83	−5.9
24.50	0.340	0.24	−1.3
24.60	0.351	0.11	−0.4
24.70	0.358	0.07	
25.00	0.373	0.050	
25.50	0.385	0.024	
26.00	0.396	0.022	
28.00	0.426	0.015	

A second approach to end-point detection is to calculate the change in potential per unit volume of titrant ($\Delta E/\Delta V$), that is, we estimate the numerical first derivative of the titration curve. A plot of the first derivative data (see Table 21-4, column 3) as a function of the average volume V produces a curve with a maximum that corresponds to the point of inflection, as shown in **Figure 21-19b**. Alternatively, this ratio can be evaluated during the titration and recorded rather than the potential. From the plot, it can be seen that the maximum occurs at a titrant volume of about 24.30 mL. If the titration curve is symmetrical, the point of maximum slope coincides with the equivalence point. For the asymmetrical titration curves that are observed when the titrant and analyte half-reactions involve different numbers of electrons, a small titration error occurs if the point of maximum slope is used.

Figure 21-19c shows that the second derivative for the data changes sign at the point of inflection. This change is used as the analytical signal in some automatic titrators. The point at which the second derivative crosses zero is the inflection point, which is taken as the end point of the titration, and this point can be located quite precisely.

All of the methods of end-point detection discussed in the previous paragraphs are based on the assumption that the titration curve is symmetric about the equivalence point and that the inflection in the curve corresponds to this point. This assumption is valid if the titrant and analyte react in a 1:1 ratio and if the electrode reaction is reversible. Many oxidation/reduction reactions, such as the reaction of iron(II) with permanganate, do not occur in equimolar fashion. Even so, such titration curves are often so steep at the end point that very little error is introduced by assuming that the curves are symmetrical.

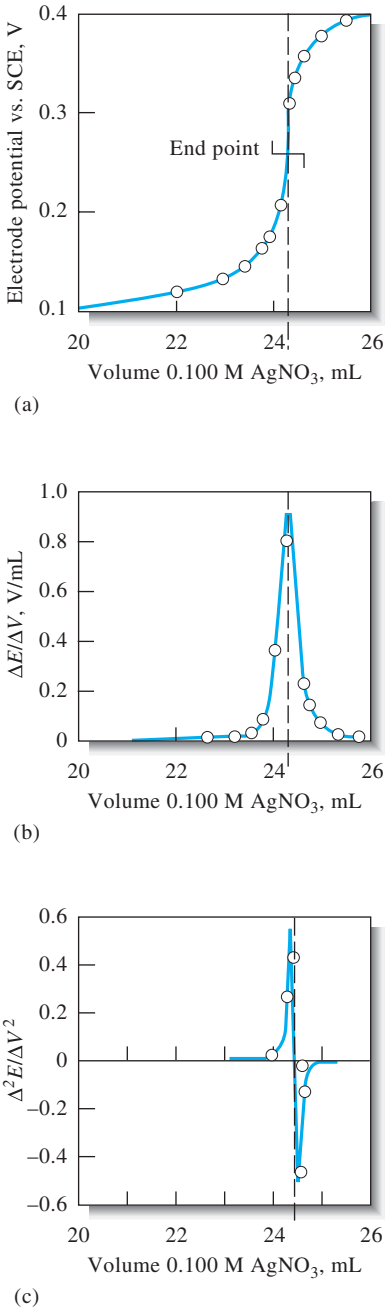

Figure 21-19 Titration of 2.433 mmol of chloride ion with 0.1000 M silver nitrate. (a) Titration curve. (b) First-derivative curve. (c) Second-derivative curve.

21G-2 Neutralization Titrations

Experimental neutralization curves closely approximate the theoretical curves described in Chapters 14 and 15. Usually, the experimental curves are somewhat displaced from the theoretical curves along the pH axis because concentrations rather than activities are used in their derivation. This displacement has little effect on determining end points, and so potentiometric neutralization titrations are quite useful for analyzing mixtures of acids or polyprotic acids. The same is true of bases.

Determining Dissociation Constants

An approximate numerical value for the dissociation constant of a weak acid or base can be estimated from potentiometric titration curves. This quantity can be computed from the pH at any point along the curve, but a very convenient point is the half-titration point. At this point on the curve,

$$[HA] \approx [A^-]$$

Therefore,

$$K_a = \frac{[H_3O^+]\cancel{[A^-]}}{\cancel{[HA]}} = [H_3O^+]$$

$$pK_a = pH$$

It is important to note the use of concentrations instead of activities may cause the value for K_a to differ from its published value by a factor of 2 or more. A more correct form of the dissociation constant for HA is

$$K_a = \frac{a_{H_3O^+} a_{A^-}}{a_{HA}} = \frac{a_{H_3O^+} \gamma_{A^-} [A^-]}{\gamma_{HA} [HA]} \qquad (21\text{-}26)$$

$$K_a = \frac{a_{H_3O^+} \gamma_{A^-}}{\gamma_{HA}}$$

Since the glass electrode provides a good approximation of $a_{H_3O^+}$, the measured value of K_a differs from the thermodynamic value by the ratio of the two activity coefficients. The activity coefficient in the denominator of Equation 21-26 doesn't change significantly as ionic strength increases because HA is a neutral species. The activity coefficient for A^-, on the other hand, decreases as the electrolyte concentration increases. This decrease means that the observed hydrogen ion activity must be numerically larger than the thermodynamic dissociation constant.

EXAMPLE 21-2

In order to determine K_1 and K_2 for H_3PO_4 from titration data, careful pH measurements are made after 0.5 and 1.5 mol of base is added for each mole of acid. It is then assumed that the hydrogen ion activities computed from these data are identical to the desired dissociation constants. Calculate the relative error incurred by the assumption if the ionic strength is 0.1 at the time of each measurement. (From Appendix 3, K_1 and K_2 for H_3PO_4 are 7.11×10^{-3} and 6.34×10^{-8}, respectively.)

Solution

If we rearrange Equation 21-26, we find that

$$K_a(\text{exptl}) = a_{H_3O^+} = K\left(\frac{\gamma_{HA}}{\gamma_{A^-}}\right)$$

The activity coefficient for H_3PO_4 is approximately equal to 1 since the free acid has no charge. In Table 10-2, we find that the activity coefficient for $H_2PO_4^-$ is 0.77 and that for HPO_4^{2-} is 0.35. When we substitute these values into the equations for K_1 and K_2, we find that

$$K_1(\text{exptl}) = 7.11 \times 10^{-3}\left(\frac{1.00}{0.77}\right) = 9.23 \times 10^{-3}$$

$$\text{error} = \frac{9.23 \times 10^{-3} - 7.11 \times 10^{-3}}{7.11 \times 10^{-3}} \times 100\% = 30\%$$

$$K_2(\text{exptl}) = 6.34 \times 10^{-8}\left(\frac{0.77}{0.35}\right) = 1.395 \times 10^{-7}$$

$$\text{error} = \frac{1.395 \times 10^{-7} - 6.34 \times 10^{-8}}{6.34 \times 10^{-8}} \times 100\% = 120\%$$

It is possible to identify an unknown pure acid by performing a single titration to determine its equivalent mass (molar mass if the acid is monoprotic) and its dissociation constant.

21G-3 Oxidation/Reduction Titrations

An inert indicator electrode constructed of platinum is usually used to detect end points in oxidation/reduction titrations. Occasionally, other inert metals, such a silver, palladium, gold, and mercury, are used instead. Titration curves similar to those constructed in Section 19D are usually obtained, although they may be displaced along the potential (vertical) axis as a consequence of the high ionic strengths. End points are determined by the methods described earlier in this chapter.

21H POTENTIOMETRIC DETERMINATION OF EQUILIBRIUM CONSTANTS

Numerical values for solubility-product constants, dissociation constants, and formation constants are conveniently evaluated through the measurement of cell potentials. One important virtue of this technique is that the measurement can be made without appreciably affecting any equilibria that may be present in the solution. For example, the potential of a silver electrode in a solution containing silver ion, cyanide ion, and the complex formed between them depends on the activities of the three species. It is possible to measure this potential with negligible current. Since the activities of the participants are not altered during the measurement, the position of the equilibrium

$$Ag^+ + 2CN^- \rightleftharpoons Ag(CN)_2^-$$

is likewise undisturbed.

EXAMPLE 21-3

Calculate the formation constant K_f for $Ag(CN)_2^-$:

$$Ag^+ + 2CN^- \rightleftharpoons Ag(CN)_2^-$$

if the cell

$$SCE \,\|\, Ag(CN)_2^- (7.50 \times 10^{-3}\ M), CN^- (0.0250\ M) \,|\, Ag$$

develops a potential of −0.625 V.

Solution

Proceeding as in the earlier examples, we have

$$Ag^+ + e^- \rightleftharpoons Ag(s) \qquad E^0 = +0.799\ V$$

$$-0.625 = E_{right} - E_{left} = E_{Ag^+} - 0.244$$

$$E_{Ag^+} = -0.625 + 0.244 = -0.381\ V$$

(*continued*)

We then apply the Nernst equation for the silver electrode to find that

$$-0.381 = 0.799 - \frac{0.0592}{1}\log\frac{1}{[Ag^+]}$$

$$\log[Ag^+] = \frac{-0.381 - 0.799}{0.0592} = -19.93$$

$$[Ag^+] = 1.2 \times 10^{-20}$$

$$K_f = \frac{[Ag(CN)_2^-]}{[Ag^+][CN^-]^2} = \frac{7.50 \times 10^{-3}}{(1.2 \times 10^{-20})(2.5 \times 10^{-2})^2}$$

$$= 1.0 \times 10^{21} \approx 1 \times 10^{21}$$

In theory, any electrode system in which hydrogen ions are participants can be used to evaluate dissociation constants for acids and bases.

EXAMPLE 21-4

Calculate the dissociation constant K_{HP} for the weak acid HP if the cell

$$SCE \,\|\, HP(0.010\ M), NaP(0.040\ M) \,|\, Pt, H_2\ (1.00\ atm)$$

develops a potential of −0.591 V.

Solution

The diagram for this cell indicates that the saturated calomel electrode is the left-hand electrode. Thus,

$$E_{cell} = E_{right} - E_{left} = E_{right} - 0.244 = -0.591\ V$$

$$E_{right} = -0.591 + 0.244 = -0.347\ V$$

We then apply the Nernst equation for the hydrogen electrode to find that

$$-0.347 = 0.000 - \frac{0.0592}{2}\log\frac{1.00}{[H_3O^+]^2}$$

$$= 0.000 + \frac{2 \times 0.0592}{2}\log[H_3O^+]$$

$$\log[H_3O^+] = \frac{-0.347 - 0.000}{0.0592} = -5.86$$

$$[H_3O^+] = 1.38 \times 10^{-6}$$

By substituting this value of the hydronium ion concentration as well as the concentrations of the weak acid and its conjugate base into the dissociation constant expression, we obtain

$$K_{HP} = \frac{[H_3O^+][P^-]}{HP} = \frac{(1.38 \times 10^{-6})(0.040)}{0.010} = 5.5 \times 10^{-6}$$

WEB WORKS

Use a Web search engine, such as Google, to find sites dealing with potentiometric titrators. This search should turn up such companies as Spectralab, Analyticon, Fox Scientific, Metrohm, Mettler-Toledo, and Thermo Orion. Set your browser to one or two of these and explore the types of titrators that are commercially available. At the sites of two different manufacturers, find application notes or bulletins for determining two analytes by potentiometric titration. For each, list the analyte, the instruments and the reagents that are necessary for the determination, and the expected accuracy and precision of the results. Describe the detailed chemistry behind each determination and the experimental procedure.

QUESTIONS AND PROBLEMS

21-1. Briefly describe or define
- *(a) indicator electrode.
- (b) reference electrode.
- *(c) electrode of the first kind.
- (d) electrode of the second kind.

21-2. Briefly describe or define
- *(a) liquid-junction potential.
- (b) boundary potential.
- *(c) asymmetry potential.
- (d) combination electrode.

***21-3.** You need to choose between determining an analyte by measuring an electrode potential or by performing a titration. Explain which you would choose if you needed to know
- (a) the absolute amount of the analyte to a few parts per thousand.
- (b) the activity of the analyte.

21-4. What is meant by Nernstian behavior in an indicator electrode?

***21-5.** Describe the source of pH dependence in a glass membrane electrode.

21-6. Why is it necessary for the glass in the membrane of a pH-sensitive electrode to be appreciably hygroscopic?

***21-7.** List several sources of uncertainty in pH measurements with a glass/calomel electrode system.

21-8. What experimental factor places a limit on the number of significant figures in the response of a membrane electrode?

***21-9.** Describe the alkaline error in the measurement of pH. Under what circumstances is this error appreciable? How are pH data affected by alkaline error?

21-10. How does a gas-sensing probe differ from other membrane electrodes?

21-11. What is the source of
- (a) the asymmetry potential in a membrane electrode?
- *(b) the boundary potential in a membrane electrode?
- (c) a junction potential in a glass/calomel electrode system?
- *(d) the potential of a crystalline membrane electrode used to determine the concentration of F^-?

***21-12.** How does information supplied by a direct potentiometric measurements of pH differ from that obtained from a potentiometric acid/base titration?

21-13. Give several advantages of a potentiometric titration over a direct potentiometric measurement.

21-14. What is the "operational definition of pH"? Why is it used?

***21-15.** (a) Calculate E^0 for the process

$$AgIO_3(s) + e^- \rightleftharpoons Ag(s) + IO_3^-$$

- (b) Use the shorthand notation to describe a cell consisting of a saturated calomel reference electrode and a silver indicator electrode that could be used to measure pIO_3.
- (c) Develop an equation that relates the potential of the cell in (b) to pIO_3.
- (d) Calculate pIO_3 if the cell in (b) has a potential of 0.306 V.

21-16. (a) Calculate E^0 for the process

$$PbI_2(s) + e^- \rightleftharpoons Pb(s) + 2I^-$$

- (b) Use the shorthand notation to describe a cell consisting of a saturated calomel reference electrode and a lead indicator electrode that could be used for the measurement of pI.
- (c) Generate an equation that relates the potential of this cell to pI.
- (d) Calculate pI if this cell has a potential of –0.402 V.

21-17. Use the shorthand notation to describe a cell consisting of a saturated calomel reference electrode and a silver indicator electrode for the measurement of
- *(a) pI.
- (b) pSCN.
- *(c) pPO_4.
- (d) pSO_3.

21-18. Generate an equation that relates pAnion to E_{cell} for each of the cells in Problem 21-17. (For Ag_2SO_3, $K_{sp} = 1.5 \times 10^{-14}$; for Ag_3PO_4, $K_{sp} = 1.3 \times 10^{-20}$.)

21-19. Calculate

*(a) pI if the cell in Problem 21-17(a) has a potential of −196 mV.

(b) pSCN if the cell in Problem 21-17(b) has a potential of 0.137 V.

*(c) pPO_4 if the cell in Problem 21-17(c) has a potential of 0.211 V.

(d) pSO_3 if the cell in Problem 21-17(d) has a potential of 285 mV.

***21-20.** The cell

$$SCE\|Ag_2CrO_4(sat'd), (x\ M)|Ag$$

is used for the determination of $pCrO_4$. Calculate $pCrO_4$ when the cell potential is 0.389 V.

***21-21.** The cell

$$SCE\|H^+(a = x)|glass\ electrode$$

has a potential of 0.2106 V when the solution in the right-hand compartment is a buffer of pH 4.006. The following potentials are obtained when the buffer is replaced with unknowns: (a) −0.2902 V and (b) +0.1241 V. Calculate the pH and the hydrogen ion activity of each unknown. (c) Assuming an uncertainty of 0.002 V in the junction potential, what is the range of hydrogen ion activities within which the true value might be expected to lie?

***21-22.** A 0.4021-g sample of a purified organic acid was dissolved in water and titrated potentiometrically. A plot of the data revealed a single end point after 18.62 mL of 0.1243 M NaOH had been introduced. Calculate the molecular mass of the acid.

21-23. Calculate the potential of a silver indicator electrode versus the standard calomel electrode after the addition of 5.00, 15.00, 25.00, 30.00, 35.00, 39.00, 39.50, 36.60, 39.70, 39.80, 39.90, 39.95, 39.99, 40.00, 40.01, 40.05, 40.10, 40.20, 40.30, 40.40, 40.50, 41.00, 45.00, 50.00, 55.00, and 70.00 mL of 0.1000 M $AgNO_3$ to 50.00 mL of 0.0800 M KSeCN. Construct a titration curve and a first and second derivative plot from these data. (K_{sp} for AgSeCN = 4.20×10^{-16}.)

21-24. A 40.00-mL aliquot of 0.05000 M HNO_2 is diluted to 75.00 mL and titrated with 0.0800 M Ce^{4+}. The pH of the solution is maintained at 1.00 throughout the titration; the formal potential of the cerium system is 1.44 V.

(a) Calculate the potential of the indicator electrode with respect to a saturated calomel reference electrode after the addition of 5.00, 10.00, 15.00, 25.00, 40.00, 49.00, 49.50, 49.60, 49.70, 49.80, 49.90, 49.95, 49.99, 50.00, 50.01, 50.05, 50.10, 50.20, 50.30, 50.40, 50.50, 51.00, 60.00, 75.00, and 90.00 mL of cerium(IV).

(b) Draw a titration curve for these data.

(c) Generate a first and second derivative curve for these data. Does the volume at which the second derivative curve crosses zero correspond to the theoretical equivalence point? Why or why not?

21-25. The titration of Fe(II) with permanganate yields a particularly asymmetrical titration curve because of the different number of electrons involved in the two half-reactions. Consider the titration of 25.00 mL of 0.1 M Fe(II) with 0.1 M MnO_4^-. The H^+ concentration is maintained at 1.0 M throughout the titration. Use a spreadsheet to generate a theoretical titration curve and a first and second derivative plot. Do the inflection points obtained from the maximum of the first derivative plot or the zero crossing of the second derivative plot correspond to the equivalence point? Explain why or why not.

***21-26.** The Na^+ concentration of a solution was determined by measurements with a sodium ion-selective electrode. The electrode system developed a potential of −0.2462 V when immersed in 10.0 mL of the solution of unknown concentration. After addition of 1.00 mL of 2.00×10^{-2} M NaCl, the potential changed to −0.1994 V. Calculate the Na^+ concentration of the original solution.

21-27. The F^- concentration of a solution was determined by measurements with a liquid-membrane electrode. The electrode system developed a potential of 0.5021 V when immersed in 25.00 mL of the sample, and 0.4213 V after the addition of 2.00 mL of 5.45×10^{-2} M NaF. Calculate pF for the sample.

21-28. A lithium ion-selective electrode gave the potentials given below for the following standard solutions of LiCl and two samples of unknown concentration:

Solution (a_{Li^+})	Potential vs. SCE, mV
0.100 M	+1.0
0.050 M	−30.0
0.010 M	−60.0
0.001 M	−138.0
Unknown 1	−48.5
Unknown 2	−75.3

(a) Construct a calibration curve of potential versus $\log a_{Li^+}$ and determine if the electrode follows the Nernst equation.

(b) Use a linear least-squares procedure to determine the concentrations of the two unknowns.

21-29. A fluoride electrode was used to determine the amount of fluoride in drinking water samples. The results given in the table below were obtained for four standards and two unknowns. Constant ionic strength and pH conditions were used.

Solution Containing F^-	Potential vs. SCE, mV
5.00×10^{-4} M	0.02
1.00×10^{-4} M	41.4
5.00×10^{-5} M	61.5
1.00×10^{-5} M	100.2
Unknown 1	38.9
Unknown 2	55.3

(a) Plot a calibration curve of potential versus log[F^-]. Determine whether the electrode system shows Nernstian response.

(b) Determine the concentration of F^- in the two unknown samples by a linear least-squares procedure.

21-30. **Challenge Problem:** Ceresa, Pretsch, and Bakker[13] investigated three ion-selective electrodes for determining calcium concentrations. All three electrodes used the same membrane but differed in the composition of the inner solution. Electrode 1 was a conventional ISE with an inner solution of 1.00×10^{-3} M $CaCl_2$ and 0.10 M NaCl. Electrode 2 (low activity of Ca^{2+}) had an inner solution containing the same analytical concentration of $CaCl_2$, but with 5.0×10^{-2} M EDTA adjusted to a pH of 9.0 with 6.0×10^{-2} M NaOH. Electrode 3 (high Ca^{2+} activity) had an inner solution of 1.00 M $Ca(NO_3)_2$.

(a) Determine the Ca^{2+} concentration in the inner solution of Electrode 2.

(b) Determine the ionic strength of the solution in Electrode 2.

(c) Use the Debye-Hückel equation and determine the activity of Ca^{2+} in Electrode 2. Use 0.6 nm for the α_X value for Ca^{2+}.

(d) Electrode 1 was used in a cell with a calomel reference electrode to measure standard calcium solutions with activities ranging from 0.001 M to 1.00×10^{-9} M. The following data were obtained:

Activity of Ca^{2+}, M	Cell Potential, mV
1.0×10^{-3}	93
1.0×10^{-4}	73
1.0×10^{-5}	37
1.0×10^{-6}	2
1.0×10^{-7}	−23
1.0×10^{-8}	−51
1.0×10^{-9}	−55

Plot the cell potential versus the pCa and determine the pCa value where the plot deviates significantly from linearity. For the linear portion, determine the slope and intercept of the plot. Does the plot obey the expected Equation 21-23?

(e) For Electrode 2, the following results were obtained:

Activity of Ca^{2+}	Cell Potential, V
1.0×10^{-3}	228
1.0×10^{-4}	190
1.0×10^{-5}	165
1.0×10^{-6}	139
5.6×10^{-7}	105
3.2×10^{-7}	63
1.8×10^{-7}	36
1.0×10^{-7}	23
1.0×10^{-8}	18
1.0×10^{-9}	17

Again, plot cell potential versus pCa and determine the range of linearity for Electrode 2. Determine the slope and intercept for the linear portion. Does this electrode obey Equation 21-23 for the higher Ca^{2+} activities?

(f) Electrode 2 is said to be super-Nernstian for concentrations from 10^{-7} M to 10^{-6} M. Why is this term used? If you have access to a library that subscribes to *Analytical Chemistry* or has Web access to the journal, read the article. This electrode is said to have Ca^{2+} uptake. What does this mean and how might it explain the response?

(g) Electrode 3 gave the following results:

Activity of Ca^{2+}, M	Cell Potential, mV
1.0×10^{-3}	175
1.0×10^{-4}	150
1.0×10^{-5}	123
1.0×10^{-6}	88
1.0×10^{-7}	75
1.0×10^{-8}	72
1.0×10^{-9}	71

Plot the cell potential versus pCa and determine the range of linearity. Again, determine the slope and intercept. Does this electrode obey Equation 21-23?

(h) Electrode 3 is said to have Ca^{2+} release. Explain this term from the article and describe how it might explain the response.

(i) Does the article give any alternative explanations for the experimental results? If so, describe these alternatives.

[13]A. Ceresa, E. Pretsch, and E. Bakker, *Anal. Chem.*, **2000**, *72,* 2054, **DOI**: 10.1021/ac991092h.